



UNIVERSITÀ DEGLI STUDI DI SALERNO



UNIVERSITÀ DEGLI STUDI DI SALERNO
Dipartimento di Farmacia

PhD Program
in **Drug Discovery and Development**

XXXIV Cycle

PhD Thesis in

*Innovative technological strategies for
the production of in situ gelling powders
containing active biomolecules for
wound healing*

Candidate

Chiara Amante

Supervisor

Prof. *Pasquale Del Gaudio*

PhD Program Coordinator Prof. Dr. *Gianluca Sbardella*

TABLE OF CONTENTS

Abbreviations.....	V
ABSTRACT	IX
1. INTRODUCTION	1
1.1 Wounds.....	3
1.1.1 Chronic wounds: characteristics, classification, and world incidence	4
1.1.1.1 Venous leg ulcers.....	5
1.1.1.2 Arterial Ulcers.....	6
1.1.1.3 Diabetic Foot Ulcers	7
1.1.1.4 Pressure Ulcers	7
1.1.1.5 Chronic wounds during COVID-19.....	8
1.2 Skin and wound healing.....	9
1.2.1 Hemostasis	10
1.2.2 Inflammation	10
1.2.3 Proliferation.....	11
1.2.4 Remodeling	12
1.2.5 Factors affecting wound healing	12
1.2.5.1 Local factors.....	13
1.2.5.2 Systemic factors	13
1.3 Wound dressing	15
1.3.1 Conventional wound dressings.....	16
1.3.2 Modern wound dressings.....	16
1.3.2.1 Interactive wound dressings	16
1.3.2.2 Advanced interactive wound dressings.....	17
1.3.2.3 Bioactive and smart bioactive wound dressings	18
1.3.3 Global wound dressings market	19
1.3.4 Regulatory aspects	20
1.4 Polymers for wound dressing	21
1.5 Micro-nanoparticle systems for drug delivery	28
1.6 Spray drying technique.....	30
1.6.1 Mini spray dryer.....	32
1.6.2 Nano spray dryer	33
1.6.3 Mini and nano spray dryer in comparison.....	35
1.6.4 Scale-up of pharmaceutical mini spray drying.....	35
1.7 Aim of the thesis	37
2. MATERIALS AND METHODS	41

2.1 Materials	43
2.1.1 Polymers	43
2.1.2 Active pharmaceutical ingredients	43
2.1.3 Salts and excipients	43
2.1.4 Lipids	44
2.1.5 Solvents	44
2.1.6 Enzymes	45
2.1.7 Cell media and others	45
2.1.8 Bacterial media	46
2.2 Encapsulation technology: nano spray drying	46
2.3 Encapsulation technology: mini spray drying	47
2.4 Preparation of feed solutions for spray drying	49
2.4.1 Alginate-pectin: feed solution	49
2.4.1.1 Alginate-pectin loaded with Ac2-26: feed solution.....	49
2.4.1.2 Alginate-pectin loaded with doxycycline: feed solution.....	49
2.4.2 Alginate-pectin-chitosan: feed solution	49
2.4.2.1 Alginate-pectin-chitosan with the co-solvents: feed solution.....	50
2.4.2.2 Alginate-pectin-chitosan with salts as excipients: feed solution.....	50
2.4.2.3 Alginate-pectin-chitosan powders loaded doxycycline: feed solution.....	50
2.4.2.4 Alginate-pectin-chitosan powders with sodium hyaluronate: feed solution.....	50
2.5 Preparation of nanocomposites	51
2.5.1 Alginate-pectin loaded with nanoemulsions (AP-NE)	51
2.5.2 Curcumin loaded nanoemulsions (NE)	51
2.6 Physico-chemical characterization of nanocomposites	52
2.7 Morphological analysis	53
2.8 Dynamic light scattering	53
2.9 Static light scattering	54
2.10 Fluid uptake ability	54
2.11 Water evaporation from hydrogel	55
2.12 Fourier Transform Infrared Spectroscopy (FT-IR) analysis	56
2.13 Residual water content	57
2.14 Differential scanning calorimetry (DSC)	57
2.15 Rheological measurements	58
2.16 Drug content and encapsulation efficiency	58
2.16.1 Ac2-26 content and encapsulation efficiency	58
2.16.2 Doxycycline content and encapsulation efficiency	60
2.16.3 Hyaluronate content and encapsulation efficiency	60
2.16.4 Curcumin content and encapsulation efficiency	61

2.17 Release studies	62
2.17.1 Ac2-26 release	62
2.17.2 Doxycycline release	63
2.17.3 Nanoemulsions release	63
2.18 Enzymatic degradation	64
2.19 Antimicrobial tests	65
2.19.1 Disc diffusion assay	65
2.19.2 Time-killing assay	65
2.20 In vitro cell studies	66
2.20.1 Cell viability and pro-inflammatory activity	66
2.20.1.1 Cell cultures.....	66
2.20.1.2 In vitro cytotoxicity: MTT test	66
2.20.1.3 Pro-inflammatory activity.....	67
2.20.1.4 Statistical analysis	67
2.20.2 Wound healing assay	68
2.20.2.1 Cell cultures.....	68
2.20.2.2 Experimental procedure	68
2.20.2.3 Statistical analysis	69
2.20.3 SDS-PAGE gelatin zymography	69
2.20.3.1 Cell culture and treatment for zymography test	69
2.20.3.2 Experimental procedure	70
3. RESULTS AND DISCUSSION	71
3.1 SECTION A	73
<i>In situ</i> gelling alginate-pectin submicropowders loaded with Ac2-26	73
3.1.1 Scientific background	75
3.1.2 Results and discussion	78
3.1.2.1 Preparation and characterization of the Ac2-26 loaded submicroparticles.....	78
3.1.2.2 In vitro Ac2-26 release studies	84
3.1.2.3 In vitro cytotoxic activity and wound healing assay	85
3.1.3 Conclusions	88
3.2 SECTION B	89
Alginate-pectin and alginate-pectin-chitosan <i>in situ</i> gelling powders	89
3.2.1 Scientific background	91
3.2.2 Results and discussion	93
3.2.2.1 Alginate-pectin and alginate-pectin-chitosan <i>in situ</i> gelling powders	93
3.2.2.2 Alginate-pectin-chitosan <i>in situ</i> gelling powders with co-solvents.....	98
3.2.2.3 Alginate-pectin-chitosan <i>in situ</i> gelling powders with salts	100
3.2.2.4 Characterization of the powders	102

3.2.2.5 <i>In vitro</i> cell studies	109
3.2.2.6 Alginate-pectin-chitosan <i>in situ</i> gelling powders: pilot scale-up.....	113
3.2.3 Conclusions	115
3.3 SECTION C	117
Alginate-pectin and alginate-pectin-chitosan <i>in situ</i> gelling powders loaded with doxycycline	117
3.3.1 Scientific background	119
3.3.2 Results and discussion	122
3.3.2.1 Preparation and characterization of the powders	122
3.3.2.2 Drug release	127
3.3.2.3 Antimicrobial tests	129
3.3.2.4 <i>In vitro</i> test: SDS-PAGE Gelatin Zymography	130
3.3.3 Conclusions	132
3.4 SECTION D	133
Alginate-pectin-chitosan <i>in situ</i> gelling powders loaded sodium hyaluronate	133
3.4.1 Scientific background	135
3.4.2 Results and discussion	137
3.4.2.1 Powders characterization	139
3.4.2.2 <i>In vitro</i> degradation	145
3.4.3 Conclusions	147
3.5 SECTION E	149
Alginate-pectin <i>in situ</i> gelling powders loaded with nanoemulsions	149
3.5.1 Scientific background	151
3.5.2 Results and discussion	155
3.5.2.1 Nanoemulsions formulation, physicochemical characterization, and stability.....	155
3.5.2.2 Production of nanocomposites.....	157
3.5.2.3 Technological characterization of nanocomposites.....	159
3.5.3 Conclusions	167
4. CONCLUSIONS AND PROSPECTS	168
Bibliography	171
Sitography	219
APPENDIX	221
List of publications and communications	221

Abbreviations

ANXA1: Annexin A1

AP: Alginate-pectin

APC: Alginate-pectin-chitosan

APCD: Alginate-pectin-chitosan with doxycycline

APCH: Alginate-pectin-chitosan with sodium hyaluronate

API: Active pharmaceutical ingredient

AP-NE: Alginate-pectin powders loaded with curcumin loaded nanoemulsions

CAGR: Compound annual growth rate

CCM: Curcumin

CFU: Colony forming unit

DCM: Dichloromethane

DE: Degree of esterification

DFU: Diabetic foot ulcer

DLS: Dynamic Light Scattering

DMEM: Dulbecco's modified eagle's medium

DSC: Differential Scanning Calorimetry

ECM: Extracellular matrix

EE: Encapsulation Efficiency

FBS: Fetal Bovine Serum

FDA: Food and Drug Administration

FPR: Formyl peptide receptors

FT-IR: Fourier Transform Infrared Spectroscopy

G: Guluronic acid

G": Loss modulus

G': Storage modulus

H: Sodium hyaluronate, Hyaluronic acid

HaCat: Human keratinocytes

HEKa: Human Epidermal Keratinocytes

HH: High molecular weight sodium hyaluronate

HM: High methoxyl

HPLC: High-Performance Liquid Chromatography

LC-MS: Liquid Chromatography-Mass Spectroscopy

LH: Low molecular weight sodium hyaluronate

LM: Low methoxyl

LOD: Limit of detection

LOQ: Limit of quantification

M: Mannuronic acid

MCT: Medium chain triglycerides

MH: Medium molecular weight sodium hyaluronate

MHA: Mueller-Hinton agar

MHB: Mueller-Hinton broth

MMPs: Matrix metalloproteinases

MTT: 3-(4,5-dimethylthiazol-2-yl)-2,5-diphenyltetrazolium

MW: Molecular weight

NADPH: Nicotinammide adenina dinucleotide fosfato

NE: Nanoemulsion

PBS: Phosphate buffered saline (Potassium dihydrogen phosphate).

PDGF: Platelet-derived growth factor

PDI: Polydispersity index

PEG: Polyethylene glycol

PES: Polyethersulfone

PGA: Poly glycolic acid

PLA: Poly lactic acid

PLGA: Poly lactic-co-glycolic

PU: Pressure ulcer

PVA: Polyvinyl alcohol

PVP: Polyvinylpyrrolidone

S1: Polyoxyethylene stearate

S2: oleoyl polyoxyl-6 glyceride

SDS: Sodium Dodecyl Sulfate

SEM: Scanning Electron Microscopy

SWF: Simulated wound fluid

TEM: Transmission electron microscopy

TGA: Thermo gravimetric analysis

TGF- β : Transforming growth factor-beta

UHPLC: Ultra high-performance liquid chromatography

UK: United Kingdom

US: United States

VEGF: Vascular endothelial growth factor

VHH: Very high molecular weight sodium hyaluronate

VLU: Venous leg ulcer

WHP: Wound healing peptides

WVTR: Water vapour transmission rate

ABSTRACT

The aim of this Ph.D. project is the development of novel topical formulations for the treatment of various wounds by innovative technologies (micro and nano spray drying). The specific objective is the production of a dry powder able to become a gel “*in situ*” in contact with wound exudates using biodegradable and biocompatible polymers. Specifically, alginate with a high content of mannuronic residues, amidated pectin with a low degree of methylation and low molecular weight chitosan are used. Such polymers active in the wound healing process, due to the formation of a hydrogel into the wound cavity, are able to control the release of encapsulated active pharmaceutical ingredients (APIs).

With this aim during the first year of this Ph.D. program, alginate-pectin (AP) submicroparticles loaded with Ac2-26 were produced through nano spray drying. Ac2-26, the N-terminal derived peptide of Annexin A1, was chosen since is able to promote cell migration and tissue repair. The FT-IR studies carried out on the formulations showed chemical interactions between Ac2-26 and polymers blend, able to improve its stability and encapsulation efficiency and control the release, till 48 h. Moreover *in vitro* wound healing assay on HaCaT cells, demonstrated the ability of Ac2-26 to accelerate closure of the wound in 24 h.

Subsequently, to enhance the properties of the powders, to the blank alginate-pectin particles, chitosan was added and a new technique was investigated: mini spray drying. To increase the gelling process, different co-solvents (ethanol and isopropanol), as well as other excipients in the form of salts (sodium bicarbonate and ammonium carbonate) were added to the alginate-pectin-chitosan (APC) formulations. Fluid uptake tests have demonstrated that the addition of sodium bicarbonate reduced the gelation time from 5 minutes to 30 seconds when the powders were in contact with wound simulated fluid. Moreover, the pro-inflammatory studies, carried out on HaCaT cells, have shown that APC powders were able to induce a higher

release of IL-8 from the human keratinocytes that could stimulate the wound healing process in difficult-healing. Having achieved good results, APC powders have been used as a vehicle for doxycycline, an antibiotic model chosen due to its inhibiting activity against matrix metalloprotease-2 (MMP-2) and metalloprotease-9 (MMP-9) hyper expressed in chronic wounds. The presence of chitosan in the powders strongly affected their size, morphology, and fluid uptake properties, as well as drug encapsulation efficiency due to chemical interactions between the polymers and the drug demonstrated by FT-IR studies. In addition, due to drug-polymer interaction, a prolonged drug release profile was observed, as well as antimicrobial activity against *Staphylococcus aureus* was enhanced (till 7 days) compared to pure doxycycline. Furthermore, doxycycline-loaded particles were able to increase drug activity against MMPs, with good activity against MMP-9 even at the lower concentration tested over 72 h.

During the third year, the polymeric blend APC has been enhanced with hyaluronic acid (H), a natural polysaccharide constituent of the extracellular matrix which plays an important role during the wound healing processes. Normally, H has a short lifecycle due to the normal turnover of the skin. However, the biodegradability test conducted *in vitro* highlighted a prolonged time degradation of H thanks to the polymeric blend thus favoring the release of the latter in the wound bed and reducing the replacement frequency of the dressings.

Lastly, during the Ph.D. course, four months were spent at the University of Lyon 1 in France, to study the feasibility of spray drying to develop nanocomposites to encapsulate lipophilic drugs. Specifically, alginate-pectin microparticles were used as a carrier to encapsulate curcumin-loaded nanoemulsions (NEs). Curcumin was used as a model drug since, exhibiting antioxidant and antimicrobial activity, can play a great role in the treatment of wounds. Stable NEs showing a droplet size of 100 nm and a neutral surface charge were obtained. NEs were efficiently encapsulated in microparticles demonstrating that the spray

drying process did not alter their properties. Furthermore, microparticles allowed to sustainably release NEs in simulated wound fluid showing a release dependently to the NEs concentration.

1. INTRODUCTION

1.1 Wounds

A wound is any type of damage or breakage of the integrity of skin, mucous membrane, or organ tissue (Kujath & Michelsen, 2008). In order to promote wound healing and limit the spread of infection and further injury, it is essential to classify wounds and identify the appropriate treatment (Wilkins & Unverdorben, 2013).

The wounds can be classified in (Sarabahi, 2012) (<https://www.woundcaresurgeons.org/>):

- Open or closed: in closed wounds, tissue damage and bleeding occur under the surface of the skin without any exposure to the underlying tissue and organs while in open wounds a break in the skin, which leaves the internal tissue or organs exposed, is involved. Open wounds can be superficial above the epidermis and deep with a loss of both epidermis and dermis.
- Simple, complex, and complicated: in simple wounds are involved only skin and subcutaneous tissue, in complex wounds, a significant tissue loss is, also, present, and in complicated wounds complications such as bacteria contamination or ischemia occur.
- Non-penetrating and penetrating wounds: the first wounds are the result of blunt trauma or friction with other surfaces (abrasions, lacerations, bruises, and concussions); penetrating wounds are the result of trauma and break of the skin (incisions and ulcerations).
- Clean, clean/contaminated, contaminated, and dirty wounds: clean wounds are uninfected without inflammation, clean/contaminated are wounds where bacteria are present endogenously such as in the gastric tract, contaminated are wounds with a wide spread of bacteria and dirty wounds are characterized from necrotic issue.
- Acute or chronic wounds: acute wounds can heal in a short time without complications (8-12 weeks), on the contrary, chronic wounds request a long time to restore normal anatomical structure and function.

1.1.1 Chronic wounds: characteristics, classification, and world incidence

Chronic wounds, called also “hard-to-heal” or “difficult-to-heal” wounds, are wounds that require for heal a time undefined ranging 4 weeks up to more than 3 months (Frykberg & Banks, 2015; Martin & Nunan, 2015; Werdin, Tennenhaus, Schaller, & Rennekampff, 2009). This kind of wound represents a serious problem for both patients and their families since causes pain infection, loss of function, and high healthcare costs (R. Zhao, Liang, Clarke, Jackson, & Xue, 2016). Chronic wounds usually occur in elderly patients with comorbidities such as stroke or diabetes (Sen et al., 2009). One of the main problems of chronic wounds is the presence of an excessive amount of exudate that inhibits fibroblast and keratinocyte proliferation (Mendez, Raffetto, Phillips, Menzoian, & Park, 1999; Trengove, Bielefeldt-Ohmann, & Stacey, 2000). In addition, cytokine and growth factor receptors may also be downregulated (Cowin et al., 2001; Harris et al., 1995) and metalloproteinases are overactive as opposed to their inhibitors (Ladwig et al., 2002; Mwaura et al., 2006; Utz et al., 2010; Yager, Zhang, Liang, Diegelmann, & Cohen, 1996). These high levels of proteases in chronic wounds result in maceration of healthy skin tissue around the wound delaying the healing.

Another serious impediment to the healing of chronic wounds is the possible occurrence of bacterial infection (Leaper, Assadian, & Edmiston, 2015). Although chronic wounds are not always infected, they may be colonized by a different microorganism that, with time, could lead to infections or complicate wound healing. Infection is defined as when the concentration of microbial species exceeds 10^5 colony-forming units (CFU) per gram of tissue (Gardner, Frantz, & Doebbeling, 2001). It occurs when pathogenic microorganisms (both planktonic and biofilms) such as *Staphylococcus aureus* and *Pseudomonas aeruginosa*, which commonly inhabit chronic wounds, attract leukocytes increasing cytokines, proteases, and reactive oxygen species from inflammatory cells that degrade the extracellular matrix (ECM) and disrupt cell migration, inhibiting wound closure (Gajula, Munnamgi, & Basu, 2020). When the bacterial

load became significant and the infection is complete, the serous exudate causes an unpleasant smell characteristic of necrotic areas (Bonadeo, Marazzi, Masina, Ricci, & Romanelli, 2004).

The impact of chronic wounds is detectable worldwide (Olsson et al., 2019), especially in the elderly population (Gould et al., 2015). In the United States (US) ~2% of the total population (5.7 million people) is estimated to be affected by chronic wounds (Järbrink et al., 2017) and this data reaches 3% in the population older than 65 years (SenCK. 2021). A 2018 retrospective analysis identified that near to 15% of Medicare beneficiaries (8.2 million) had at least one type of wound or infection. Medicare cost estimates for all wound types ranged from \$28.1 billion to \$96.8 billion, with the highest costs for surgical wounds and diabetic ulcers (Nussbaum et al., 2018).

Chronic injuries are divided into four types: venous ulcers, arterial ulcers, diabetic ulcers, and pressure ulcers (Figure 1).



Figure 1. *From left to right: examples of venous ulcer, arterial leg ulcer, diabetic foot ulcer, and pressure ulcer.*

1.1.1.1 Venous leg ulcers

Venous leg ulcers (VLUs) are a common manifestation of chronic venous insufficiency and are responsible for about 50-70% of chronic ulcers of the lower limbs (Gillespie, 2010; O'Donnell et al., 2014). It has been estimated that VLUs affect up to 2% of the adult population worldwide, with a higher prevalence in women and the elderly (Chi & Raffetto, 2015; Eberhardt

& Raffetto, 2014). VLU's are a worldwide problem: Europe has up to 2.2 million people affected, and in the United States over 6 million individuals are involved (Broszczak, Sydes, Wallace, & Parker, 2017). VLU's are a defect in the skin with surrounding pigmentation and dermatitis, located in the gaiter region, an area extending from midcalf until below the malleolus, which has been present for greater than 30 days, as a consequence of venous hypertension and congestion due to venous thrombosis (Gillespie, 2010). They may be single or multiple lesions, with a frequent presence of red granulation tissue or yellow fibrinous rarely necrotic (Morton & Phillips, 2016; Zielins et al., 2014). The treatment of VLU's involves many resources, including doctor's visits, nursing care, wound care, and in some cases hospitalization. Therefore, the annual cost associated with each patient in seven different geographies (United States, United Kingdom, Germany, Australia, Italy, Spain, and France) is estimated to total \$10.73 billion (US dollar), nothing compared to the psychosocial impact due to with isolation, embarrassment, lack dependency and sleep (Kolluri et al.; Raffetto, Ligi, Maniscalco, Khalil, & Mannello, 2020).

1.1.1.2 Arterial Ulcers

Arterial ulcers also mentioned as ischemic ulcers are less common than venous lesions and interest 25% of lower limb ulcers. They occur as a consequence of arterial insufficiency due to atherosclerosis, thrombosis, or radiation damage and have a higher incidence in smokers, diabetics, and people with hyperlipidemia and hypertension. The narrowing of the vessel lumen reduces perfusion, leading to ischemia and hypoxia in the affected area and causing open wounds (Morton & Phillips, 2016). Arterial ulcers are characterized by well-defined wound margins, extremely deep with necrotic tissue. Arterial ulcers are often found below the knee, extending to the foot presenting a non-bleeding wound yellow, brown, grey, or black. Often the

limb appears cold to the touch and very painful, especially during the night and all this can last 10 weeks or more (<https://www.woundsource.com>).

1.1.1.3 Diabetic Foot Ulcers

Diabetic foot ulcers (DFUs) are defined as localized injury to the skin, below the ankle, in a person with diabetes (Graves, Phillips, & Harding, 2021). In this pathology, the deficits lead to poor sweating and alteration of blood flow, causing poor oxygenation of the distal extremities and making the skin more susceptible to cracking (Gershater et al., 2009; Lepäntalo et al., 2011). Generally, this phenomenon is born from neuropathy and/or peripheral arterial disease, involving both a macro and microvascular problem (Margolis, Hofstad, & Feldman, 2008). The risk of developing a diabetic foot ulcer during life is estimated between 19% and 34% with 15% of individuals with diabetes that can develop foot ulcers every year (David G. Armstrong, Andrew J.M. Boulton, & Sicco A. Bus, 2017) and 60% that will have recurring ulcers after three years (D. G. Armstrong, A. J. M. Boulton, & S. A. Bus, 2017). Patients with diabetic foot ulcers have a 15-time higher risk of limb amputation and death compared that healthy individuals, due to the high likelihood of infection in the presence of an open wound (Yazdanpanah, Nasiri, & Adarvishi, 2015). The total medical cost for the management of diabetic foot disease in the US in 2017 was estimated at \$237 billion, a 26% increase from 2012 (Armstrong et al., 2020), while in the United Kingdom (UK) in 2014-2015 was estimated at between £837 million and £962 million, 0.8-0.9% of the National Health Service budget for England (Kerr et al., 2019).

1.1.1.4 Pressure Ulcers

Pressure ulcers (PUs), also referred to as bedsores or decubitus ulcers, are defined by Global Burden of Disease as an injury to the skin and surrounded tissue resulting from an obstruction

of blood flow caused by pressure or pressure in combination with shear ("Global burden of 369 diseases and injuries in 204 countries and territories, 1990-2019: a systematic analysis for the Global Burden of Disease Study 2019," 2020). They are common in patients with reduced or impaired mobility, such as paralyzed or unconscious individuals due to their inability to reposition themselves (Z. Moore, Cowman, & Conroy, 2011). Despite the medical knowledge and new effective prevention and treatments, the impact of pressure ulcers on the patient's quality of life is still enormous and debilitating and the costs associated are also considerable (Borojeny, Albatineh, Dehkordi, & Gheshlagh, 2020; Hajhosseini, Longaker, & Gurtner, 2020; Niemiec, Louiselle, Liechty, & Zgheib, 2021). Different studies revealed that the incidence of PUs across Europe is around 10.8% (Z. Moore et al., 2019) while in the United States, annually, around 3 million patients are treated for PUs (Mervis & Phillips, 2019). In the US the healthcare system spends, annually about \$11 billion for the prevention and treatment of pressure ulcers, while in the UK, 4% of the total health costs are used for bedsores (Afzali Borojeny, Albatineh, Hasanpour Dehkordi, & Ghanei Gheshlagh, 2020).

1.1.1.5 Chronic wounds during COVID-19

Recent studies highlighted the increase of risk associated with chronic wounds in patients infected with COVID-19 due to the lack of regular wound care visits to avoid the exposition to the virus (Oropallo, Lantis, Martin, Rubaiay, & Wang, 2021). Data suggested that 40% in the US wound centers visited 40% less of the patient in 2020 compared to 2019 (Rogers et al., 2020) with a \$9.4 billion reduction, a 19% decrease, relative to projected spending levels in the first half of 2020 (<https://www.ama-assn.org/practice-management/sustainability/physician-survey-details-depth-pandemic-s-financial-impact>). The use of medical devices to treat COVID-19-positive individuals blocked in the bed led to the risk of PUs, also in atypical sites on the body, increased from malnutrition and covid issues (Britton et al., 2020).

1.2 Skin and wound healing

Skin, the largest organ of the body, with an area of 1.5–2 m², forms a protective barrier between the body and the external environment against physical damage and pathogens, maintaining body homeostasis (Nejati, Kovacic, & Slominski, 2013). Its structure is composed of three layers: epidermis, dermis, and hypodermis. The epidermis, the outermost layer of skin, provides a waterproof barrier and contains keratinocytes, melanocytes, dendritic cells known as Langerhans cells, and other immune cells (Nejati et al., 2013; Rousselle, Braye, & Dayan, 2019). The dermis, beneath the epidermis, is mainly composed of connective tissue produced by dermal fibroblasts. It contains, also, hair follicles extracellular matrix complex that supports intercellular connections, cellular movement, and regulates cytokine and growth factors functions (Cañedo-Dorantes & Cañedo-Ayala, 2019). The hypodermis is made of fat, protects bones and muscles, and maintains the temperature (Lai-Cheong & McGrath, 2017). The skin is involved when other tissues are injured and takes part in the wound healing process to allow the survival of the organism (Takeo, Lee, & Ito, 2015). Wound healing is a spontaneous and dynamic process that involves an interaction among cells, signaling molecules, and extracellular matrix components allowing the wound closure (Muzzarelli, 2009). This process can be divided into four overlapped phases (Figure 2): hemostasis, inflammation, proliferation, and tissue remodeling (Harper, Young, & McNaught, 2014; Mt, Mohapatra, Kumar, Chittoria, & Nandhagopal, 2015).

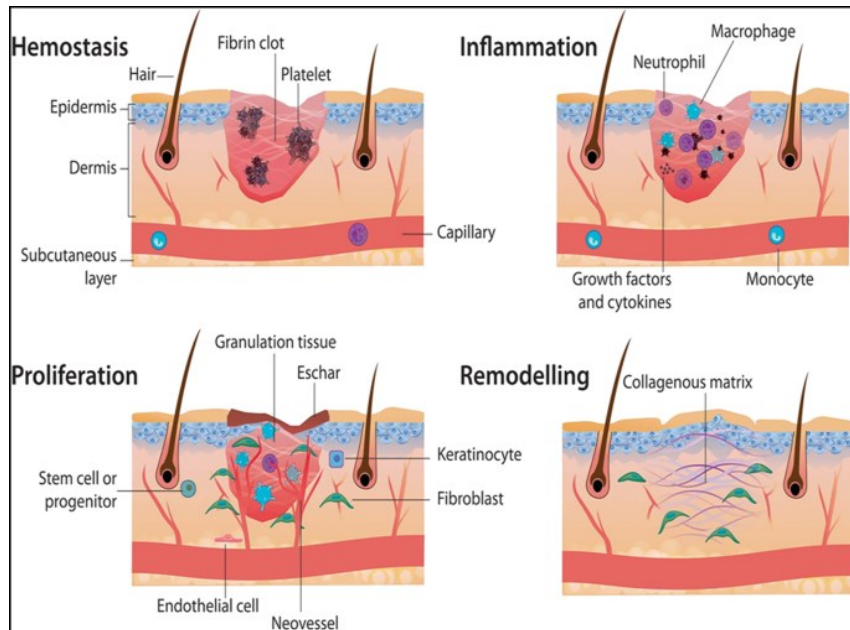


Figure 2. Schematic of the wound healing process (Nour et al., 2019).

1.2.1 Hemostasis

After an injury, the immediate response of the body is to prevent bleeding promoting the formation of fibrin clots (Ellis, Lin, & Tartar, 2018). The clot is constituted by platelets crosslinked fibrin fibers derived by the cleavage of fibrinogen in soluble fibrin. As a consequence of the platelets aggregation, the intrinsic part of the coagulation cascade is activated. The healing cascade initiates through the release of pro-inflammatory cytokines, chemokines, and growth factors that lead to a migration of immune cells like neutrophils and monocytes into the wounded area that determines the start of the inflammatory phase (Beldon, 2010).

1.2.2 Inflammation

This stage of wound healing aims to prevent infection. Neutrophils are the first inflammatory cells that are recruited at the site of injury to destroy damaged tissues and bacteria (Diegelmann & Evans, 2004; Dovi, He, & DiPietro, 2003; Guo & DiPietro, 2010). They kill bacteria by

phagocytosis, resulting in the further release of growth factors, cytokines, reactive oxygen species, and proteolytic enzymes (R. Zhao et al., 2016). When the neutrophils have completed their activity, generally after 48 hours, they are sloughed from the wound surface or are phagocytosed by macrophages (Harper et al., 2014). Macrophages, 48-72 hours after the formation of the injury, attracted to the wound by the chemical messengers released from platelets and damaged cells, secret growth factors that stimulate angiogenesis and fibrous tissue formation (L. A. Dipietro, Reintjes, Low, Levi, & Gamelli, 2001). Macrophages can be divided into M1 and M2 macrophages, depending on the cytokines secreted (Koh & DiPietro, 2011). M1 secreted the pro-inflammatory cytokines, such IL-6, IL-8, and TNF α , important factors to attract additional immune cells (Mosser, 2003). After the removal of neutrophils M1 switches in the M2 phenotype that secretes IL-10 determining the initiation of the proliferation and migration phase (Bratton & Henson, 2011; Landén, Li, & Ståhle, 2016).

1.2.3 Proliferation

The proliferative phase generally follows and overlaps with the inflammatory phase, including re-epithelization and angiogenesis, matrix deposition, and collagen synthesis resulting in the formation of granulation tissue. Re-epithelization occurs under the fibrin clot when epithelial cells start to migrate in the wound site. Fibroblasts, attracted towards the wound edge, proliferate, and then stimulate the migration and further proliferation of keratinocytes.

Neovascularization is necessary to provide nutrients and oxygen to the new tissue. Platelets, releasing transforming growth factor beta (TGF- β), platelet-derived growth factor (PDGF), and fibroblast growth factor, triggered angiogenesis. Vascular endothelial growth factor (VEGF), in combination with the other cytokines, induce endothelial cells to trigger neovascularization and the repair of damaged blood vessels.

After that, fibroblasts, stimulated by growth factors (predominantly by TGF- β and PDGF), produce collagen as well as glycosaminoglycans and proteoglycans, which are major components of the ECM. The result is pink, vascular, fibrous tissue which replaces the clot at the site of a wound, termed granulation tissue. After proliferation and ECM synthesis, wound healing enters the final remodeling phase, which can last for years (Harper et al., 2014; Kurahashi & Fujii, 2015; Wallace, Basehore, & Zito, 2021).

1.2.4 Remodeling

The final stage of wound healing can take up to 2 years involving a delicate process of synthesis and degradation. Fibroblasts, differentiate into myofibroblasts, increase collagen synthesis causing wound contraction and reduction of the wound size (Darby, Laverdet, Bonté, & Desmoulière, 2014). Type III collagen, a characteristic constituent in the granulation tissue, is remodeled into type I collagen, a prevalent constituent in the normal human dermis through the help of MMPs (Gonzalez, Costa, Andrade, & Medrado, 2016; Gurtner, Werner, Barrandon, & Longaker, 2008). After the remodeling of collagen, the vascular density of the wound returns to normal, myofibroblasts undergo apoptosis, and the number of immune cells decreases (Desmoulière, Redard, Darby, & Gabbiani, 1995; Luisa A. DiPietro, 2013). However, although repaired epithelia are almost the same as before wounding, the skin never achieves the same level of tissue strength and elasticity, but only 80% (Harper et al., 2014).

1.2.5 Factors affecting wound healing

Wound healing can be affected by local factors, which directly influence the characteristics of the wound as oxygen and infection or systemic factors health status, and pathologies (Guo & DiPietro, 2010).

1.2.5.1 Local factors

- The lack of oxygen impairs the wound process, while hypoxia stimulates wound healing such as the release of growth factors and angiogenesis, therefore the adequate level of oxygen is an essential requirement for wounds to heal (Bishop, 2008; Yip, 2015).
- All skin breaks can determine micro-organisms to enter the wound site. *Staphylococcus aureus*, *Pseudomonas aeruginosa*, and β -hemolytic streptococcus are common bacteria in infected and non-infected wounds. Due to the formation of biofilm, many chronic ulcers do not heal becoming resistant to conventional antibiotic treatment (Davis et al., 2008; Edwards & Harding, 2004).

1.2.5.2 Systemic factors

- Elderly patients show slower inflammatory, migratory, and proliferation responses (Gosain & DiPietro, 2004). This effect is more evident in aged males, in fact, studies reported that female estrogens (estrone and 17β -estradiol) can improve healing, on the contrary androgens (testosterone and 5α -dihydrotestosterone, DHT) affect wound healing negatively (Gilliver, Ashworth, & Ashcroft, 2007).
- Stress has a great impact on human health and social behavior. Stress up-regulates glucocorticoids and reduces the levels of the pro-inflammatory cytokines IL- 1β , IL-6, TNF- α , and IL- 1α and IL-8 at wound sites essential for the inflammatory phase of wound healing (Boyapati & Wang, 2007; Godbout & Glaser, 2006). In addition to anxiety and depression, stressed individuals tend to assume incorrect behaviors like lack of adequate sleep, not properly cleaning the wound, inadequate nutrition, and excessive drinking or smoking, worsening the state of the wounds.
- Deficit of different nutrients can hurt wound healing, including vitamin A (involved in collagen and hyaluronate synthesis), vitamin C (involved in angiogenesis and capillary

fragility), vitamin E (anti-oxidant), carbohydrates, and protein (involved in collagen synthesis), and omega-3 fatty acids (essential for the systemic immune function) (Arnold, Barbul, & surgery, 2006; Burgess, 2008; Campos, Groth, Branco, & Care, 2008).

- Different studies have demonstrated that the assumption of alcohol increases the incidence of infection by impairing the early inflammatory response, reducing wound closure and collagen production (Gentilello et al., 1993; Szabo, Mandrekar, & Research, 2009).
- Smoke determines more postoperative complications for a smoker than nonsmoker patients (J. Kean, 2010; Sørensen, 2012). Paradoxically, despite the effect of smoking, low doses of nicotine can enhance angiogenesis (Jacobi et al., 2002; Liem, Morimoto, Ito, Kawai, & Suzuki, 2013; Morimoto, Takemoto, Kawazoe, & Suzuki, 2008).
- Different chronic diseases and drugs can affect negatively wound healing. Patients with diabetes show different complications that influence the heal such as hypoxia (Mathieu, 2006), damage derivate under hyperglycemia from advanced glycation end-products, and the interaction with their receptors (Huijberts, Schaper, & Schalkwijk, 2008) and high level of metalloproteases (Tsioufis, Bafakis, Kasiakogias, & Stefanadis, 2012). Obesity generates different negative effects on the body including issues related to wound healing. Healthy adipose tissue is beneficial to the human body isolating paracrine and endocrine organs, secreting cytokines, growth factors, and immune mediators, but the excessive adiposity alters the physiology of the skin and subcutaneous tissues (Pierpont et al., 2014). In addition, many drugs delay wound healing including glucocorticoid steroids, non-steroidal anti-inflammatory drugs, anticoagulants, and chemotherapeutic drugs ("Drugs that delay wound healing," 2013).

1.3 Wound dressing

Wound dressings are essential devices in healthcare that cover wounds to protect them from contamination and damage promoting healing (Derakhshandeh, Kashaf, Aghabaglou, Ghanavati, & Tamayol, 2018). The choice of the ideal dressing should be based on an accurate diagnosis of the type of wound (Olsson et al., 2019). To do so, it is essential to know the dressings and their characteristics. In the last years, different wound dressing has been developed to provide an efficacy environment for accelerating the healing process, especially for chronic wounds that take a long time to heal (Boateng, Matthews, Stevens, & Eccleston, 2008). Wound dressing can be classified as traditional and modern (Figure 3).

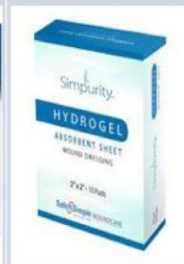
Traditional WDs		Modern WDs		
Gauzes	Bandages	Interactive	Advanced interactive	Bioactive
Xeroform™ non – occlusive petrolatum gauze	Applied as secondary WDs Made from polyesters, cotton or nylon	Semipermeable films and foams	Hydrocolloids and hydrogels	Tissue engineered skin equivalents
				
				
Lacerations, skin graft recipient sites, newly sutured wounds, abrasions and minor or partial-thickness burns	Partial burns, infected and low – to – mild exudating wounds	Lower limbs ulcers, I-II stages burns and I-IV pressure ulcers	Pressure ulcers, diabetic foot ucler, lower as well as upper limbs ulcers	Partial and full-thickness venous ulcers, full-thickness diabetic neuropathic ulcers

Figure 3. *Traditional and modern wound dressings (Brumberg, Astrelina, Malivanova, & Samoilov, 2021).*

1.3.1 Conventional wound dressings

Conventional dressings (gauzes, sterilized absorbent cotton, and bandages) have always been used in clinical practice due to low cost, simple manufacturing processes (Broughton, Janis, & Attinger, 2006), biocompatibility, and skin affinity (Souza et al., 2019). Thanks to their structure are used for absorbing wound exudates, however, the inability to maintain the wound bed moistly and to prevent microbial invasion have made them less desirable at present (Z. E. Moore & Webster, 2013; Uzun, 2018). To improve this lacks, researchers have developed different methods to introduce functional components in gauze such as polymerization with antibacterial polymers (Lumbreras-Aguayo et al., 2019). However, the mechanical properties of the matrix limit the development of these formulations. Therefore, today traditional dressings are mainly used for clean and dry wounds, or as secondary dressings.

1.3.2 Modern wound dressings

Modern wound dressings may be more suitable candidates owing to their properties better biocompatibility, degradability, and moisture retention. When compared with traditional dressings used to cover wounds, modern dressings provide a moist environment and interact with the wound surface to promote wound healing (Han & Ceilley, 2017; Sussman, 2014; C. D. Weller, Team, & Sussman, 2020). Modern dressings can be divided into interactive (films and foams), advanced interactive (hydrocolloids and hydrogels), bioactive (tissue-engineered skin), and smart bioactive (Pilehvar-Soltanahmadi et al., 2018; Przekora, 2020).

1.3.2.1 Interactive wound dressings

Semipermeable film dressings consist of a porous transparent and adhesive polyurethane structure permeable to gas and impermeable to bacteria and liquid. Transparency of film makes it possible to monitor wound healing without removing the dressing (C. Weller & Team, 2019).

The advantage of these dressings is that they can be left on the wound for up to seven days, however, may be traumatic their removal. Moreover, the scars can absorb the exudate (Arroyo, Casanova, Soriano, & Torra, 2015; Vowden & Vowden, 2017), therefore they are used for superficial wounds and abrasions. Opsite™, Tegaderm™, Bioocclusive™, and Hydrofilm™ are examples of films approved by the FDA (Food and Drug Administration) (Michelin, Ahdoot, Zakhary, McDowell, & French, 2021).

Foam is a porous structure made from polyurethane and in some cases has a coating of soft silicone to be allowed removed without pain for the patient. These products can have hydrophobic or hydrophilic, adhesive or no adhesive properties (C. Weller & Team, 2019). Foam dressings absorb the excess of exudate and do not require frequent changes. Since the effectiveness of these dressings depends on the exudative process they can use for burns and pressure ulcers (Jung, Yoo, Han, Dhong, & Kim, 2016). Allevyn, Permafoam, Lyofoam Max, Mepilex, Suprasorb P are examples of foams in commerce (Y.-C. Wang et al., 2021).

1.3.2.2 Advanced interactive wound dressings

Hydrocolloids are dressings that combine gel-forming agents, such as gelatin, sodium carboxymethylcellulose, and pectin with elastomer and adhesive materials. In powder or paste, in the presence of wound exudate, hydrocolloids absorb liquid, forming a gel and maintaining a moist environment (Vries, 2018). The main advantages of the hydrocolloid dressings are moisture retention and the occlusive properties providing a good barrier to water, oxygen, or bacteria. They are adapted to wounds with low to medium exudation and wounds with scab formation, but, not for neurotrophic ulcers and wounds with abundant exudate (C. D. Weller et al., 2020). Hydrocolloid accelerates autolytic debridement to reduce dressing frequency until one time a week, depending on the type of hydrocolloid dressing and the amount of exudate.

Granuflex™, Comfeel™, and Tegaserb™ are examples of hydrocolloid dressings (Westby, Dumville, Soares, Stubbs, & Norman, 2017).

Hydrogels can be defined as highly hydrated polymer materials with a high (90%) water content that structural integrity is ensured by physical and chemical intermolecular crosslinks between polymer chains (Gun'ko, Savina, & Mikhalovsky, 2017). The main advantages of hydrogels are their ability to adapt to the different surfaces on the wounds, the ability to absorb the exudate and maintain a moist environment, and the possibility to incorporate antimicrobial agents and antibiotics. The main disadvantage of hydrogel dressings is that they provide a poor bacterial barrier. Hydrogel dressings are suitable for uninfected low exuding wounds, pressure ulcers, skin tears, and surgical wounds. They can remain in place for no longer than three days and can be covered with a secondary dressing, such as film or foam (Vowden & Vowden, 2017). Intrasite™ Aquaform® Granugel® Nugel™ Purilon® are examples of hydrogel in commerce.

1.3.2.3 Bioactive and smart bioactive wound dressings

Tissue-engineered skin refers to bioactive wound dressings. They are engineered constructs composed of scaffold, cells, or growth factors to accelerate wound healing and recuperate skin functions (Goodarzi et al., 2018). Some examples are layers of keratinocytes and fibroblasts with an underlying layer of collagen (ApliGraf®), composites of an acellular dermal matrix, and components of human or animal origin (AlloDerm®, AlloMax®, GraftJacket®, Integra®, etc.). Even if these formulations are FDA-approved they are still limited by the high cost, a lot of time required to treat cells, and the risk of infection and antigenicity (Miller, Brown, Ibrahim, Ramchal, & Levinson, 2015).

Recently, smart wound dressings integrated with the sensors able to interact with the wounds and react to the wound condition or environment changing have been developed. Since wound healing is characterized by changes in temperature, pH, and redox status, thermo-responsive,

pH-responsive, photo-responsive, and ROS-responsive materials were used in smart wound dressings. However, many challenges still need to be addressed such as balancing the various function without compromising any and creating a dressing safe and biocompatible with the human body. Moreover, large-scale production is another challenge, as many products are still in the experimental phase and request different steps for commercialization (R. Dong & Guo, 2021; Farahani & Shafiee, 2021).

1.3.3 Global wound dressings market

The global advanced wound care market size was valued at US\$ 17.94 billion in 2020 and is predicted to reach nearly US\$ 29.96 billion, registering a compound annual growth rate (CAGR) of 7.6% through 2021 to 2027. The increasing prevalence of chronic injuries is one of the key factors leading to the rise in demand for advanced wound care products. The advanced wound care market is segmented based on product, type, end-user, and region. By product, the global market is divided into traditional/basic wound care products, surgical wound care products, and advanced wound management products (Figure 4).

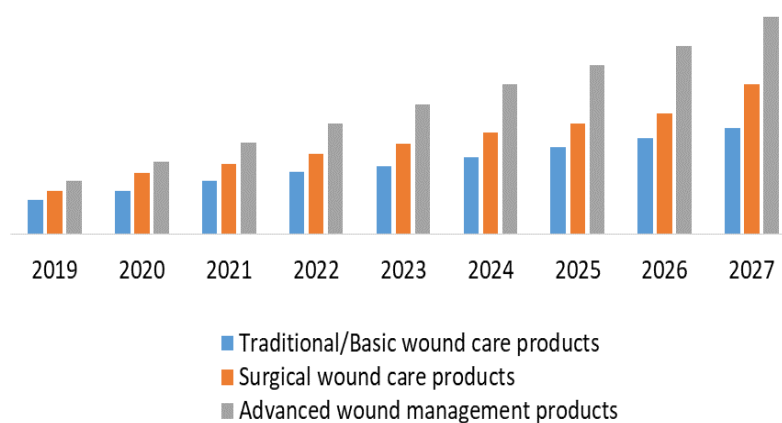


Figure 4. Global wound care market segmented by product 2020-2027.

Based on application, the advanced wound care market is bifurcated into chronic wounds and acute wounds, while regarding end-user depending on where the patient is treated, the market is classified into Hospital, Home healthcare, and Long term care (Figure 5).

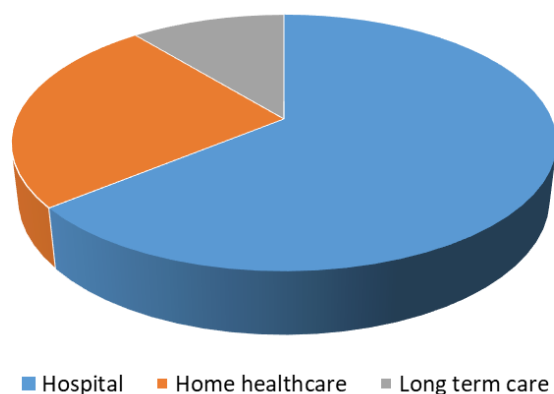


Figure 5. *Global wound care market segmented by End-User (%) in 2020.*

Region-wise, the market is analyzed across North America, Europe, Asia Pacific, South America, Middle East, and Africa (<https://www.maximizemarketresearch.com/market-report/global-wound-care-market/15340/>).

1.3.4 Regulatory aspects

World Health Organization defines as medical devices, any materials, instrument, apparatus, appliance/software, whether used alone or in combination, for specific medical purpose. This new regulation entered into force on May 25th, 2020 after a transition time of 3 years. According to this definition wound dressings are classified as medical devices (Ravizza et al., 2019). According to the US FDA guidelines, bandages and gauze are designated as Class I of wound dressings, dressing products that contain drugs/bioactive molecules, biomaterials are considered as Class II while dressing products with human or animal cellular belong to Class III. In European Medical Device Directive guideline, wound dressings used for the injured skin

are in Class I, dressings that enhance the healing process by monitoring the level of moisture, pH, and temperature at the wound site, are classified as Class II, and dressings containing animal tissues as Class III (Farahani & Shafiee, 2021).

1.4 Polymers for wound dressing

Polymers play an important role as an excipient in any dosage form since they influence formulations properties and drug release. In the last years the interest versus biodegradable polymers, distinguished in synthetic and natural polymers, has been increased. Some of the synthetic polymers frequently used for controlled release in dressing formulations are (Hamid Akash, Rehman, & Chen, 2015; Kamoun, Kenawy, & Chen, 2017):

- Polyethylene glycol (PEG), a water-soluble synthetic viscous amphiphilic polymer, is widely studied and approved by FDA for drug delivery. Due to its biocompatibility, biodegradability, nontoxicity, non-antigenicity, and cost-efficient, it is a good candidate for several medical applications. It is often used in combination with other polymers and molecules, often as hydrogels since it exhibits attractive swelling properties due to its capability to absorb water (Masood et al., 2019; W.-K. Xu et al., 2019).
- Polyvinylpyrrolidone (PVP), a water-soluble and biocompatible/biodegradable synthetic polymer, is extensively used as hydrogel membranes for skin substitutes, because of its low toxicity, good water vapor transmission rate, and impermeability to the bacteria. The best formulation known with PVP is the disinfectant povidone-iodine (Goldenheim, 1993).
- Poly lactic-co-glycolic acid (PLGA) is a copolymer of poly lactic acid (PLA) and poly glycolic acid (PGA). It is FDA-approved biodegradable polymer due to its biocompatibility and changeable biodegradability. The block copolymers of PLGA

with PEG are extensively studied, especially PEG-PLGA-PEG, due to gel-sol transition in water, which make them solid at room temperature and gel at body temperature (Ghahremankhani, Dorkoosh, Dinarvand, & technology, 2008; Jeong, Bae, & Kim, 2000; Khodaverdi et al., 2012).

- Polyvinyl alcohol (PVA), hydrophilic synthetic polymer (Mbhele et al., 2003), is used as a wound dressing due to its biocompatibility, swelling capacity, transparent, flexibility, non-toxic, and biodegradable properties (Jannesari, Varshosaz, Morshed, & Zamani, 2011; Kim et al., 2008).

Natural polymers are organic molecules synthesized by fungi and bacteria, plants, algae, and animals widely used in pharmaceutical applications for their biocompatibility, biodegradability, and lower antigenicity (Rehm, 2010; Sezer & Cevher, 2011; Smith, Moxon, & Morris, 2016). They have a wide range of pharmacological activities (e.g. antitumor, antioxidant or anti-inflammatory effects) very useful in the healing process. Moreover, they can be modulated into different scaffolds mixed with other polymers and functionalized to improve their properties (Yu, Shen, Song, & Xie, 2018). Below are the polymers generally used for wound dressing.

- Collagen, the major component of ECM, is a biocompatible abundant mammalian protein. Twenty-nine collagen types have been identified but Type I collagen is the main component implicated in tissue repair. Collagen and, gelatin its proteolytic cleavage fragment, assume an important role in wound healing (Brett, 2008). Collagen in form of sponges, hydrogels, films, membranes, and powders are commercialized as a wound dressing: Biopad, Stimulen, CellerateRX, Cutimed, etc. (Sahana & Rekha, 2018).
- Cellulose, composed of repeating units of β -D-glucose held by β -1, 4-glycosidic linkages, is the most abundant biopolymer available in nature. It maintains moist wound supplying of growth factors and other molecules to the healing tissues and

due to its porosity mimics ECM of the skin improving tissue regeneration (Czaja, Krystynowicz, Bielecki, & Brown, 2006; Kucińska-Lipka, Gubanska, & Janik, 2015; Sulaeva, Henniges, Rosenau, & Potthast, 2015). Generally, it is functionalized or used in a blend with other materials to improve its properties (El Fawal, Abu-Serie, Hassan, & Elnouby, 2018; Pasaribu, Gea, Ilyas, Tamrin, & Radecka, 2020). Durafiber and Exu-Dry Cellulose are examples of cellulose-based products commercially available.

- Dextran consists primarily of α -1,6-linked D-glucopyranose residues with a few percent of α -1,2-, α -1,3- or α -1,4-linked side chains (Mehvar, 2000). Dextran is a promising candidate for biomedical applications due to good biocompatibility and the ability to facilitate neovascularization and skin regeneration *in vivo* (J.-Y. Liu et al., 2018; G. Sun et al., 2011; Unnithan et al., 2012).
- Hyaluronic acid (H) is a glycosaminoglycan made up of repeating units of d-glucuronic acid and N-acetyl-d-glucosamine linked by alternating β -1,4 and β -1,3 glycosidic linkages. It plays an important role in wound healing by promoting fibroblast proliferation, remodeling of ECM, and keratinocyte migration (Price, Myers, Leigh, & Navsaria, 2005). It is widely used as a wound dressing, in form of sponges, foam and hydrogels. Fiorica et al. developed a hydrogel able to incorporate and vehicle VEGF, through a crosslinking between copolymer of HA- carbamate acid with α -elastin. The experiments demonstrated that the hydrogels favor an appropriate VEGF release profile, essential to stimulate the formation of the new blood vessels during the wound healing process (Fiorica et al. 2018). Another work describes the production of porous nanoparticles of HA using the gas anti-solvent precipitation method for the incorporation of growth factors in order to obtain controlled-release carrier systems (Zavan B., et al. 2009). In addition, there are a lot

of wound care commercial products containing hyaluronic acid such as Hyalomatrix, Hyalofill and Ialuset plus.

- Alginate is a polysaccharide copolymer constituted of β -D-mannuronic acid and α -L-guluronic acid (Figure 6) isolated from brown algae through alkaline extraction and marketed as a sodium or calcium salt, in a range of molecular weight (MW) of 32,000-400,000 Da (K. Y. Lee & D. J. Mooney, 2012). It is composed of sequences of M-blocks and G-blocks residues and it was demonstrated that high mannuronic content alginate stimulates the production of cytokines in the wound healing process (Pawar & Edgar, 2012). It is widely used for wound dressing due to its biocompatibility, biodegradation, hemostatic properties as well as its ability to absorb exudate forming a hydrogel *in situ* (Balakrishnan, Mohanty, Pr, & Athipettah, 2005; Z. Dong, Wang, & Du, 2006; J. Sun & Tan, 2013). When alginate is in contact with fluid the ion exchange between the calcium ions in the alginate and the sodium ions in exudate occurs. This phenomenon determines the forming of a typical harsh structure, defined as “egg-box”, very useful for controlled drug release (A. Thomas, Harding, & Moore, 2000). Alginate is a versatile polymer that can be used in a wide range of applications (films, gels, hydrogels, foams, wafers, nanofibers, gauzes, *etc.*) in order to maintain a moist environment around the wound, which is necessary to facilitate fast wound healing. Due to their functional groups, alginate can be easily blended with other biopolymers especially chitosan to form bioactive inter-polymer (polyelectrolyte) complexes due to its ionic character. Mndlovu et al. produced a film performed *via* polyelectrolyte complexes able to incorporate a huge amount of water and have a prolonged biodegradation time (Mndlovu et al. 2019). Jin and his research group produced novel hemostatic microspheres composed of carboxymethyl chitosan, sodium alginate and collagen having a good blood-absorption ability useful

for wound healing applications (Jin et al., 2018). Singh et al., have reported antibiotic moxifloxacin released in a controlled manner from a biocompatible alginate hydrogel to improve wound healing (Singh et al., 2017). There are several commercially available wound care products such as Algosteril, Comfeel Alginate Dressing, CarrasorbH, Kaltostat, etc.

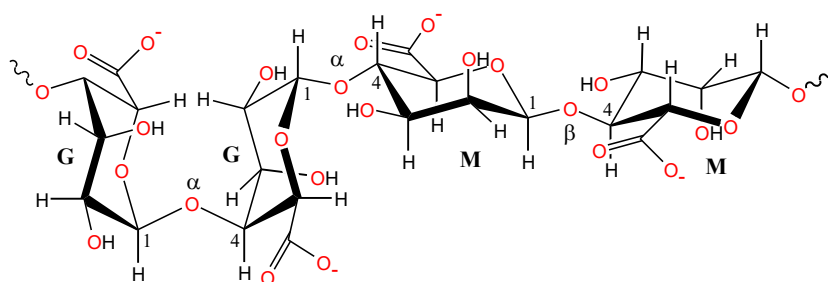


Figure 6. Chemical structure of alginate.

- Pectin, a water-soluble polysaccharide easily available and cheap, has recently been explored for use in numerous biomedical applications including drug delivery (H. Y. Lin, Chen, Chang, & Ni, 2013). It is one of the major constituents of citrus, poly α 1-4-galacturonic acids, with varying degrees of methylation of carboxylic acid residues (Figure 7). The MW of pectin varies in the range of 50,000-150,000 Da. According to the number of carboxyl groups that can be esterified with methyl groups, pectins are classified based on their degree of esterification (DE) into two main groups: high methoxyl (HM) with a degree of esterification of more than 50% and low methoxyl (LM) with less than 50% of carboxyl groups esterified (Thakur, Singh, Handa, Rao, & Nutrition, 1997). One of the main characteristics and attractiveness of pectins is their capacity to form gels and the strength of the gelification depends mainly on its DE (P. J. S. U. I. J. Sriamornsak, 2003; Sundar Raj et al., 2012). HM pectin requires low pH (2.5-3.5), an acidic environment, and the presence of an adequate amount of soluble

solids as sucrose to reduce the water activity to stabilize junction zones through hydrophobic interactions (Löfgren, Walkenström, & Hermansson, 2002; D. Oakenfull & Scott, 1984). LM pectin follows the "egg-box" model in the presence of bivalent cations such as alginate, creating intermolecular junction zones between pairs of carboxyl groups of different chains in close contact (Axelos, Thibault, & pectin, 1991; Munarin, Tanzi, & Petrini, 2013). In literature, a lot of works are reported based on a combination of pectin with others polymers as wound dressings. Rezvanian's group produced simvastatin-loaded crosslinked alginate-pectin hydrogel films by ionic crosslinking to enhance the thermal stability of the wound fluid uptake and drug release behavior (Rezvanian et al., 2017). Another work reported the production of clindamycin-loaded composite hydrogel films using alginate, pectin and hyaluronic acid for the treatment of Methicillin-resistant *Staphylococcus aureus* infection (Hasan et al., 2021).

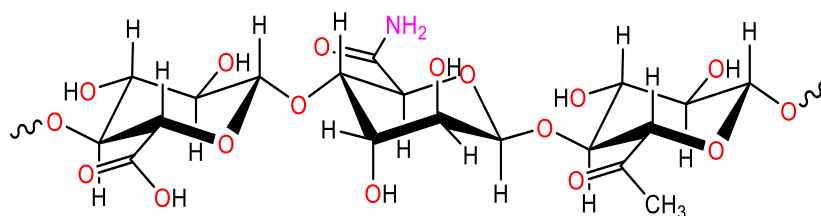


Figure 7. Chemical structure of pectin.

- Chitin is the second most abundant biopolymer in nature after cellulose, present mainly as a structural component in the exoskeleton of crustaceans and the cell wall of fungi and yeasts. It is a linear heteropolymer composed of D-glucosamine and N-acetyl-D-glucosamine linked via β (1 \rightarrow 4) glycosidic bonds. When chitin is brought to an acetylation level of less than 50% in an alkaline environment, it is called chitosan (Figure 8). Chitosan is soluble in a dilute acidic solution of pH \sim 2, producing a rigid

crystalline structure (Krajewska & technology, 2004). The molecular weight of chitosan can influence its physicochemical properties such as viscosity, solubility, and elasticity (Moeini, Pedram, Makvandi, Malinconico, & Gomez d'Ayala, 2020). Low molecular weight chitosan (310,000-375,000 Da) is preferred since it has a higher solubility and less viscosity than the high molecular weight (50,000-190,000 Da). Chitosan is widely used for wound healing, due to its antimicrobial and antifungal activity site (Raafat, von Bargen, Haas, & Sahl, 2008; Seyfarth, Schliemann, Elsner, & Hipler, 2008), hemostatic effect, and proliferative activities essential for efficient healing. Chitosan also stimulates fibroblast proliferation (Ueno, Mori, & Fujinaga, 2001) and accelerates tissue regeneration (Ahmed & Ikram, 2016; Kozen, Kircher, Henao, Godinez, & Johnson, 2008). Due to these interesting characteristics, chitosan and its derivatives can be considered the most promising materials for wound dressing applications. Lv et al. produced injectable hydrogels, based on carboxymethyl chitosan/alginate polyelectrolyte complexes demonstrating good viability and acceleration of wound healing process in a mouse skin defect model (Lv et al., 2019). In another work, a facile flow injection method to fabricate chitosan beads was developed. These beads are able to induce blood coagulation suggesting the potential use as a hemostatic dressing for trauma hemostasis (Li et al., 2020). Suprasorb, Celox, and Opticell are examples of chitosan-based dressings are available in the market.

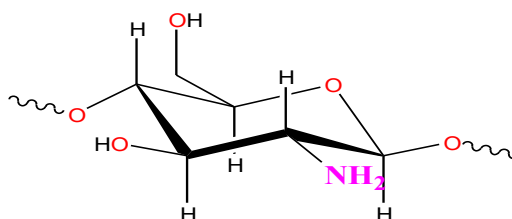


Figure 8. Chemical structure of chitosan.

1.5 Micro-nanoparticle systems for drug delivery

Controlled drug delivery technology has grown and diversified enormously in the last years. Drug delivery systems can be used for different applications from inhalation to topical, offering numerous clear advantages respecting conventional formulations. Among them, micro and nanoparticles have unique properties based on their structural and functional abilities. Particles can be injected or deposited directly at the site of action, prolonging the release of drug and the efficacy, minimizing system toxicity, and improving patient's compliance (Kohane, 2007; Ravi Kumar, 2000). From the viewpoint of technology, micro and nanoencapsulation offer numerous advantages: masking an unpleasant taste, separating incompatible materials, protecting the body from the side effects and, improving the stability of the active pharmaceutical ingredients (API) prolonging their effects (Lengyel, Kállai-Szabó, Antal, Laki, & Antal, 2019). Pharmaceutical particles consist of a variety of sizes and shapes including micro and nano particles, powders, granules, and tablets (Figure 9). Microparticle systems are defined as solid particles with a size ranging between 1 and 1000 μm , but the most interesting, from a pharmaceutical point of view, are located up to 100 μm , while nanoparticle systems are defined as particles smaller than 1 μm divided into submicroparticles (300-1000 nm) and nanoparticles proper (1- 300 nm).

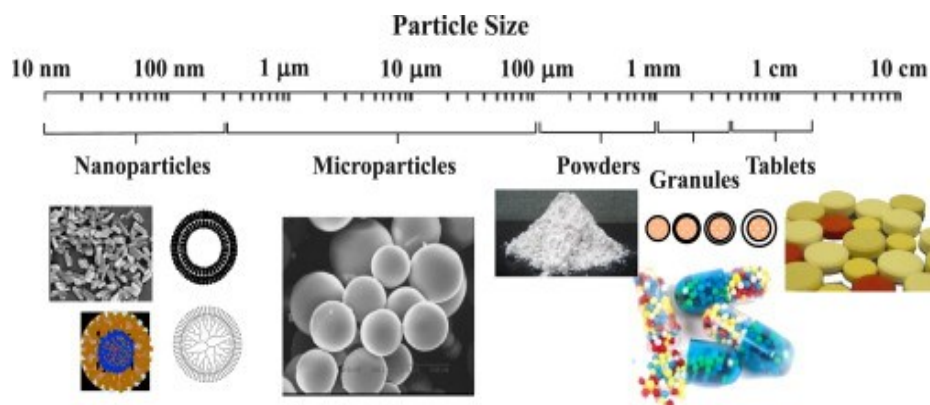


Figure 9. Representation of different solid pharmaceutical forms concerning their size (B. K. Lee, Yun, & Park, 2015).

Particles can be divided into micro-nanospheres and micro-nanocapsules.

Micro-nanospheres exhibit matrix systems in which the drug is dispersed, either dissolved or suspended, while micro-nanocapsules have typical core-shell morphology where a membrane shell is surrounding the core forming a reservoir system (Anton, Jakhmola, & Vandamme, 2012; Peanparkdee, Iwamoto, & Yamauchi, 2016; Whelehan & Marison, 2011).

The release of drugs is the result of various phenomena and mechanisms, always in combinations: dissolution/diffusion, erosion, and osmotic-mediated events (Ebube et al., 1997; Miyazaki, Yakou, & Takayama, 2004). Although a zero-order release profile is desired, most drug delivery systems show a triphasic release profile. The first consist phase of an initial burst (Ebube et al., 1997) is attributed to drug precipitates at the particle surface. The second phase is a lag period depending on the polymer and the release is mostly governed by the diffusion of the drug through the polymeric matrix or the pores (Miyazaki et al., 2004). In the third phase, a faster release is observed due to erosion of the formulation (Panyam et al., 2003). The drug release depends on many factors: drug formulations properties, flexibility and swelling behavior of the polymer matrix, interactions between polymers and drug, and release medium (E. S. Tang, Chan, & Heng, 2005). A decrease in particle size and higher porosity of the particles, inducing an increase in the surface area, can facilitate the contact with the fluid and, as a consequence, the drug diffusion (Panyam et al., 2003; Wischke & Schwendeman, 2008). In the case of micro-nanospheres, the drug release occurs mainly by diffusion through polymers that in contact with water swell creating new pores that allow the transition of the active. The second event possible is the erosion of the polymers matrix. In the case of micro-nanocapsules, the polymers form a water-insoluble, permeable or semipermeable barrier and the diffusion mechanism is predominant. With the exposure of water, the pores and channels of the reservoir filled with fluid and driven by an osmotic gradient, drug molecules can diffuse (Figure 10) (Prajapati, Jani, & Kapadia, 2015; Siepmann & Siepmann, 2012).

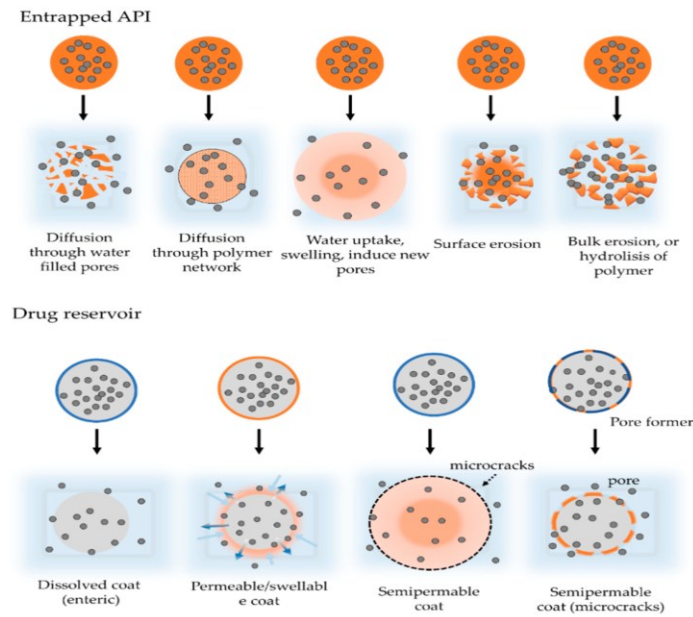


Figure 10. *Schematic drug release from micro-nanospheres and micro-nanocapsules*
(Lengyel et al., 2019).

1.6 Spray drying technique

In the last year, it was considered increasingly important to control particle size and morphology (Suh, Jang, Suh, & Suslick, 2006) for various applications: electronics, sensors, pigments, drug carriers, etc. (Iskandar, 2009). Many alternative methods have been proposed to realize the production of particles with a controllable morphology: precipitation, lyophilization, freeze-drying, spray-drying, pyrolysis, supercritical fluid, and emulsion-based methods. Among them, spray drying due to its reproducibility, fast and continuous mode of operation, short exposure of the product to high processing temperatures, and industrial applicability is widely used in pharmaceutical applications since the 1940s (J. Wang, de Wit, Boom, & Schutyser, 2015). The application in pharmaceutical included solid preparation (Sawicki, Beijnen, Schellens, & Nuijen, 2016) spray-dried nanocomposites (Azad, Arteaga, Abdelmalek, Davé, & Bilgili, 2015; M. Li et al., 2018), carrier for extracts (Sansone et al., 2011) and inhalation powders (Manniello, Del Gaudio, Aquino, & Russo, 2017). Spray drying is a continuous process that transforms, directly, various liquids (e.g. solutions, emulsions, or

dispersions) into solid particles with well-defined size and distribution, as well as morphology and chemical composition (Nandiyanto & Okuyama, 2011) (Figure 11).

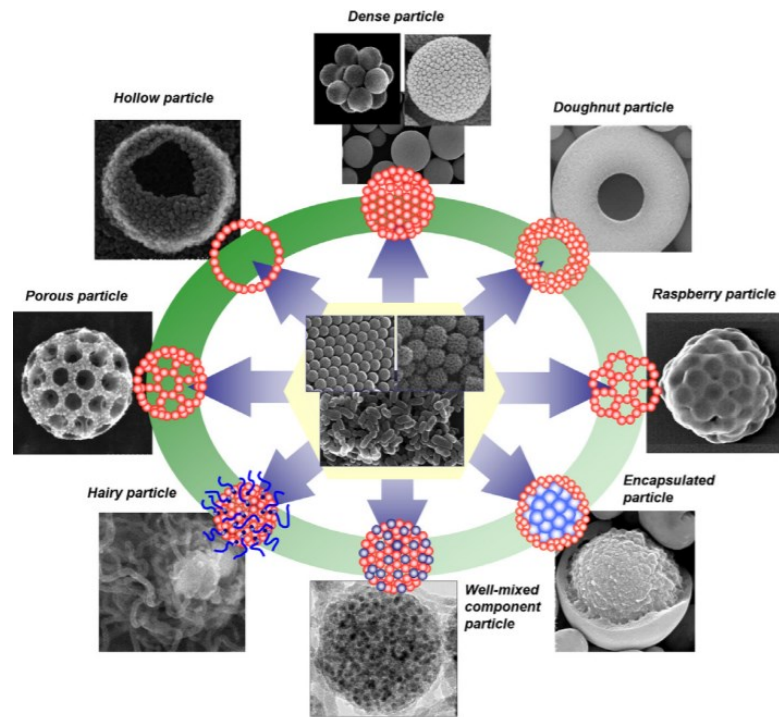


Figure 11. *Different particles prepared by the spray-drying (Nandiyanto & Okuyama, 2011).*

The process involves heating of the drying gas, droplet generation through atomization, drying of the droplet and conversion in particle, and particle collection. The first step is the atomization based on the passage of liquid feed in specific atomization equipment to obtain droplets. Different atomizations are available: a rotary disk that produces droplets with a size of 200 μm , a two-fluid nozzle and an ultrasonic nebulizer that can generate droplets ranging from 10-1000 and 1–10 μm , respectively. The droplets generated to atomization enter the drying chamber where the solvent is quickly removed by the continuous flow of a hot drying gas (Iskandar, 2009). The carrier gas used to transport aerosol droplets into this chamber generally is air or inert gas (e.g. nitrogen, argon, carbon dioxide). For aqueous feeds, the typical system configuration is an open mode with air as drying gas, on the contrary when flammable organic solvents are used, a closed mode operation was applied. Dry particles so formed are

collected in a collector and the gas is filtered. The spray drying process is affected by different parameters including the spray rate intensity, the feed composition and concentration, the drying gas inlet temperature, the solvent type, the temperature, and the drying gas flow rate. All of these parameters influence the final product (i.e. particle size and morphology, moisture content, encapsulation efficiency and drug loading yield, and stability), therefore is essential to optimize process parameters.

1.6.1 Mini spray dryer

There are a different number of mini spray dryers available commercially but, the most widely used is the Büchi laboratory spray dryer, currently available as its Model B-290.

The feed solution is injected by a pump into a spray nozzle and atomized at the entrance of the drying chamber, where is converted into a spray of tiny drops. Drops in contact with hot gas at the proper temperature for the moisture evaporation, develop particles that started to move in a helical direction toward the bottom. The dry particles are then separated from the drying gas employing a cyclone that uses centrifugal force to separate solid particles from the gas. The fluid behavior is affected by cyclone design. The cyclone consists of a cylindrical upper part and a conical lower part. The air charged with solid particles enters the upper part tangentially assuming a spiral movement inside the conical part. The solid, cannot follow the movement of the air, so it collides with the walls of the cyclone and it precipitates in the collector under the effect of gravity, while the air rises upwards together with the finer dust, exits from the cyclone, and is filtered (Figure 12).

Mini spray dryers can be fitted with cyclone separators of different sizes that produce variations in the drying gas flow rate, with an impact on the final product. The small-dimensioned cyclone, in comparison with the larger standard cyclone, allows to obtain a higher yield, very attractive when the start material is little and expensive (Bögelein & Lee, 2010).

Spray drying allows to obtain small size (1-5 μm), medium size (5-25 μm), and large size (10-60 μm) particles (Piñón-Balderrama et al., 2020).

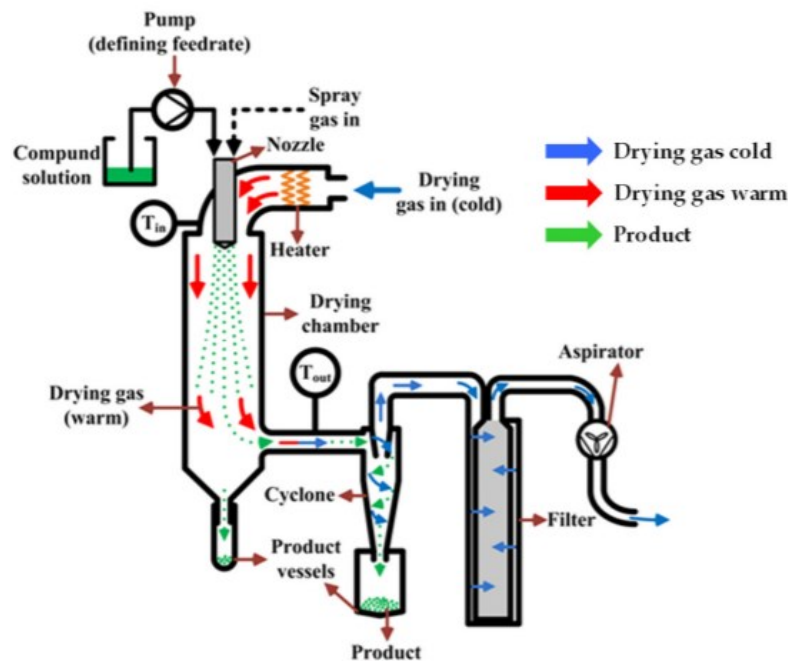


Figure 12. Schematic representation of mini spray dryer (Piñón-Balderrama et al., 2020).

1.6.2 Nano spray dryer

Recent progress in spray drying technology led to the introduction of an advanced spray dryer, the Nano Spray Dryer B-90, developed by Büchi Labortechnik AG (Switzerland) in 2009. The droplet generation is based on a piezoelectric crystal actuator, in direct contact with a thin stainless steel membrane (spray mesh) in a small spray cap. The membrane is characterized by a series of micrometer-sized holes from the diameter of 4.0, 5.5, or 7.0 μm (Arpagaus, John, Collenberg, & Rütli, 2017; Schmid, Arpagaus, & Friess, 2011). The liquid feed is fed through a peristaltic pump, at the desired flow rate. The piezoelectric vibration, due to the application of ultrasonic frequency (60-140 kHz) leading to a fast upward and downward movement of the spray mesh, produces millions of narrow droplets into the drying chamber (X. Li, Anton, Arpagaus, Belleiteix, & Vandamme, 2010). The resulting spray contains drops in the

mean droplet size varied from 4.8 to 7.2 μm for the spray mesh of 4 and 7 μm , respectively (Piñón-Balderrama et al., 2020). A drying gas, generally air, heated up based on a set of inlet temperatures, enters in laminar flow from the top into the drying chamber and directs the particles to the electrostatic collector. The vertical configuration of the spray dryer minimizes particle adhesion to the glass of the chamber, increasing collection yields (Arpagaus, 2012; S. H. Lee, Heng, Ng, Chan, & Tan, 2011) and provides homogeneous heat distribution, thus avoiding the risk of the temperature-sensitive material degrading. Before the collection, the solid particles are electrostatically charged and deposited at the surface of the collecting electrode consisting of a grounded star electrode (cathode) and cylindrical particle collecting electrode (anode). A high voltage of 17 kV at the collecting electrode (electrical current of a few 10 mA) accelerates the deposition of negatively charged particles into the inner wall of the particle collecting electrode. At the end of the process, the particles are gently removed from the surface of the collecting electrode by using a scraper, and the drying gas is purified (Figure 13).

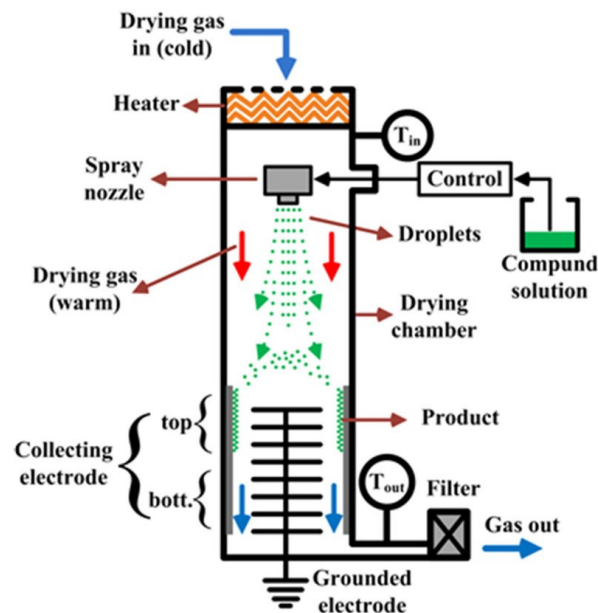


Figure 13. Schematic representation of nano spray dryer (Piñón-Balderrama et al., 2020).

1.6.3 Mini and nano spray dryer in comparison

The main limitation of the mini spray dryer is the minimum volume of feed solution required (50 mL) and the yield is not very high (max. 70%). Using the B-90 Nano Spray Dryer with modern atomization head technology, the minimum volume of the feed solution is up to 2 ml and the yield is increased by up to 90%. The high yields enable the economical use of valuable APIs. Moreover, the inlet temperature used contributes to maintaining the stability and activity of heat-sensitive materials, such as peptides and proteins. The main advantage of nano spray dryer, however, is the reduction of particle size up to 300 nm, improving bioavailability, and release of APIs. However, the long process times do not make a nano spray dryer suitable for industrial scale-up, differently from a mini spray dryer.

1.6.4 Scale-up of pharmaceutical mini spray drying

Pharmaceutical spray dryers are available in a broad range of scales: from lab units to large commercial instruments. In the first case milligrams of powders can be produced with low risk, on the contrary in the second case multiple tons of powder per day where product losses and risk are very high (Figure 14). Therefore is essential that the spray drying process be scaled up directly from the laboratory to the industrial (Faure, York, & Rowe, 2001). Based on a recent report of the spray drying market in the pharmaceutical industry, it is predicted an increase 17% of the production between 2018 and 2028.

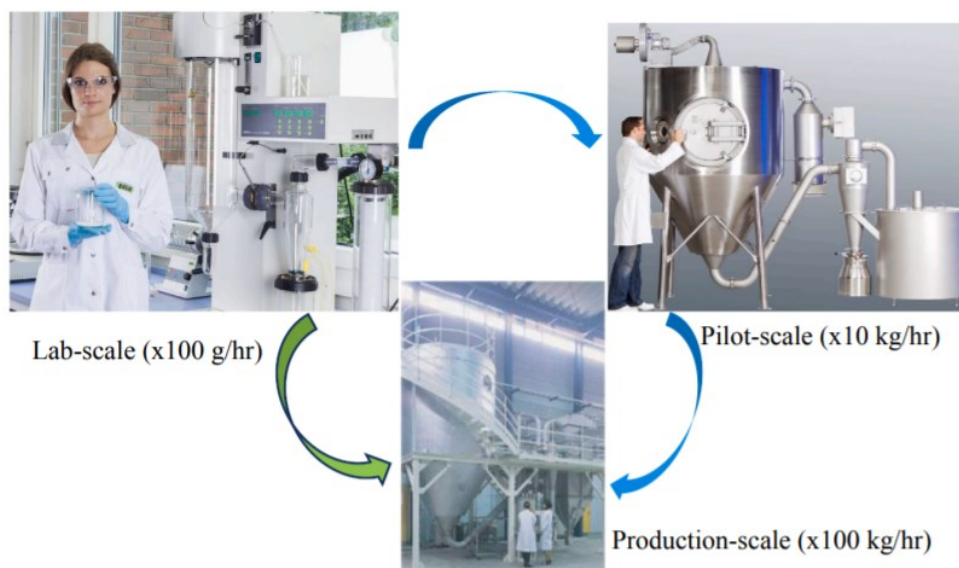


Figure 14. Scale-up of the spray drying process (Poozesh & Bilgili, 2019).

Pharmaceutical spray dryers often combine the most sophisticated control systems with simple designs to obtain a fast process and an easy-to-clean instrument. Commonly, small-scale dryers operate in a single-pass mode in which fresh drying gas is introduced to the chamber, whereas larger spray dryers operate in recycle mode in which the drying gas is recycled. In many cases, nitrogen is the preferred drying gas with respect to the air. Pressure and two-fluid nozzles are mostly used in the pilot and large-scale equipment. The choice depends on the type of feed and particle size of the final product. Two-fluid nozzles provide for the passage of liquid and gas through the nozzle. Shear forces induced by the relative impact of high-speed gas on liquid create instabilities on the bulk liquid surface, which results in droplets formation. In pressure atomization a liquid is forced through a small aperture under high applied pressure, the pressure energy is transformed into kinetic energy to overcome surface tension force and break up bulk liquid.

The principal goal during scale-up is to maintain product quality and yield. To do this is extremely important to keep response variables to the process unchanged across different

scales. Small-scale experiments can be used to identify commercial operating parameters and they can be confirmed by offline tools process modeling, computer simulations, thermodynamic models, and scale correlations. In this way, waste of time and materials is avoided, especially very expensive APIs required to develop a robust commercial spray-drying process (Poozesh & Bilgili, 2019) (<https://www.europeanpharmaceuticalreview.com/article/27768/spray-drying-pharmaceutical-industry/>; <https://drug-dev.com/spray-dried-dispersions-efficient-scale-up-strategy-for-spray-dried-amorphous-dispersions/>).

1.7 Aim of the thesis

In the last decades, the researchers have widely examined the complexity of the repair tissue process "wound healing", mediated by interdependent cellular events aimed to restore tissue integrity. In many diseases such as diabetes, tumors, and vasculopathy the wounds are not able to close turning into chronic wounds that request more than six weeks to heal, necessitating daily medical care, sometimes difficult to manage and expensive to sustain. In recent years, several dressings have been commercialized for the treatment of chronic wounds, such as hydrocolloids and hydrogels, foams and films, among others. The ideal wound dressing should have proper adhesion to the wound site, good absorbance of the exudate, easy application, and atraumatic removal and should be able to favor the release of loaded APIs directly to the wound. The main technological challenge in the development of wound dressing is to balance the ability to absorb high amounts of exudate present in chronic wounds and the ability to maintain a proper moisturized environment.

My project has proponed the production of micro-nanoparticle carriers in the form of dry powders, able to be converted quickly in hydrogels when in contact with the biological fluids of a wound, thus tailoring the release of APIs at the site of action and overcoming some problems related to conventional devices as traumatic removal, poor conformability, and high

costs. These formulations have been developed using a mixture of biocompatible, biodegradable, multifunctional, and economic polymers. Specifically, alginate with a high content of mannuronic residues, amidated pectin with a low degree of methylation, and low molecular weight chitosan were chosen. Thanks to their mucoadhesive and gelling properties, these polymers can strongly promote the absorption of exudates and, gelling directly on the lesion and not in the periwound skin, the formulation is able to reduce pain during the removal. Moreover, alginate and chitosan are able to stimulate tissue repair processes and pectin to speed up *in situ* gel formation. The objective of my study was to verify the feasibility of the combination of these materials using mini spray drying, spray drying pilot for the production of a prototype able to fit pharmaceutical company requirements and, novel manufacturing technology nano spray drying. As a consequence another important objective was to optimize process parameters, in order to obtain high yields reducing the time process and encapsulating efficiently different APIs, improving their stability and their activity in the wound healing treatment.

In particular, the specific aims of this PhD program have been the development and characterization of:

- Alginate-pectin submicroparticles loaded with Annexin N-terminal residue Ac2-26 as wound healing promoter due to its ability to promote cell migration and tissue repair.
- Alginate-pectin-chitosan *in situ* gelling powders, evaluating the different atomization techniques, mini and nano spray drying, and the influence of different polymer and other excipients on powder properties.
- Alginate-pectin-chitosan *in situ* gelling powders loaded with doxycycline, chosen as an antimicrobial model to enhance the healing process, in an infected wound, by contrasting bacterial spreading.

- Alginate-pectin-chitosan *in situ* gelling powders loaded with two different molecular weights of sodium hyaluronate, high molecular weight, and low molecular weight, in order to compare their characteristics in a complex blend as a medical device.
- Nanocomposites combining alginate-pectin microparticles with nanoemulsions to vehicles lipophilic drug, during a research period of 4 months at the University of Lyon 1, France.

2. MATERIALS AND METHODS

2.1 Materials

2.1.1 Polymers

- Chitosan low molecular weight, 1% viscosity in acetic acid 20-80 mPa s, 75–85% deacetylated, (Sigma-Aldrich, Milan, Italy)
- Pectin Amid CF 025 D, amidated low methoxyl grade, degree of esterification 23-28%, degree of amidation 22-25%, molecular weight 120 kDa (Herbstreit&Fox Corporate group, Neuenbürg/Württ, Germany)
- Sodium alginate from brown algae, 1% viscosity 65 mPa s, medium molecular weight 180 kDa, mannuronic/guluronic ratio 70/30 (Carlo Erba reagents, Milan, Italy)
- Sodium hyaluronate low molecular weight (184 kDa) (Altergon, Avellino, Italy)
- Sodium hyaluronate, from *Streptococcus equi*, high molecular weight (1500-1800 kDa) (Sigma Aldrich, Milan, Italy)

2.1.2 Active pharmaceutical ingredients

- ANXA1 N-terminal peptide Ac2-26 with the following sequence: Ac-Ala-Met-Val-Ser-Glu-Phe-Leu-Lys-Gln-Ala-Trp-Phe-Ile-Glu-Asn-Glu-Glu-Gln-Glu-Tyr-Val-Gln-Thr-Val-Lys (Tocris Bioscience, Bristol, UK)
- Curcumin (CCM) Sigma-Aldrich (St Quentin-Fallavier, France)
- Doxycycline monohydrate (Carbosynth, Compton, UK)

2.1.3 Salts and excipients

- Ammonium carbonate (Sigma-Aldrich, Milan, Italy)
- Calcium chloride (Sigma Aldrich, Milan, Italy)
- Lactose (Sigma Aldrich, Milan, Italy)

- Mycological peptone (Oxoid Ltd, Basingstoke, Hants, United Kingdom)
- Phosphate buffered saline (PBS) tablets (pH 7.4) (VWR International, Fontenay-sous-Bois, France)
- Potassium dihydrogen phosphate (PBS) (VWR Chemicals, Fontenay sous Bois Île-de-France, France)
- Sodium bicarbonate (Sigma-Aldrich, Milan, Italy)
- Sodium chloride (Sigma Aldrich, Milan, Italy and VWR International, Fontenay-sous-Bois, France)
- Sodium dodecyl sulfate (Sigma Aldrich, Milan, Italy)
- Tween® 85 (Sigma-Aldrich, Milan, Italy)

2.1.4 Lipids

- Medium chain triglycerides, MCT (Miglyol®812) (CREMER OLEO GmbH & Co. KG Hamburg, Germany)
- Oleoyl polyoxyl-6 glycerides (Labrafil®M1944CS) (Gattefossé, Saint-Priest, France)
- Polyoxyethylene(40) stearate, (Myrj®52) (Sigma-Aldrich, St Quentin-Fallavier, France)

2.1.5 Solvents

- Acetic acid (Sigma-Aldrich, Milan Italy)
- Acetone (VWR International, Fontenay sous Bois Île-de-France, France)
- Acetonitrile for HPLC (VWR Chemicals, Fontenay sous Bois Île-de-France, France and Fisher Scientific, Illkirch, France)
- Acetonitrile LC-MS grade and HPLC (Sigma Aldrich, Milan, Italy)

- Dichloromethane (Merck KGaA, Darmstadt, Germany)
- Ethanol 96 and absolute (VWR International, Fontenay sous Bois Île-de-France, France)
- Formic acid HPLC grade (Fisher Scientific, Illkirch, France)
- Hydrochloric acid 37% w/w (ACS reagent, Sigma-Aldrich, Italy)
- Methanol, HPLC grade (Fisher Scientific, Illkirch, France)
- Milli-Q water (Millipore, Saint Quentin, Yvelines France)
- Orthophosphoric acid 99% (Carlo Erba Reactifs, Cornaredo, Italy)
- Sodium hydroxide (Sigma Aldrich, Milan, Italy)
- Ultrapure milli-Q water (Millipore, Milan, Italy)
- Water for HPLC (VWR Chemicals, Fontenay sous Bois Île-de-France, France)

2.1.6 Enzymes

- Hyaluronidase from bovine testes, Type IV-S (Sigma-Aldrich Milan, Italy)

2.1.7 Cell media and others

- 10,000 U/mL penicillin and 10 mg/mL streptomycin (Euroclone, Milan, Italy)
- 3-(4,5-dimethylthiazol-2-yl)-2,5-diphenyltetrazolium (MTT) (VWR Chemicals, Fontenay sous Bois Île-de-France, France)
- Brij-35 (Sigma Aldrich, Milan, Italy)
- Coomassie Brilliant Blue G-250 (Sigma Aldrich, Milan, Italy)
- Dulbecco's modified Eagle's medium (DMEM) (Sigma Aldrich, Milan, Italy)
- EpiLife[®] Medium (Gibco, Thermo Fischer Scientific)
- Fetal bovine serum (FBS) (Sigma Aldrich, Milan, Italy)
- Gelatin (Sigma Aldrich, Milan, Italy)

- Human Keratinocyte Growth Supplement (HKGS) (Gibco, Thermo Fischer Scientific)
- Mitomycin C (SigmaAldrich, Missouri, USA)
- NADPH (Sigma Aldrich, Milan, Italy)
- Polyacrylamide (Sigma Aldrich, Milan, Italy)
- Triton® X-100 (Sigma Aldrich, Milan, Italy)
- Trizma® Hydrochloride (Sigma Aldrich, Milan, Italy)

2.1.8 Bacterial media

- Muller Hinton Broth (Biolife Italiana S.r.l, Milan, Italy)
- Muller Hinton Agar (Biolife Italiana S.r.l, Milan, Italy)

2.2 Encapsulation technology: nano spray drying

Nano spray dryer Buchi B-90 HD (Buchi Laboratoriums-Tecnik, Flawil, Switzerland) is constituted by (Figure 15):

- a cold gas entrance in co-current, on the top;
- a piezoelectric actuator that allows feed atomization;
- a drying glass chamber, where feed droplets become dry;
- a collecting electrode for particle collection on the bottom of the system;
- a grounded electrode.

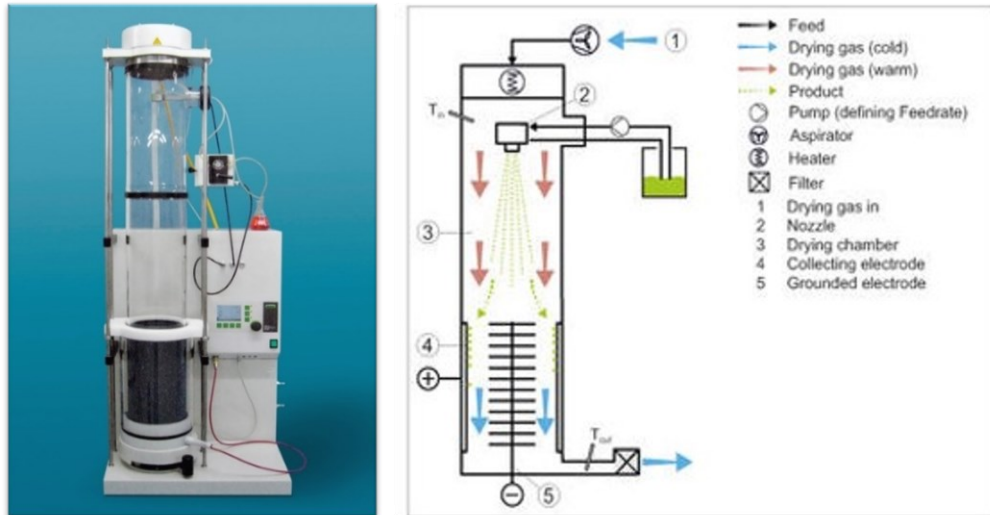


Figure 15. Nano spray dryer Buchi B-90 with a schematic representation of its components.

Feed solutions were processed with optimized operational conditions set as follows: inlet temperature 70 °C, outlet temperature 37-39 °C, feed rate 0.5 mL/min, nozzle mesh 5.5 µm, frequency 110 kHz, Pressure 40 hPa. The powders obtained, at the end of the process, were collected in closed vials to avoid moisture sorption and analysed in terms of yield calculated as the ratio between the amount of product obtained and the total amount of the material processed.

2.3 Encapsulation technology: mini spray drying

Mini Spray Dryer Buchi B-290 (Buchi Laboratoriums-Tecnik, Flawil, Switzerland) includes (Figure 16):

- a peristaltic pump for the feed transport to the drying chamber and a spray gas connection to the atomizator;
- a concentric nozzle for the pneumatic atomization;
- a cold drying gas entrance in co-current;
- a drying chamber where feed droplets are transformed into dried particles;

- two collectors, one at the bottom of the drying chamber for liquid droplets, one at the bottom of cyclone for a dried product;
- a cyclone for the powder collection;
- a filter at the end to purify the air from particulate before the reestablishment.

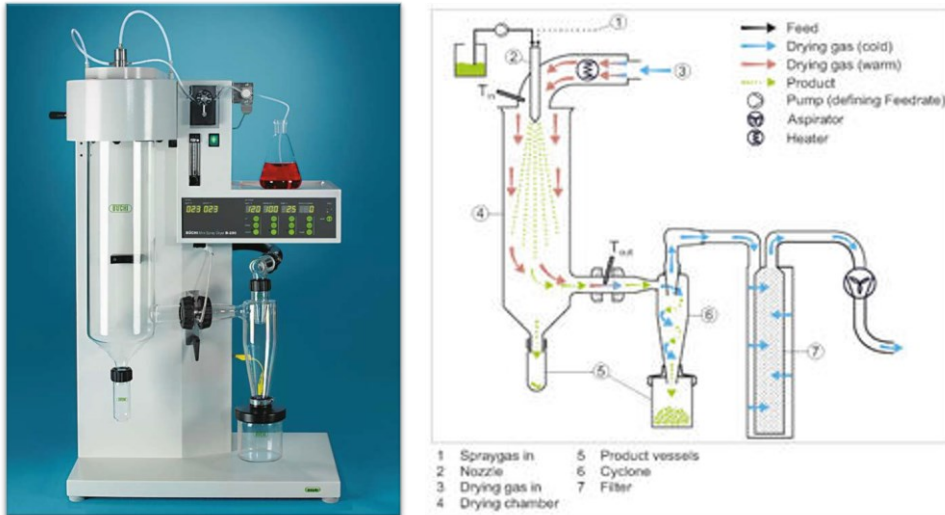


Figure 16. Mini spray dryer Buchi B-290 with a schematic representation of its components.

All feed solutions were processed with the optimized parameters reported in the table below:

Table 1. Parameter of the mini spray drying.

Inlet Temperature (°C)	Outlet Temperature (°C)	Aspirator (%)	Air pressure (atm)	Drying air flow (L/h)	Feed rate (mL/min)	Nozzle diameter (mm)
120 or 130	71-77	100	6	560-580	5	0.5-0.7

The spray-dried powders were recovered and kept in closed vials to avoid moisture sorption. The process yield was calculated as the ratio between the amount of powders obtained and the total amount of the material processed.

2.4 Preparation of feed solutions for spray drying

2.4.1 Alginate-pectin: feed solution

The alginate-pectin solution was prepared dissolving before alginate and, after complete dissolution of it, the pectin in milli-Q water under vigorous stirring for 1h (500 rpm). The total concentration of polymers was set at 0.15, 0.25, 0.5 and 1.00% (w/v), while different alginate-pectin ratio (1:1, 1:3, 3:1) were evaluated.

2.4.1.1 Alginate-pectin loaded with Ac2-26: feed solution

Peptide stock solution (0.125 mg/mL) was prepared dissolving Ac2-26 in a filtrated aqueous solution with 20% (v/v) of acetonitrile and 0.25% (v/v) ammonium hydroxide. Ac2-26 (diluted in milli-Q water) was added employing a Gilson pipet (Pipetman Classic, Gilson, Inc., Middleton, WI, USA), under gentle magnetic stirring, to the polymers solution alginate-pectin to obtain a final peptide/polymer blend ratio ranging between 0.01 and 0.02 (w/w).

2.4.1.2 Alginate-pectin loaded with doxycycline: feed solution

Doxycycline was added to the AP solution under gentle stirring (250 rpm) comparing two different concentrations (2% and 1% w/w).

2.4.2 Alginate-pectin-chitosan: feed solution

Feed solutions to obtain micro or nanoparticles through mini spray drying or nano spray drying were prepared as follows:

- chitosan was dissolved in an acid aqueous solution (1% v/v CH₃COOH), so that the acidity of the solution (pH=3.22) favours the dissolution of chitosan, through protonation of the amine residues at room temperature, under gentle stirrer (250 rpm) overnight;

- pectin was dispersed in an aqueous solution after solubilization of alginate at room temperature, under vigorous stirrer (500 rpm for 1 h) obtaining AP solution.

So prepared, the two solutions were mixed through the use of Ultra-Turrax® T25 (IKAWorks GmbH & Co. Staufen, Germany) thus obtaining the final solution (APC solution) to be submitted to the spray drying process. Total concentration of polymers was set at 0.15% (w/v), while different APC ratio (1:1:1, 1:1:3, 1:1:7) were evaluated.

2.4.2.1 Alginate-pectin-chitosan with the co-solvents: feed solution

To prepare APC feed solution with different percentages of co-solvents, various mixtures of water/ethanol, water/isopropanol, or /ethanol/acetone, in a 1:1 ratio were prepared. Subsequently, each of them and AP solution were added to chitosan dissolved in an acid aqueous solution and homogenized thanks to Ultra-Turrax.

2.4.2.2 Alginate-pectin-chitosan with salts as excipients: feed solution

The adding of excipients, sodium bicarbonate or ammonium carbonate in unlike concentration, was happened directly on APC solution under a gentle stirrer.

2.4.2.3 Alginate-pectin-chitosan powders loaded doxycycline: feed solution

Doxycycline was added to the APC solution under gentle stirring (250 rpm) comparing two different concentrations (2% and 1% w/w).

2.4.2.4 Alginate-pectin-chitosan powders with sodium hyaluronate: feed solution

Feed solutions were obtained by adding the sodium hyaluronate to an aqueous solution of APC under gentle stirring (250 rpm). Three different concentrations of two different molecular weights of sodium hyaluronate were investigated: 0.5, 1.00, and 2.00% (w/w).

2.5 Preparation of nanocomposites

For the production of nanocomposites composed of alginate-pectin with curcumin loaded nanoemulsions (AP-NE), mini spray drying was used.

2.5.1 Alginate-pectin loaded with nanoemulsions (AP-NE)

The alginate-pectin solution was prepared dissolving both polymers in milli-Q water under vigorous stirring for 1h (500 rpm). The total concentration of polymers was set at 1% (w/v) and an alginate-pectin mass ratio at 1:1 was used. After the complete dissolution of the polymers, the nanoemulsions (NEs) were added, under a slight stirrer (250 rpm) for 15 minutes before the spray drying process (Mini Spray dryer Büchi B 290, Büchi, Rungis, France). The applied process parameters were: aspirator 100%, drying airflow 560–580 L/h, air pressure 6 atmospheres, feed rate 5 mL/min, 120 °C inlet temperature, 65-68 °C outlet temperature, and a nozzle diameter of 0.7 mm.

The spray-dried powders were recovered and kept in closed vials to avoid moisture sorption. The process yield was calculated as the ratio between the amount of product obtained and the total amount of the material processed.

2.5.2 Curcumin loaded nanoemulsions (NE)

NEs were prepared by emulsion phase inversion technique coupled with high stirring energy input (Figure 17). Briefly, NEs were composed of an MCT oil core stabilized by a surfactant shell, made of a mixture of hydrophilic and hydrophobic surfactants, namely polyoxyethylene (40) stearate (Myrj 52) and oleoyl polyoxyl-6 glycerides (Labrafil M1944CS), respectively. To prepare the oil phase, MCT and surfactants were mixed and magnetically stirred (750 rpm) using a thermostated bath at 80 °C. The aqueous phase (PBS 5 mM,), heated up to 80 °C as well, was added into the organic melt phase. Stirring was then performed by two cycles of 10 min using a rotor-stator disperser (T25 digital Ultra-Turrax® equipped with an S25N10G shaft,

IKA®-Werke GmbH & Co. KG, Staufen, Germany) rotating at 11000 rpm at 80 °C. The resulting colloidal system was cooled to room temperature under magnetic stirring for 30 min. Curcumin (CCM) was solubilized in the oil phase and magnetically stirred (750 rpm) for 1 h at 80 °C to obtain a homogeneous mixture. during NEs preparation for its encapsulation. The final concentration of NEs in colloidal suspension was 142.89 mg/mL

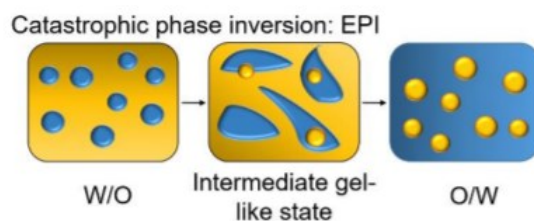


Figure 17. Method of nanoemulsion formulation: emulsion phase inversion.

2.6 Physico-chemical characterization of nanocomposites

The size distribution and surface potential of the NE droplets were determined using the Malvern Zetasizer® Nano ZS instrument (Malvern Instruments S.A., Worcestershire, UK). Particle size and polydispersity index (PDI) were determined by Dynamic light scattering (DLS) diluting all samples with milli-Q water to ensure the correct calculation of size distribution. The PDI indicates the size distribution. Analyses were carried out at 25 °C with an angle of detection of 173°. The ζ -potential was calculated from the mean electrophoretic mobility measured for samples diluted in milli-Q water. Measurements were performed in triplicate.

The stability of NEs in a colloidal suspension was followed during 28 days upon storage at 20 °C. At scheduled time points, particle size, PDI, and ζ -potential were measured.

2.7 Morphological analysis

The morphology of all powders was investigated by scanning electron microscopy (SEM), using a Carl Zeiss EVO MA 10 microscope with a secondary electron detector (Carl Zeiss SMT Ltd., Cambridge, UK) and with 20 KeV accelerating voltage. Before microscopy, the powders were distributed on a carbon stub (Agar Scientific, Stansted, UK) and were coated with a thick gold layer (18 ± 0.2 nm) of Au–Pd (200–400 Å) in an inert argon atmosphere and a high vacuum (0.05 mbar) (LEICA EMSCD005 metallizator). To verify the uniformity of the particles, no less than 20 SEM images were taken.

The morphology of the nanocomposites was analysed by scanning electron microscopy (SEM) at the “Centre Technologique des Microstructures” (CT μ) facility of the University of Lyon. SEM images were obtained with an FEI Quanta 250 FEG microscope. The powder was deposited on a flat steel holder. The sample was coated under vacuum by cathodic sputtering with copper (10nm layer) and observed by SEM under an accelerating voltage of 10 kV.

Transmission electron microscopy (TEM) was executed with a Philips CM120 microscope at the Centre Technologique des Microstructures (CT μ) of the University Lyon 1 (Villeurbanne, France). Diluted NE (10 μ L) was deposited on a microscope grid (copper support coated with carbon) and slowly dried in the open air. The dry samples were observed by TEM under 120 kV acceleration voltage.

2.8 Dynamic light scattering

Dynamic light scattering N5 (Beckman Spray Dryer, Miami, FL) was used to analyse the particle size distribution and mean diameter of powders produced by the nano spray dryer. Each formulation was diluted in dichloromethane (DCM) and sonicated three times for 10 min, with and without the presence of a surfactant 1% (v/v) in DCM. The effectiveness of the particle

dispersion was verified by performing the measurements after different sonication times ranging between 5 and 30 min.

Results were expressed as d_{50} and span defined below:

$$Span = \frac{d_{90}-d_{10}}{d_{50}} \quad (1)$$

where d_{90} , d_{50} , and d_{10} indicate the volume diameters at the 90th, 50th, and 10th percentiles, respectively. In all time intervals, good reproducibility of results was obtained.

2.9 Static light scattering

Static light scattering Coulter LS 13320 (Beckman Coulter, Inc., Fullerton, CA, USA), which allows analysis of particles in the range of 0.017 μm to 2000 μm , was used to analyse the particle size distribution and mean diameter of powders produced by spray drying.

Each formulation was diluted in DCM and sonicated three times for 10 min, with and without the presence of a tween 1% (v/v) in DCM. After sonication, some drops of each one were placed in DCM under constant stirring, using the micro liquid module, to obtain an obscuration between 8 and 12%. Results, calculated by instrument software using the Fraunhofer model, were expressed as mean diameter d_{10} , d_{50} , d_{90} .

2.10 Fluid uptake ability

Powders fluid uptake studies were conducted to evaluate the behavior of the powders when in contact with simulated wound fluid (SWF) consisting of 50% FBS and 50% of diluent composed by 0.1% (w/v) peptone, a peptic digest of animal tissue, and 0.9% (w/v) sodium chloride (Bowler et al., 2012; Cerciello et al., 2017). For fluid uptake ability studies, conducted on dry powders Franz-type diffusion cell was used in an open configuration, without the donor chamber, with a total volume of 5 mL and a permeation area of 0.6 cm^2 (Figure 18).

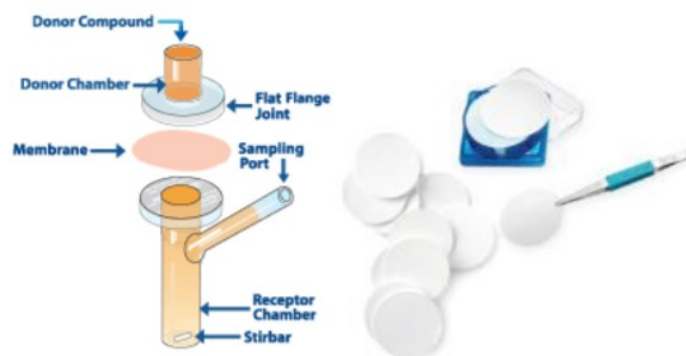


Figure 18. Franz-type diffusion cell and Merck Millipore HVLP membranes.

About 8 mg of dried powder, weighed using a microbalance (MTS Mettler Toledo, USA), was spread over a previously weighed HVLP nitrocellulose membrane (0.45 μm , Merck-Millipore, Darmstadt, Germany) or PES membrane disc filter (Polyethersulfone, 0.45 μm , 25 mm, Pall Corporation, USA). The membrane was in contact with a Franz cell (Hanson Research, USA), filled with SWF, thermostated at 37 $^{\circ}\text{C}$, with 200 rpm of stirring. At regular time intervals, the membrane with the sample was weighted, to test the quantity of fluid absorbed by the dry formulation, and the Franz cell was filled to maintain constant fluid during the entire experiment. All experiments were performed at least in triplicate.

Fluid uptake was calculated as the ratio between the weight of the gel and the weight of the dried powder producing the gel, using the following equation (Yoon et al., 2016):

$$\text{Fluid uptake (100\%)} = \frac{W_w}{W_d} \times 100 \quad (2)$$

where W_w is the weight of the wet formulation, and W_d is the weight of the dry formulation.

2.11 Water evaporation from hydrogel

Water vapor transmission rate (WVTR) was performed as described by ASTM standard (ASTM Standard, 2010). 25 mm hydrogel disc of each formulation was mounted on the top of

a plastic tube filled with 20 mL of distilled water. The edge of the disc was covered with teflon tape to avoid boundary loss. The assembly was maintained inside an incubator at 37 ± 0.5 °C at a relative humidity of $32 \pm 0.2\%$ (Figure 19). At regular time intervals, weight loss was noted and plotted against time.

WVTR was calculated as the ratio between the slope of the plot and the area of the disc, by the following formula:

$$WVTR = \frac{Slope}{A} \quad (3)$$

where A is the test area of the sample in m^2 .

Water evaporation rate from *in situ* formed hydrogel was acquired as loss of weight over time by using the same procedure described above and noting the weight of the hydrogel at regular time intervals. Weight loss percentage was estimated by the following equation:

$$Weight (\%) = \frac{W_t}{W_0} \times 100 \quad (4)$$

where W_t is the weight at the specific time and W_0 is the initial weight.

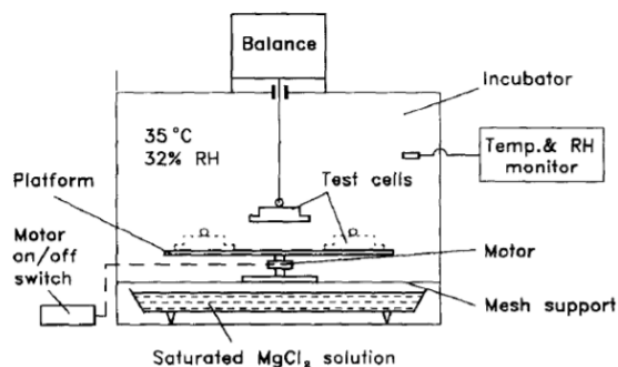


Figure 19. System for water vapor transmission rate.

2.12 Fourier Transform Infrared Spectroscopy (FT-IR) analysis

Samples, put on the crystal plate, were subjected to IR characterization in the range of 4000-600 cm^{-1} using Spotlight 400N (FT-NIR Imaging System, Perkin Elmer Inc, USA) equipped

Spectrum Software version 10.5.2 with ZnSe crystal plate. The spectra were obtained at room temperature, resolution of 1.0 cm^{-1} using 128 scans.

2.13 Residual water content

Water content was studied by Thermo Gravimetric Analysis (TGA, TG50 - Mettler Toledo, Columbus, OH, USA) by using about 15 mg of each powder. Results were expressed as the mean of the obtained results at least in triplicate for each powder.

For the powders produced at the University of Lyon thermogravimetric analysis was performed on NETZSCH TG 209F1 (NETZSCH-Gerätebau, Germany) and NETZSCH Proteus 6.1 software was used to evaluate the data. The measurements were completed on samples of about 5 mg, placed in ceramic crucibles, and heated from 20 to 1000 °C at a heating rate of 10 °C/min, under a nitrogen atmosphere with a nominal gas flow rate of 30 mL/min.

In addition, the water content of the particles was quantified by the Karl-Fischer titration using an 889 KF Coulometer (Metrohm Ltd., Herisau, Switzerland) equipped with an oven (860 KF Thermoprep). The air flow rate was 100 mL/min and the oven temperature was set to 120 °C. The extraction time was set at 500 s and the drift time was 10 µg/min. A solution of hydranal (HYDRANAL™ - Coulomat AG) was used as the titrant. Each powder was tested in triplicate.

2.14 Differential scanning calorimetry (DSC)

Differential scanning calorimetry (Mettler Toledo DSC 822e module controlled by Mettler Star E software, Columbus, Ohio) was used to determine the thermal characteristics of raw materials and microparticles. 5-6 mg of the powder sample was weighed with a microbalance (MTS Mettler Toledo, OH, USA) before being placed in an aluminum pan (40 µL) perforated. The sample was heated from 25 °C to 400 °C at a rate of 25 °C/min and the characteristic peaks were recorded. All DSC analysis was performed in a nitrogen atmosphere of 150 mL/min. Data

were collected with Mettler Toledo STARe software and analysed using Thermal Analysis Instruments to characterize thermal events and degradation profiles of materials.

For the powders produced at the University of Lyon the structural characterizations of powders were performed by DSC using a Q200® instrument from TA Instruments (New Castle, DE, USA). A nitrogen purge of 50 mL·min⁻¹ was used for all measurements. The temperature range was -80 °C to +180 °C. Samples (about 7 mg) were accurately weighed and sealed in 40 µL aluminum pans with a perforated aluminum lid.

2.15 Rheological measurements

The rheological properties of *in situ* gelling powders were evaluated using Anton Paar MCR-102 Rheometer fitted with plate-plate geometry (PP25 with a diameter of 24,985 mm). Each powder (200 mg) was placed directly on the plate, previously heated, and treated with PBS 100 mM pH 7.4 to form a gel in around 10 minutes. The distance between the plates was determined according to the stickiness of the gels formed. Amplitude sweep tests were chosen setting strain amplitude in the range 0,01-200% and angular frequency at $\omega = 10$ rad/s. All measurements were performed at 37 °C.

The software used to do the studies and to analyse the data obtained was RheoCompass™ Software (Anton Paar, Austria).

2.16 Drug content and encapsulation efficiency

2.16.1 Ac2-26 content and encapsulation efficiency

The effective amount of Ac2-26 in the submicropowders was evaluated by Liquid Chromatography/Mass Spectrometry (LC/MS), an analytical chemistry technique that combines the physical separation capabilities of liquid chromatography (LC) with the mass analysis capabilities of mass spectrometry (MS). After 6 h of incubation under vigorous stirring,

1 mL of each sample was pre-purified on a Chromabond HR-X SPE cartridge (Macherey-Nagel, Düren, Germany) using water/acetonitrile (30:70) as elution solution. LC/MS analyses were performed on an LTQ XL instrument (Thermo Fisher Scientific, MA, USA) provided with an ESI ion source and a hybrid quadrupole/linear trap analyser and coupled with an Accela 600 HPLC system. Chromatography was performed on an Aeris C18 (2.0 × 150- millimeters. 3µm) reversed-phase column, using mobile phases A (0.1% formic acid in water, v/v) and B (0.1% formic acid in acetonitrile, v/v). Linear gradient increase from 25 to 70% B in 30 min was resulted optimal for this analysis, while the flow rate was set at 200 µL/min. Mass spectra were acquired in positive ion mode over the m/z range from 700 to 1600. The specific ions at m/z 773.37 [M +4H]⁴⁺, 1030.82 [M+3H]³⁺, and 1545.73 [M+2H]²⁺ were selected to quantify Ac2-26.

Ac2-26 content was calculated as the ratio between the amount of active ingredient determined experimentally by LC/MS analysis and the weight of the total powder used for the analysis.

$$Ac2 - 26 \text{ content } (\%) = \frac{Ac2-26 \text{ calculated weight}}{\text{Total powder weight}} \times 100 \quad (5)$$

The Encapsulation Efficiency (E.E.) was obtained as the ratio between the experimental weight of the peptide and the amount of active ingredient theoretically present in the feed solutions subjected to the spray drying process.

$$E. E. (\%) = \frac{Ac2-26 \text{ calculated amount}}{Ac2-26 \text{ theoretical amount}} \times 100 \quad (6)$$

Each analysis was effectuated in triplicate and the results were expressed as mean ± standard deviation.

In order to evaluate the stability of the powder, the formulations were stored at 40 °C and 75% relative humidity for 1 month as described by the ICH Q1AR2 C Guideline “Stability Testing of New Drug Substances and Products”. At defined time points, samples were recovered and Ac2-26 content was determined with LC-MS.

2.16.2 Doxycycline content and encapsulation efficiency

Doxycycline content was calculated as the ratio between experimental drug and total powder weight while E.E. was determined as the ratio of the experimental drug to theoretical drug content in the formulation. About 5 mg of the different formulations were dissolved in 5 mL PBS 0.1 M, pH 7.4 to obtain a uniform dispersion. The dispersion was sonicated for ten minutes to allow the permeation of the drug from the formulation and centrifuged (6000 rpm for 10 min) to remove polymers. The supernatant obtained was filtered (45 µm filter Chromafil RC-45/25, Macherey-Nagel, Germany) and analysed by HPLC (Sunarić, Denić, Bojanić, & Bojanić, 2013) to evaluate the amount of doxycycline. The Agilent 1100 Series instrument (Agilent 1100 Series HPLC, Agilent Technologies, USA) with a UV detector was used for the HPLC analysis. The separation was performed on a reversed-phase column (Kinetex XB-C18, 100A, 75x2.10 mm, 2.6 µm, Phenomenex, USA), using as mobile phase a mixture of acetonitrile (A) and water a pH 2.5 with orthophosphoric acid (B). After different proves the volume ratio of solvent A against solvent B was set at 22:78, the flow rate at 0.5 mL/min, and the injection volume at 20 µL. Based on the absorption spectrum of the molecule, performed by UV-vis spectrophotometer, two peaks of interest (270 and 349 nm) were detected. However, the wavelength was set at 349 nm because being further away from the absorption of water allowed us to obtain a greater reproducibility in the analysis. The results were compared with a calibration curve in a range of concentrations between 0.5 and 34.0 µg/mL.

2.16.3 Hyaluronate content and encapsulation efficiency

Sodium hyaluronate (H) content from APCH formulations was quantized via HPLC (Agilent 1260 Infinity) with DAD detector (Agilent Technologies, USA) as the ratio between actual H weight calculated and the total powder weight while E.E. was calculated as the ratio of actual to theoretical H content (Aquino et al., 2013).

The stock solutions were diluted in the mobile phase to prepare various concentrations of sodium hyaluronate and the calibration curve was performed in a range of 0.6 - 0.08 mg/mL (regression coefficient value $R^2=0.9997$) and 0.6 - 0.03 mg/mL, ($R^2=0.9999$), for high molecular weight H and low molecular weight H, respectively. About 3 mg of the different formulations was solubilized in 10 mL of potassium dihydrogen phosphate buffer (0.05 M, pH 7.00) to obtain a uniform dispersion. This dispersion was sonicated for 10 minutes, centrifuged (3000 rpm for 10 min) and the supernatant obtained was filtered (45 μ m filter Chromafil RC-45/25, Macherey-Nagel, Germany) and analysed. The separation was performed on size exclusion column (PolySep-GFC-P 6000, 300 x 7.8 mm, Phenomenex, USA) with guard column (PolySep-GFC-P 35 x 7.8 mm) using as isocratic mobile phase a potassium dihydrogen phosphate buffer (0.05 M) with pH adjusted to 7.0 using potassium hydroxide (10% w/v), at room temperature (Ruckmani, Shaikh, Khalil, Muneera, & Thusleem, 2013). The flow-rate of the mobile phase was 1 mL/min, the column temperature was set at 25 °C and the chromatograms were acquired at a wavelength of 205 nm. The injection volume was 20 μ L and the H peak/retention time was evident at 8 min.

2.16.4 Curcumin content and encapsulation efficiency

The amount of CCM loaded NE was quantified by UHPLC (Ultra High Performance Liquid Chromatography) equipped with a UV-vis detector using the method reported in the literature (Y. Liu et al., 2018; Lollo et al., 2018). 1 mg of CCM was dissolved in 1 mL of methanol/acetonitrile (50:50) and the sample was vortexed for 5 min. The dilutions were filtered using a Nylon filter 0.22 μ m (Whatman GmbH, Dassel, Germany) before injection in the UHPLC system. The UHPLC apparatus consisted of UHPLC Waters Acquity Arc Quaternary Solvent Manager-R, Waters Acquity Arc Sample Manager FTN-R, equipped with Waters Acquity UHPLC 2998 PDA Detector. CCM was detected using an RPC18 column (Kinetex 5

μm C18 100 Å, 150 × 4.6 mm, Phenomenex, Torrance, CA, USA), set at 30 °C, using acetonitrile and deionized water with 0.1% formic acid (50:50) as mobile phases at a flow rate of 1 mL/min. The injection volume was 10 μL , the detection wavelength 423 nm and the total run time was 8 min. The chromatogram of CCM exhibited a characteristic peak at a retention time of 4.7 min. The UHPLC calibration curve was linear ($R^2 = 0.999$) in the concentration range of 0.04-40 $\mu\text{g/mL}$. The method was validated according to ICH Q2(R1) guidelines. Detection and quantification limits (LOD and LOQ) were 1.27 $\mu\text{g/mL}$ and 4,25 $\mu\text{g/mL}$, respectively.

AP-NE powders were solubilized in methanol/acetonitrile (50:50) and maintained under stirrer for two hours to allow the dissolution of curcumin from formulations. NE content was calculated by analyzing CCM encapsulated in NE. CCM content was calculated as the ratio between actual CCM weight calculated and the total powder weight, while the E.E. as the ratio of CCM detected, to the amount of CCM initially loaded in the NE.

2.17 Release studies

2.17.1 Ac2-26 release

The release of Ac2-26 was evaluated using a slide analyser mini dialysis units, 10 K molecular weight cut off (Thermo Fisher Scientific Inc., Waltham, MA, USA) with an exposed surface area of 0.33 cm^2 . 20 mg powder with 250 μL of SWF was placed in the dialysis cup to promote the formation of the gel. Experiments were conducted in a 5 mL receptor compartment filled with 3 ml of SWF thermostated at 37°C and magnetically stirred at 200 rpm by a teflon-coated stirring bar.

At specific time points, 100 μL aliquots of the receptor solution were taken and analysed by LC-MS to quantify the amount of AC2-26 permeated through the dialysis membrane, as previously described (subparagraph 2.16.1).

2.17.2 Doxycycline release

The release of doxycycline encapsulated in microparticles was evaluated using Franz-type vertical diffusion cells (15 mm, 7 mL, Hanson research corporation, CA, USA), which allows keeping the powders in a humid environment like the wound bed. The Franz cell is composed of donor and receptor compartments (Figure 20). About 20 mg of the formulation was placed on the membrane (PES, 0.45 μm , 25 mm, Pall Corporation, USA) that was inserted between the donor and the receptor compartment. The receptor chamber was filled with PBS 0.1 M, pH 7.4 and thermostated at 37 °C thanks to the water jacket and magnetically stirred at 250 rpm. At the set time intervals, the aliquots (250 μL) were withdrawn from the receptor compartment and replaced with the equal volume of the fresh buffer solution to maintain the total volume constant into the chamber. The drug released was identified by HPLC as previously described (subparagraph 2.16.2) performing the experiments in triplicate.

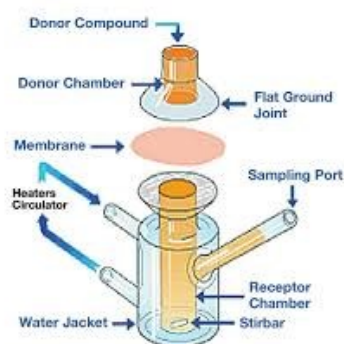


Figure 20. Structure of Franz cell.

2.17.3 Nanoemulsions release

The *in vitro* release of NEs via curcumin from the powders was evaluated in SWF by cumulative study, in non-sink conditions. Therefore, the solubility of CCM in SWF has been assessed. 2 mg of it was dissolved in 2 mL of SWF under stirred (750 rpm) at room temperature and left overnight to reach equilibrium. Then, the sample was centrifuged two times at 8000

RCF for 10 min and the supernatant was collected and filtrated with a 0.22 µm Nylon syringe filter (Whatman GmbH, Dassel, Germany). 100 µL of supernatant was mixed with 500 µL of methanol/acetonitrile (50:50) and the sample was injected into the UHPLC system for curcumin detection as previously reported (subparagraph 2.16.4).

To study NE release, 2.5 mL of SWF was added on top of the AP-11-NE0.1 and AP-11-NE0.2 placed in a glass vial of 3 mL. 60 mg of each sample were used. At predetermined time points, 200 µL of SWF was removed and replaced with fresh fluid. Aliquots were diluted in 600 µL of methanol/acetonitrile (50:50) vortexed for 5 min and centrifugated for two minutes at 1200 RCF, to remove the polymers. In the supernatants, 10 µg/ml of curcumin as an internal standard was added to allow correct detection of the drug. The amount NEs was quantified by UHPLC-UV detecting the curcumin, present only in the NEs. The analyses were performed in triplicate.

2.18 Enzymatic degradation

The biodegradability of alginate-pectin-chitosan with sodium hyaluronate was evaluated by incubating powders with sodium hyaluronidase. The dry samples, accurately weighted (about 25 mg), were placed in a 1.5 mL tube with 1 mL of medium with 200 U/mL of hyaluronidase and maintained at 37 °C under stirring (100 rpm). At regular time intervals (1, 3, 5, and 7 days), the samples were removed, washed, and centrifuged, then the precipitates were lyophilized at 0.100 bar for 28 h and weighed. The samples treated with only PBS were used as a negative control. Sodium hyaluronate was used as a positive control.

The degradation rate is given by:

$$\text{Degradation rate} = \frac{W_i - W_t}{W_i} \times 100 \quad (7)$$

Where W_i is the initial weight of the dressing and W_t is the weight of the dressing after degradation at a specific time interval. The measurements were performed three times ($n = 3$).

2.19 Antimicrobial tests

Each bacterial strain has been manipulated using a Class II biological safety hood (Thermo Scientific HeraSafe KS with H14 HEPA filters).

2.19.1 Disc diffusion assay

Disc diffusion assay was carried out on Mueller-Hinton agar (MHA) according to Clinical and Laboratory Standard Institute (CLSI) guidelines, with suitable modifications (De Falco et al., 2017). *Staphylococcus aureus* (ATCC 6538) and *Pseudomonas aeruginosa* (ATCC 9027) which normally colonize wounds have been studied. The bacterial suspension (10^8 cells/mL) was spread on a sterile MHA agar plate. The bacterial inoculum was prepared by dipping the sterile cotton swabs in Mueller-Hinton broth (MHB) and incubated under stirring in an incubator at 37°C, overnight (New Brunswick Scientific Co. G24 Environmental Incubator Shaker). For the preparation of plates, the powder of MHA was dissolved in milli-Q water and autoclaved at 120 °C for 25 min. After sterilization of the broth, this is poured into empty Petri dishes and left at room temperature to allow the solidification of agar. The agar plates, so prepared, were spotted with powders mixing with a diluent (lactose in powder) to test different concentrations of doxycycline encapsulated in the formulations. Raw doxycycline was used as a positive control. After incubation at 35 °C for 24 h, the zone of inhibition was determined, by measuring the diameter of the clearing zone produced by each powder.

2.19.2 Time-killing assay

Time-killing studies were performed on *S. aureus* (A 170) incubating the bacteria, diluted 30-fold, in prewarmed MHB, at 35°C under constant shaking overnight. 2.5×10^8 cells/mL were used to inoculate sterile 96-well plates further treated with the different APC formulations corresponding to 0.50 mg/mL of doxycycline encapsulated. At specific time points (1, 2, 3, and

7 days), serial dilutions were plated on MHA incubated at 35°C to calculate the vital bacteria expressed as CFU/mL (colony forming unit per mL). Kill curves were plotted with time against the number of CFU found. Each antimicrobial assay was performed in triplicate on separate days.

2.20 In vitro cell studies

2.20.1 Cell viability and pro-inflammatory activity

2.20.1.1 Cell cultures

Human immortalized keratinocyte (HaCaT) cells, purchased from CLS Cell Lines Service GmbH (Germany), were used to perform the MTT (3-(4,5-dimethylthiazol-2-yl)-2,5-diphenyltetrazolium bromide) assays. Cell culture medium was Dulbecco's modified Eagle's medium (DMEM) supplemented with 10% (v/v) FBS and antibiotics (10,000 U/mL penicillin and 10 mg/mL streptomycin). Cells were cultured at 37 °C in a humidified atmosphere with 5% CO₂ and 95% air incubator and were serially passed at 70-80% confluence.

2.20.1.2 In vitro cytotoxicity: MTT test

In order to evaluate the possible cytotoxicity of alginate, pectin, chitosan, alginate-pectin, and alginate-pectin-chitosan blend in different polymer ratios, the viability of HaCaT cells was evaluated by the MTT colorimetric assay.

Cells were maintained overnight at 37 °C with 5% of CO₂. Then, the culture medium was removed, and cells were treated with an increasing concentration of powders (0.01–10 µg/mL) diluted in milli-Q water. The latter concentration is a function of the maximum amount of acetic acid allowed in vitro (0.1%), used to dissolve the chitosan, alone or in combination. Water was used as a positive control (100% viability), while 1% (w/v) Sodium dodecyl sulfate (SDS) was the negative control.

Cells were exposed to the formulations for 24 h at 37 °C. After the indicated treatment, samples were replaced with 100 µL of fresh medium added with 25 µL of MTT solution in each well. The plates were incubated for 3 h at 37 °C. The formazan purple crystals formed by the reaction of MTT with nicotinamide adenine dinucleotide fosfato (NAD(P)H) of metabolically active cells were dissolved in 100 µL of an aqueous solution containing 50% (v/v) N, N-dimethylformamide, and 20% (w/v) SDS, with an adjusted pH of 4.5. The optical density of each well was measured with a microplate reader (Titertek Multiskan MCC/340, LabSystem) at 550 nm. The analyses were performed no less than five times.

2.20.1.3 Pro-inflammatory activity

To evaluate the pro-inflammatory activity of powders, pro-inflammatory cytokines IL-6 and TNF α , and chemokine IL-8 (CXCL-8), were revealed in cell-free supernatants using commercial enzyme-linked immunosorbent assay kits (ELISAs). The ELISA test involves the use of two antibodies and a detection system to identify in immunoabsorbent plates the above cytokines after spectrophotometric reading (wavelength: 450 nm, corrected to 550nm). Based on the results obtained for cell viability, HaCaT cells were plated in multiwells and serially treated for 24 hours, with 0.1-0.5-1 µg/mL of the same components used in the MTT test.

2.20.1.4 Statistical analysis

Statistical analysis of the *in vitro* cytotoxicity and pro-inflammatory activity data was performed using GraphPad Prism version 7.04 for Windows (GraphPad Software, San Diego, California, USA). The statistic test was One Way ANOVA, followed by Bonferroni's multiple comparison post-test or Tukey's post-test.

2.20.2 Wound healing assay

2.20.2.1 Cell cultures

Human immortalized keratinocyte (HaCaT) cells, purchased from CLS Cell Lines Service GmbH (Germany), were used to perform the wound healing assay. Cell culture medium was Dulbecco's modified Eagle's medium (DMEM) supplemented with 10% (v/v) FBS and antibiotics (10,000 U/mL penicillin and 10 mg/mL streptomycin). Cells were cultured at 37 °C in a humidified atmosphere with 5% CO₂ and 95% air incubator and were serially passed at 70-80% confluence.

2.20.2.2 Experimental procedure

HaCaT cells were seeded in the presence of a hydrogel bed formed by alginate or pectin or alginate-pectin or Ac2-26 loaded alginate-pectin particles, in DMEM. Two experiments were conducted in parallel, using a 12-well plastic plate with at 5×10^5 and 10×10^5 cells, respectively, per well. The grown medium was used as a negative control. After 24 h incubation, cells reached 100% confluence and a wound was produced at the center of the monolayer by gently scraping the cells with a sterile plastic p10 pipette tip. All experimental points were further treated with 10 µg/mL of mitomycin C to guarantee the block of mitosis.

The wounded cells were then incubated at 37 °C in a humidified and equilibrated (5% v/v CO₂) incubation chamber of an Integrated Live Cell Workstation Leica AF-6000 LX. To record cell movements, a 10x phase contrast objective with a frequency of acquisition of 10 min, was used. The migration rate of individual cells was defined by measuring the wound closure from the initial time to the selected time-points (bar of distance tool, Leica ASF software). For each wound, ten different positions were recorded, and for each position, ten different cells were randomly selected to measure the migration distances.

2.20.2.3 Statistical analysis

The normality of data distribution of the wound healing assay was assessed. For the wound healing assay data analyses and statistical evaluations were performed by using Microsoft Excel™. Data were analysed using an unpaired, two-tailed t-test comparing two variables. All results are the mean ± standard deviation of at least 3 experiments performed in triplicate. Differences were considered significant if $p < 0.05$, $p < 0.01$ and $p < 0.001$.

2.20.3 SDS-PAGE gelatin zymography

2.20.3.1 Cell culture and treatment for zymography test

Human Epidermal Keratinocytes adult cell line (HEKa) were cultivated in EpiLife® Medium complemented with Human Keratinocyte Growth Supplement, without serum. In fact, as serum contains gelatinases, for gelatin zymography it is important to obtain serum-free conditioned media (Toth & Fridman, 2001). The cells were maintained at 95% humidity and 37 °C in an atmosphere of 5% CO₂. 1×10^5 cells/well were seeded in the upper compartment of trans-well filters (12 mm in diameter with 0.4 µm pore polycarbonate membrane insert, Corning) to pass at a confluence in 24h. Before treatment with the hydrogels, prepared to treat the powders with sterile PBS, cells were washed in PBS, and EpiLife® Medium without supplement was added in the upper compartment of all wells. The lower chambers of different wells were filled with the hydrogels with different doxycycline amounts: 0.5, 1, and 5 µg in a total volume of 1 mL. EpiLife® Medium without supplement was used as a negative control. The conditioned media in the upper compartments were taken after 24, 48, and 72h of treatment, centrifuged and stored at -80 °C until subsequent uses.

2.20.3.2 *Experimental procedure*

SDS-PAGE gelatin zymography was conducted to detect and quantitate gelatinases in the conditioned media from HEKa cultures after treatments with hydrogels according to a previously reported method (Toth & Fridman, 2001). A 10% polyacrylamide gel containing 0.1% gelatin was prepared and loaded with 20 μ L of each supernatant mixed to SDS-PAGE sample buffer without boiling or reducing to not degrade the protein. After electrophoresis, to remove SDS, the gel was washed in 0.25% (v/v) Triton X-100 for 30 minutes at room temperature with gentle stirring and then incubated in a digestion buffer (50 mM Tris-HCl [pH 7.4], 150 mM NaCl, 10 mM CaCl₂, and 0.01% Brij-35), at 37 °C overnight, to allow gelatin digestion. Gels were stained with Coomassie Brilliant Blue G-250 (0.5% v/v) composed by Coomassie blue in 30% (v/v) methanol and 10% (v/v) acetic acid and destained with an aqueous solution with 10% (v/v) acetic acid and 25% (v/v) methanol until clear bands indicating proteolytic activity, have become visible.

Image analysis was performed by Image Quant LAS 4000 (GE Healthcare, Waukesha, WI, USA) digital imaging system and quantified by Image Quant TL software.

3. RESULTS AND DISCUSSION

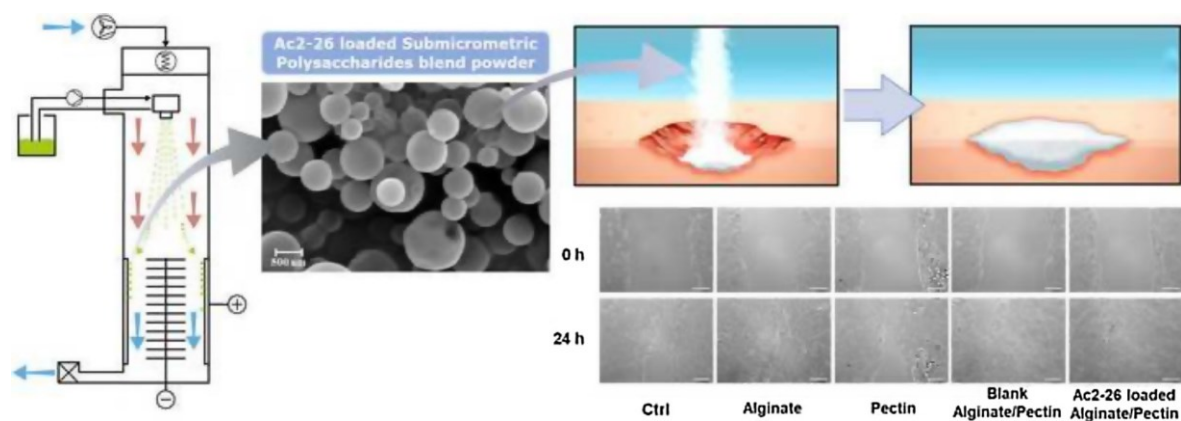
3.1 SECTION A

In situ gelling alginate-pectin submicropowders loaded with Ac2-26

Based on the article:

Pasquale Del Gaudio, **Chiara Amante**, Roberta Civale, Valentina Bizzarro, Antonello Petrella, Giacomo Pepe, Pietro Campiglia, Paola Russo, Rita P. Aquino. *In situ* gelling alginate-pectin blend particles loaded with Ac2-26: A new weapon to improve wound care armamentarium. *Carbohydrate Polymers*. Volume 227, 2020, 115305, ISSN 0144-8617.

<https://doi.org/10.1016/j.carbpol.2019.115305>



3.1.1 Scientific background

In the last years, the attention of researchers has focused on active ingredients such as growth factors and wound healing peptides (WHP) for their mechanisms of action able to promote one or more stages of the healing process (Mangoni, McDermott, & Zasloff, 2016). Ac2-26, the N-terminal derived peptide of Annexin A1 (ANXA1), containing the pharmacophoric portion of ANXA1, can be considered biomimetic of the protein itself and WHP (Figure 21).

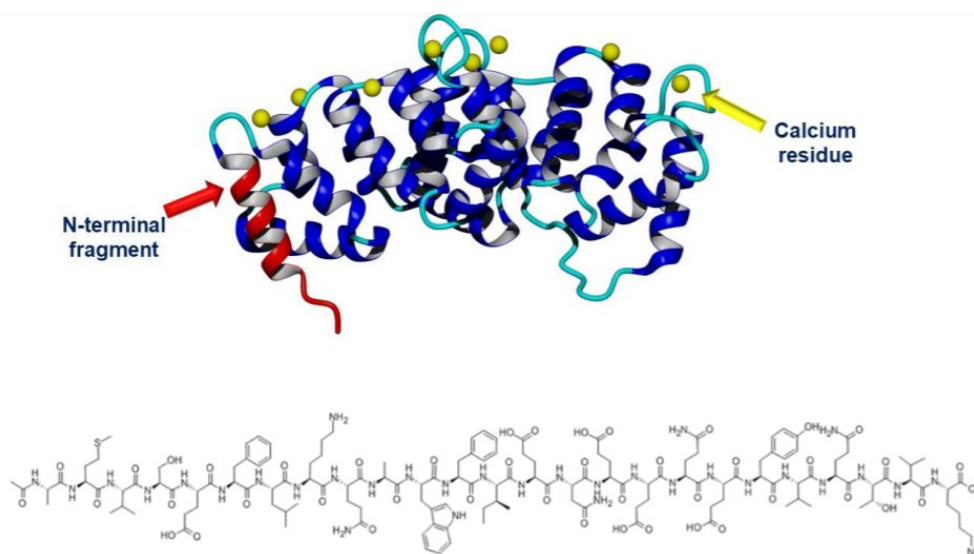


Figure 21. *ANXA1 3D image with N-terminal fragment (represented in red) and aminoacidic sequence of Ac-2-26.*

ANXA1, a 37 kDa protein, is the first characterized member of the 13 proteins identified in mammals (Hoehenwarter et al., 2008; Raynal & Pollard, 1994) that contains a central domain consisting of 4-8 repetitions of a highly conserved aminoacid sequence, varying in length and composition, and a small functional N-terminal domain. These kinds of proteins are so called for their binding (i.e., to annex) to cellular membranes in a Ca^{2+} -dependent manner (Mauro Perretti & D'Acquisto, 2009). Crystallography studies have revealed that part of the N-terminal domain is naturally folded into the annexin domain and the presence of calcium ions causes an

outward flip, making it available for interactions (Rosengarth & Luecke, 2003). The ANXA1 effects are dependent on phosphorylation and interaction with formyl peptide receptors (FPR), especially FPR2, a G-protein coupled receptor, which involves a broad range of molecular and cellular processes, including anti-inflammatory signaling, maintenance of cytoskeleton and extracellular matrix integrity, tissue growth, apoptosis and cellular differentiation (Gobbetti & Cooray, 2016; Leoni & Nusrat, 2016). The peptide Ac2-26, able to interact with both FPR1 and FPR2 (Cooray et al., 2013) exhibits functions similar to those of ANXA1 (Mauro Perretti & Dalli, 2009), as the activation of the skeletal muscle cells and cell surface translocation (Bizzarro, Belvedere, Dal Piaz, Parente, & Petrella, 2012). Furthermore, Ac2-26 promotes skin regeneration modulating inflammation and angiogenesis (Lacerda et al., 2018).

A recent study revealed that Ac2-26 could be applied in diabetic wounds by up-regulating the percentage of macrophages M2 (J. J. Huang et al., 2020) and stimulating the migration of fibroblasts. In diabetes, hyperglycemia can cause activation of pro-inflammatory M1 macrophage and inhibition of the pro-repair M2 phenotype, leading to severe inflammation and failure to wound healing (Hesketh, Sahin, West, & Murray, 2017; Okizaki et al., 2015; Torres-Castro et al., 2016). Moreover, in high glucose conditions, Ac2-26 stimulates fibroblast migration maybe through interaction with FPRs, up-regulated in hyperglycemia conditions (Bizzarro, Fontanella, et al., 2012). Together, these data highlight the potential application of the peptide as a pharmacological tool.

In a previous study (Del Gaudio et al., 2015) it was demonstrated that the alginate was able to stabilize Ac2-26, via hydrogen bonding, and promote its release in a controlled manner. When released from alginate hydrogel in a model murine, Ac2-26 was able to promote wound healing over 72 h and wound closure in 14 days.

In the first phase of this Ph.D. project, submicroparticles carriers composed of high M content alginate and high amidated pectin loaded with Ac2-26 to obtain an *in situ* forming

hydrogel were developed. Nano spray drying is the technology chosen for the production of submicroparticles since makes possible to obtain tiny particles down to only 350-500 nm and to reach high yields of the process up to around 90 % (Arpagaus, 2012). Moreover, nano spray drying is well suited for heat-sensitive materials like proteins and peptides since the temperature used for the atomization remains relatively low due to fast solvent removal (Abdel-Mageed et al., 2020).

Alginate is a natural polysaccharide composed of mannuronic (M) and guluronic (G) acid units isolated from brown algae. The ratio between M and G units influences physiochemical and mechanical characteristics, specifically, alginate with a high M content induces cytokine release, involved in wound healing, more than alginate with a high G content (Kuen Yong Lee & David J. Mooney, 2012; Szekalska, Puciłowska, Szymańska, Ciosek, & Winnicka, 2016). However, the alginate with $M/G > 1$ has a low amount of guluronic acid that can provide a soft structure gel (Gómez-Ordóñez & Rupérez, 2011), therefore, the combination with other natural polysaccharides, like pectin, can speed up *in situ* gel-forming rate (Felicetta De Cicco, Porta, Sansone, Aquino, & Del Gaudio, 2014).

This polymeric blend was used to encapsulate Ac2-26, stabilizing the peptidomimetic and controlling its release into the wound cavity. FT-IR studies to analyse the chemical interactions between Ac2-26 and polymers blend, as well as fluid uptake ability of the powders and release of the peptide have been performed. Furthermore, a cytotoxicity test to evaluate the compatibility of the polymers on the wound and the wound healing assay has been evaluated on an *ex vivo* model, using HaCaT cell line.

3.1.2 Results and discussion

3.1.2.1 Preparation and characterization of the Ac2-26 loaded submicroparticles

To produce alginate-pectin particles loaded with different amounts of Ac2-26 a novel technology, Nano Spray Dryer B-90, was used. Preliminary experiments were conducted to optimize all the process parameters and the feed solution preparation steps, in order to determine the adequate operating spray conditions avoiding aggregates or particle clusters into the produced powders. Nozzle mesh diameter of 5.5 μm was chosen to obtain submicrometric powder and the inlet temperature was set at 70 °C to minimize the moisture content of the powders and at the same time avoid the degradation of Ac2-26. Three different polymer ratios (from 3:1 to 1:3) and 0.25, 0.50%, and 1.00% (w/v) as the total concentration of the polymers were set. Moreover, based on a previous study two different amounts of Ac2-26 (0.01% and 0.02% w/w) were investigated (Del Gaudio et al., 2015) (Table 2).

Table 2. *Composition, process yield, particle size, drug content, and encapsulation efficiency (E.E.) of Ac2-26 loaded alginate-pectin submicroparticles obtained by nano spray drying.*

Sample	Polymers concentration % (w/v)	Alginate-pectin ratio	Ac2-26 polymers ratio	Yield (%)	Mean diameter (nm) ± SD	Drug content (%) ± SD	E.E. (%) ± SD	Drug content (%) ± SD*
NAP_31-25	0.25	3:1	-	73.9 ± 1.8	583 ± 62	n.d.	n.d.	n.d.
NAP_31-25_Ac1			0.01	73.6 ± 2.8	569 ± 71	0.82 ± 0.04	86 ± 5	0.78 ± 0.05
NAP_31-25_Ac2			0.02	71.9 ± 3.2	593 ± 58	1.73 ± 0.03	88 ± 4	1.64 ± 0.06
NAP_11-25		1:1	-	72.0 ± 1.7	611 ± 72	n.d.	n.d.	n.d.
NAP_11-25_Ac1			0.01	70.2 ± 2.2	599 ± 58	0.72 ± 0.04	78 ± 4	0.69 ± 0.05
NAP_11-25_Ac2			0.02	71.3 ± 1.9	583 ± 92	1.62 ± 0.05	78 ± 5	1.52 ± 0.07
NAP_13-25		1:3	-	69.2 ± 1.9	595 ± 81	n.d.	n.d.	n.d.
NAP_13-25_Ac1			0.01	67.9 ± 1.7	582 ± 84	0.71 ± 0.03	79 ± 3	0.63 ± 0.05
NAP_13-25_Ac2			0.02	68.8 ± 2.4	605 ± 74	1.69 ± 0.04	77 ± 4	1.48 ± 0.07
NAP_31-50	0.50	3:1	-	75.8 ± 1.9	656 ± 92	n.d.	n.d.	n.d.
NAP_31-50_Ac1			0.01	76.4 ± 2.7	684 ± 86	0.82 ± 0.04	84 ± 5	0.79 ± 0.05
NAP_31-50_Ac2			0.02	74.9 ± 2.1	678 ± 106	1.46 ± 0.04	86 ± 3	1.72 ± 0.07
NAP_11-50		1:1	-	71.4 ± 3.0	667 ± 94	n.d.	n.d.	n.d.
NAP_11-50_Ac1			0.01	72.8 ± 2.3	689 ± 90	0.76 ± 0.05	80 ± 2	0.73 ± 0.04
NAP_11-50_Ac2			0.02	71.9 ± 2.9	674 ± 88	1.53 ± 0.06	80 ± 4	1.54 ± 0.07
NAP_13-50		1:3	-	72.9 ± 2.6	691 ± 96	n.d.	n.d.	n.d.
NAP_13-50_Ac1			0.01	73.4 ± 2.5	704 ± 106	0.72 ± 0.04	77 ± 5	0.72 ± 0.06
NAP_13-50_Ac2			0.02	72.8 ± 3.1	686 ± 97	1.73 ± 0.06	78 ± 4	1.50 ± 0.07
NAP_31-100	1.00	3:1	-	84.9 ± 2.1	822 ± 112	n.d.	n.d.	n.d.
NAP_31-100_Ac1			0.01	85.3 ± 2.2	769 ± 98	0.79 ± 0.05	85 ± 5	0.75 ± 0.05
NAP_31-100_Ac2			0.02	85.7 ± 1.9	831 ± 89	1.72 ± 0.07	89 ± 3	1.63 ± 0.06
NAP_11-100		1:1	-	82.6 ± 2.4	814 ± 106	n.d.	n.d.	n.d.
NAP_11-100_Ac1			0.01	81.8 ± 1.8	882 ± 114	0.73 ± 0.04	80 ± 2	0.69 ± 0.05
NAP_11-100_Ac2			0.02	83.5 ± 2.3	834 ± 91	1.54 ± 0.07	81 ± 4	1.46 ± 0.08
NAP_13-100		1:3	-	80.8 ± 2.2	855 ± 93	n.d.	n.d.	n.d.
NAP_13-100_Ac1			0.01	82.1 ± 2.6	876 ± 104	0.72 ± 0.06	78 ± 5	0.63 ± 0.04
NAP_13-100_Ac2			0.02	81.4 ± 1.8	865 ± 94	1.50 ± 0.07	79 ± 4	1.33 ± 0.08

*Data acquired after 1 month in accelerated storage condition

The innovative atomization mechanism, due to a piezoelectric membrane and the electrostatic collector of nano spray dryer, has allowed obtaining high process yields and low particle size distribution (up to 200 nm), despite the use of small quantities of feed solution and the employ of long times. Formulations were obtained in good yield (68-85%) dependent on feed solution: the higher the total polymer concentration and ratio, the higher the yield. Particles size and particle size distribution as well as water content were affected by feed concentration: the lower the feed concentration the smaller particle size and the water content that ranged between 5.6 and 3.5% (w/w). This is due to the decrease in surface tension of the droplets generated by the vibrating membrane (Del Gaudio et al., 2017; Y. Y. Xu, Howes, Adhikari, & Bhandari, 2012). On the contrary, the presence of the peptide had no impact on both the size and spherical morphology of the particles (Figure 22).

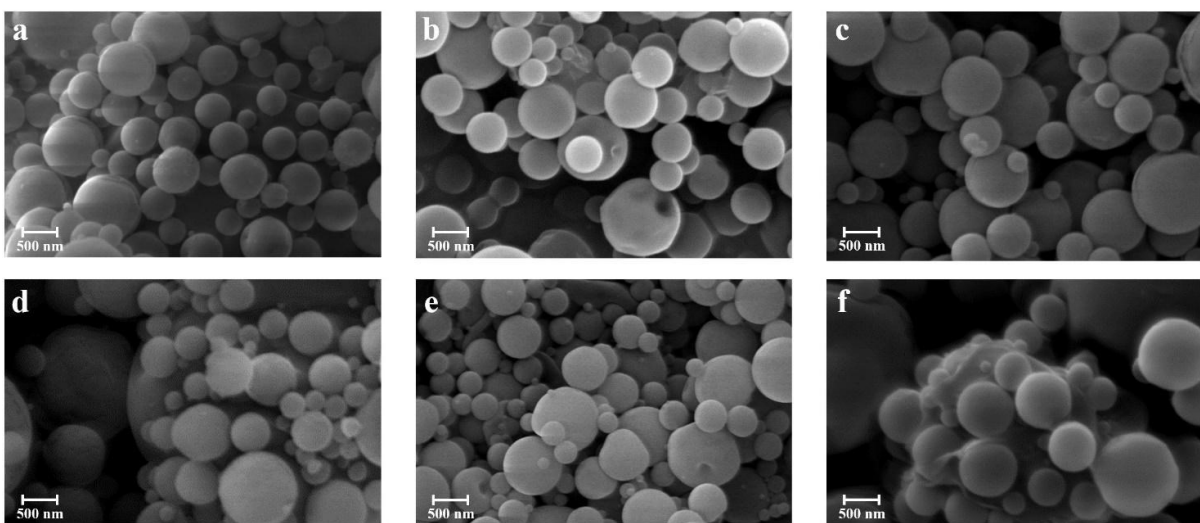


Figure 22. SEM microphotographs. Blank submicroparticles: NAP_31-25 (a), NAP_31-50 (b) and NAP_31-100 (c); Ac2-26 loaded submicroparticles: NAP_31-25_Ac2 (d), NAP_31-50_Ac2 (e) and NAP_31-100_Ac2 (f).

All formulations were reported a high encapsulation efficiency (77-89%) due to the formation of hydrogen bonding between peptide and free alginate carboxyl groups confirmed

by spectroscopy FT-IR analysis. As shown in Figure 23-a,b, amidated pectin presented two peaks at 1680 cm^{-1} and 1592 cm^{-1} related to amide I and the amide II and the signal of COO stretching at 1410 cm^{-1} , while alginate presented at 1613 cm^{-1} and 1418 cm^{-1} the characteristics bands belonging to the antisymmetric and symmetric stretching vibration of the alginate carboxyl group. Blank alginate-pectin particles (Figure 23-c) exhibited a shift both in the vibration bands of amide bonds and symmetric and asymmetric COO stretching, and due to the formation of hydrogen bonding (Sinitsya, J, Prutyaynov, Skoblya, & V, 2000) during the spray drying process. In fact, the band correlated to the amide I was shifted at 1675 cm^{-1} , and the band belonging to amide II was overlapped with the antisymmetric carboxyl band shifted at 1602 cm^{-1} ; furthermore symmetric stretching vibration of the carboxyl group was shifted at 1412 cm^{-1} . As shown in Figure 23-e, alginate-pectin loaded with Ac2-26 presented a new band at 1547 cm^{-1} , probably due to a partial shifting of the alginate carboxyl groups that can be associated with hydrogen bonding between Ac2-26 and some alginate chains.

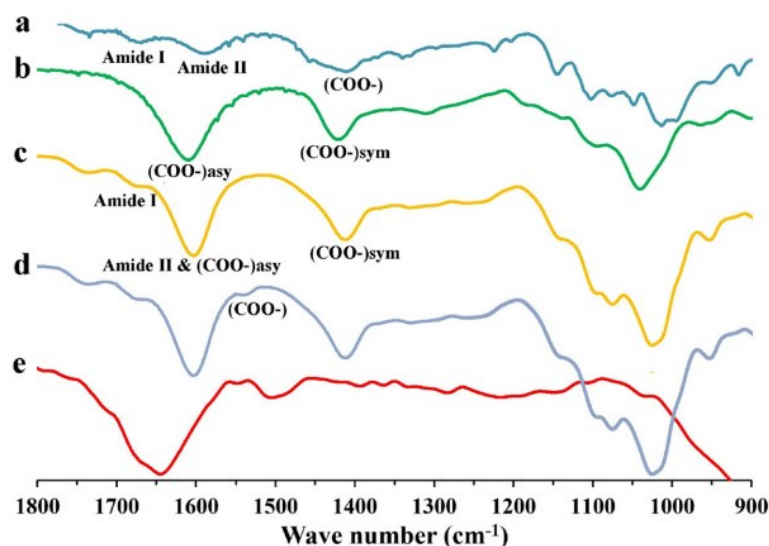


Figure 23. FTIR spectra. Amidated pectin (a), alginate (b), alginate-pectin particles, (c), 0.01 % (w/V) AC2-26 solution (d) and NAP_31-50_Ac2 (e).

Such interactions could be responsible for the increase in stability of the Ac2-26 when encapsulated into the polymer blend matrix. Quantitative LC/MS analyses, performed on the powders stored at -20 and 4°C, showed a very low decrease of Ac2-26 encapsulated in NAP_31s and NAP_11s, less than 5% after one month, regardless of the amount of loaded peptide, but, on the contrary, a reduction around 13% in case of NAP_13s. The same formulations stored at room temperature showed a similar reduction of the Ac2-26 titer. This aspect represents a huge advantage since it allows to overcome the considerable limitations related to the chemical stability of substances of peptide nature. Ac2-26 in solution needs a storage temperature of -20 °C but, from the data obtained during this work, if encapsulated in a matrix with the prevalence of alginate able to interact with the peptide via hydrogen bonding, the peptide can be stored even at room temperature remaining chemically stable for at least 1 months (Qin et al., 2019).

Fluid uptake studies were performed in order to evaluate the ability of the powders to become a hydrogel when in contact with SWF, using Franz cells (Figure 24). All formulations exhibited maximum swelling between 15 and 20 minutes depending on the relative amount of amidated pectin; the higher the pectin the faster the gelling of the formulation (Capel, Nicolai, Durand, Boulenguer, & Langendorff, 2006). After maximum swelling, all powders reached an equilibrium phase with partial loss of water due to reorganization of the gel elastic network (Azevedo & Kumar, 2012).

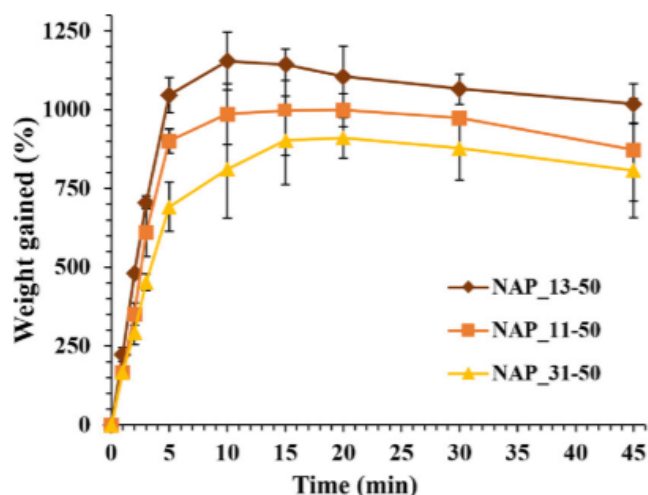


Figure 24. Simulated wound fluid uptake of the blank alginate-pectin submicrometric powder prepared by nano spray drying. Mean \pm SD; ($n = 6$).

In situ formed hydrogel fluid loss was evaluated in order to verify the ability of the gel to maintain correctly hydrated the wound during therapy. The fluid loss was evaluated as the weight decrease of the different gel after removal of SWF. As shown in Figure 25 all gels demonstrated an increased fluid loss within 12 h, between 53% and 34%, related to the pectin concentration. In fact, the higher the concentration the lower the loss. Nevertheless, after 24 h, all formulations were able to retain at least 25% of the incorporated fluid and about 40% in the case of powders with a high amount of pectin, maybe due to the higher pectin water affinity (Yamamoto, Saeki, & Inoshita, 2002). These results suggest the ability of the powders to continue to be gel if there is no more fluid supplied by the wound. Ac2-26 encapsulated, as well as total polymers concentration of the feed, did not influence significantly the fluid uptake ability or water loss.

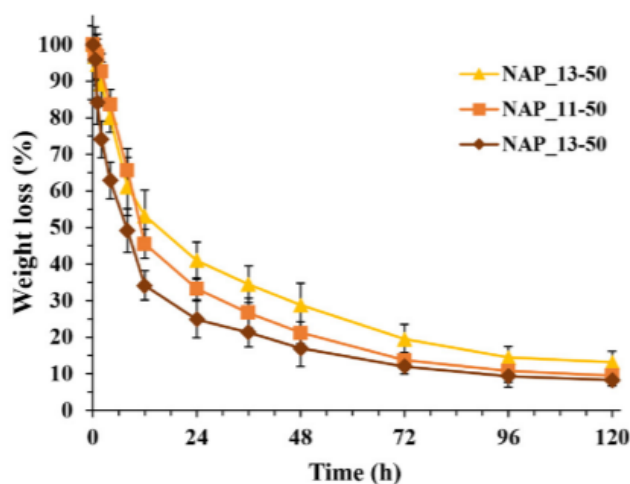


Figure 25. Water evaporation from blank alginate-pectin hydrogel prepared by nano spray drying. Mean \pm SD; (n = 6).

3.1.2.2 *In vitro* Ac2-26 release studies

To assess the Ac2-26 release behaviour from different formulations, *in vitro* permeation experiments were conducted using slide-a-lyzer mini dialysis units, as a loading chamber for the powder, inserted into acceptor compartment of Franz-type vertical diffusion cells filled with SWF.

All formulations, analysed by LC-MS, exhibited burst effect within 3 hours followed by a prolonged release between 24 and 48 hours (Figure 26). The burst effect was dependent on the rate of gel formation. In fact, NAP_11s and NAP_13s powders with a higher amount of amidated pectin having a faster gelling rate, released 42% and 37% of the loaded peptide, respectively. On the contrary NAP_31s powder released about 50% of their load. Total release of Ac2-26 was reached between 24 and 36 h depending on the alginate pectin ratio that determined the resistance of the gel, the higher the alginate concentration, the faster the release. NAP_31-50_Ac formulations released 95% of their load in 24 h, while NAP_11-50_Acs and NAP_13-50_Acs released 88% and 82% of the loaded peptide in 30 and 48 h, respectively. The intensive release of the Ac-26 in the first hours of analysis, followed by a prolonged release,

may be very useful during the healing process that could benefit from effects related to the strong anti-inflammatory and promigratory activity of Ac2-26 (R. A. P. Teixeira, Mimura, Araujo, Greco, & Oliani, 2016). Due to the interaction between alginate carboxyl residues and Ac2-26 via hydrogen bonding, as reported in FT-IR analyses, and partial degradation of the peptide in SWF after its release, it was impossible to detect the total release of the peptide encapsulated. However, these results demonstrated that polymers can protect the peptide for a long time compared to peptide alone that degrades in a few hours (M. Perretti et al., 2002).

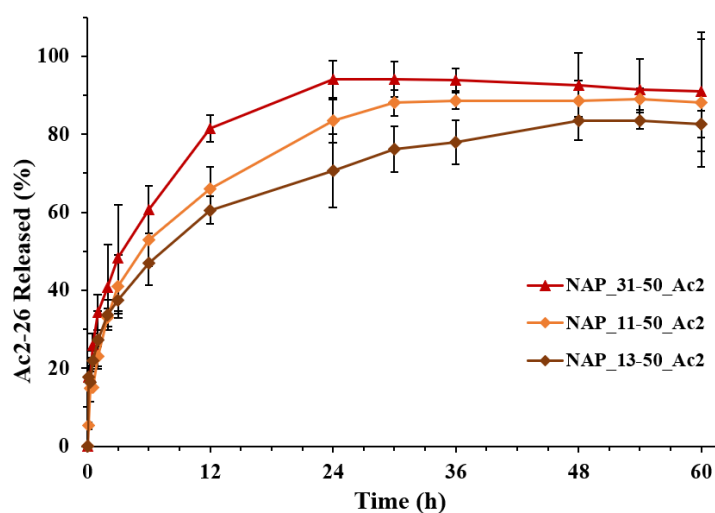


Figure 26. Release profiles of Ac2-26 loaded alginate-pectin powders with different polymer blend ratio: NAP_31-50_Ac2, NAP_11-50_Ac2, NAP_13-50_Ac2. Mean \pm SD; (n = 6).

3.1.2.3 *In vitro* cytotoxic activity and wound healing assay

Since the powders are intended to be dispensed directly to the wounds, *in vitro* cytotoxicity, conducting MTT assay against HaCaT cells was evaluated. HaCaT cells were treated for 24 hours with alginate, pectin, and alginate-pectin blend testing different concentrations between 0.01 to 10 μ g/mL. The treatment did not show a statistically significant reduction in the optical density (OD) at 550 nm, compared to the positive control (SDS 1%), for none combinations and concentration tested (Figure 27).

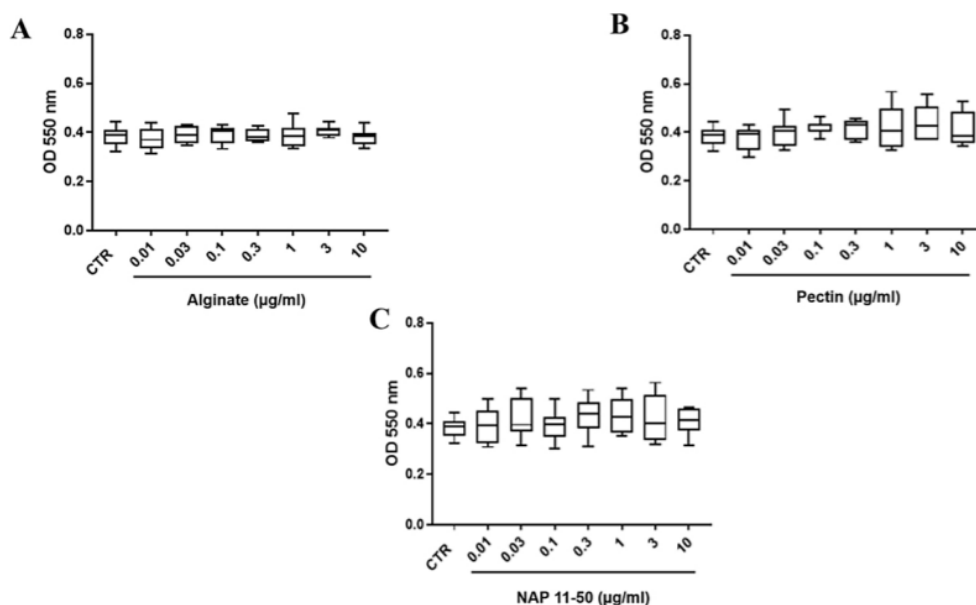


Figure 27. Cell viability was conducted on HaCaT cells after 24 h treatment with alginate (A), pectin(B), and representative of alginate-pectin blend powders(C). Data are represented as median \pm interquartile range ($n = 7$).

Wound healing experiments were conducted to evaluate the efficacy of formulations in wound repair using HaCaT cells. After 24 hours, blank alginate-pectin particles were less efficient than alginate particles in improving cell migration, whereas the treatment with pure amidated pectin particles was comparable to the control. On the contrary, the powders containing the Ac2-26, even in a lower amount, showed a very good ability to improve migration leading to wound complete closure after 24 hours, 79%, and 25% better than control and pure alginate, respectively (Figure 28).

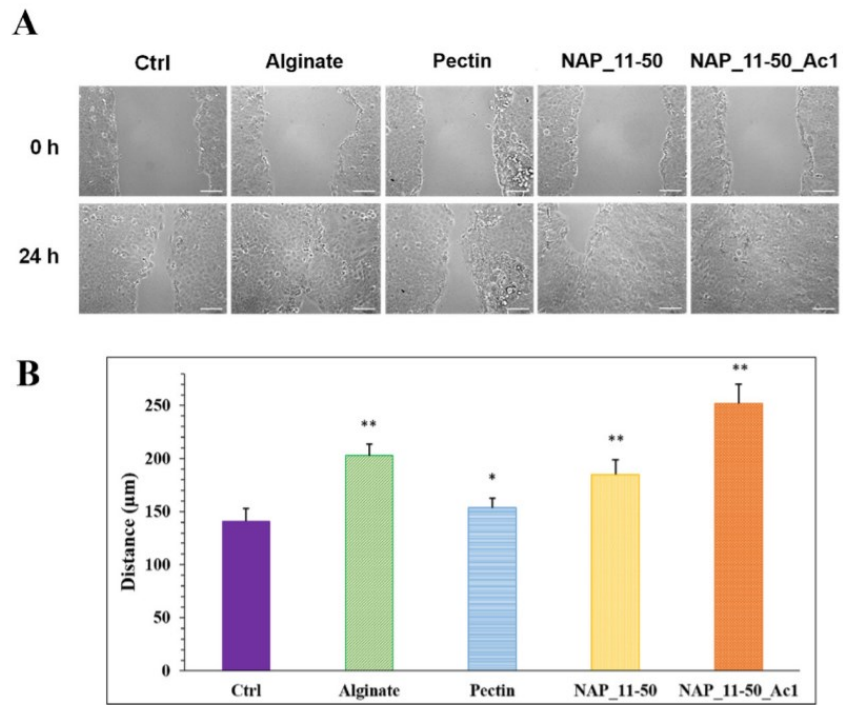


Figure 28. Results of wound healing assay on HaCaT cells. Panel A: representative bright fields of wound healing assay at 0 and 24 hours after the creation of the lesion on a cell monolayer. Scale Bar 100 µm; Panel B: the migration rate of cells treated with Ctrl (not treated cells), Alginate, pectin, NAP_11-50, and NAP_11-50_Ac2. The data are representative of 3 independent experiments \pm SD. * $p < 0.05$; ** $p < 0.01$.

3.1.3 Conclusions

In conclusion, this study demonstrated that incorporating the ANXA1 mimetic peptide Ac2-26 in high M content alginate improves its stability over time, one of the main problems related to the use of peptide, which needs to be stored at -20 °C. The powders were produced by spray drying technology using the nano spray dryer that allowed to obtain particles of submicrometric size with high yields of the process (67-85 %). Ac2-26 encapsulation efficiency was very high, till 83%, even after 1 month in accelerated storage conditions. Fluid uptake ability showed complete gelling of the formulations between 10 and 15 min depending on pectin relative amount. FTIR studies suggested a binding between the negatively charged portion of the peptide and free alginate carboxyl groups of the polysaccharide blend that stabilize and control the release of Ac2-26 from the *in situ* formed hydrogels. In fact, the release of encapsulated Ac2-26 from the gel exhibited a burst effect, within 3 h, followed by a prolonged release, between 24 and 48 h, relating the alginate-pectin ratio. *In vitro* wound healing tests on HaCaT cells showed that Ac2-26 loaded formulations, compared to the blank alginate-pectin particles, were able to promote the cell migration to close lesions. These promising results suggest that nano spray drying technology has been successfully used to produce stable submicrometric alginate-pectin particles loaded with the peptide Ac2-26 that might have potential application as dressings for wound healing processes.

3.2 SECTION B

Alginate-pectin and alginate-pectin-chitosan *in situ* gelling powders

Manuscript to be submitted.

3.2.1 Scientific background

Owing to its high reproducibility, continuous mode of operation, broad application, fast drying capability, and reduced exposure of the product to high processing temperatures, spray drying is considered a powerful technological process for the pharmaceutical and biotechnology application (Al-Khattawi, Bayly, Phillips, & Wilson, 2018; Sansone et al., 2018). During this study *in situ* gelling micro-nanoparticles carriers were produced to evaluate two different atomization techniques, the influence of different polymers and other excipients on powder final properties. Mini spray drying and nano spray drying technologies were compared since the latter allows to obtain smaller particle sizes than conventional spray dryers with a higher surface-volume ratio when in contact with the biological fluid (Arpagaus, Collenberg, Rütli, Assadpour, & Jafari, 2018).

In acute wounds, the exudate contains proteins and essential nutrients for the epithelial cells, and also proteolytic enzymes and their inhibitors, balanced between them to prepare wound bed before closure and remodeling (Benbow, 2016). On the contrary, chronic wound exudate is rich in proteinases that block the proliferation of key cells involved in the wound healing process (Cutting, 2003). The porosity structure and high-water content, allowing the absorption of the exudates maintaining a moist healing environment, make hydrogel a good candidate as a wound dressing (Miguel, Ribeiro, Brancal, Coutinho, & Correia, 2014; Xue et al., 2019). However, since conventional hydrogels need several hours to reach maximum water absorption, the aim of this work is the development of *in situ* gelling powders as a wound dressing, using a mixture of natural polysaccharide with specific characteristics: alginate with high content of mannuronic acid, amidated pectin, and chitosan low molecular weight.

Alginate with high residues of M is able to induce the production of cytokines (Szekalska et al., 2016; A. Thomas et al., 2000) improving the wound healing process. Amidated pectin with a low degree of methylation can speed up *in situ* gel formation (Felicetta De Cicco, Reverchon,

et al., 2014). Low molecular weight chitosan is able to interact with acetylated residues of mannose receptors inducing macrophages activation (Porporatto, Bianco, Riera, & Correa, 2003). Moreover, regardless of molecular weight, chitosan can accelerate wound healing thanks to anti-inflammatory, homeostatic and antimicrobial activity (Bhattarai, Gunn, & Zhang, 2010; Liow et al., 2017; Paomephan et al., 2018).

Subsequently, to increase the gelling process of the best formulation, different co-solvents (ethanol, isopropanol, and acetone), as well as other excipients in the form of salts (sodium bicarbonate and ammonium carbonate) were added to the feed solution.

The powders, produced through spray dryer, have been characterized in terms of process yield, morphology, dimensional distribution, and fluid uptake ability. Moreover, the chemical structure was obtained by FTIR spectra, the thermal analysis was evaluated by DSC, as well as the elasticity was determined through rheological studies. Finally, MTT test and ELISA assay for cytotoxic and pro-inflammatory activity were performed to assess the safety and efficacy of the particles on wounds.

3.2.2 Results and discussion

3.2.2.1 Alginate-pectin and alginate-pectin-chitosan in situ gelling powders

For the development of formulations capable of gelling in contact with fluids present in the wound bed of chronic wounds and at the same time able to release in a controlled manner active particles, a polymeric blend, using three different natural polysaccharides, were produced. Specifically, alginate-pectin (AP) and alginate-pectin-chitosan (APC) polymeric blends with three different total polymeric ratios were produced, AP 1:1,1:3,3:1 and APC 1:1:1, 1:1:3, 1:1:7 respectively. Preliminary studies were conducted to optimize the process parameters and the operating conditions for feed solution preparation performed in the first part of this thesis when chitosan was included in the polysaccharides blend. In fact, due to the formation of insoluble polyelectrolyte complex between the cationic group of the chitosan and the anionic groups of the alginate (Lai, Abu'Khalil, & Craig, 2003; Lawrie et al., 2007; Simsek-Ege, Bond, & Stringer, 2003), the feed was limited in its final pH and concentration. Therefore, the optimal concentration of the polymers in terms of feasibility and yield of the process was found at 0.15% since the amount of chitosan affected the appearance of the final feed, the spray drying process, which in some situations could not be conducted due to the formation of insoluble agglomerates in the feed solution, and consequently, the final characteristics of the powders.

As reported in Table 3, a comparison between mini spray dried particles obtained from AP and APC at different ratios shows that process yield is affected by the presence of chitosan. In fact, in the feed prepared with the higher amount of chitosan a slight increase in process yield was registered, from about 60% to 70%, probably due to an increase in viscosity of the feed related to alginate-chitosan interaction able to promote crosslinking of the polymer chains during the formation of the powders (Alsharabasy, Moghannem, & El-Mazny, 2016; Hashad, Ishak, Fahmy, Mansour, & Geneidi, 2016).

Table 3. *Composition, process yield, and particle size of powders obtained with different polysaccharides ratio by mini spray drying.*

Sample	Alginate-Pectin-Chitosan Ratio	Yield (%)	Mean diameter (μm) \pm SD
AP-11	1:1	63	2.07 \pm 0.08
AP-31	3:1	65	2.16 \pm 0.11
AP-13	1:3	61	2.85 \pm 0.49
APC-111	1:1:1	60	3.24 \pm 0.13
APC-113	1:1:3	72	2.75 \pm 0.10
APC-117	1:1:7	73	2.58 \pm 0.04

AP particles showed a mean diameter ranging between 2.07 and 2.85 μm depending on the polymer ratio. Smaller particles were obtained when a 1:1 polymer ratio was used, whereas the largest particles were obtained processing feeds with the highest amount of pectin, AP-13. In APC powders, higher chitosan concentration led to smaller particles (see Table 3). Polymers ratio have, also, influenced powders surface. In fact, the formulation with more pectin AP-13 particles exhibited wide size distribution, a tendency to agglomerate, and a partially shrank shape that might be related to the presence of xylose, galactose, and arabinose in the structural side chains of the pectin that reduce the interactions with the alginate consequently to a collapsed particle structure after the drying process (Jaya, Durance, & Wang, 2009) (Figure 29-a,b,c). Whereas the addition of chitosan led to particles being rougher and rougher accordingly to the amount of chitosan used to prepare the feed. Such modification could be ascribed to the precipitation of chitosan on the matrix of alginate and pectin during the drying phase due to its lower solubility in the feed solution (Figure 29-d,e,f).

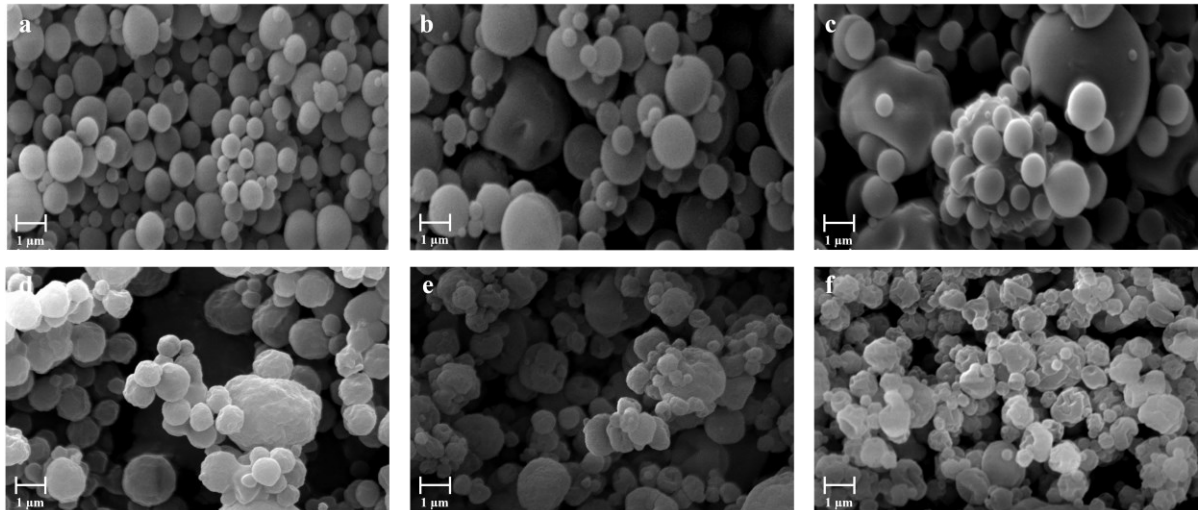


Figure 29. SEM microphotographs of alginate-pectin and alginate-pectin-chitosan particles produced by mini spray drying with different polymers ratio: AP-11 (a), AP-31 (b), AP-13 (c), APC-111 (d), APC-113 (e), APC-117 (f).

Since the main goal of these formulations is the ability to gel quickly in contact with wound exudates, to test this property, fluid uptake ability was studied using a Franz cell filled with SWF to mimic *in vitro* the wound bed environment. As reported in the graphs below (Figure 30), AP 11 reported the maximum swelling in about 15 minutes, while all APC formulations have reached it in about 10 minutes. However, it is possible to observe that the speed of absorption of the fluid is different and strongly dependent on the concentration of chitosan. In fact, although the formulation APC-117 had a slower uptake it was able to absorb higher amounts of SWF, compared to other APC powders, around 50% and 60% more than APC-113 and APC-111, respectively. This phenomenon can be explained by taking into account that APC-117 particles exhibit smaller sizes and higher surface area due to the very wrinkled surface for the precipitation of chitosan on the particles (Dresvyanina et al., 2020).

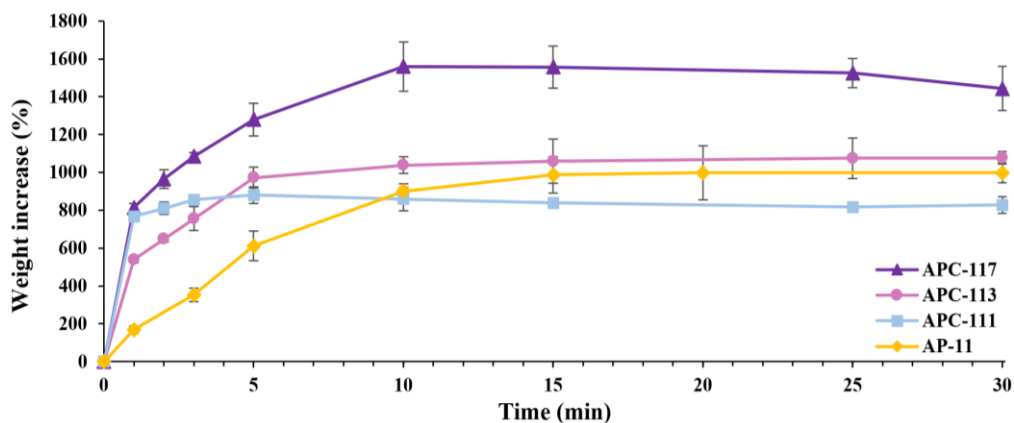


Figure 30. Simulated wound fluid uptake of powders produced by mini spray drying: alginate-pectin-chitosan particles in comparison with alginate-pectin particles.

From the preliminary studies carried out on these formulations, interesting results in terms of fluid uptake were obtained with the APC formulations (1:1:3) and (1:1:7), therefore these formulations were produced using nano spray drying technology to test which of them was able to produce the particles with the most suitable characteristics for direct administration. As reported in Table 4 these formulations showed a process yield similar to particles produced by mini spray drying and not higher yields as expected from this process, probably because were produced also particles of size < 200 nm that are lost by the collection system.

Table 4. Composition, process yield, and particle size of powders produced by nano spray drying.

Sample	Alginate-Pectin-Chitosan Ratio	Yield (%)	Mean diameter (µm) ± SD
NAPC-113	1:1:3	73.5	0.540 ± 0.25
NAPC-117	1:1:7	74.8	0.600 ± 0.26

These particles did not show surface roughness, on the contrary, they appeared not homogeneous with particles ranging from 900 nm to extremely small particles around 200 nm as reported in SEM images (Figure 31).

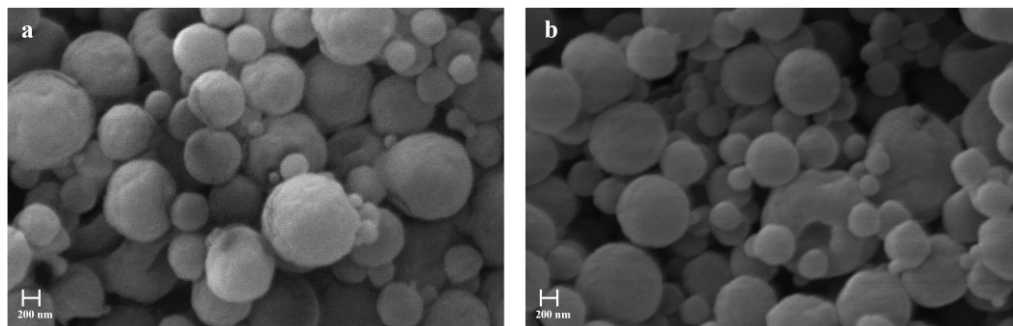


Figure 31. SEM images of powders produced by nano spray drying: NAPC-113 (a) and NAPC-117 (b).

However, although small size (about 0.6 μm), probably for the lack of homogeneity these particles did not show an increase in fluid uptake, on the contrary NAPC-117 showed a lower capacity to absorb the fluids than to the equivalent APC-117 produced by mini spray as reported in Figure 32.

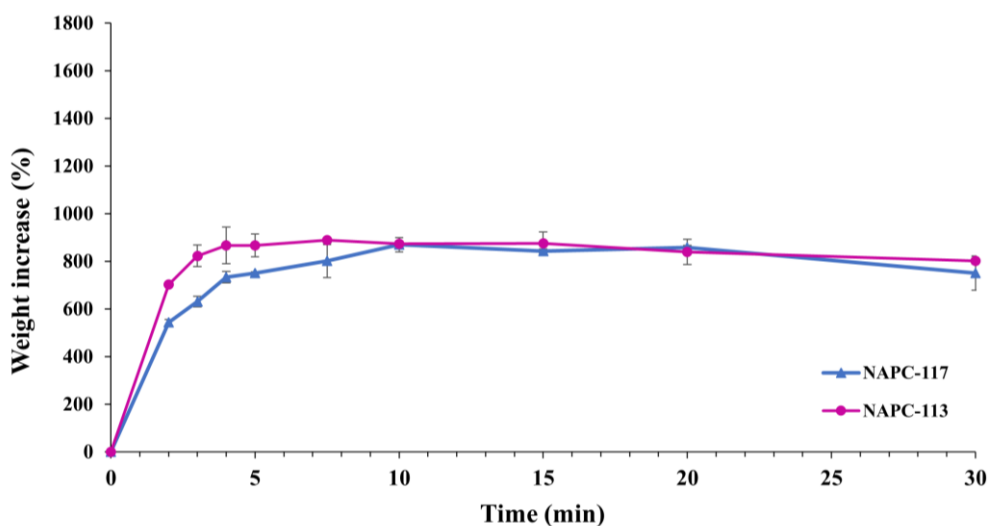


Figure 32. Simulated wound fluid uptake of alginate-pectin-chitosan particles produced by nano spray drying.

3.2.2.2 Alginate-pectin-chitosan *in situ* gelling powders with co-solvents

In order to speed up gelling rate, APC 117, which produced better results in terms of gelling rate, was prepared with different co-solvents. The addition of a more volatile solvent in the feed for spray drying might modify the crystallization kinetics leading to different particle properties (Wan et al., 2013; Z. Wang, Ordoubadi, Wang, & Vehring, 2021). Compared to feed based on pure water, due to less energy input required for the evaporation rate of the volatile organic solvent, this kind of feed solution favours the drying of the particles with the formation of hollow or porous powders (Cal & Sollohub, 2010). Formulations with 5, 10, 20% v/v of ethanol, 20% v/v of ethanol/acetone (1:1), and 5% v/v of isopropanol were tested. Ethanol, a volatile and miscible solvent with water, was chosen because is a commonly used solvent in the pharmaceutical industry. As reported in Table 5 the yield of the process decreased with an addition of co-solvents in the feed solution, especially with 20% of ethanol in the feed, the yield was passed from 61% to 45%. In addition, the ethanol led to an increase of mean diameter meanwhile the presence of acetone determined a reduction of diameter. However, no clear correlation between these characteristics and co-solvent content was observed.

Table 5. *Composition, process yield, and particle size of powders added with different co-solvents produced by mini spray drying.*

Sample	APC ratio	Ratio H ₂ O/Co-solvent	Process yield (%)	Mean diameter (µm) ± SD
APC-117	1:1:7	H ₂ O 100	61.5	3.65 ± 0.01
APC-117-5Et		H ₂ O/CH ₃ OH 95:5	55.8	5.05 ± 0.06
APC-117-10Et		H ₂ O/CH ₃ OH 90:10	55.8	4.09 ± 0.02
APC-117-20Et		H ₂ O/CH ₃ OH 80:20	45.7	4.80 ± 0.19
APC-117-20EtA		H ₂ O/CH ₃ OH/CH ₃ COCH ₃ 80:10:10	55.6	2.91 ± 0.01
APC-117-5Iso		H ₂ O/CH ₃ CH(OH)CH ₃ 95:5	50.3	3.27 ± 0.05

The addition of co-solvents has influenced the morphology of the particles, generating more corrugated and irregular particles due to the faster removal of the solvent (Figure 33).

During a multi solvent-system drying process, the evaporation rate and the diffusion coefficients vary with time due to variation of Péclet number. This number represents the behavior of solutes inside an evaporating droplet. It is constant in a single solvent droplet but changes with time in a multi-solvent system. A higher percentage of solvent leads to a higher evaporation rate, higher Péclet number, and as a consequence cracked surfaces and low-density hollow particles (Vehring, Foss, & Lechuga-Ballesteros, 2007). Moreover, the insolubility of chitosan in ethanol and isopropanol might result in precipitation faster from the ethanol-water feed related to only water during the atomization process. In fact, the particles not having the strong enough to maintain the spherical shape collapse becoming wrinkled particles (Ji et al., 2016).

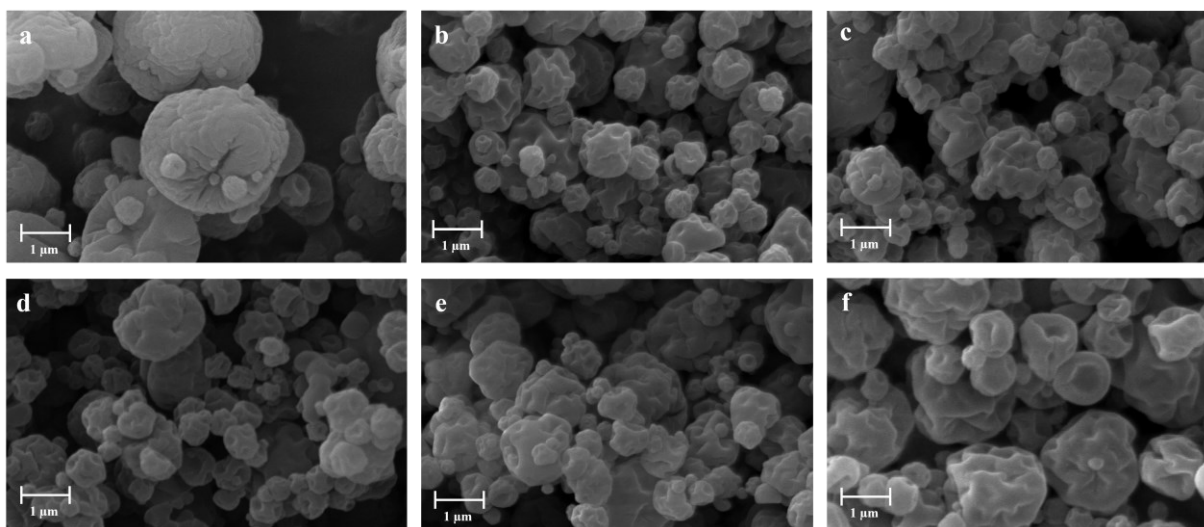


Figure 33. SEM images of powders produced by mini spray drying with different co-solvents: APC-117(a), APC-117-5Et (b), APC-117-10Et (c), APC-117-20Et (d), APC-117-20EtA (e), and APC-117-5Iso (f).

The formulations with different blends of solvents were subjected to fluid uptake experiments in order to evaluate their ability to absorb the SWF compared to the blank

formulation (Figure 34). Except for APC-117-5Iso, all formulations showed a higher value of swelling than the blank formulation APC-117. Especially for APC-117-5Et, the swelling was immediate, less than 5 minutes, while APC-117-20Et reached the higher swelling value although in greater times. This behavior could be explained due to the corrugation of the particles which reduces the contact area and the inter particulate forces between particles, as compared to spherical particles, which consequently higher contact surface with the fluid.

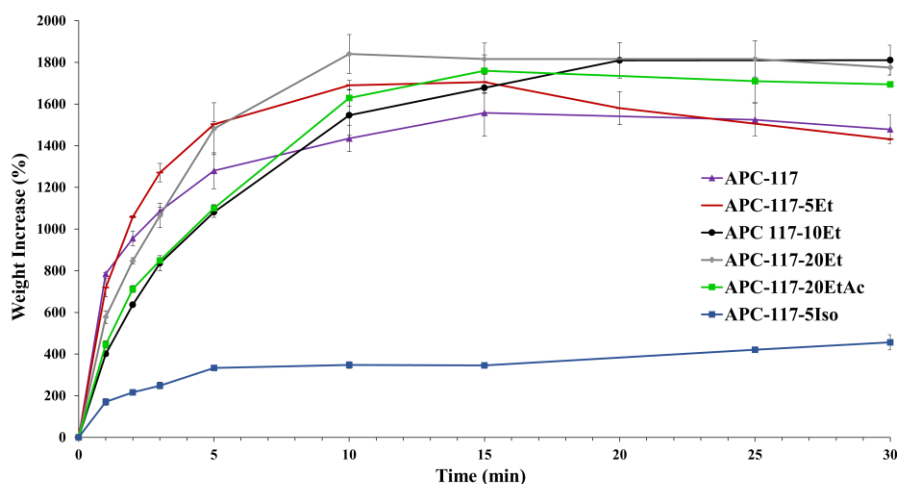


Figure 34. Simulated wound fluid uptake of in situ gelling powders. Blank particles APC 117 in comparison with particles produced with different co-solvents: APC-117-5Et, APC-117-10Et, APC-117-20Et, APC-117-20EtA, APC-117-5Iso.

3.2.2.3 Alginate-pectin-chitosan in situ gelling powders with salts

To avoid problems of precipitation and leave organic solvent residues, formulations APC-117 with sodium bicarbonate (NaHCO_3) and ammonium carbonate ($(\text{NH}_4)_2\text{CO}_3$) were prepared. Since these formulations were very reactive to water, they were collected under a nitrogen hood to avoid contact with air. Different amounts of salts were added from 400 to 1 % w/w but the formulations with 10% of salts were the most promising, therefore further analyses were carried

out. The presence of the salts did not influence the process yield, on the contrary, led to an increase in particle sizes for the formulations APC-117-10Bic and APC-117-10Car (Table 6).

Table 6. *Composition, process yield, and mean diameter of particles prepared with the addition of salts produced by mini spray drying.*

Sample	APC ratio	Salt concentration % (w/w)	Yield of the process (%)	Mean diameter (μm) \pm SD
APC-117	1:1:7	-	61.5	3.65 \pm 0.01
APC-117-10Bic		10 Sodium Bicarbonate	64.1	9.58 \pm 0.07
APC-117-10Car		10 Ammonium Carbonate	59.3	9.70 \pm 0.10

Moreover, as reported in SEM images (Figure 35), the particles made with NaHCO_3 appear aggregated in each other, while those with $(\text{NH}_4)_2\text{CO}_3$ show mainly a discoidal structure but not rough.

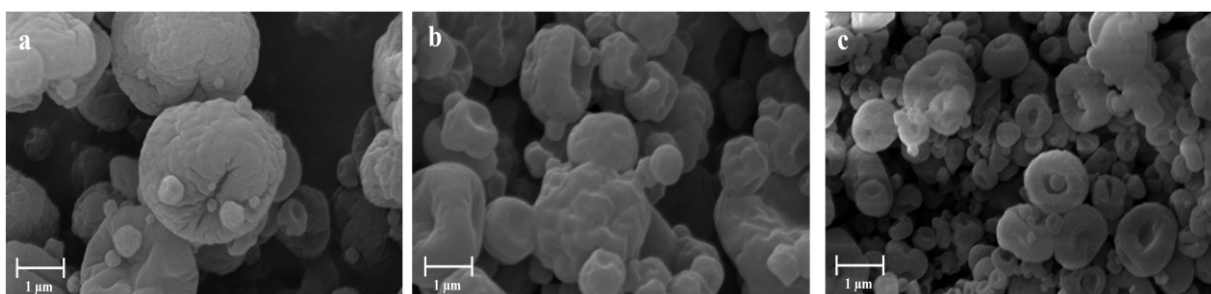


Figure 35. *SEM microphotographs. APC-117 (a), APC-117-10Bic (b), APC-117-10Car (c).*

The gelation rate studies showed that the addition of 10% w/w of NaHCO_3 led to the formation of gel in about 5 seconds, a result that was not obtained with other quantities of bicarbonate or with $(\text{NH}_4)_2\text{CO}_3$. The gel formed when the powder APC-117-10Bic was in contact with SWF appeared transparent and well-structured (Figure 36). As there must be an equilibrium between protonated and deprotonated units, it is probably that the lack of this led

to poor gelling for the solutions with a higher salt concentration. Based on the results, feeds containing ethanol and sodium bicarbonate were also tested, combining different concentrations but, although of acceptable size, all the formulations produced showed rather a slow gelation, so no further tests were carried out.



Figure 36. Gel obtained from APC-117-10Bic in contact with simulated wound fluid.

3.2.2.4 Characterization of the powders

Additional analyses were performed on the powders that reported better results in terms of gelling rate, APC-117-5Et, and APC-117-10Bic. The infrared spectrum was used to analyse the formation of intermolecular interactions. Panel A of Figure 37 reports the spectra of the powders of a single polymer and powders of alginate-pectin-chitosan blends in different polymers ratios, while in panel B APC-117-5Et and APC-117-10Bic are compared to the blank formulation APC-117. As reported in previous work (Pasquale Del Gaudio et al., 2020) blank alginate particles (Figure 37-a) presented two characteristic bands at 1602 cm^{-1} and 1408 cm^{-1} associated with the antisymmetric and symmetric stretching vibration of the carboxyl group the alginate. Blank pectin particles (Figure 37-b) also presented characteristic amide I band at 1675 cm^{-1} and 1590 cm^{-1} the amide II band, while COO stretching was observed at 1418 cm^{-1} . At 1552 cm^{-1} the bending vibration from the primary amine group was overlapped to the amide II vibration of the chitosan and the amide I band at 1655 cm^{-1} as well as the band associated with CH_2 bending at 1375 cm^{-1} . Moreover, associated with chitosan (Figure 37-c) the band related with C-O-C asymmetric stretching was visible at 1149 cm^{-1} while at 1059 cm^{-1} and 1023 cm^{-1}

were reported the stretching of C-O for CH₂-OH and CH-OH respectively (Assaad, Maire, & Lerouge, 2015).

Moreover, a broad absorption of OH around 3000-3600 cm⁻¹ masked the characteristics signal of the amino group present (Y. Tang et al., 2010). APC particles presented several bands related to the single polymers overlapped. However, COO bands of alginate, amide stretching of pectin, and NH bending band of chitosan shifted at lower wavenumbers according to the increase of chitosan in the blend (Figure 37-d,e,f), namely ranging from 1528 cm⁻¹ to 1521 cm⁻¹ for chitosan characteristic band and between 1402 cm⁻¹ and 1396 cm⁻¹ for alginate COO bands. The presence of ethanol in APC-117-5Et (Figure 37-g) was not detectable, and this may indicate that the addition of a co-solvent did not involve structural changes in the polymer matrix. On the contrary, in APC-10Bic (Figure 37-h), probably due to mixing with the acid solution, although at low intensity, at 1648 cm⁻¹ and 1336 cm⁻¹ were visible the anti-symmetric and symmetric stretching vibrations of the carboxyl group of NaHCO₃ (Baldassarre & Barth, 2014).

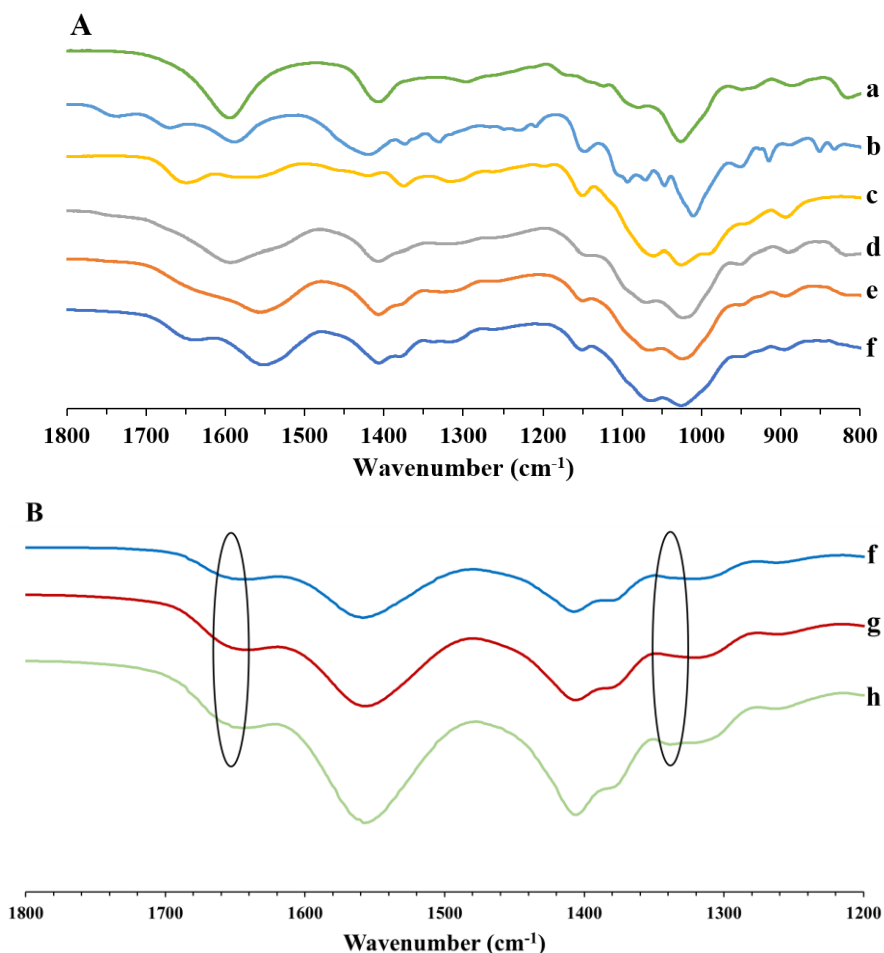


Figure 37. FTIR spectra alginate-pectin-chitosan. Panel A: alginate (a), amidated pectin (b), low MW chitosan (c), and APC-111 (d), APC-113 (e), APC-117 (f). Panel B: APC-117 (f), APC-117-5Et (g) and APC-117-10Bic (h).

Figure 38 reports the calorimetric thermograms of polymers as raw material compared to APCs formulations (panel A) and the thermograms of formulations APC-117-5Et and APC-117-10Bic compared to the blank formulation APC-117 (panel B). Alginate showed an exothermic peak at 240 °C (Figure 8-a) whereas chitosan at 305 °C (Figure 38-b) due to polymer degradation (De Cicco, Porta, et al., 2014; Saeed, Dmour, & Taha, 2020). Amidated pectin (Figure 38-c) showed a crystalline endothermic peak at 145°C, a broad peak at 170 °C followed by an exothermic one at 240°C (G. Auriemma et al., 2013). In the panel B, the peak at 120 °C presented in APCs, associated with the surface and crystallization water (Mladenovska et al.,

2007) in the material and its release during heating, was shifted to a higher temperature for AP-11. Moreover, AP-11 presented a broad peak at 180 °C related to the melting peak of pectin and an exothermic peak at 250 °C associated with both alginate and pectin (Figure 38-d). APCs exhibited a structural rearrangement at 250 °C and a broad peak around 300 °C related to the degradation of chitosan (Figure 38-e,f,g). Specifically, APC-111 showed an exothermic peak at 250 °C similar to AP because the polymers were present in the same concentration and one around at 300 °C correlated to chitosan degradation, less evident than previous (Figure 38-e). APC-117, on the contrary, showed the opposite trend for the higher concentration of chitosan. The first peak was more widened respected to the peak at 285 °C due to the formation of an interaction between the carboxylate group (-COO-) of alginate and the ammonium group (-NH³⁺) of chitosan as reported from IR analysis (Figure 38-g). APC-117-10Bic presented the exothermic peak around 300 °C related to the decomposition of chitosan shifted at a lower temperature, maybe for the different rearrangement of matrix polymeric, on the contrary APC-117-5Et did not show significant differences (Figure 38-h, i).

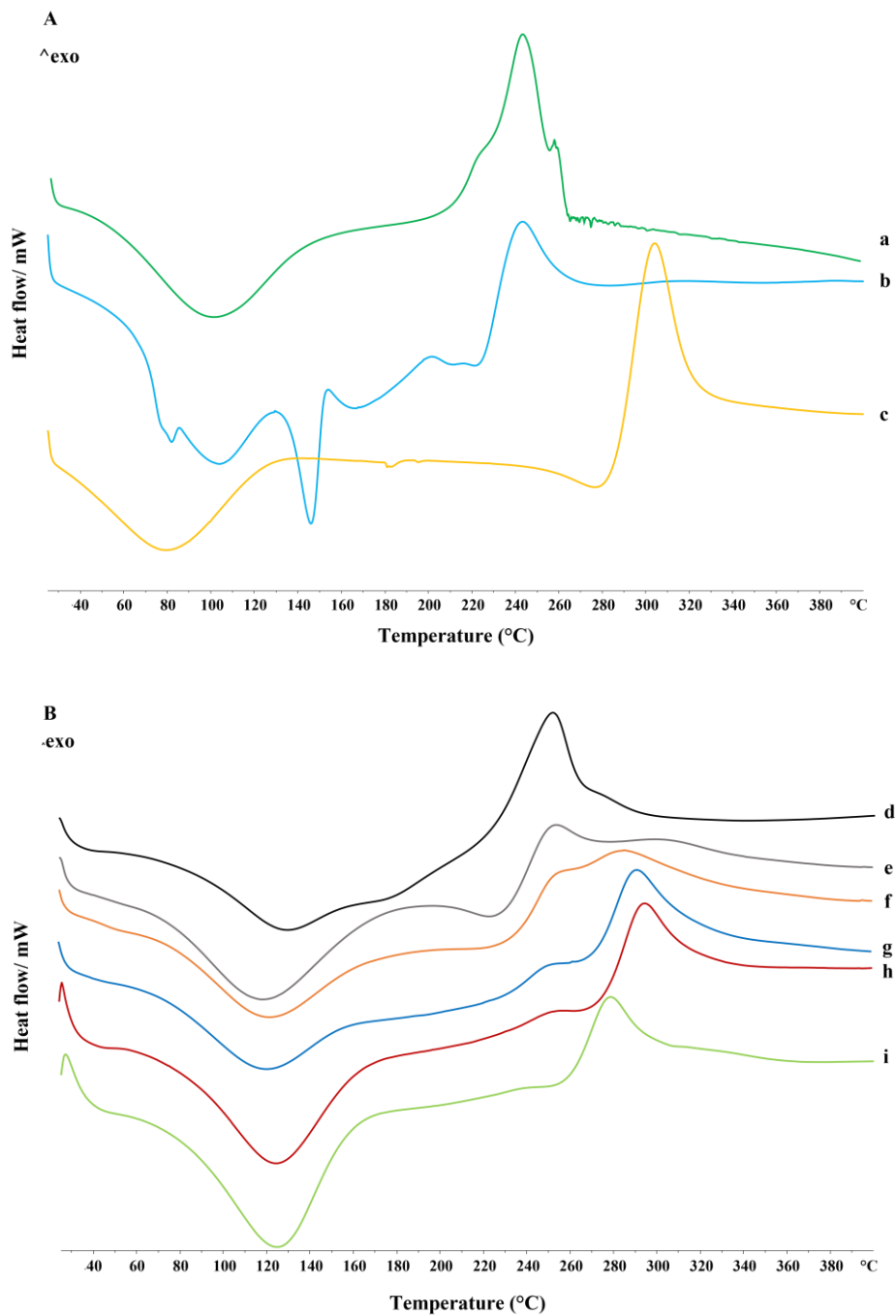
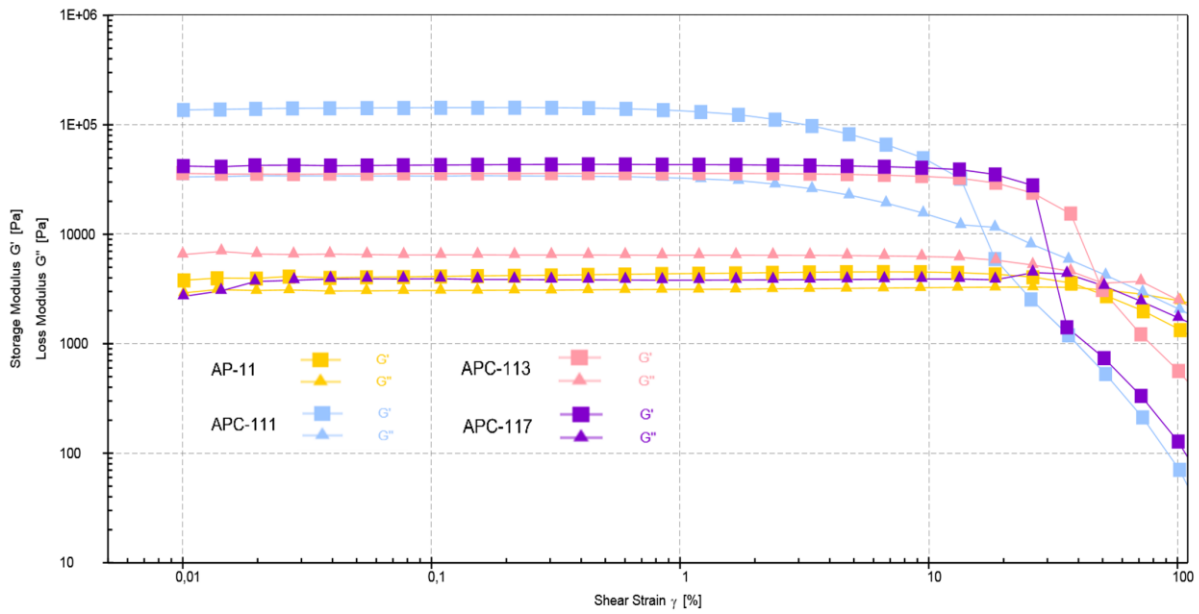


Figure 38. Differential scanning calorimetry (DSC) thermograms. Panel A: alginate (a), amidated pectin (b), low MW chitosan (c). Panel B: AP-11 (d), APC-111 (e), APC-113 (f), APC-117 (g), APC-117-5Et (h) and APC-117-10Bic (i).

The amplitude sweep test was employed to evaluate the viscoelastic properties of the *in situ* gel powders. By analyzing panel A of figure 39 the dynamic moduli curves of the systems

showed a similar viscoelastic trend, with storage modulus (G') greater than loss modulus (G'') indicating that the samples showed a gel-like behavior. Since the storage modulus is correlated with the number of junctions per unit volume higher value of G' than G'' means that the formulations had the characteristics of a gel. While in AP these values were almost overlapping, APC-117 showed a G' about 10% higher than APC-113 and 18% higher than APC-111 with a reduction more noticeably which caused the collapse of the gel (Belali et al., 2017). This behavior can be better explained through $\tan \delta$ (Figure 39 panel B), the factor that represents the ratio between viscous and elastic behavior, which highlighted an increase in the viscoelastic behavior of the hydrogels according to the amount of chitosan. Usually, in practical applications, $0.01 < \tan \delta < 1$ describes a gel-like behavior, where 0.5 represents the transition point from a prevalent solid-like to a prevalent liquid behavior. In the AP formulation, $\tan \delta$ is > 0.5 , on the contrary, in APC formulations, this value decreases proportionally to the increase of chitosan concentration, demonstrating that in this kind of hydrogels, the corpuscular part predominates over the liquid part.



B

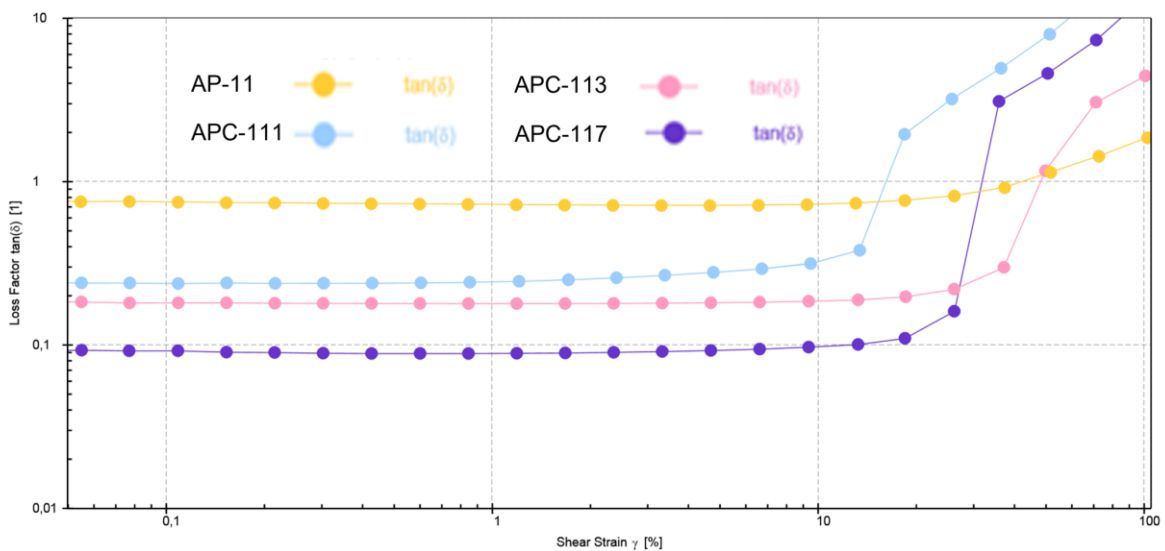


Figure 39. Rheological characterization of AP-11, APC-111, APC-113, and APC-117.

Storage G' and loss G'' moduli evaluated via amplitude sweep test (Panel A) and strain dependent tangent of loss factor (Panel B).

The rheology curves of the formulations APC 117-5Et and APC-117-10Bic showed the similar viscoelastic character of blank formulation APC-117, predominantly gel, with a higher value of G' than G'' (Figure 40). However, the addition of the ethanol induced an increase of

these values demonstrating that the addition, had a slight reinforcing effect on the polymeric matrix, soft and elastic membranes being obtained. The same results have been obtained with NaHCO_3 maybe due to the neutralization of chitosan with bicarbonate through H-bonding that increased gel structuring (L. Liu, Tang, Wang, & Guo, 2011).

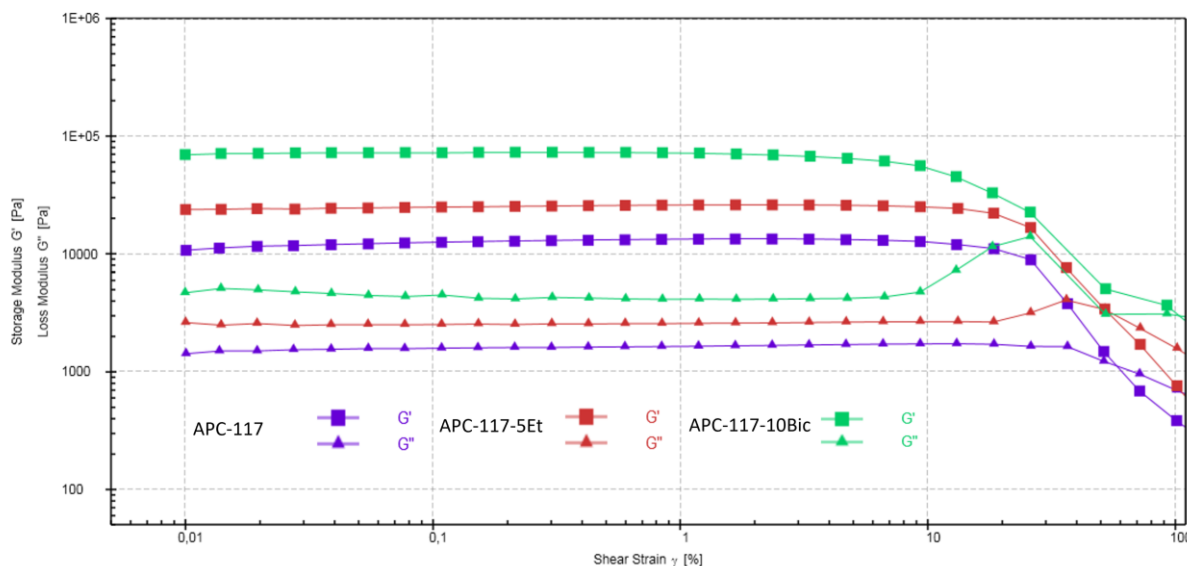


Figure 40. Rheological characterization of AP-117, APC-117-5Et, and APC-117-10Bic.

Storage G' and loss G'' moduli evaluated via amplitude sweep test.

3.2.2.5 In vitro cell studies

Biocompatibility of the polysaccharides blend powders was assessed by monitoring cytotoxic activity (MTT assay) on human keratinocyte cells (HaCaT). Cells were exposed to single polymers alginate, pectin, and chitosan, two polymers blended in different combinations, and alginate-pectin-chitosan blends at different ratios (1:1:1, 1:1:3, and 1:1:7). Treatment with the individual components of the formulation did not show any statistically significant cytotoxicity at the concentrations used (0.01-10 $\mu\text{g}/\text{mL}$), in contrast to what is observed with the positive control (SDS 1%). Furthermore, the vehicle of chitosan (0.01-0.1% acetic acid) did not induce alteration of cellular respiration, such that it did not prove to be cytotoxic (Figure 41).

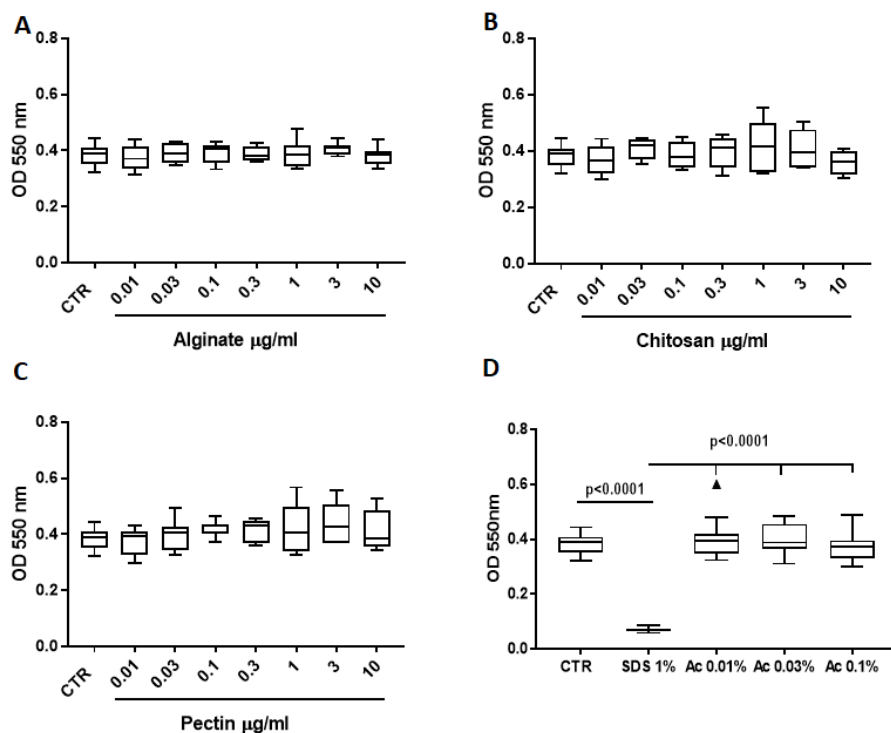


Figure 41. Results of MTT assay after treatment of HaCaT cells (human keratinocytes) with alginate (A) chitosan (B) and pectin (C) and SDS 1% or acetic acid (D). In abscissas, the concentrations of the single products tested, in ordinates the optical density (OD) value, the function of the cell viability according to the MTT assay. The statistical analysis was determined by one-way ANOVA with the Bonferroni test as a post-test.

Moreover, as shown in Figure 42, no formulation made of the two or three polymers blend produces any significant cytotoxic activity in the range of 0.01-10 $\mu\text{g/mL}$.

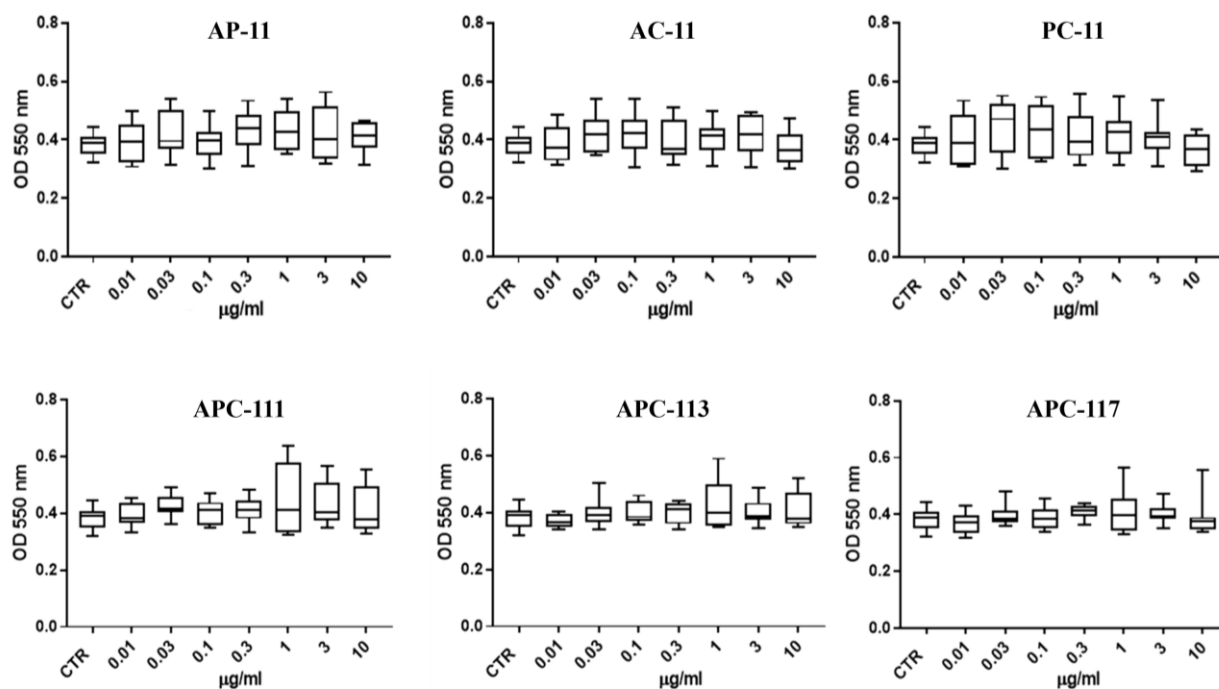


Figure 42. Cell viability assessed by MTT test on HaCaT cells after 24 h of treatment with blends of alginate-pectin (AP-11), alginate-chitosan (AC-11), pectin-chitosan (PC-11), and blends of alginate-pectin-chitosan in different polymer ratios: APC-111, APC-113, and APC-117. Data are represented as median \pm interquartile range ($n = 7$). The statistical analysis was determined by one-way ANOVA with the Bonferroni test as a post-test.

The toxicity test results were used to evaluate the pro-inflammatory activity of the powders by the release of the cytokines IL-6 and $\text{TNF}\alpha$ and of the chemokine IL-8 (CXCL-8) mediators in the inflammatory process (Ashcroft et al., 2012; Z. Q. Lin, Kondo, Ishida, Takayasu, & Mukaida, 2003) For these experimental assays, 0.1-0.5-1 $\mu\text{g/mL}$ concentrations were chosen, not only because they were non-cytotoxic, but also because these solutions did not show any solid residues in the culture medium for the formation of hydrogel in contact with aqueous solutions. The presence of these residues, visible in the solutions at concentrations 3 $\mu\text{g/mL}$ and

10 μ g/ml could cause technical alterations in the ELISA assay. The results indicated that treatment with alginate, pectin, or chitosan did not alter basal levels of IL-6 (Figure 43 A), TNF- α (Figure 43 B), after 24 hours of treatment. Nevertheless, there is a trend toward a non-statistically significant increase in IL-8 (Figure 43 C) after treatment with each of the three components.

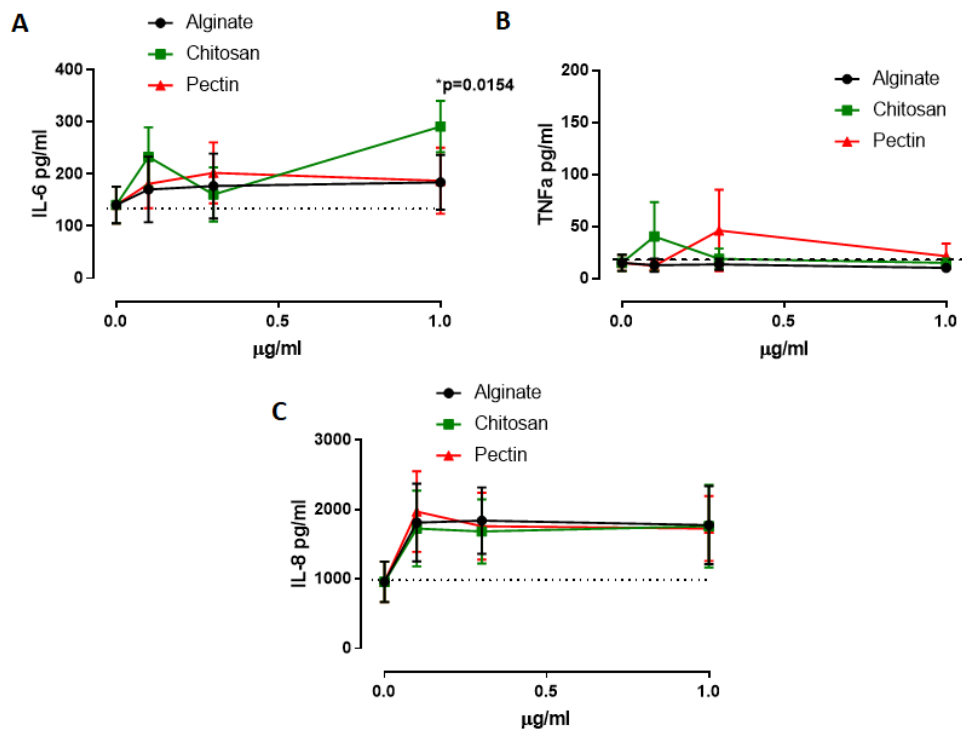


Figure 43. Levels of IL-6 (A), TNF- α (B), and IL-8 (C) after treatment of HaCaT cells with single components alginate, chitosan, and pectin. The dashed line represents basal levels which are represented by the value 0 in the abscissa. In abscissas, the concentrations of the single products tested, in ordinates, the quantitative value, expressed in pg/mL, of the cytokines under investigation. The statistical analysis, obtained through the Two-Way ANOVA followed by Tukey's post-test, was carried out concerning the basal levels.

As shown in Figure 44, APCs did not alter the levels of IL-6 and TNF- α compared to their basal levels. On the contrary, APC formulations were able to induce, even within the limits of

significance ($p = 0.04$), a higher release of IL-8 from the human keratinocytes when tested at the concentration of 1 $\mu\text{g}/\text{mL}$. This result might be due to the interaction between chitosan and alginate that led to the reduction of positive charge and the increase of hydrophobicity of the chitosan. Consequently, the chitosan interacting with cells might have favored the release of IL-8 (Park, Gabrielson, Pack, Jamison, & Wagoner Johnson, 2009). Although could be a negative datum, as reported in the literature, IL-8 is able to increase the keratinocytes migration rate suggesting that the APC powders could stimulate the wound healing process in difficult-healing wounds (Jiang, Sanders, Ruge, & Harding, 2012).

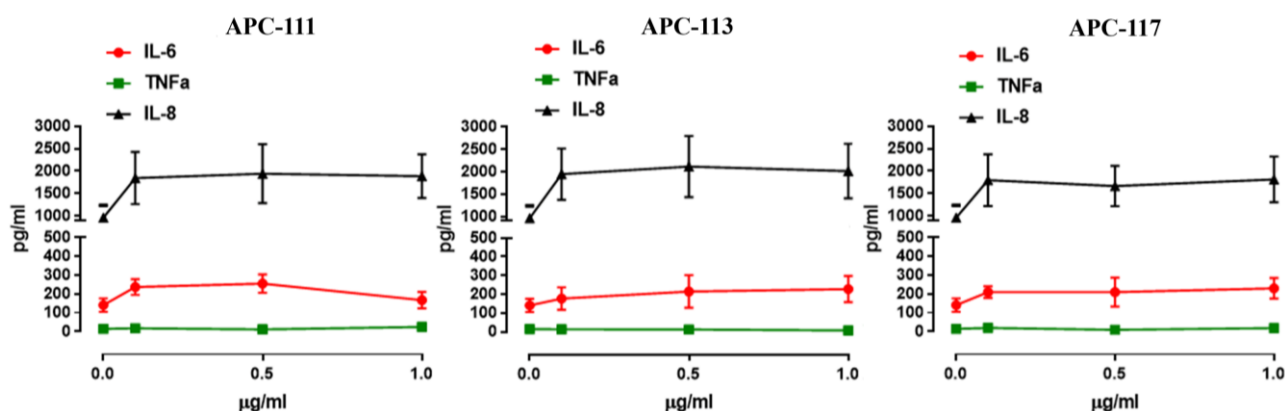


Figure 44. Pro-inflammatory effect of APCs particles at various concentrations in terms of release of IL-6, TNF α , and IL-8. The statistical analysis, obtained through the Two-Way ANOVA followed by Tukey's post-test, was carried out concerning the basal levels.

3.2.2.6 Alginate-pectin-chitosan in situ gelling powders: pilot scale-up

Based on the results obtained from the production in the laboratory, according to the aim of this industrial doctoral program, formulation alginate-pectin-chitosan (APC) with three different total polymeric ratios 1:1:1, 1:1:3, 1:1:7 with 10% of NaHCO_3 were produced on large scale. The specific objective was to produce powders increasing the concentration of the total polymer and improving the feeding rate. This objective was divided into 2 distinct phases:

- Phase 1: optimization of the process maintaining the product quality attributes.

- Phase 2: up scaling of formulation and process on spray dryer pilot plant.

In order to verify the feasibility of the production process on an industrial scale, a pre-pilot and pilot spray drying plant were tested to produce the *in situ* gelling powders. The preparation of the feed solutions remained unchanged and so did the type of atomization, using a two-fluid nozzle. In order to increase the amount/h of the powder the nozzle used to spray the feeds was larger, diameter 1.1 mm, compared to the one used in the laboratory apparatus (0.5 mm). The second variable changed to increase the production rate of the powder was the concentration of the total polymer: various tests were conducted until it was set at 0.9%, a strong increment compared with the 0.15% reached with the spray drying at laboratory scale. The feeding rate was increased from 4 mL/min to 60, 468, and 318 mL/min for APC 111-APC 113 and APC 117, respectively. This made it possible to obtain a larger quantity of product in less time in order to reach companies production standards. The powders obtained with a pre-pilot plant were all white with few exceptions where the powders resulted in pale yellow; in all cases, process yield and size distribution was in line with the experiments made up in the laboratory. The formulation APC-117 with a higher chitosan ratio produced a higher process yield (69.5%). Based on these results, the formulation APC-117 was produced using a spray drying pilot plant obtaining, however, a lower yield of 47.7% (Table 7).

Table 7. *Composition, process yield, and particle size of powders produced by mini spray drying.*

Sample	Alginate-Pectin-Chitosan Ratio	Yield (%)	d ₅₀ (µm)
APC-111	1:1:1	26.9	3.3
APC-113	1:1:3	42.0	3.3
APC-117	1:1:7	69.5	3.1
APC-117 (pilot)	1:1:7	47.7	3.0

3.2.3 Conclusions

This part of the thesis focused on the production of alginate-pectin and alginate-pectin-chitosan powders capable to move rapidly from powder to gel at the site of chronic tissue lesions creating an optimal environment for the healing process using spray drying technology. The choice of excipients was related not only to the high biocompatibility, biodegradability, and high capacity to absorb exudate but also to their ability to stimulate the healing process. The powders were produced both with the mini spray dryer and nano spray dryer to compare the two different atomization techniques. All formulations showed a good process yield, however in the presence of chitosan the yields were higher than formulations consisting only of alginate and pectin. SEM showed that particles consisting of alginate, pectin, and chitosan presented a wrinkled surface as chitosan tended to deposit on the alginate-pectin matrix, and this phenomenon was more and more evident with the increase of the amount of chitosan present. Particles made of alginate and pectin, on the other hand, had a smooth surface and a regular spherical shape. Moreover, the powders showed a good fluid uptake capacity and a rapid gelation process and these results were more evident in the particles produced by mini spray drying. Specifically, the formulations with a higher amount of chitosan, APC-117, have shown themselves to be the most promising since were able to produce immediate gelling powders in around 5 minutes. Among these, the APC-117 with ethanol at 5% V/V or with the addition of sodium bicarbonate 10% w/V were the best. Specifically, the formulation with sodium bicarbonate could be more promising since does not involve the use of organic solvents. Moreover, *in situ* gelling powders showed a good level of elasticity useful for topical application. Furthermore, formulations did not show cytotoxic activity on HaCat cells and pro-inflammatory activity in terms of the levels of IL-6 and TNF- α , whereas they were able to induce the release of IL-8 from the human keratinocytes that could stimulate the wound healing process in difficult healing. In addition, these formulations have been tested on a large-scale

production plant, which has resulted in the possibility to process feeds with a higher polymer concentration in the feed solution and higher feeding rates, while retaining the characteristics of the powder prepared in the laboratory. Such results, and taking also into account the process yield, are very promising regarding the cost/effectiveness of the final product and it is encouraging about the possibility to move the production to the industrial scale.

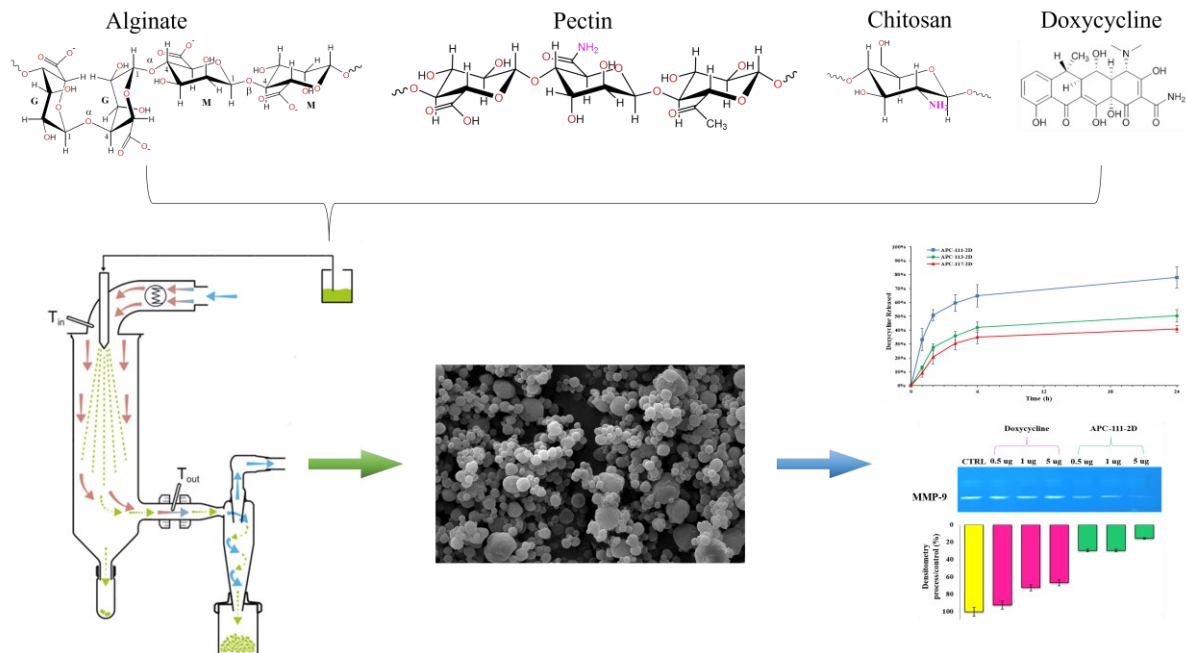
3.3 SECTION C

Alginate-pectin and alginate-pectin-chitosan *in situ* gelling powders loaded with doxycycline

Based on the article:

Chiara Amante, Tiziana Esposito, Pasquale Del Gaudio, Veronica Di Sarno, Amalia Porta, Alessandra Tosco, Paola Russo, Luigi Nicolais, Rita P. Aquino. A Novel Three-Polysaccharide Blend in Situ Gelling Powder for Wound Healing Applications. *Pharmaceutics*. Volume 13, 2021, 101680, ISSN 1999-49.

<https://doi.org/10.3390/pharmaceutics13101680>



3.3.1 Scientific background

In large or difficult-to-heal chronic wounds, healing can be altered by pathogens and microorganisms leading to severe wound and systemic infections, especially in aged people (Demidova-Rice, Hamblin, & Herman, 2012; Yang et al., 2017). In these cases, the encapsulation of active agents is extremely important for the resolution of the injury. To remedy chronic or bacteria-infected wounds, in the last years, numerous dressings have been developed based on natural polymers, not only for their biocompatibility and biodegradability, but, also due to the ability to improve the healing process (F. De Cicco et al., 2016; R. Huang et al., 2015; Jeon, Samorezov, & Alsberg, 2014; Kucińska-Lipka et al., 2019). Polysaccharide-based hydrogels, due to their ability to manage the exudates, can be used as dressings to prevent the formation of a substrate for bacteria proliferation (Giulia Auriemma et al., 2020; Percival, McCarty, Hunt, & Woods, 2014). However, most dressings based on natural polysaccharides lack conformability and exudate absorbance (Rabiee, Yeganeh, & Gharibi, 2019), on the contrary *in situ* gelling hydrogel are able to properly fill the wound site, absorbing and retaining the excess of exudate (Tran, Joung, Lih, & Park, 2011), while the use of an appropriate mixture of polysaccharides allows the formation of a transparent cover to follow the healing process (Pal, Banthia, Majumdar, & organs, 2006).

This part of the thesis was focused on the production of innovative *in situ* gelling powders based on different polymers used as adjuvants in the wound healing process and as a carrier for doxycycline. Based on the results obtained from the blank formulations in section III of this thesis alginate-pectin and alginate-pectin-chitosan blends have been studied with particular attention to the amount of chitosan considering its influence on drug encapsulation and its release.

Alginate, with high mannuronic content, is able to induce cytokine production by human monocytes more than alginate with a high G content, a very useful process in wound healing

(Szekalska et al., 2016; A. Thomas et al., 2000). As demonstrated in a previous work reported in section II the combination alginate-pectin blends allowed to obtain *in situ* gelling submicropowders with appropriate wound dressing properties in terms of adhesiveness and transpiration that can quickly gel when in contact with wound fluids (P. Del Gaudio et al., 2020).

Chitosan represents a good candidate for wound healing due to its numerous biological properties, including excellent bioactivity as hemostatic properties, antimicrobial and anti-inflammatory activity (Dash, Chiellini, Ottenbrite, & Chiellini, 2011; Dragostin et al., 2016; Lupascu et al., 2015; Patrulea, Ostafe, Borchard, & Jordan, 2015; Xia, Liu, Zhang, & Chen, 2011). The antimicrobial effect of chitosan is strongly dependent on its molecular weight and degree of deacetylation and at the same time on the intrinsic differences in target bacterial wall structure (Huh & Kwon, 2011; T. Kean & Thanou, 2010). Three models of chitosan antibacterial activity have been proposed (Abdeltwab, Abdelaliem, Metry, & Eldeghedy, 2019; Goy, Britto, & Assis, 2009): (I) interaction between positively charged chitosan molecules and negatively charged microbial cell membranes, resulting in the cell wall structure and the permeability of the cell membrane, (II) binding of chitosan with microbial DNA and consequent inhibition of the mRNA and protein synthesis, and (III) chelation of metals and consequent decrease in the activities of metalloproteins.

Doxycycline, a semisynthetic analog of tetracycline (Figure 45), has been used as an antimicrobial model drug due to its broad spectrum bacteriostatic drug against Gram-positive and Gram-negative bacteria (Golub et al., 1995) by binding reversible to the bacterial 30S ribosomal subunit and blocking incoming aminoacyl tRNA from binding to the ribosome acceptor site. Furthermore, doxycycline is able to inhibit host matrix metalloproteinases (MMPs), hyper expressed in chronic wounds, through the chelation of calcium or zinc ions necessary for the enzymatic activity of metalloproteinases (García et al., 2005; Stechmiller,

Cowan, & Schultz, 2010). In the normal tissue, MMPs are expressed at basal levels, but, when tissue remodeling is mandatory, as in wound healing, MMPs can be rapidly expressed and activated, involving the bond with zinc ions in the active site (Van Wart & Birkedal-Hansen, 1990). MMPs play a vital role in wound healing modifying the wound matrix, allowing cell migration and tissue remodeling; however, excessive expression of MMPs may inhibit wound closure (Caley, M. P., Martins, V. L., & O'Toole, E. A. 2015).

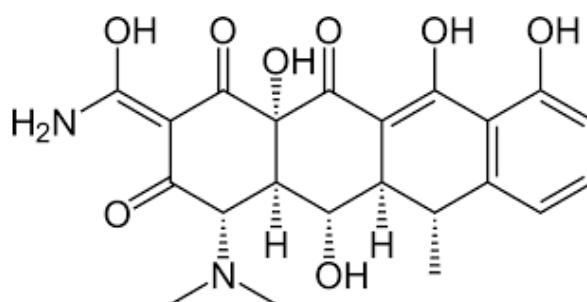


Figure 45. *Molecular structure of doxycycline.*

The *in situ* gelling powders have been characterized in terms of yield, morphology, size distribution, FT-IR analysis, and drug encapsulation efficiency. Moreover, the fluid uptake ability of the powders and drug release have been evaluated. Antimicrobial tests against bacteria that normally colonize the wounds and zymography to evaluate the inhibition of MMPs, using HaCaT cells, were performed in order to assess the efficacy of the doxycycline encapsulated in the APC formulations when used to treat infected wounds.

3.3.2 Results and discussion

3.3.2.1 Preparation and characterization of the powders

The blank formulations reported in the previous chapter of this manuscript, alginate-pectin (AP), and alginate-pectin-chitosan (APC), were used as a carrier to vehicle a drug model: doxycycline. Mini spray and nano spray drying were used to produce *in situ* gelling powders with different polymer ratios. The total polymer was found at 0.15% (w/v) as high chitosan content did not allow an effective preparation of powders, whereas two different concentrations of doxycycline were studied (1 and 2 % w/w). Three different polymers ratio were considered: AP 1:1, 1:3, 3:1 and APC 1:1:1, 1:1:3, 1:1:7. These concentrations were chosen to ensure, during the release of the active ingredient a concentration above the MIC (minimum inhibitory concentration), but within the therapeutic window. Ac2-26 loaded alginate-pectin submicropowders (II section) and alginate-pectin-chitosan submicropowders (III section) were prepared with a nano spray dryer. However, the addition of doxycycline to APC formulations did not allow to obtain nanoparticle formulations with an adequate yield, and in the case of APC-111, it was not possible to conclude the process and collect a product, since the starting feed solution was already more turbid and tending to gelling. Probably due to the formation of a neutral adduct between the active and the polymers, which involved the -NH₂ residues of the chitosan and the -OH residues of the active, a feed solution more difficult to atomize was obtained. Moreover, the formation of neutral adducts affected the variation of the electric field induced by the piezoelectric crystal, causing the formation of a layer of gel that occluding the membrane of the instrument made it impossible to complete the atomization process.

The same difficulties did not concern the mini spray drying process, as atomization is not affected by the formation of such neutral adducts. As reported in Table 8, the comparison between mini spray dried particles obtained from AP and APC at different ratios shows that the presence of the drug did not affect the yield of the process instead, was influenced by chitosan.

Higher the concentration of chitosan the higher the yield (60-70 %), due to an increase in viscosity of the feed related to alginate-chitosan interaction. In the same way, the increase of chitosan concentration conducted greater encapsulation of the drug, evaluated via HPLC analysis. Alginate-pectin powders showed an E.E. of about 70% not significantly influenced by the polymeric blend whereas the E.E. for alginate-pectin-chitosan particles ranged between 67% and 78%, according to the relative amount of chitosan in the formulation. Such results indicated an interaction between amino residues of the chitosan and hydroxyl groups of doxycycline

Table 8. *Composition, process yield, particle size, drug content, and encapsulation efficiency (E.E.) of powders obtained with different polysaccharides ratio by mini spray drying.*

Samples	Alginate-Pectin-Chitosan Ratio	Doxycycline % (w/w)	Yield (%)	Drug Content (%)	E.E. (%)	Mean Diameter (μm) \pm SD
AP-11	1:1	-	63	-	-	2.07 \pm 0.08
AP-31	3:1		65			2.16 \pm 0.11
AP-13	1:3		61			2.85 \pm 0.49
AP-11-1D	1:1	1.0	62	0.70	69	2.11 \pm 0.12
AP-11-2D	1:1	2.0	62	1.41	70	2.13 \pm 0.15
AP-31-2D	3:1		64	1.33	66	2.21 \pm 0.13
AP-13-2D	1:3		66	1.38	69	2.74 \pm 0.43
APC-111	1:1:1	-	60	-	-	3.24 \pm 0.13
APC-113	1:1:3		72			2.75 \pm 0.10
APC-117	1:1:7		73			2.58 \pm 0.04
APC-111-1D	1:1:1	1.0	62	0.69	69	3.25 \pm 0.08
APC-113-1D	1:1:3		68	0.72	72	2.78 \pm 0.09
APC-117-1D	1:1:7		70	0.78	78	2.24 \pm 0.13
APC-111-2D	1:1:1	2.0	62	1.33	67	3.59 \pm 0.09
APC-113-2D	1:1:3		71	1.41	71	2.69 \pm 0.12
APC-117-2D	1:1:7		74	1.56	78	2.42 \pm 0.11

The polymers concentration influenced, also, the size and morphology of the powders, on the contrary, the loading of doxycycline did not affect these characteristics, as shown in SEM images (Figure 46-d,e,f and 47-d,e,f).

AP particles showed a mean diameter ranging between 2.07 and 2.85 μm , which increases as the concentration of pectin increases. Furthermore, although all AP formulations presented a spherical shape (Figure 46-a,b,c) AP-13 exhibited a partially shrunken shape (Figure 46-c).

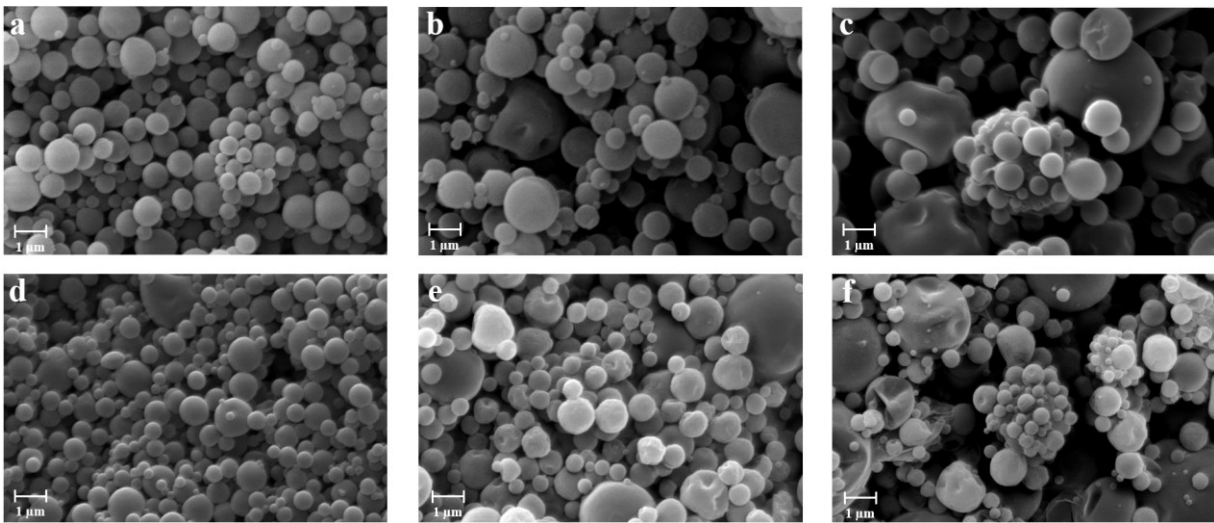


Figure 46. SEM microphotographs of alginate-pectin powders produced by mini spray drying with different polymers ratios: blank particles AP-11 (a), AP-31 (b), AP-13 (c), and doxycycline loaded particles AP-11-2D (d), AP-31-2D (e), AP-13-2D (f).

In APC powders, the amount of chitosan influenced both particle size and size distribution, in fact, SEM images showed that concerning the increase of chitosan in the formulations, the particles gradually assumed greater surface roughness, reducing, in the same time, mean diameter and the tendency to agglomerate with each other during the drying phase (Figure 47-a,b,c).

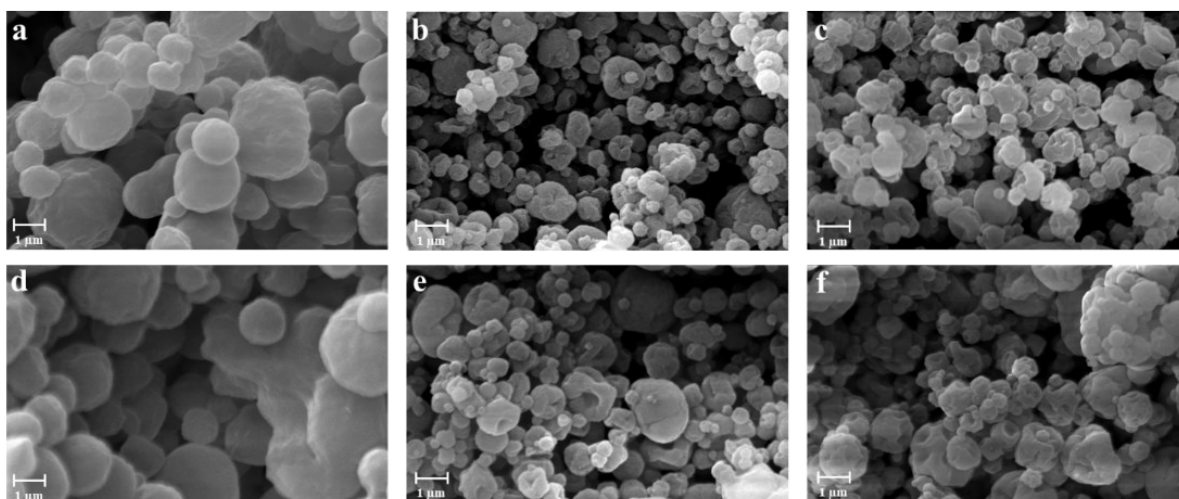


Figure 47. SEM microphotographs of alginate-pectin powders produced by mini spray drying with different polymers ratios: blank particles APC-111 (a), APC-113 (b), APC-117 (c), and 2% (w/w) doxycycline-loaded particles APC-111-2D (d), APC-113-2D (e), APC-117-2D (f).

As *in situ* gelling formulation should become rapidly a gel when in contact with wound exudates and should be able to cover the wound bed homogeneously, all formulations were placed in contact with SWF and at a defined time point the increase in weight was calculated. As reported in Section II, all formulations exhibited quick interaction with SWF, with APCs formulations having a faster fluid uptake ability than powders without chitosan. In fact, APC-117 powders were able to become a gel within 2 min on the surface on which they were spread (Figure 48).

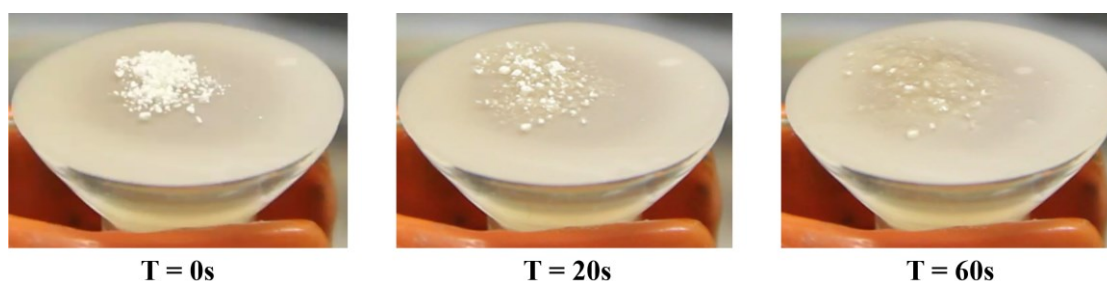


Figure 48. The ability of APC-117 to move into a gel from dry powder.

Doxycycline-loaded APCs formulations showed lower fluid uptake ability compared to their blank homologs, in which APC 117 increased more than 1500 times its weight, as reported in

the previous part of this thesis (Section III). Such a trend was related to the amount of doxycycline loaded into the particles. According to the hypothesis that doxycycline interacts with chitosan APCx-1D formulations exhibited a higher fluid uptake than APCx-2D. This phenomenon might be related to interaction via hydrogel bonding able to reduce the ability of the powders to interact with a fluid (Figure 49).

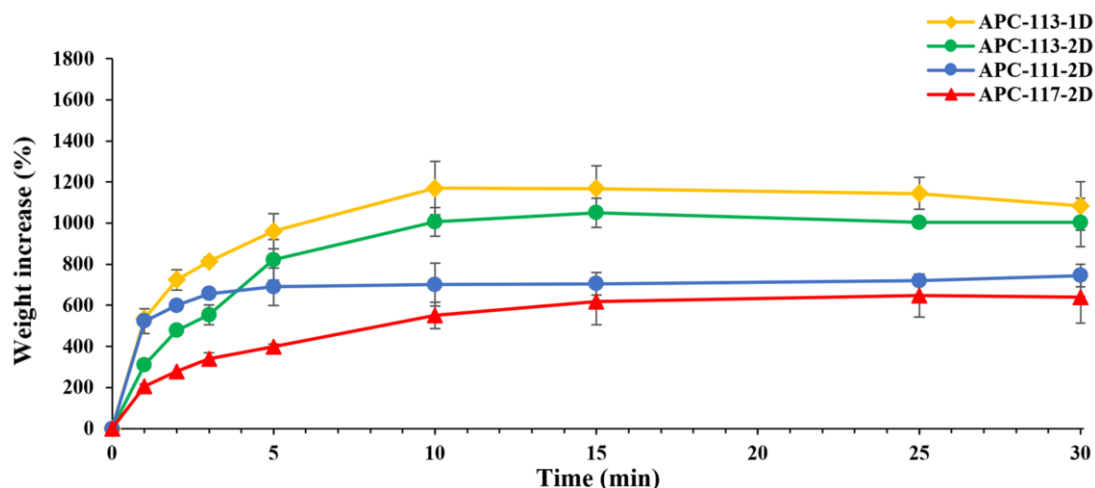


Figure 49. Simulated wound fluid uptake of alginate-pectin-chitosan powders loaded with different amounts of doxycycline.

FT-IR studies have been performed to evaluate the formation of interactions between the drug and the polymer matrix after the production of the loaded particles. These interactions could be useful to promote the prolonged drug release from powders extending its efficacy. Figure 50 reports the spectra of the drug, blank polymer particles APC-111, and loaded particles APC-111-2D in the region where doxycycline shows the most characteristic peaks, between 1800 and 1300 cm^{-1} (Silva et al., 2015). In the spectrum of doxycycline stretches of C=O were present at 1680 and 1614 cm^{-1} , while the carbonyl groups of the two rings were shown at 1602 and 1573 cm^{-1} . At 1525 cm^{-1} , the band corresponding to the amino group of the amide was shown, whereas the band at 1455 cm^{-1} corresponded to the C=C skeleton vibration (Figure 50-a). In the same region, APC presented several bands of the single polymers overlapped (Figure

50-b). The broad peak at 1600 cm^{-1} represented the asymmetric stretching band of the carboxylate ion of the alginate, the characteristic amide I and amide II bands of pectin and chitosan. Moreover, alginate presented symmetric stretching vibration of the carboxyl group at 1408 cm^{-1} where pectin showed COO stretching. The spectrum of alginate-pectin-chitosan particles loaded with doxycycline (Figure 50-c) showed a similar spectrum of APC, but, with a shift in both amide carbonyl and amino groups of doxycycline. In fact, the peaks of the amide C=O were shifted to 1674 cm^{-1} , while the -NH_2 shifted from 1525 to 1533 cm^{-1} , indicating that an interaction between the polymeric blend and the drug happened via the amide group.

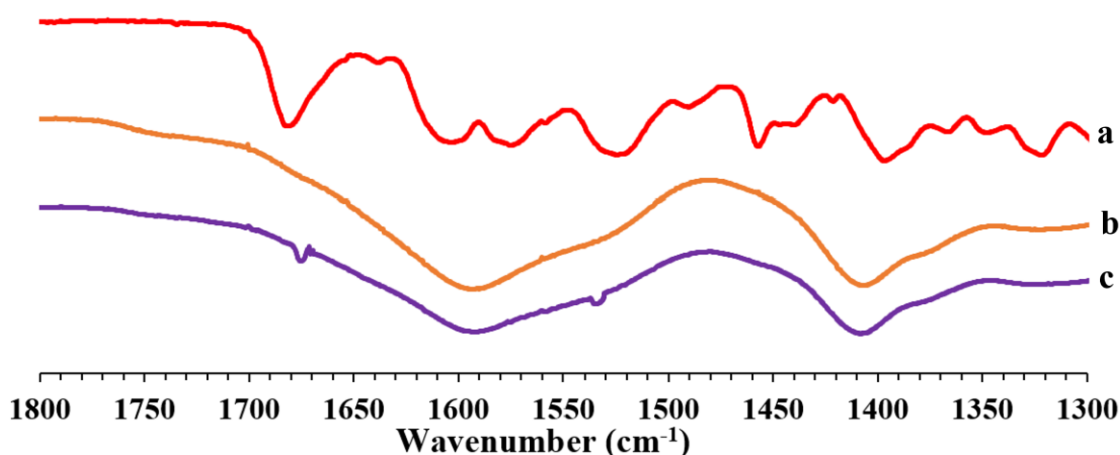


Figure 50. FTIR spectra of drug raw material in comparison with alginate-pectin-chitosan particles and doxycycline-loaded polymeric particles: doxycycline raw material (a), APC-111 (b), and APC-111-2D (c).

3.3.2.2 Drug release

To study the drug release, *in vitro* release experiments were performed using Franz cells and SWF as acceptor fluid. Figure 51 exhibits representative release curves of doxycycline from APC powders obtained from different polysaccharides ratios. Results were compared to doxycycline raw material that was completely released in less than 15 min. All formulations showed a burst effect in the first hours (4 h) followed by a prolonged release over the next hours or days related to the formulation. An initial burst effect within 3 or 4 h from an administration

can result very useful to prevent infection from spreading at the beginning of local antibiotic therapy (Cover, Lai-Yuen, Parsons, & Kumar, 2012). APC-111-2D showed a 60% drug release in 6 hours reaching the total release of the doxycycline in 72 hours, while powders containing more chitosan, APC-113-2D and APC-117-2D, released at the same time about 40% and 35% in 6 hours, and 50% and 65% at 72 hours, respectively. Increasing the percentage of chitosan in the formulation resulted in an inversely proportional effect to the amount of doxycycline released from the gel framework, in fact, the total release of doxycycline in APC-113-2D and APC-117-2D was achieved respectively in 5 and 7 days. Prolonged release of the drug in formulations corroborates the interactions between doxycycline and chitosan, as demonstrated by FT-IR studies. The kinetics of the release can be related to the solubility and/or swelling of the matrix. In this case, although alginate and pectin are water-soluble and chitosan is soluble in acid water, the matrix thanks to the chemical interaction behaves as a single entity. The pH of the feed solutions is the same for the formulations with different concentrations of chitosan, as well as, the pH of gel when in contact with SWF. In addition, the formulations determine the reduction of pH of the medium, leading it to a value closer to neutrality, more convenient to avoid tissue maceration.

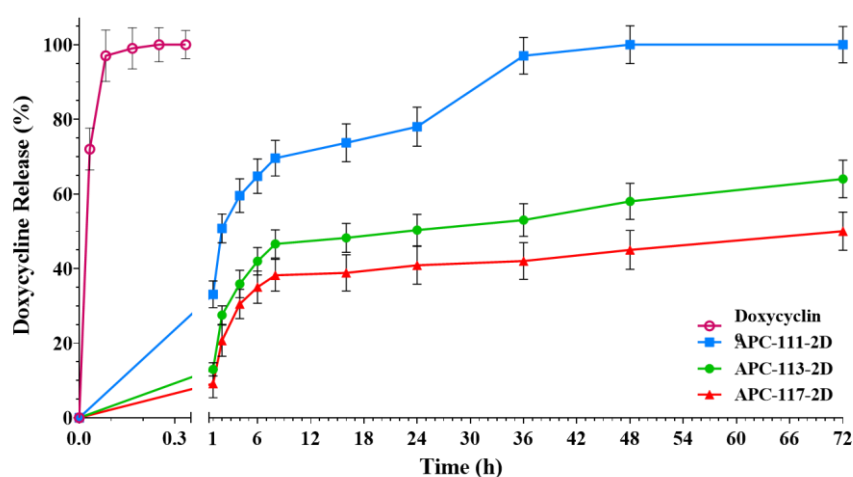


Figure 51. Release profiles of doxycycline loaded alginate-pectin-chitosan powder compared to the pure doxycycline.

3.3.2.3 Antimicrobial tests

To test the antimicrobial activity of doxycycline loaded in APC formulations preliminary antimicrobial assay, disc diffusion test, was carried out against both *Staphylococcus aureus* and *Pseudomonas aeruginosa*, which normally colonize the wounds (Omar, Wright, Schultz, Burrell, & Nadworny, 2017; Serra et al., 2015). A modified disc diffusion test conducted on a Muller-Hinton agar plate spread with *P. aeruginosa*, showed an inhibition zone for none formulations tested since this bacteria is resistant to doxycycline (Figure 52). Unlike what was obtained for *P. aeruginosa*, on agar plate spread with *S. aureus* inhibition zones produced by APC-113-2D, and APC-117-2D were larger than pure doxycycline and APCD-111-2D at 24 h. By normalizing the area concerning the amount of the powder tested on *S. aureus*, Figure 52 shows an inhibition zone with a diameter of 30.64, 29.87, 32.01, and 32.86 mm, for pure doxycycline, APC-111-2D, APC-113-2D and APC-117-2D, respectively.

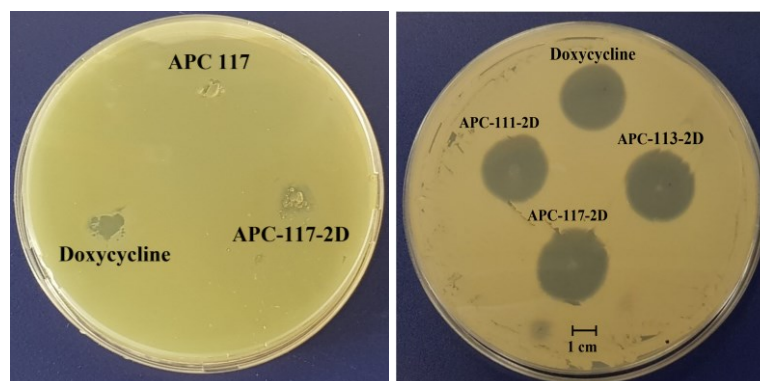


Figure 52. Representative modified diffusion assay conducted against *Pseudomonas aeruginosa* (on the left) and *Staphylococcus aureus* (on the right) at 24 h by APCs-2D at different ratios in concentrations equivalent to 1.55 μg of pure doxycycline, used as control.

Based on results of disc diffusion, a time-killing assay at 1, 2, 3, and 7 days, against *S. aureus* was carried out. Figure 53 shows that all formulations had better antimicrobial activity than pure doxycycline. Pure doxycycline lost its activity after 2 days, on the contrary, all drug-loaded

APCs formulations maintained their activity longer, with APC-117-2D able to preserve most of the antimicrobial activity over the 7-day experiment due to the prolonged release of the drug. Moreover, as demonstrated in blank formulation APC-117, the bacteriostatic effect of chitosan favored the antimicrobial activity of doxycycline (Tao, Qian, & Xie, 2011).

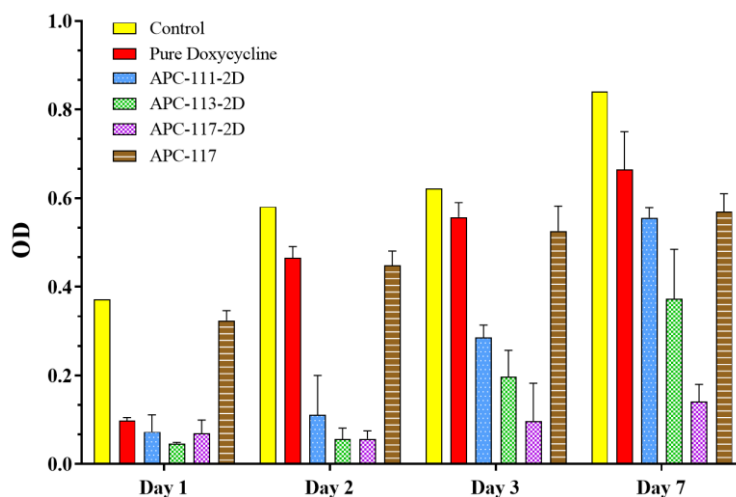


Figure 53. *Time-kill assay against Staphylococcus aureus for doxycycline loaded APC powders in comparison with pure doxycycline and APC-117.*

3.3.2.4 *In vitro* test: SDS-PAGE Gelatin Zymography

Parallel to the antimicrobial activity of the formulation the behavior of doxycycline against metalloproteinases (MMPs) was investigated (Castro, Tanus-Santos, & Gerlach, 2011). Gelatinases (Metalloproteinases 2 and 9) are involved in acute and chronic wounds, playing a crucial role in regulating cell migration, essential for wound re-epithelialization. However, uncontrolled protease activity can lead to a delay in healing (Caley, Martins, & O'Toole, 2015). For this reason inhibitors of MMPs are considered excellent adjuvants to promote wound healing and among them, clinical and experimental studies reported that doxycycline at low doses, is an inhibitor of MMP-2 and 9, reducing the expression and activity of these proteases

(H. Lee, Park, Kim, Lo, & Lee, 2009; H. M. Lee et al., 2004; Ryan, Usman, Ramamurthy, Golub, & Greenwald, 2001; Uitto, Firth, Nip, & Golub, 1994).

To analyse the activity of the doxycycline loaded powders on the MMPs, human epidermal keratinocyte model cells (HEKa) were placed in trans-wells and treated with pure doxycycline and hydrogel containing an increasing amount of doxycycline (0.5, 1 and 5 μg) and avoiding any direct contact with cells. After 24, 48, and 72 h of incubation, the culture media were harvested and subjected to gel zymography. As shown in Figure 54, only MMP-9 (as deduced from the molecular weight) was detected in HEKa conditional media. The gels showed that doxycycline released from hydrogels inhibited the activity of MMP-9 more than the only doxycycline already at the lowest concentration tested and its effect was stable until 72h. This result confirmed that drug encapsulation did not modify the bioactivity of doxycycline but, on the contrary, was able to enhance it perhaps due to the prolonged release of the drug compared to drug solution.

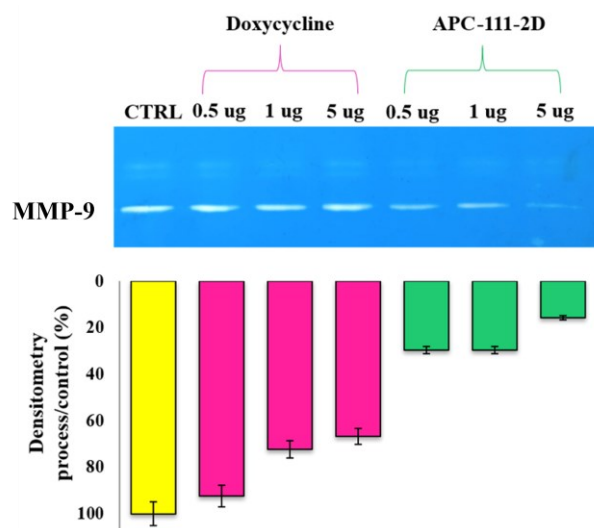


Figure 54. Representative gel zymograms on HEKa cells after 72 hours of treatment with pure doxycycline and APC-111-2D comparing different amounts of doxycycline.

3.3.3 Conclusions

In conclusion, this part of the thesis highlighted the possibility to use mini spray drying with optimized conditions successfully to produce *in situ* gelling powders capable of controlling the release of doxycycline, an antimicrobial model drug with a wide spectrum and the ability to inhibit host matrix metalloproteinases, hyper expressed in chronic wounds. Alginate, pectin, and chitosan were chosen not only for their high biocompatibility, biodegradability, and high capacity to absorb exudate but also for their influence on the stimulation of the healing process. Size, morphology, fluid uptake ability of the particles, as well as drug encapsulation efficiency, were influenced by the presence of chitosan. The increased amount of chitosan led to obtaining particles more wrinkled but more homogeneous in size able to absorb a significantly greater amount of fluid. However, the interaction between polymers and doxycycline led to a reduction in fluid uptake in the formulations loaded. Fluid uptake ability could correlate to the drug release profiles: the slower fluid uptake, the more prolonged the release. In fact, the release of the doxycycline encapsulated in APC powders exhibited a controlled release depending on the alginate-pectin-chitosan ratio, with a burst effect within 4 h, followed by a prolonged release over 24 h for APC-111-2D and with the slower release for the formulations with more chitosan due to minor absorption of the fluid for extensive interaction between the polymeric blend and the drug via the amide group, as demonstrated by FTIR studies. Such interaction did not affect the antimicrobial activity of doxycycline, but, on the contrary, the increased amount of chitosan enhanced antibiotic efficacy. Interestingly, doxycycline-loaded particles were able to increase drug activity against MMPs, with great activity against MMP-9 even at 0.5 µg/mL after 72 h.

3.4 SECTION D

Alginate-pectin-chitosan *in situ* gelling powders loaded sodium hyaluronate

Manuscript to be submitted.

3.4.1 Scientific background

Hyaluronic acid (H) is a natural linear polyanionic polysaccharide composed of alternating units of a repeating disaccharide D-glucuronic acid and D-N-acetyl-d-glucosamine bound with β -glycosidic linkages (H. Li et al., 2018) (Figure 55). H is an essential component of the extracellular matrix and exists in connective tissues, skin, synovial joint fluid, human vitreous humor, joints, and an umbilical cord (Fallacara, Baldini, Manfredini, & Vertuani, 2018). In addition, H can also be obtained through microbial fermentation (Gupta, Lall, Srivastava, & Sinha, 2019). H could have different molecular weights (MW), low molecular weight H (LH, $1-25 \times 10^4$ Da), medium molecular weight H (MH, $25-10 \times 10^4$ Da), high molecular weight H (HH, $> 1 \times 10^6$ Da), and very high molecular weight H (VHH, $> 6 \times 10^6$ Da) (Tavianatou et al., 2019). It is synthesized as high molecular weight and is degraded very fast by hyaluronidases enzymes or reactive oxygen species with the formation of fragments having decreasing sizes (Nyman, Henricson, Ghafouri, Anderson, & Kratz, 2019; Schanté, Zuber, Herlin, & Vandamme, 2011).

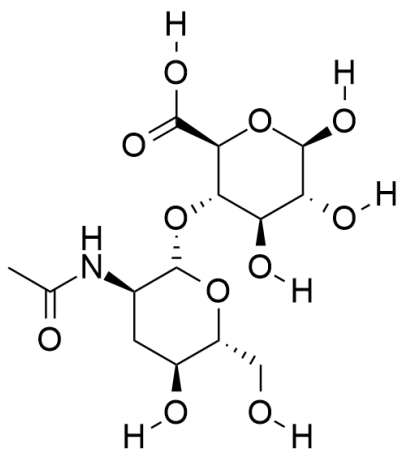


Figure 55. Chemical structure of hyaluronic acid.

The biological effects of hyaluronic acid depend heavily on molecular weight. In the first phase of wound healing, HH through the control of the inflammatory cells recruitment and cytokines production demonstrates an anti-inflammatory effect. Furthermore, HH can interact

with the CD44 receptors available on the monocytes and granulocytes surfaces modulating biological processes such as angiogenesis, cell migration, proliferation, and adhesion to ECM components, the elimination of intracellular reactive oxygen species as well as the reduction of the DNA damage (Litwiniuk, Krejner-Bienias, Speyrer, Gauto, & Grzela, 2016). On the other hand, LH is pro-angiogenic, stimulates the production of pro-inflammatory cytokines as well as promotes leukocyte chemotaxis and growth factors enrolled in the remodeling of skin ECM (Ghatak et al., 2015; Prosdocimi & Bevilacqua, 2012; Tamer et al., 2018).

The intent of this part of the work section has been to the development micropowders composed of an alginate-pectin-chitosan blend loaded sodium hyaluronate to accelerate wound healing. Specifically, two different molecular weights of sodium hyaluronate were introduced into the polymeric blend to compare their potential application as a medical device for tissue regeneration, in a complex polymeric blend. The powders, produced through spray drying, have been described in terms of process yield, morphology and dimensional distribution, and sodium hyaluronate loading. Moreover, fluid uptake ability, FT-IR analysis, thermal behavior, as well as elasticity through rheological studies were determined. In addition, a degradation test was performed to assess the possible application on the wounds.

3.4.2 Results and discussion

Hydrogels formed by sodium hyaluronate (H) can adhere well to the skin surface, enhance skin hydration, and improve drug permeation time (Y.-T. Zhang et al., 2017). Therefore, in this part of the work, the possibility to add two different sodium hyaluronate to an *in situ* gelling powder of alginate, pectin, and chitosan was assessed.

Starting from the formulation with the lowest amount of chitosan, APC 111, produced by mini spray drying, increasing amounts (0.50, 1.00 and 2.00% w/w) of H were added, comparing two different molecular weights, high molecular weight (HH) and low molecular weight (LH). Having obtained encouraging results, the formulations with the higher concentration of chitosan APCH 113 and APCH 117 were investigated.

Initially, knowing that H is soluble in water in the range of pH 5.5-7.5, the polymer was added to the alginate-pectin solution, which has a pH of 5.6, before the addition of chitosan dissolved in an aqueous acidic solution with a pH of 3.5. However, the atomization process of this feed solution to the mini spray dryer was not optimal resulting in a low process yield (< 40%) and material loss. Therefore H was added directly to complete feed solutions of alginate-pectin-chitosan obtaining good process yields from 56 to 72%. As observed in a work made by Liu et al., where the correlation between chitosan concentration and particle size of spray-dried microparticles was studied, also in this work the yield process was influenced by chitosan as the higher the concentration of chitosan the higher the yield, reaching values around 70% (Wenjie Liu, Wu, Selomulya, & Chen, 2011). Interestingly, the increase of hyaluronate concentration, regardless of its molecular weight, led to a higher yield, moving from 56 to 68%, as well as to an encapsulation efficiency reaching a value around 98% in the formulations with 2% of H (Table 9). However, it was not possible to produce formulations APCH 113 and APCH 117 with an H concentration higher than 0.5% since, probably due to polymer interactions, flocculates were formed with loss of material before the spray drying process.

Table 9. *Composition, process yield, drug content, encapsulation efficiency (E.E.), dimension of powders obtained by mini spray drying.*

Samples	Hyaluronate concentration % (w/w)	Yield (%)	Hyaluronate content (%) ± SD	E.E. (%) ± SD	Mean diameter (µm) ± SD
APC 111	-	60	-	-	3.24 ± 0.13
APC 113	-	72	-	-	2.55 ± 0.10
APC 117	-	73	-	-	2.58 ± 0.04
APCH 111-0.5HH	0.5	56	0.37 ± 0.04	73.98 ± 6.87	6.43 ± 0.02
APCH 111-1HH	1	59	0.98 ± 0.03	94.76 ± 3.12	9.00 ± 0.04
APCH 111-2HH	2	66	1.85 ± 0.03	98.61 ± 1.50	12.55 ± 0.01
APCH 113-0.5HH	0.5	72	0.42 ± 0.02	84.15 ± 4.13	3.19 ± 0.04
APCH 117-0.5HH	0.5	71	0.40 ± 0.02	80.58 ± 3.82	3.55 ± 0.01
APCH 111-0.5LH	0.5	57	0.36 ± 0.03	71.45 ± 5.73	9.11 ± 0.2
APCH 111-1LH	1	58	0.96 ± 0.01	96.71 ± 1.96	12.61 ± 0.06
APCH 111-2LH	2	68	1.94 ± 0.02	99.21 ± 1.24	13.95 ± 0.23
APCH 113-0.5LH	0.5	69	0.41 ± 0.03	85.85 ± 4.07	2.95 ± 0.02
APCH 117-0.5LH	0.5	70	0.39 ± 0.01	78.42 ± 2.04	3.50 ± 0.06

As reported in Table 9 chitosan influenced particle size distribution with smaller particles obtained when the concentration was higher. Moreover, in APCH 111, according to the concentration of H, powders had a higher distribution range, probably due to the increase in the viscosity of the solution that led to a particle aggregation (Fallacara et al., 2018; Fatnassi et al., 2014).

SEM images (Figure 56) showed that the formulations containing more chitosan presented particles with greater surface roughness, pores, and clusters due to the alginate-chitosan interaction but a narrower size distribution shown by laser scattering analysis (Kulig, Zimoch-

Korzycka, Jarmoluk, & Marycz, 2016). On the contrary, sodium hyaluronate did not influence the morphology of the powders.

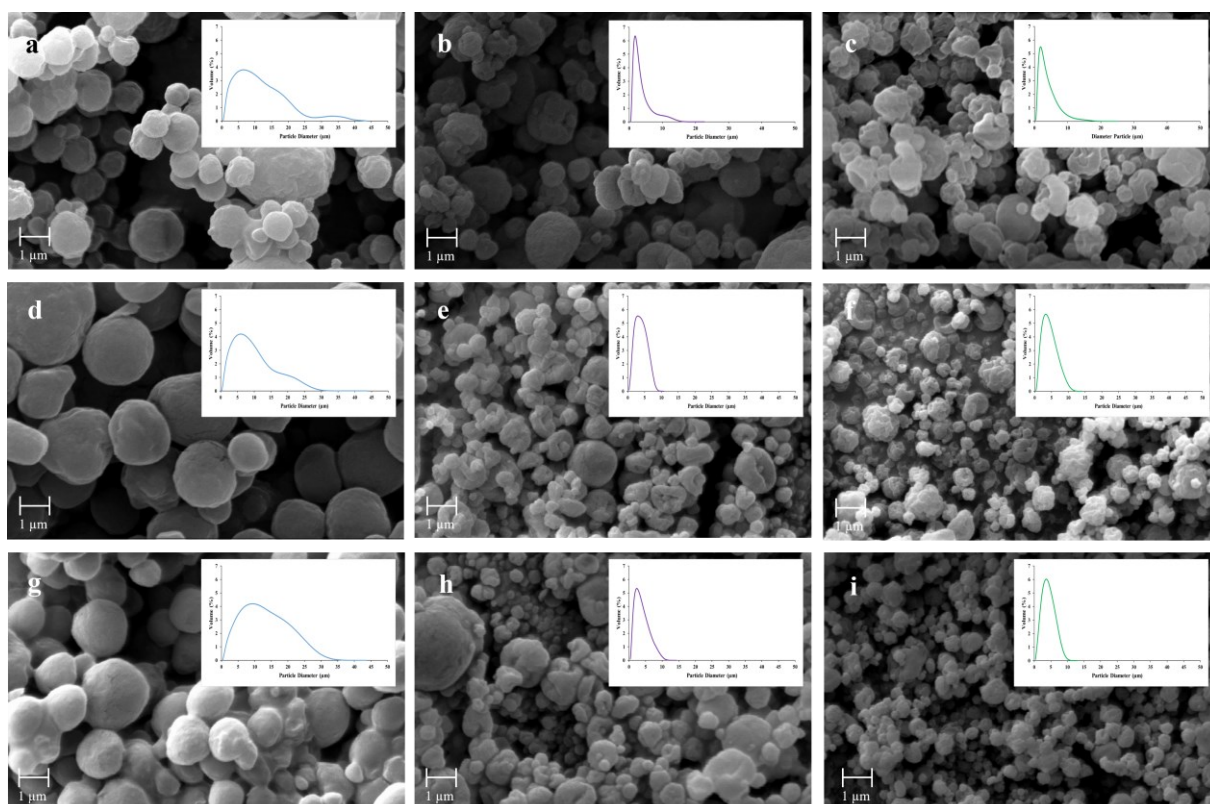


Figure 56. SEM microphotographs with graphs of dimensional analysis (x axis: particle diameter (μm); y axis: volume (%)). First line blank particle: APC 111 (a), APC 113 (b), APC 117 (c); second line particles with high molecular weight hyaluronate: APCH 111-0.5HH (d), APCH 113-0.5HH (e), APCH 117-0.5HH (f); third line particles with low molecular weight hyaluronate: APCH 111-0.5LH (g), APCH 113-0.5LH (h), APCH 117-0.5LH (i).

3.4.2.1 Powders characterization

To evaluate the swelling ability, a key feature for *in situ* gelling powders to favor the release of the bioactive molecules, the powders were subjected to fluid absorption experiments. These studies were conducted using Franz cells and placing the different formulations on a membrane in contact with SWF to mimic *in vitro* the wound environment. Once placed on the membrane, all APCH powders became a gel in a maximum time of 2 min and within 5-15 min reached the

maximum degree of swelling, then establishing an equilibrium for the entire duration of the experiment.

APCH 111, 113 and 117 showed different behavior, according to the concentration of chitosan, due to the size of the microparticles and the different types of interaction of particles with fluid (Figure 57). As chitosan concentration increased, the surface roughness of the particles and their contact with the simulated fluid increased. In fact, although the APCH 117 formulation took a longer time to reach the maximum swelling value due to the poor interaction of chitosan with water, the value reached was considerably higher than the other formulations. Nevertheless, it was interesting to find out that formulation with LH showed swelling lower than formulation with HH and this trend is more evident in the formulation with more chitosan, APCH 113, and APCH 117, due to the formation of a polyelectrolyte complex between positively charged chitosan and negatively charged sodium hyaluronate (Ran Shi et al., 2018). This comportment can be attributed to the structure of low molecular weight sodium hyaluronate that has less hydrophilic groups, such as COOH and OH, available to form bonds with the fluid (Wu et al., 2017).

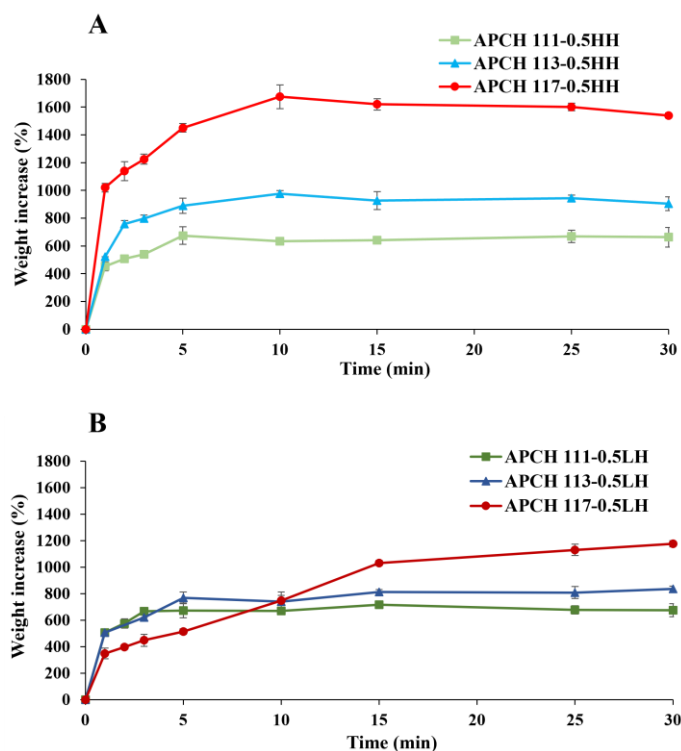


Figure 57. Simulated wound fluid uptake of different APCH formulations ranging from high to low molecular weight hyaluronate. Panel A: APCH 111-0.5HH, APCH 113-0.5HH, APCH 117-0.5HH; Panel B: APCH 111-0.5LH, APCH 113-0.5LH, APCH 117-0.5LH (down).

In order to verify the interaction between polymers, FT-IR studies on the different formulations were conducted. Figure 58 reports the spectra of the blank formulation and sodium hyaluronate loaded particles comprised in the region ranging between 1750 cm^{-1} and 1300 cm^{-1} , where H presents the most characteristic peaks. Figure 58-a shows overlapped bands characteristic of the stretching vibration of the hyaluronate carbonyl group ($1500\text{-}1700\text{ cm}^{-1}$). At 1603 cm^{-1} , a peak related to stretching vibration in the carbonyl of the carboxylate group of the d-glucuronic acid and, at 1650 cm^{-1} and 1558 cm^{-1} two signals related to the amide I band and amide II band are represented (Bigucci et al., 2015). APC particles presented several bands of the single polymers overlapped (Figure 58-b). The broad peak at 1600 cm^{-1} represented the asymmetric stretching band of the carboxylate ion of the alginate and the distinctive amide I

and amide II bands of pectin and chitosan. Furthermore, at 1410 cm^{-1} , alginate symmetric stretching vibration of the carboxyl group and COO pectin stretching were reported. Moreover, the chitosan showed the absorption bands at 1371 cm^{-1} characteristic of the $-\text{CH}_3$ symmetrical vibration. APCH 111-2H formulation (Figure 58-c) showed a similar spectrum of APC with the band characteristic of protonate amine at 1558 cm^{-1} present in hyaluronate spectrum slightly shifted to 1539 cm^{-1} (Luppi et al., 2009). This shift can be caused by sharing of electrons that vibrate at a lower frequency, (W. Zhang, Dehghani-Sanij, & Blackburn, 2008) indicating an interaction between the carboxylate group of H and the NH_3^+ group of chitosan. In the graph was reported only one type of sodium hyaluronate because no differences were found between the two.

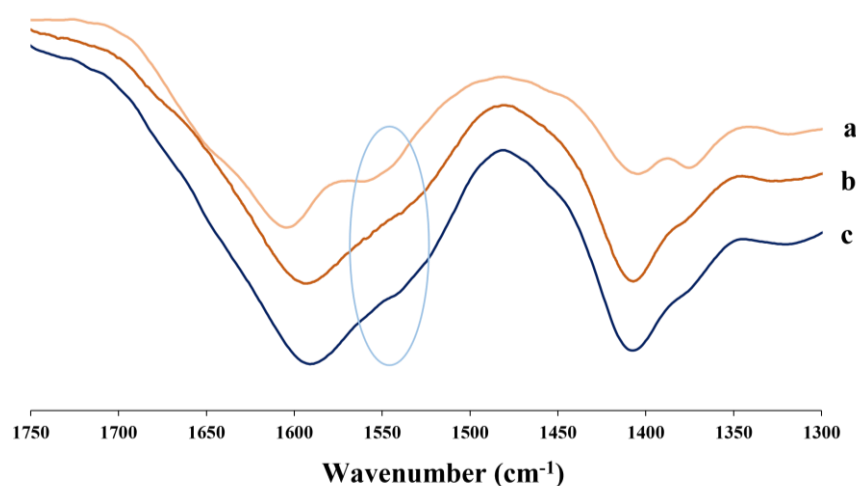


Figure 58. FTIR spectra of drug raw material in comparison with particles of alginate-pectin-chitosan and alginate-pectin-chitosan with sodium hyaluronate: sodium hyaluronate raw material (a), APC 111 (b), and APCH111-2HH (c).

To study the impact of sodium hyaluronate on the physical properties of alginate-pectin-chitosan powders, their thermal behavior was analyzed by DSC. The study was carried out in the temperature range from 25 to 400 $^{\circ}\text{C}$, with a temperature rise rate of 25 $^{\circ}\text{C}/\text{min}$. All

polymers showed a large endothermic band from 90 to 145 °C which underlines the presence of bonded water (Xie, Yi, Wang, Hou, & Jiang, 2018). Moreover, alginate (Figure 59-b) presented an exothermic peak around 240 °C related to the oxidative degradation of polymers (Falcone et al., 2022), amidated pectin (Figure 59-a) showed an endothermic peak at 145 °C related melting point (Deshmukh, Harwansh, Paul, & Shukla, 2020), a broad peak at 190 °C followed by an exothermic one at 250°C and chitosan (Figure 59-c) exhibited a broad peak around 300 °C related to its degradation (Amirian et al., 2021). H (Figure 59-d,e) contains three types of functional groups capable of hydrogen bonding with water molecules: hydroxyl, carboxylic, and acetamide groups that have been responsible for the endotherm peak related to the removal of water, up to 200 °C. Moreover H presented an exothermic peak at 238 °C due to the thermal decomposition (Benešová, Pekař, Lapčík, Kučerík, & calorimetry, 2006). All APCH formulations showed a similar calorimetric profile regardless of the concentration and type of sodium hyaluronate (Figure 59 Panel B). Specifically, an endothermic peak around 120 °C is related to the removal of water, a peak at 249 °C is related to the exothermic rearrangement of alginate pectin and hyaluronate indicating a formation of a homogeneous blend between polymers (Meng et al., 2021) and a broad peak around 300 °C related to the degradation of chitosan.

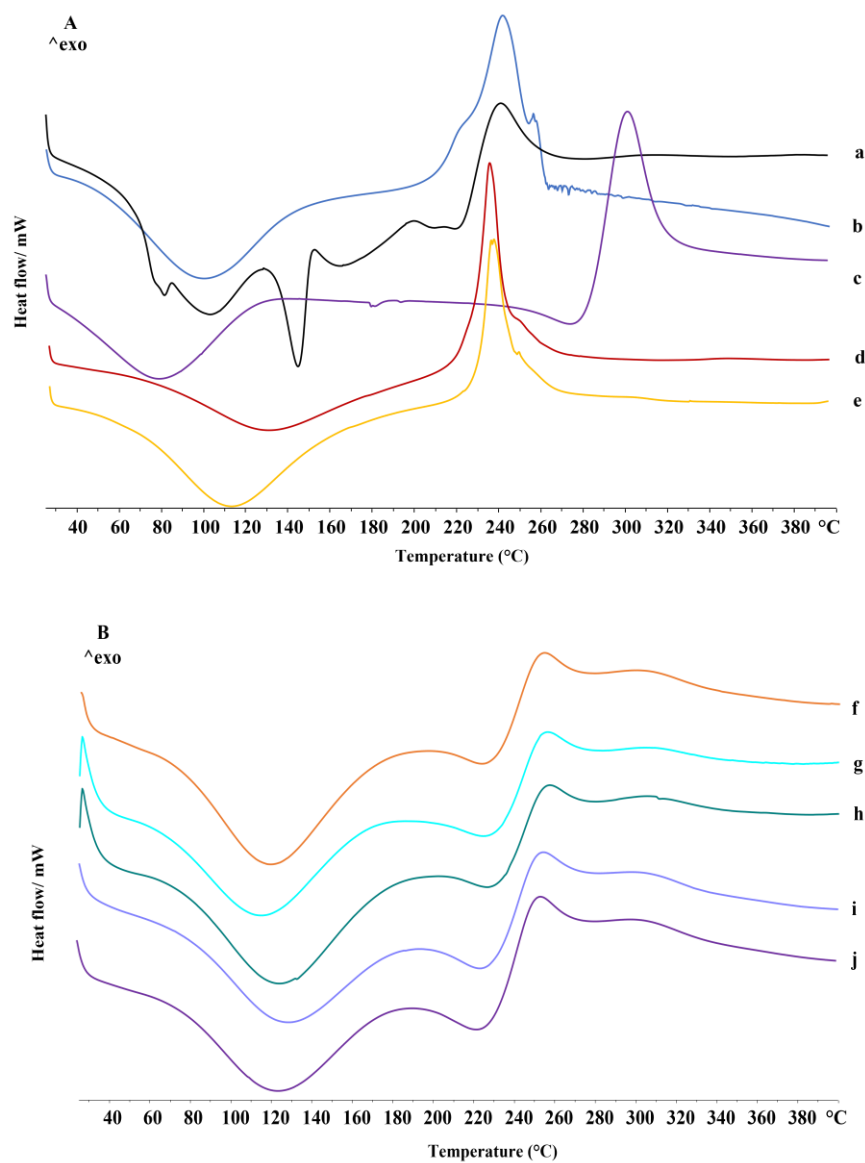


Figure 59. *Differential scanning calorimetry thermograms of alginate, amidated pectin, chitosan and sodium hyaluronate raw material in comparison with alginate-pectin-chitosan polymeric blend with sodium hyaluronate. Panel A: amidated pectin (a), alginate (b), chitosan (c), sodium hyaluronate high molecular weight (d), sodium hyaluronate low molecular weight (e). Panel B: APC 111 (f), APCH 111-0.5HH (g), APCH 111-2HH (h), APCH 111-0.5LH (i) and APCH 111-LH (j).*

The amplitude sweep test was employed to evaluate the viscoelastic properties of the *in situ* gel powders. APC and APCH showed a similar viscoelastic trend, with storage modulus (G') greater than loss modulus (G'') indicating that the samples show a gel-like (Figure 60). APCH 111-2LH reported an increase of both moduli, respect APC 111, obtaining a more elastic and organized gel respect APCH 111-2HH that, on the contrary, showed lower values (Butnaru, Cheaburu, & Vasile, 2012).

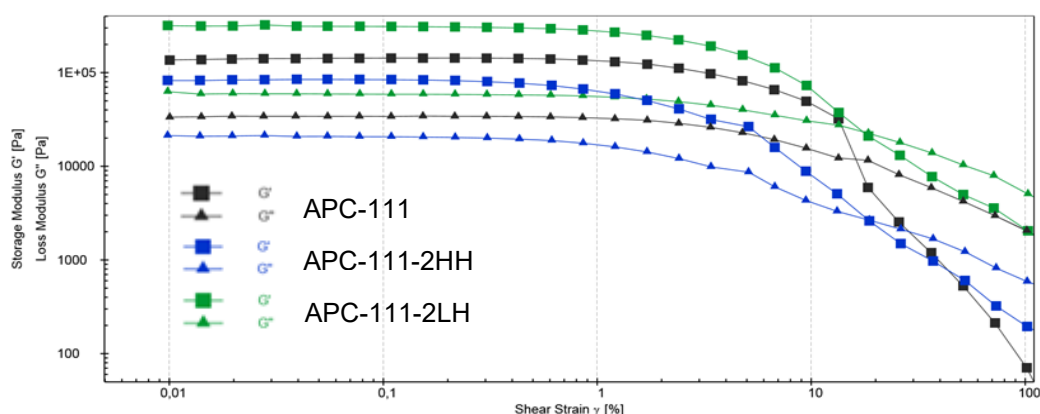


Figure 60. Rheological study. Amplitude sweep test. Storage modulus (G') and loss modulus (G'') of APC 111 in comparison with APCH 111-2HH and APCH 111-2LH.

3.4.2.2 *In vitro* degradation

The principal aim of the degradation studies is to estimate the required time for degradation of dressings when applied to the wounds. Consequently, the degradation of the powders was evaluated in PBS with and without hyaluronidase, enzymes that catalyze the degradation of hyaluronic acid, to compare the hydrolytic degradation and enzymatic degradation. Both formulations tested showed in PBS an initial burst phase (the first day) followed by a slower continuous degradation, reaching 20-25% after one week (Figure 61). Since hydrogels were formed due to the establishment of ionic interactions between the interaction of the polymers and, since these bounds are nonpermanent in nature, the weight loss observed on the first day

is probably due to the dissolution of the weakly ionic bounded chains of biopolymers. When the powders were treated to hyaluronidase solutions, similar degradation trends were found, with a slight increase due to the cleavage of β -(1-4) glucoside bonds present in H (only 2% of the formulations) and chitosan that show similar bonds thank the action of hyaluronidase (Chen et al., 2020). Only H, regardless of its molecular weight, reached maximum degradation in three days. Therefore these powers could have an extended usage period, reducing replacement frequency.

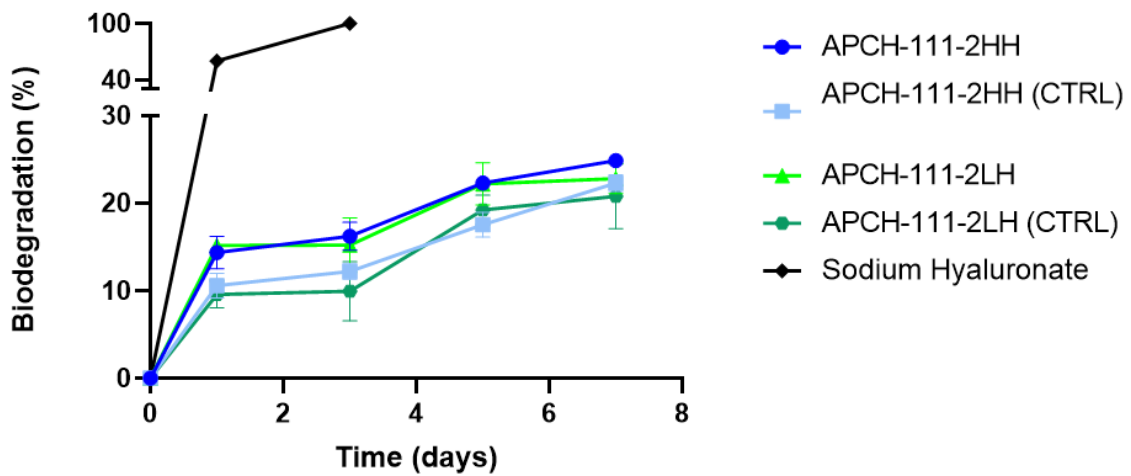


Figure 61. Degradation behavior of APCH 111-2LH and APCH 111-2HH with and without hyaluronidase (CTRL) in comparison with sodium hyaluronate. Treatment for 7 days (data = mean \pm SD; n = 3).

3.4.3 Conclusions

In this work, *in situ* gelling powders based on natural polymers of natural containing sodium hyaluronate were produced and characterized for the treatment of tissue injuries. A mini spray dryer with optimized conditions successfully was used for the production of complex dry powders using alginate, pectin, and chitosan as the polymeric blend and two different molecular weights of sodium hyaluronate. All constituents have the biocompatibility, biodegradability, non-toxicity, and non-immunogenicity inherent in bioactive formulations, and can interact with the wound environment to promote wound healing, with hyaluronic acid, a physiological constituent of the skin's extracellular matrix and a stimulator of tissue regeneration, playing the major role. All formulations were obtained with a good encapsulation efficiency (up to 72%), related to the chitosan concentration. The increase of hyaluronate concentration, regardless of its molecular weight, led to better encapsulation efficiency (up to 98 %). When in contact with a simulated wound fluid they were able to swell and move into a gel, between 1-5 minutes, absorbing large quantities of wound fluid, due to dextran blend swelling properties. This ability was directly related to the concentration of chitosan in the liquid feeds processed by mini spray dryer. However, the formulation containing more chitosan and low molecular weight of sodium hyaluronate absorbed less amount water due to the reduced availability of groups to form interactions with the fluid. Acting as a barrier to sodium hyaluronate permeation due to the interaction between polymers as confirmed FT-IR analysis, formulations influenced hyaluronate degradation. In fact, the *in situ* gelling powders were able to prolong their degradation when in contact with sodium hyaluronidase for over seven days.

3.5 SECTION E

Alginate-pectin *in situ* gelling powders loaded with nanoemulsions

Based on the results obtained during the period spent at Université Claude-Bernard Lyon 1, LAGEPP group, under the supervisor of professor Giovanna Lollo.

Manuscript to be submitted.



LAGEPP



3.5.1 Scientific background

A large number of lipophilic compounds, presenting a logP higher than 4, such as α -tocopherol, β -carotene, and curcumin are used in the treatment of skin diseases (Akbik, Ghadiri, Chrzanowski, & Rohanizadeh, 2014; Cichewicz, Pacleb, Connors, Hass, & Lopes, 2013; Moser, Kriwet, Naik, Kalia, & Guy, 2001). However, being poorly water soluble these compounds tend to localize in the superficial stratum corneum after topical application. Therefore, it is essential to develop a formulation capable of stabilizing and incorporating such drugs, releasing them in control manner. Lipid-based drug delivery systems have drawn increasing attention in the last decade for their great potential regarding the enhancement of solubility and dissolution of lipophilic drugs (Kalwar, 2017; L. Thomas et al., 2017). Among them, nanoemulsions (NEs), thermodynamically stable systems, composed of oil, surfactants, and water (Anwer, Jamil, Ibnouf, & Shakeel, 2014; Solans & Solé, 2012) can be used for wound healing applications (Gong et al., 2013). NEs, incorporating the poorly water-soluble drugs in the oil droplet phase, are able to vehicle a greater amount of them than other conventional topical formulations like creams or gels (Ahmad et al., 2019). However, these systems do not have sufficient viscosity to be used for topical application. Therefore, the encapsulation of these nanoparticles in secondary vehicles such as polymeric scaffolds can enhance their use and co-delivery of ingredients pharmaceutical active to the application site (Oyarzun-Ampuero et al., 2015).

Recently, nanosystems have been combined with macro and microstructures to develop nanocomposites (Kung et al., 2016; Y. Li et al., 2015; Parani, Lokhande, Singh, & Gaharwar, 2016; M. A. Teixeira, Paiva, Amorim, & Felgueiras, 2020), hybrid delivery devices consisting of at least one of the dispersed particles in the nanometer range, such as lipid dispersed in a polymeric matrix (Merino, Martín, Kostarelos, Prato, & Vázquez, 2015). The incorporation of two distinct materials into one formulation enhances the single properties obtaining the unique

physicochemical and biological characteristics, that neither one of the two systems can achieve individually. This kind of system increases the stability of the encapsulated drug and can promote its controlled release at the active site (Xiao et al., 2014). Nanocomposite macrosystems include hydrogels, aerogels, sponges, films, microneedles, tablets, and capsules. While microsystems, identified as microparticles, consist of microspheres, microgels, and microcapsules (Figure 62).

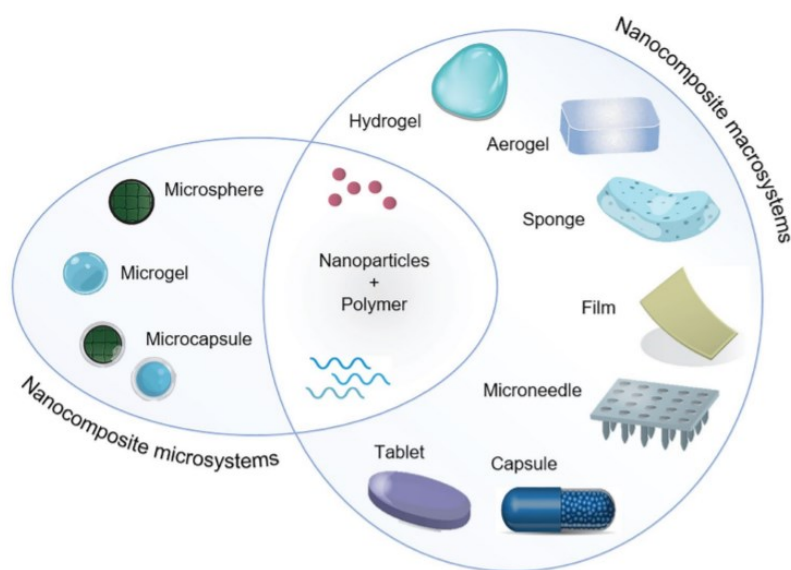


Figure 62. Different types of nanocomposite systems for drug delivery categorized based on their micro or macrostructure (Andretto, Rosso, Briançon, & Lollo, 2021).

The nanocomposite hydrogels for wound healing can encapsulate antibiotics, drugs, and anti-inflammatory agents or other biomolecules, delivering them at the wound sites to prevent bacterial penetration and infection and to promote faster tissue healing and regeneration. Desimone et al., reported that the antibiotics (gentamicin and rifamycin) were released from the nanocomposite hydrogel in a sustained manner within the wound inhibiting bacterial growth (Alvarez et al., 2014; Mebert et al., 2018). Since it is necessary to have a formulation that is not only capable of promoting the controlled release of the nano formulation but also has favorable

wound healing characteristics like exudate absorption maintaining a moist environment (Nair, Raman, & Doble, 2016; Rui Shi et al., 2018), the purpose of this part of the work was to produce, by spray drying, nanocomposites to deliver lipophilic drug: alginate-pectin *in situ* gelling powders loaded with curcumin loaded nanoemulsions. Sodium alginate is able to form a soft and flexible hydrophilic gel, due to its high mannuronic content, through an ionic exchange Ca/Na process when in contact with the wound exudates. Pectin can gelify ionotropically when in contact with bivalent cations presented in the exudate due to its low methoxyl grade thus enhancing the in-situ gel-forming rate (P. Sriamornsak, Thirawong, & Puttipipatkachorn, 2004). Curcumin, 1,7-bis-(4-hydroxy-3-methoxyphenyl)-1,6-heptadiene-2,5-dione, is a yellow phenolic pigment obtained from turmeric oleoresin, which is the organic extract obtained from turmeric (*Curcuma longa*) rhizomes, a tropical plant native from Southern Asia (Venkatasubbu & Anusuya, 2017). Curcumin has been chosen as a model drug since, when applied topically, is able to significantly improve wound healing and prevent oxidative damage (Gopinath et al., 2004). One of the most important factors responsible for all the activity of curcumin is its capability to scavenge reactive oxygen and nitrogen free radicals (Masuda et al., 2002; Panchatcharam, Miriyala, Gayathri, & Suguna, 2006; Venkatesan & Rao, 2000). Curcumin can modulate physiological and molecular events involved in the inflammatory, proliferative, and remodeling phases of the wound healing process (Figure 63). Moreover, recent years' studies showed that curcumin has, also antibacterial activity (Krausz et al., 2015; Salehi et al., 2021; Zorofchian Moghadamtousi et al., 2014). Its bacteriostatic activity involves interference on cellular processes by targeting DNA and proteins, damage to the cell wall and cell membrane, and inhibition of bacterial quorum sensing (the ability to detect and respond to cell population density by gene regulation through the use of signal molecules) (Zheng et al., 2020).

Antimicrobial properties of curcumin have been reported against a broad range of microorganisms, including common bacteria that are detected on the wounds: *Staphylococcus aureus*, *Escherichia coli*, and *Pseudomonas aeruginosa* (Basniwal, Buttar, Jain, Jain, & chemistry, 2011; Mun et al., 2013; Rai, Singh, Roy, & Panda, 2008).

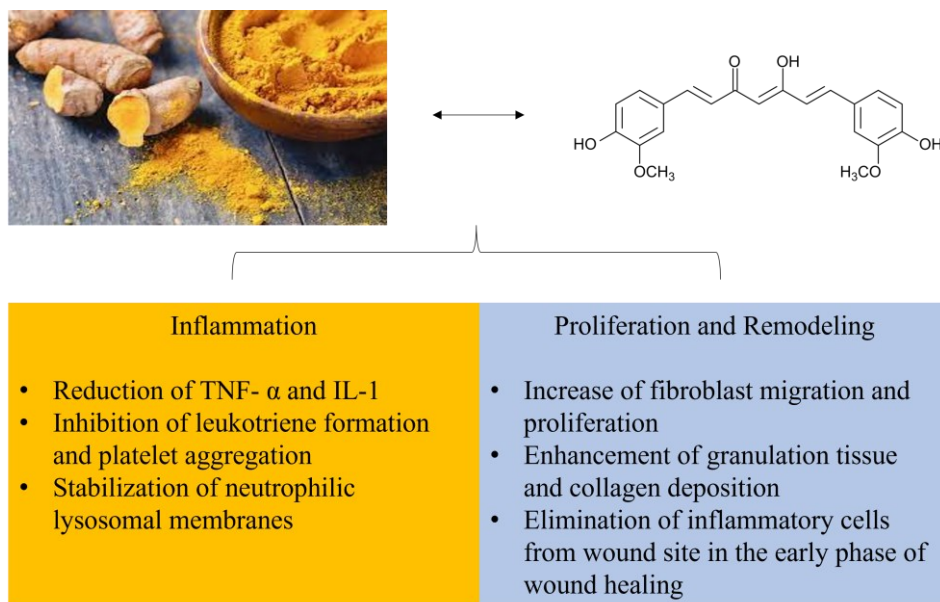


Figure 63. Structure and effects of curcumin on wound healing.

During this work, preliminary studies have been devoted to NEs characterization regarding their structural, mechanical properties, and stability. In a successive phase, the nanocomposites were produced and analyzed in order to evaluate the influence of the addition of NEs on the alginate-pectin *in situ* gelling powders and the effect of the spray drying process on NEs. Moreover, morphology and distributional dimension, thermal behavior, fluid uptake ability, and viscoelastic properties of the nanocomposites were assessed, as well as encapsulation efficiency and NEs release from the *in situ* formed hydrogel.

3.5.2 Results and discussion

3.5.2.1 Nanoemulsions formulation, physicochemical characterization, and stability

Nanoemulsions (NEs) loaded with curcumin (CCM) were produced by emulsion phase inversion.

In this part of the work, the organic phase was prepared by mixing the oil (MCT) stabilized with hydrophilic and hydrophobic surfactants, namely polyoxyethylene (40) stearate (S1) (HLB 16.9), and oleoyl polyoxyl-6 glyceride (S2) (HLB 4), respectively. The hydrophilic surfactant, S1, was selected since PEGylated stearates create a steric barrier against droplet coalescence and permit the formation of small particle size (Komaiko & McClements, 2016). S2 was used as a hydrophobic surfactant to enhance NEs stability by positioning itself between NE oil core and hydrophilic surfactant shell (Choi, Aditya, & Ko, 2014). The aqueous phase consisted of PBS 5 mM, pH 7.4. The preparation of this type of NE is based on an exhaustive study carried out on NEs prepared by emulsion phase inversion technique evaluating the influence of NE composition, physicochemical properties, and stability (Rosso et al., 2020).

CCM, as a wound healing agent (Andrabi, Majumder, Gupta, & Kumar, 2020; Jagetia & Rajanikant, 2012; Krausz et al., 2015; Mohanty & Sahoo, 2017), was encapsulated into the NE, as a hydrophobic model drug. NEs were prepared (14.29% w/w) with different concentrations of CCM (1.33, 2.66, and 5.33% w/w) leading to NE with different properties in terms of mean size and PDI (Table 10).

Table 10. *Physicochemical characteristics of curcumin loaded nanoemulsions.*

	Size (nm) ± SD	PDI ± SD	ζ-potential (mV) ± SD
NE1 (1.33)	103.90 ± 2.10	0.17 ± 0.01	-14.67 ± 1.10
NE2 (2.66)	160.43 ± 28.73	0.30 ± 0.02	-19.60 ± 1.51
NE5 (5.33)	285.23 ± 51.61	0.40 ± 0.02	-14.47 ± 0.23

Since NEs are defined as very small particles (<100 nm) (Salvia-Trujillo, Martín-Belloso, & McClements, 2016) and polymer-based nanoparticle materials with a value of PDI < 0.2 are considered monodispersed systems (Danaei et al., 2018), the CCM loaded NE chosen to be used in nanocomposites has been NE1 with a size of 104 nm, a low PDI (0.180), and a stable zeta potential (-14.67) (Table 10). Due to the lipophilic character of CCM, the drug encapsulation efficiency was very high 96.46 ± 5.66 , and the drug content was 1.29 ± 0.10 .

The stability of NE1 in colloidal suspension, upon storage at 4 °C, was followed over 28 days. Macroscopic aspect (presence of aggregates, cream formation, or changes in color), physicochemical properties (particle size, polydispersity, and zeta potential), and drug loss were evaluated. No sample degradation or changing of color was observed and mean size, PDI, and surface potential remained stable during the studied period (Figure 64). In addition, the amount of encapsulated curcumin remained unchanged of storage at 4 °C.

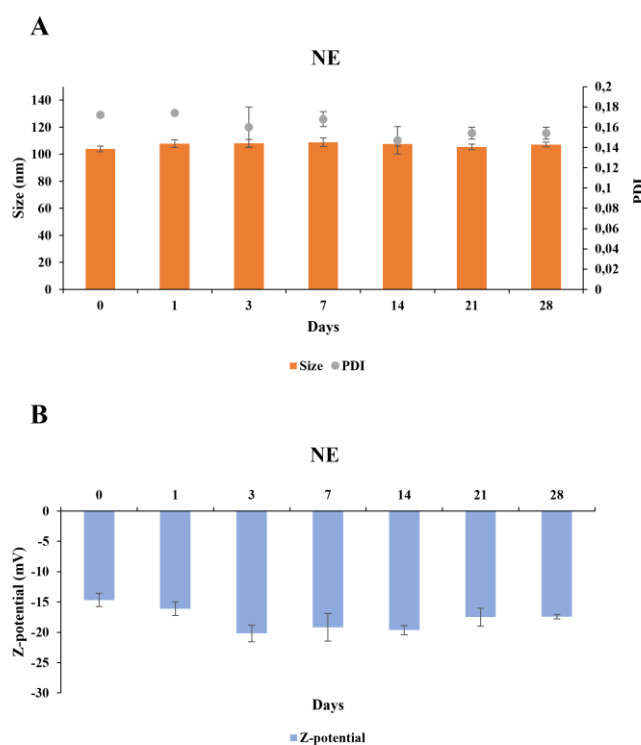


Figure 64. Stability study of NE1 upon storage at 4°C for 28 days. Data are shown as mean \pm S.D., $n = 3$.

TEM images showed that NEs appeared as a monodispersed population of spherical droplets with a smooth surface (Figure 65-a,b).

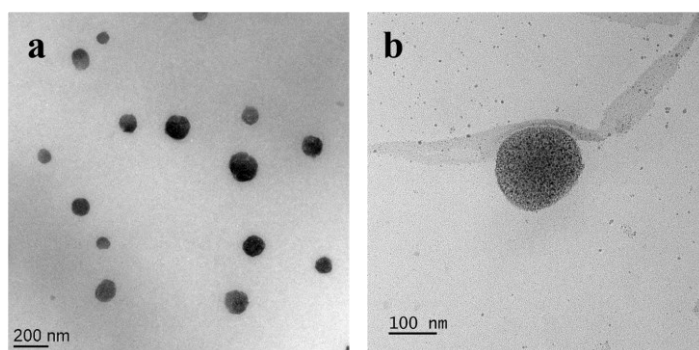


Figure 65. TEM of NEs at a magnification of 200 nm and 100 nm.

3.5.2.2 Production of nanocomposites

Once assessed the stability and encapsulation efficiency of CCM in NEs, an original nanocomposite composed of alginate-pectin blend with CCM-loaded NEs was produced using spray drying. Based on the previous work reported in section II, alginate-pectin (AP) powders in ratio 1:1 were chosen as a carrier. While total polymer concentration was fixed at 1% (w/w), two different concentrations of CCM-loaded NEs were compared (0.1 and 0.2% w/w). The main characteristics of nanocomposites, represented by yellow powder, were reported in table 11. Both nanocomposites AP-11-NE0.1 and AP-11-NE0.2 were characterized by relatively high process yield without difference than microparticles AP-11. The E.E. of the NEs in microparticles, studied analyzing the curcumin, ranged between 57.6 and 50.47% depending on the amount of NE, the higher concentration the lower was the encapsulation. These values suggest a saturation of the polymers when NE is present in higher concentrations. This hypothesis is supported by earlier work on encapsulation of essential oil in alginate microparticles that revealed the same trend (Hosseini et al., 2013).

Table 11. *The main characteristics alginate-pectin microparticles and nanocomposites.*

Sample	Polymers concentration % (w/w)	NE % (w/w)	Process Yield (%)	Drug content (%) ± SD	E.E. (%) ± SD
AP-11	1	-	67.0	-	-
AP-11-NE0.1	1	0.1	65.0	0.08 ± 0.00	57.60 ± 3.89
AP-11-NE0.2	1	0.2	65.1	0.14 ± 0.00	50.47 ± 0.59

The stability of the nanocomposites after spray drying was assessed by evaluating the physicochemical properties of the NE encapsulated in AP microparticles, after solubilization in water (Table 12). An increase of NE diameter in AP-11-NE0.1 and AP-11-NE0.2 (from 103 nm to 205 nm and 238 nm, respectively) and of PDI (from 0.17 to around 0.3, respectively) were observed. These results could indicate the absorption of the polymers on the NE more evident in AP-NE.0.1. Moreover, the ζ -potential of the NE-loaded AP microparticles went from a negative value to a highly negative value (-14.68 mV to -21 and -29 mV). Importantly, the microparticles had a relatively high negative charge (about -52 mV), at pH 5.5. In this range of pH, alginate has several carboxyl groups along its backbone, which account for its anionic characteristics (Pallandre, Decker, & McClements, 2007). Structural diversity and surface charge of the polysaccharides play a critical role to encapsulate NE and CCM. Probably the negative surface charge of AP-11 determines a repulsion between polymers and NE that leading a reduction in encapsulation efficiency.

Table 12. *Physicochemical characteristics of NE, NE encapsulated in AP microparticles and AP microparticles.*

	Size (nm) ± SD	PDI ± SD	ζ-potential (mV) ± SD
NE	103.90 ± 2.10	0.172 ± 0.00	-14.68 ± 1.10
AP-11-NE0.2	205.13 ± 2.44	0.28 ± 0.01	-21.20 ± 1.93
AP-11-NE0.1	238.97 ± 4.82	0.36 ± 0.03	-29.65 ± 2.19
AP-11	817.93 ± 29.10	0.33 ± 0.03	-51.93 ± 1.72

3.5.2.3 Technological characterization of nanocomposites

AP-11 microparticles showed a relatively small mean diameter ($3.60 \pm 0.04 \mu\text{m}$), with particle size distributions containing only a single peak. In the nanocomposites as the amount of NE increased, so did the mean diameter (Figure 66). These results could be the cause of the thermal instability of NE droplets, which during the spray drying process, has led to the aggregation of them, increasing the diameter of the particles (El-Messery, Altuntas, Altin, & Özçelik, 2020). However, also nanocomposite has reported a single peak indicating that uniform particles were formed and that the majority of NE were embedded inside the microparticles (Wei Liu, Wang, McClements, & Zou, 2018).

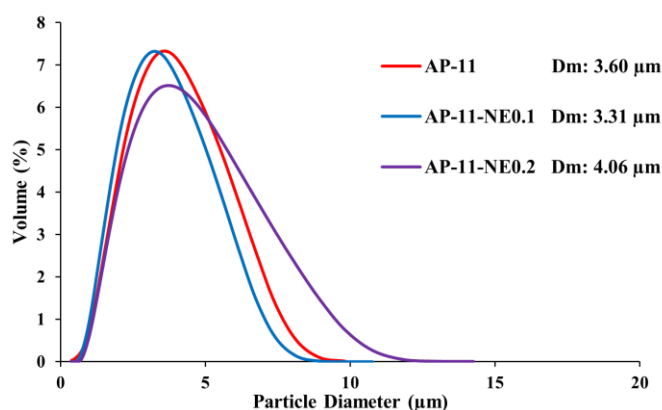


Figure 66. *Dimensional distribution with values of mean diameters of AP-11 and nanocomposites AP-11-NE0.1 and AP-11-NE0.2.*

Particles obtained by spray drying can have different morphologies depending on the features of the initial raw material and process conditions (Nandiyanto & Okuyama, 2011). AP-11 presented a morphology of “deflated balloons” (Figure 67-1,2a) (Felicetta De Cicco, Reverchon, et al., 2014).that in the nanocomposites has been replaced by spherical shapes (Figure 67-1,2b and 67-1,2c), maybe due to the global increase of droplet loading before drying (Xiang Li et al., 2011). In addition, Nanocomposites particles presented cracks and fissures probably due to the presence of NEs on the surface of the microparticles.

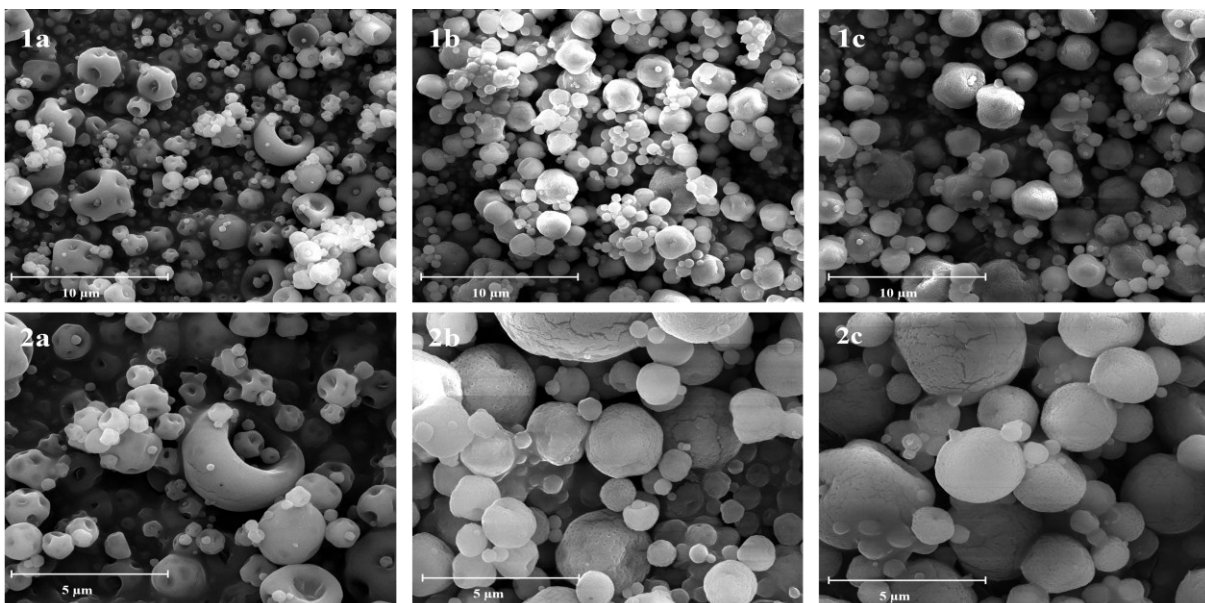


Figure 67. SEM microphotographs of AP-11 (a) AP-11-NE0.1(b) and AP-11-NE0.2, (c). 1: sample surface at low magnification (scale bar: 10 μm); 2: sample surface at higher magnification (scale bar: 10 μm).

The thermal properties of the materials are compared using both thermogravimetric analysis (TGA) and differential scanning calorimetry (DSC). Figure 68 shows the TGA profiles of alginate and pectin in comparison with that of microparticles. The degradation profile of alginate consisted of a three-stage process: below 150 °C the weight loss was associated with the humidity release while at 237 °C and 750 °C it was correlated to the rupture of chains,

fragments, and monomers (Y. Zhao et al., 2010). Pectin had two main weight loss steps. The degradation patterns of the other samples revealed very similar to alginate and pectin with a weight loss below 150 °C due to the removal of moisture, followed by sharp weight loss at 230 °C due to the degradation of the polymer backbone.

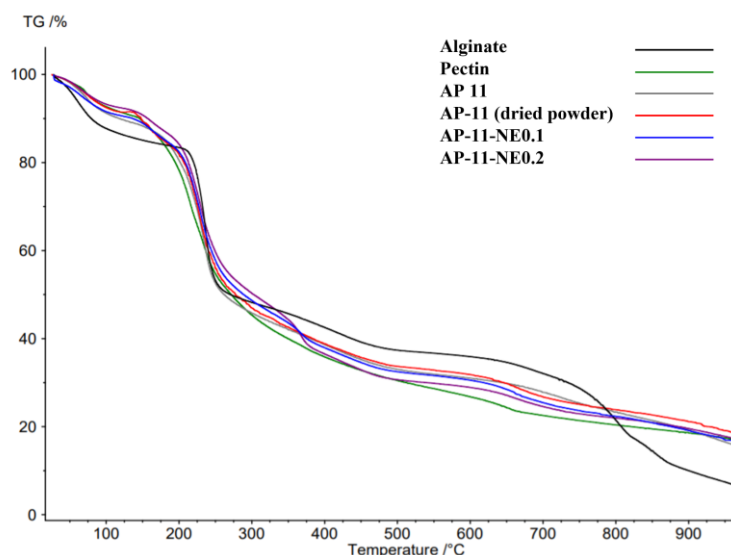


Figure 68. Thermogravimetric curves of alginate raw material (black), pectin raw material (green), AP in combination before spray drying (grey), AP-11 after spray drying (red), AP-11-NE0.1 (blue), and AP-11-NE0.2 (violet).

The water content, indicated in the TGA as the first peak of thermal degradation, was evaluated also by Karl Fisher titration, (Table 13) which highlighted that the addition of NE to AP polymers led to a reduction of the amount of water entrapped during the spray drying process, probably due to its hydrophobicity character, improving the stability of these samples (Makaremi et al., 2019; Siracusa et al., 2018).

Table 13. *Moisture content evaluated using Karl Fisher titration of spray dried powders: AP-11, AP-11-NE0.1, and AP-11-NE.0.2.*

	H₂O % (w/w) ± SD
AP-11	9.27 ± 0.04
AP-11-NE0.1	6.07 ± 0.05
AP-11-NE0.2	5.54 ± 0.09

The state of the shell (crystalline or amorphous) of the NE in colloidal suspension and of the micropowders was investigated using DSC (Figure 69). NE showed a melting endotherm at 48 °C and, a second peak at lower temperatures (below 40 °C) suggesting the presence of a second crystalline phase, attributable to a polymorphic form of the stearic acid of S1 (Figure 69-1a). In addition, it showed a broad crystallization exotherm from 0 to 30 °C upon cooling and a second melting peak at -50 °C (Figure 69-2a) referred to as MCT polymorphism (Jenning, Thünemann, & Gohla, 2000; Ribeiro et al., 2015). AP-11-NE powders were analyzed to estimate the influence of the drying process on the structure of NE loaded. Once the water had been evaporated, the melting and crystallization peaks of S1 were visible in according to the amount of NE in powders (Figure 69-b,c). These peaks were shifted at a lower temperature in the AP-NEs due to the presence of polymers alginate and pectin that on the contrary did not show any signal (Figure 69-d,e,f,g) (Rosso et al., 2020).

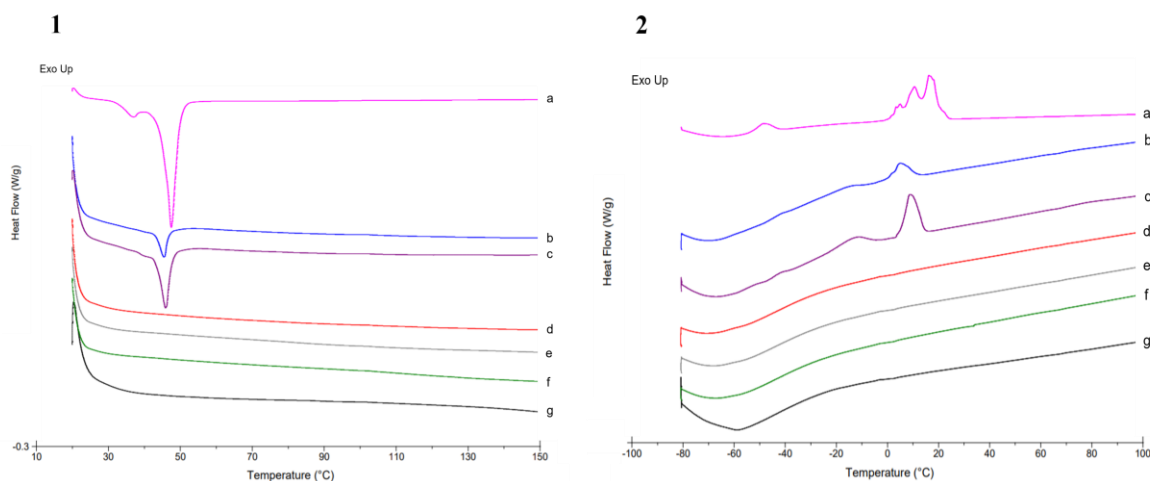


Figure 69. DSC thermograms of NE in a colloidal suspension (a), AP-11-NE0.1 (b), AP-11-NE0.2 (c), AP in combination before spray drying (d), AP-11 after spray drying (e), pectin raw material (f), and alginate raw material (g). Panel 1 represents the second cooling cycle from +20 °C to 180 °C while panel 2 third heating performed from +180 °C to -80 °C, both at 10 °C /min.

To evaluate the influence of NE on the powders ability to become a gel in situ, AP-11 and AP-11 NEs were placed in contact with simulated wound fluid (SWF) and at defined time points the increase in weight was calculated. Figure 70 shows that AP-11 became gel in less than 5 minutes increasing almost 700 times its weight after 15 minutes. As expected a different trend was observed for AP-11-NEs. The swelling was immediate ma the amount of water uptake was less due to the presence of NE that enhanced the hydrophobicity of the systems as confirmed also by Karl Fisher analysis (Rosso et al., 2021). Moreover, the presence of the NEs physically reduced the freedom of polymer movement and, taking up the space of the water, resulted in the reduction of fluid uptake into the polymer structure (Schoener, Hutson, & Peppas, 2012).

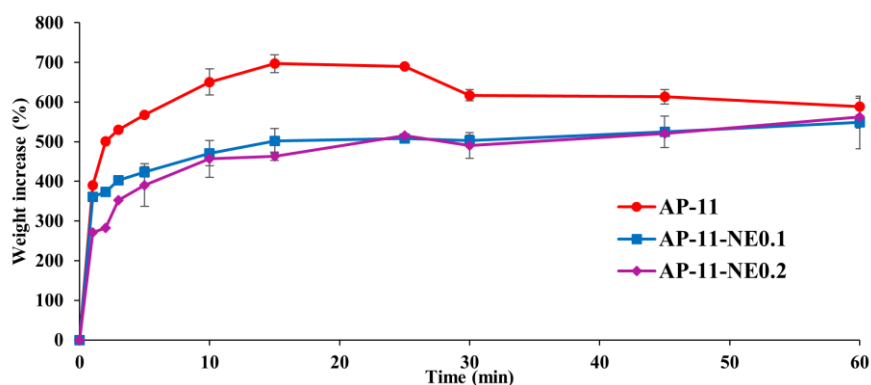


Figure 70. Simulated wound fluid uptake of AP-11, AP-11-NE0.1, and AP-11-NE0.2.

To verify the elasticity of the *in situ* gel powders viscoelastic properties were assessed through rheological measurements via amplitude sweep test, which depicts the variation of dynamic storage modulus (G') and loss modulus (G'') with shear strain (γ). All formulations (Figure 71) showed G' was much higher than G'' suggesting an interconnected gel-like network structure. For the AP-11-NEs was reported an increase of the gap between the storage and loss modulus, according to the NE concentration, demonstrating the prevalent gel behaviour. This behavior can be better explained through $\tan \delta$ the factor that represents the ratio between viscous and elastic components (purely elastic, $\delta = 0$; purely viscous, $\delta = 90$). This value (Figure 71 panel B) highlighted an increase in the elastic behavior of the hydrogels according to the amount of NE (Zou, Yang, & Scholten, 2018).

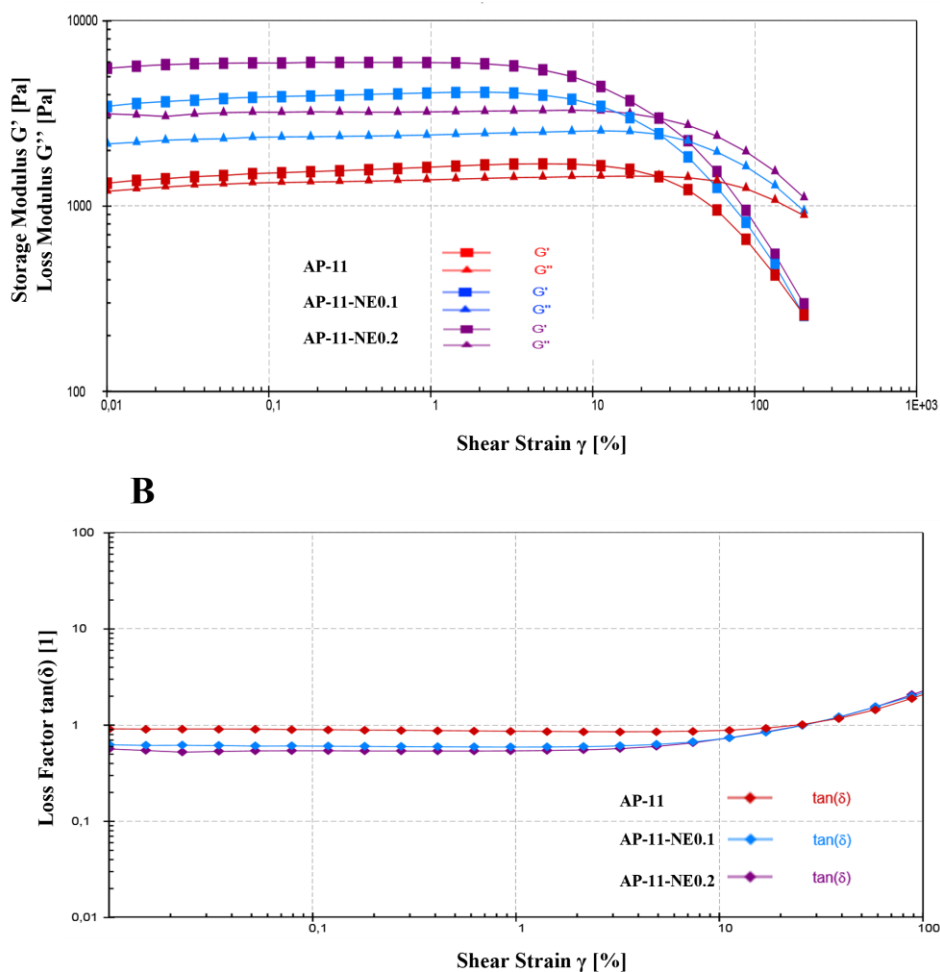


Figure 71. Rheological characterization of AP-11, AP-11-NE0.1, and AP-11-NE0.2. Storage G' and loss G'' moduli evaluated via amplitude sweep test and (Panel A) and strain dependent tangent of loss factor (Panel B).

3.5.2.4 *In vitro* release study

In vitro release studies of the NE from nanocomposite powders via curcumin were carried out in SWF. The release studies aimed to analyze the behaviour of the nanosystem *per se*, therefore, non-sink conditions were used. Making sure to stay below the solubility of curcumin to avoid its release, a cumulative release study was performed. All formulations have shown the same trend. A burst effect in the first hours and a sustained release until 24 hours (Figure 72). The initial burst release could be correlated to the NEs adsorbed on and near the surface of

the microparticles as reported in SEM images. In addition, the swelling of the powder in contact with SWF can favor the release of the NEs. This burst release was followed by a second phase characterized by slow release in the second stage could be due to the diffusion of NE dispersed into the microparticles (Faisant, Siepmann, Richard, & Benoit, 2003). However, although nanocomposites showed the same trend, AP-11-NE0.1 has reported a faster release than AP-11-NE0.2 with higher concentrations of NE. AP-11-NE0.1 released about 55% of the encapsulated NE after 5 h, followed by a sustained release profile for 24h reaching 100%. When NEs content was doubled release decreased from 55% to 47% after 5h and from 100 to 98% after 24h. These observations are in agreement with the distributional dimension, in fact, AP-11-NE0.1, being smaller, exposed a more surface to fluid contact favoring the release of NE (Hosseini et al., 2013). This pattern means that by varying the concentration of encapsulated NEs, the release rate can be modulated, very useful in topical application.

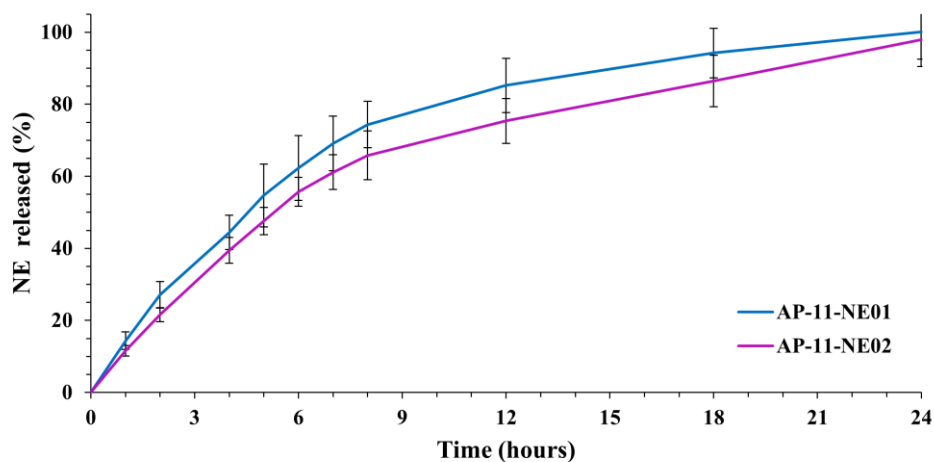


Figure 72. CCM-loaded NE release from the nanocomposite AP-11-NE0.1 and AP-11-NE0.2 performed in SWF.

3.5.3 Conclusions

Nanocomposites combining NE alginate-pectin powders intended for the encapsulation of lipophilic drugs for wound healing application were successfully designed. This study proposed a novel technique using a spray-drying process to microencapsulate NEs loaded with hydrophobic molecules. The results have shown that the spray drying process did not alter the NEs physicochemical properties. The combination of polymers and NE improve the elastic properties of the gel formed in situ and determined the sustained release of NEs.

Further analyses should be carried out to test the stability of NE in formulations over time and the activity of the released curcumin. However, the system based on the data obtained can be used to deliver lipophilic drugs other than curcumin to improve wound healing.

4. CONCLUSIONS AND PROSPECTS

This Ph.D. project was focused on innovative technological strategies for polymeric micro-nanoparticulate systems made by biocompatible and biodegradable polysaccharide-based excipients (alginate, pectin, and chitosan) for the manufacturing of new wound dressing formulations. Natural polymers have been chosen as a carrier due to their intrinsic properties, such as biodegradability and biocompatibility, as well as the ability to induce the wound healing process by different mechanisms. In particular, the project focused on the production and characterization of “*in-situ*” gelling powders obtained by mini and nano spray drying. The optimized process parameters have permitted the production of dried powders with reproducible results and very good yields. Powders made with a blend of alginate-pectin and alginate-pectin-chitosan showed proper technological characteristics to be administered directly to the wounds, since they were able to become gel when in contact with the fluids present into the wound bed, in less of 5 minutes. The addition of sodium bicarbonate to a polymeric blend has allowed reducing this time at 30 seconds. It was demonstrated the applicability of the spray drying technique to produce stable powders with uniform morphology and narrow size distribution, proper technological properties, and without cytotoxic activity on HaCat cells. Alginate and pectin were used for the delivery of a thermolabile macromolecule, Ac2-26 Annessin1-like N-terminal peptide, known for its ability to promote wound healing, increasing its stability and activity. Alginate-pectin-chitosan microparticles were used to vehicle doxycycline, a hydrophilic drug model, modulating its release and enhancing its activity. In addition, this polymeric blend was enhanced with sodium hyaluronate useful in wound healing application. Moreover, the development of nanocomposites, performed at the University of Lyon 1, has allowed to vehicle lipophilic drug in a hydrophilic blend, modulating its release *in vitro*. Lastly, alginate-pectin-chitosan microparticles have been tested on a large-scale production plant demonstrating the possibility to move the production to the industrial

scale. Therefore, all these results suggest that *in situ* gelling powders loaded with different APIs could be a promising wound dressing to improve wound care armamentarium.

However, further investigations will be needed to optimize these novel wound dressings. Based on the data obtained by the production on a large-scale could be interesting to know the total cost of powders production and, the best device to vehicle them. In addition, these data must be corroborated from *in vivo* studies in order to test their capability as restorative agents on murine or pig skin wound models, evaluating the closure of the wounds and the others process connected to tissue repair as cellular proliferation and migration and inflammatory process. Moreover, since the design of wound dressings for injuries has to face up different challenges day by day, the incorporation of growth factors or siRNAs, which could silence genes that encode inflammatory proteins, in the formulations could be an exciting proposal to add the formulations to enhance the wound healing.

Bibliography

- Abdel-Mageed, H. M., Fouad, S. A., Teaima, M. H., Radwan, R. A., Mohamed, S. A., & AbuelEzz, N. Z. (2020). Engineering Lipase Enzyme Nano-powder Using Nano Spray Dryer BÜCHI B-90: Experimental and Factorial Design Approach for a Stable Biocatalyst Production. *Journal of Pharmaceutical Innovation*.
- Abdeltwab, W. M., Abdelaliem, Y. F., Metry, W. A., & Eldeghedy, M. (2019). Antimicrobial effect of Chitosan and Nano-Chitosan against some Pathogens and Spoilage Microorganisms. *Journal of Advanced Laboratory Research in Biology*, 10(1), 8-15.
- Afzali Borojeny, L., Albatineh, A. N., Hasanpour Dehkordi, A., & Ghanei Gheshlagh, R. (2020). The Incidence of Pressure Ulcers and its Associations in Different Wards of the Hospital: A Systematic Review and Meta-Analysis. *Int J Prev Med*, 11, 171.
- Ahmad, N., Ahmad, R., Al-Qudaihi, A., Alaseel, S., Fita, I., Khalid, M., & Pottoo, F. (2019). Preparation of a novel curcumin nanoemulsion by ultrasonication and its comparative effects in wound healing and the treatment of inflammation. *RSC Advances*, 9, 20192-20206.
- Ahmed, S., & Ikram, S. (2016). Chitosan Based Scaffolds and Their Applications in Wound Healing. *Achievements in the Life Sciences*, 10(1), 27-37.
- Akbik, D., Ghadiri, M., Chrzanowski, W., & Rohanizadeh, R. (2014). Curcumin as a wound healing agent. *Life Sciences*, 116(1), 1-7.
- Al-Khattawi, A., Bayly, A., Phillips, A., & Wilson, D. (2018). The design and scale-up of spray dried particle delivery systems. *Expert Opinion on Drug Delivery*, 15(1), 47-63.
- Alsharabasy, A. M., Moghannem, S. A., & El-Mazny, W. N. (2016). Physical preparation of alginate/chitosan polyelectrolyte complexes for biomedical applications. *Journal of Biomaterials Applications*, 30(7), 1071-1079.

- Alvarez, G. S., H elary, C., Mebert, A. M., Wang, X., Coradin, T., & Desimone, M. F. (2014). Antibiotic-loaded silica nanoparticle–collagen composite hydrogels with prolonged antimicrobial activity for wound infection prevention. *Journal of Materials Chemistry B*, 2(29), 4660-4670.
- Amirian, J., Zeng, Y., Shekh, M. I., Sharma, G., Stadler, F. J., Song, J., . . . Zhu, Y. (2021). In-situ crosslinked hydrogel based on amidated pectin/oxidized chitosan as potential wound dressing for skin repairing. *Carbohydrate Polymers*, 251, 117005.
- Andrabi, S. M., Majumder, S., Gupta, K. C., & Kumar, A. (2020). Dextran based amphiphilic nano-hybrid hydrogel system incorporated with curcumin and cerium oxide nanoparticles for wound healing. *Colloids and Surfaces B: Biointerfaces*, 195, 111263.
- Andretto, V., Rosso, A., Brian on, S., & Lollo, G. (2021). Nanocomposite systems for precise oral delivery of drugs and biologics. *Drug Deliv Transl Res*, 11(2), 445-470.
- Anton, N., Jakhmola, A., & Vandamme, T. F. (2012). Trojan microparticles for drug delivery. *Pharmaceutics*, 4(1), 1-25.
- Anwer, M. K., Jamil, S., Ibnouf, E. O., & Shakeel, F. (2014). Enhanced antibacterial effects of clove essential oil by nanoemulsion. *J Oleo Sci*, 63(4), 347-354.
- Aquino, R. P., Auriemma, G., Mencherini, T., Russo, P., Porta, A., Adami, R., . . . Del Gaudio, P. (2013). Design and production of gentamicin/dextrans microparticles by supercritical assisted atomisation for the treatment of wound bacterial infections. *International journal of pharmaceutics*, 440(2), 188-194.
- Armstrong, D. G., Boulton, A. J. M., & Bus, S. A. (2017). Diabetic Foot Ulcers and Their Recurrence. *N Engl J Med*, 376(24), 2367-2375.
- Armstrong, D. G., Swerdlow, M. A., Armstrong, A. A., Conte, M. S., Padula, W. V., & Bus, S. A. (2020). Five year mortality and direct costs of care for people with diabetic foot complications are comparable to cancer. *Journal of Foot and Ankle Research*, 13(1), 16.

- Arnold, M., Barbul, A. J. P., & surgery, r. (2006). Nutrition and wound healing. *Plastic and reconstructive surgery*, 117(7S), 42S-58S.
- Arpagaus, C. (2012). A Novel Laboratory-Scale Spray Dryer to Produce Nanoparticles. *Drying Technology*, 30(10), 1113-1121.
- Arpagaus, C., Collenberg, A., Rütli, D., Assadpour, E., & Jafari, S. M. (2018). Nano spray drying for encapsulation of pharmaceuticals. *International Journal of Pharmaceutics*, 546(1), 194-214.
- Arpagaus, C., John, P., Collenberg, A., & Rütli, D. (2017). 10 - Nanocapsules formation by nano spray drying. In S. M. Jafari (Ed.), *Nanoencapsulation Technologies for the Food and Nutraceutical Industries* (pp. 346-401): Academic Press
- Arroyo, A. A., Casanova, P. L., Soriano, J. V., & Torra, I. B. J. E. (2015). Open-label clinical trial comparing the clinical and economic effectiveness of using a polyurethane film surgical dressing with gauze surgical dressings in the care of post-operative surgical wounds. *Int Wound J*, 12(3), 285-292.
- Ashcroft, G. S., Jeong, M. J., Ashworth, J. J., Hardman, M., Jin, W., Moutsopoulos, N., . . . Wahl, S. M. (2012). Tumor necrosis factor-alpha (TNF- α) is a therapeutic target for impaired cutaneous wound healing. *Wound Repair Regen*, 20(1), 38-49.
- Assaad, E., Maire, M., & Lerouge, S. (2015). Injectable thermosensitive chitosan hydrogels with controlled gelation kinetics and enhanced mechanical resistance. *Carbohydrate Polymers*, 130, 87-96.
- Auriemma, G., Mencherini, T., Russo, P., Stigliani, M., Aquino, R. P., & Del Gaudio, P. (2013). Prilling for the development of multi-particulate colon drug delivery systems: pectin vs. pectin-alginate beads. *Carbohydr Polymers*, 92(1), 367-373.

- Auriemma, G., Russo, P., Del Gaudio, P., García-González, C. A., Landín, M., & Aquino, R. P. (2020). Technologies and Formulation Design of Polysaccharide-Based Hydrogels for Drug Delivery. *Molecules (Basel, Switzerland)*, 25(14), 3156.
- Axelos, M., Thibault, J. J. T. c., & pectin, t. o. (1991). The chemistry of low-methoxyl pectin gelation. *The chemistry and technology of pectin*, Chapter 6, 109-108.
- Azad, M., Arteaga, C., Abdelmalek, B., Davé, R., & Bilgili, E. (2015). Spray drying of drug-swallowable dispersant suspensions for preparation of fast-dissolving, high drug-loaded, surfactant-free nanocomposites. *Drug Development and Industrial Pharmacy*, 41(10), 1617-1631.
- Azevedo, E. P., & Kumar, V. (2012). Rheological, water uptake and controlled release properties of a novel self-gelling aldehyde functionalized chitosan. *Carbohydrate Polymers*, 90(2), 894-900.
- Balakrishnan, B., Mohanty, M., Pr, U., & Athipettah, J. (2005). Evaluation of an in Situ Forming Hydrogel Wound Dressing Based on Oxidized Alginate and Gelatin. *Biomaterials*, 26, 6335-6342.
- Baldassarre, M., & Barth, A. (2014). The carbonate/bicarbonate system as a pH indicator for infrared spectroscopy. *The Analyst*, 139.
- Basniwal, R. K., Buttar, H. S., Jain, V., Jain, N. (2011). Curcumin nanoparticles: preparation, characterization, and antimicrobial study. *J Agric Food Chem*, 59(5), 2056-2061.
- Belali, S., Emandi, G., Cafolla, A. A., O'Connell, B., Haffner, B., Möbius, M. E., . . . Senge, M. O. (2017). Water-soluble, neutral 3,5-diformyl-BODIPY with extended fluorescence lifetime in a self-healable chitosan hydrogel. *Photochemical & Photobiological Sciences*, 16(11), 1700-1708.
- Beldon, P. (2010). Basic science of wound healing. *Surgery - Oxford International Edition*, 28(9), 409-412.

- Benbow, M. (2016). Best practice in wound assessment. *Nurs Stand*, 30(27), 40-47.
- Benešová, K., Pekař, M., Lapčík, L., Kučerík, J. (2006). Stability evaluation of n-alkyl hyaluronic acid derivatives by DSC and TG measurement. *Journal of Thermal Analysis and Calorimetry*, 83(2), 341-348.
- Bhattarai, N., Gunn, J., & Zhang, M. (2010). Chitosan-based hydrogels for controlled, localized drug delivery. *Adv Drug Deliv Rev*, 62(1), 83-99.
- Bigucci, F., Abruzzo, A., Saladini, B., Gallucci, M. C., Cerchiara, T., & Luppi, B. (2015). Development and characterization of chitosan/hyaluronan film for transdermal delivery of thiocolchicoside. *Carbohydrate Polymers*, 130, 32-40.
- Bishop, A. (2008). Role of oxygen in wound healing. *Role of oxygen in wound healing. J Wound Care*, 17(9), 399-402.
- Bizzarro, V., Belvedere, R., Dal Piaz, F., Parente, L., & Petrella, A. (2012). Annexin A1 Induces Skeletal Muscle Cell Migration Acting through Formyl Peptide Receptors. *PLOS ONE*, 7(10), e48246.
- Bizzarro, V., Fontanella, B., Carratù, A., Belvedere, R., Marfella, R., Parente, L., & Petrella, A. (2012). Annexin A1 N-Terminal Derived Peptide Ac2-26 Stimulates Fibroblast Migration in High Glucose Conditions. *PLOS ONE*, 7(9), e45639.
- Boateng, J. S., Matthews, K. H., Stevens, H. N. E., & Eccleston, G. M. (2008). Wound Healing Dressings and Drug Delivery Systems: A Review. *Journal of Pharmaceutical Sciences*, 97(8), 2892-2923.
- Bögelein, J., & Lee, G. (2010). Cyclone selection influences protein damage during drying in a mini spray-dryer. *Int J Pharm.* 401(1-2), 68-71.
- Bonadeo, P., Marazzi, M., Masina, M., Ricci, E., & Romanelli, M. (2004). *Wound bed preparation: evoluzione della pratica clinica secondo i principi del time.*

- Borojeny, L. A., Albatineh, A. N., Dehkordi, A. H., & Gheshlagh, R. G. (2020). The Incidence of pressure ulcers and its associations in different wards of the hospital: A systematic review and meta-analysis. *Int J Prev Med*, 11.
- Bowler, P. G., Welsby, S., Towers, V., Booth, R., Hogarth, A., Rowlands, V., . . . Jones, S. A. (2012). Multidrug-resistant organisms, wounds and topical antimicrobial protection. *Int Wound J*, 9(4), 387-396.
- Boyapati, L., & Wang, H. L. (2007). The role of stress in periodontal disease and wound healing. *Periodontol*, 44(1), 195-210.
- Bratton, D. L., & Henson, P. M. (2011). Neutrophil clearance: when the party is over, clean-up begins. *Trends in immunology*, 32(8), 350-357.
- Brett, D. (2008). A Review of Collagen and Collagen-based Wound Dressings. *Wounds*, 20(12), 347-356.
- Britton, J. D. G.-B., Costa, T. R., Grosso, M. B. R. P., Horrocks, C. M. C., Kaes, L. B. L. C., Kennedy-Evans, K. R. A.-B.(2020). How covid-19 is changing skin: post-acute care wound experts from across the united states speak out. *Wound Management Prevention*, 66 (9).
- Broszczak, D. A., Sydes, E. R., Wallace, D., & Parker, T. J. (2017). Molecular Aspects of Wound Healing and the Rise of Venous Leg Ulceration: Omics Approaches to Enhance Knowledge and Aid Diagnostic Discovery. *The Clinical biochemist. Reviews*, 38(1), 35-55.
- Broughton, G., 2nd, Janis, J. E., & Attinger, C. E. (2006). A brief history of wound care. *Plast Reconstr Surg*, 117(7 Suppl), 6s-11s.
- Brumberg, V., Astrelina, T., Malivanova, T., & Samoilov, A. (2021). Modern Wound Dressings: Hydrogel Dressings. *Biomedicines*, 9(9), 1235.
- Burgess, C. (2008). Topical vitamins. *J Drugs Dermatol*, 7(7 Suppl), s2-6.

- Butnaru, E., Cheaburu, C., & Vasile, C. (2012). Morphological, thermal and rheological characterization of polyvinyl alcohol/chitosan blends. *Cellulose Chemistry and Technology*, 46, 571-581.
- Cal, K., & Sollohub, K. (2010). Spray Drying Technique. I: Hardware and Process Parameters. *Journal of Pharmaceutical Sciences*, 99(2), 575-586.
- Caley, M. P., Martins, V. L. C., & O'Toole, E. A. (2015). Metalloproteinases and Wound Healing. *Advances in wound care*, 4(4), 225-234.
- Calogero Fiorica, Fabio S. Palumbo, Giovanna Pitarresi, Mario Allegra, Roberto Puleio, Gaetano Giammona. (2018). Hyaluronic acid and α -elastin based hydrogel for three dimensional culture of vascular endothelial cells. *Journal of Drug Delivery Science and Technology*, 46 28-33
- Campos, A. C., Groth, A. K., Branco, A.B. (2008). Assessment and nutritional aspects of wound healing. *Current Opinion in Clinical Nutrition Metabolic Care*, 11(3), 281-288.
- Cañedo-Dorantes, L., & Cañedo-Ayala, M. (2019). Skin Acute Wound Healing: A Comprehensive Review. *International journal of inflammation*, 2019, 3706315-3706315.
- Capel, F., Nicolai, T., Durand, D., Boulenguer, P., & Langendorff, V. (2006). Calcium and acid induced gelation of (amidated) low methoxyl pectin. *Food Hydrocolloids*, 20(6), 901-907.
- Castro, M. M., Tanus-Santos, J. E., & Gerlach, R. F. (2011). Matrix metalloproteinases: targets for doxycycline to prevent the vascular alterations of hypertension. *Pharmacol Res*, 64(6), 567-572.
- Cerciello, A., Del Gaudio, P., Granata, V., Sala, M., Aquino, R. P., & Russo, P. (2017). Synergistic effect of divalent cations in improving technological properties of cross-

- linked alginate beads. *International Journal of Biological Macromolecules*, 101, 100-106.
- Chi, Y.-W., & Raffetto, J. D. (2015). Venous leg ulceration pathophysiology and evidence based treatment. *Vasc Med*, 20(2), 168-181.
- Choi, K.-O., Aditya, N. P., & Ko, S. (2014). Effect of aqueous pH and electrolyte concentration on structure, stability and flow behavior of non-ionic surfactant based solid lipid nanoparticles. *Food Chemistry*, 147, 239-244.
- Cichewicz, A., Pacleb, C., Connors, A., Hass, M. A., & Lopes, L. B. (2013). Cutaneous delivery of α -tocopherol and lipoic acid using microemulsions: influence of composition and charge. *J Pharm Pharmacol*, 65(6), 817-826.
- Cooray, S. N., Gobbetti, T., Montero-Melendez, T., McArthur, S., Thompson, D., Clark, A. J., Flower R.J., Perretti, M. (2013). Ligand-specific conformational change of the G-protein-coupled receptor ALX/FPR2 determines proresolving functional responses. *Proc Natl Acad Sci U S A*, 110(45), 18232-18237.
- Cover, N. F., Lai-Yuen, S., Parsons, A. K., & Kumar, A. (2012). Synergetic effects of doxycycline-loaded chitosan nanoparticles for improving drug delivery and efficacy. *International journal of nanomedicine*, 7, 2411-2419.
- Cowin, A. J., Hatzirodos, N., Holding, C. A., Dunaiski, V., Rayner, T. E., Harries, R. H., . . . Belford, D. A. (2001). Effect of Healing on the Expression of Transforming Growth Factor β s and their Receptors in Chronic Venous Leg Ulcers. *Journal of Investigative Dermatology*, 117(5), 1282-1289.
- Cutting, K. F. (2003). Wound exudate: composition and functions. *Br J Community Nurs*, 8(Sup3), S4-S9.
- Czaja, W., Krystynowicz, A., Bielecki, S., & Brown, R. M., Jr. (2006). Microbial cellulose--the natural power to heal wounds. *Biomaterials*, 27(2), 145-151.

- Danaei, M., Dehghankhold, M., Ataei, S., Hasanzadeh Davarani, F., Javanmard, R., Dokhani, A., . . . Mozafari, M. R. (2018). Impact of Particle Size and Polydispersity Index on the Clinical Applications of Lipidic Nanocarrier Systems. *Pharmaceutics*, 10(2), 57.
- Darby, I. A., Laverdet, B., Bonté, F., & Desmoulière, A. (2014). Fibroblasts and myofibroblasts in wound healing. *Clinical, cosmetic and investigational dermatology*, 7, 301-311.
- Dash, M., Chiellini, F., Ottenbrite, R. M., & Chiellini, E. (2011). Chitosan—A versatile semi-synthetic polymer in biomedical applications. *Prog Polym Sci*, 36(8), 981-1014.
- Davis, S. C., Ricotti, C., Cazzaniga, A., Welsh, E., Eaglstein, W. H., & Mertz, P. M. (2008). Microscopic and physiologic evidence for biofilm-associated wound colonization in vivo. *Wound Repair Regen*, 16(1), 23-29.
- De Cicco, F., Porta, A., Sansone, F., Aquino, R. P., & Del Gaudio, P. (2014). Nanospray technology for an in situ gelling nanoparticulate powder as a wound dressing. *International Journal of Pharmaceutics*, 473(1), 30-37.
- De Cicco, F., Reverchon, E., Adami, R., Auriemma, G., Russo, P., Calabrese, E. C., . . . Del Gaudio, P. (2014). In situ forming antibacterial dextran blend hydrogel for wound dressing: SAA technology vs. spray drying. *Carbohydrate Polymers*, 101, 1216-1224.
- De Cicco, F., Russo, P., Reverchon, E., García-González, C. A., Aquino, R. P., & Del Gaudio, P. (2016). Prilling and supercritical drying: A successful duo to produce core-shell polysaccharide aerogel beads for wound healing. *Carbohydr Polymers*, 147, 482-489.
- De Falco, G., Porta, A., Petrone, A. M., Del Gaudio, P., El Hassanin, A., Commodo, M., . . . D'Anna, A. (2017). Antimicrobial activity of flame-synthesized nano-TiO₂ coatings. *Environmental Science: Nano*, 4(5), 1095-1107.
- Del Gaudio, P., Amante, C., Civale, R., Bizzarro, V., Petrella, A., Pepe, G., . . . Aquino, R. P. (2020). In situ gelling alginate-pectin blend particles loaded with Ac2-26: A new weapon to improve wound care armamentarium. *Carbohydrate Polymers*, 227, 115305.

- Del Gaudio, P., De Cicco, F., Aquino, R. P., Picerno, P., Russo, P., Dal Piaz, F., . . . Petrella, A. (2015). Evaluation of in situ injectable hydrogels as controlled release device for ANXA1 derived peptide in wound healing. *Carbohydrate Polymers*, 115, 629-635.
- Del Gaudio, P., Russo, P., Rodriguez Dorado, R., Sansone, F., Mencherini, T., Gasparri, F., & Aquino, R. P. (2017). Submicrometric hypromellose acetate succinate particles as carrier for soy isoflavones extract with improved skin penetration performance. *Carbohydrate Polymers*, 165, 22-29.
- Demidova-Rice, T. N., Hamblin, M. R., & Herman, I. M. (2012). Acute and impaired wound healing: pathophysiology and current methods for drug delivery, part 1: normal and chronic wounds: biology, causes, and approaches to care. *Adv Skin Wound Care*, 25(7), 304-314.
- Deshmukh, R., Harwansh, R. K., Paul, S. D., & Shukla, R. (2020). Controlled release of sulfasalazine loaded amidated pectin microparticles through Eudragit S 100 coated capsule for management of inflammatory bowel disease. *Journal of Drug Delivery Science and Technology*, 55, 101495.
- Desmoulière, A., Redard, M., Darby, I., & Gabbiani, G. (1995). Apoptosis mediates the decrease in cellularity during the transition between granulation tissue and scar. *Am J Pathol*, 146(1), 56-66.
- Diegelmann, R. F., & Evans, M. C. (2004). Wound healing: an overview of acute, fibrotic and delayed healing. *Front Biosci*, 9, 283-289.
- DiPietro, L. A. (2013). Angiogenesis and scar formation in healing wounds. *Curr Opin Rheumatol*, 25(1), 87-91.
- Dipietro, L. A., Reintjes, M. G., Low, Q. E., Levi, B., & Gamelli, R. L. (2001). Modulation of macrophage recruitment into wounds by monocyte chemoattractant protein-1. *Wound Repair Regen*, 9(1), 28-33.

- Dong, R., & Guo, B. (2021). Smart wound dressings for wound healing. *Nano Today*, 41, 101290.
- Dong, Z., Wang, Q., & Du, Y. (2006). Alginate/gelatin blend films and their properties for drug controlled release. *Journal of Membrane Science*, 280, 37-44.
- Dovi, J. V., He, L. K., & DiPietro, L. A. (2003). Accelerated wound closure in neutrophil-depleted mice. *J Leukoc Biol*, 73(4), 448-455.
- Dragostin, O. M., Samal, S. K., Dash, M., Lupascu, F., Pânzariu, A., Tuchilus, C., . . . Profire, L. (2016). New antimicrobial chitosan derivatives for wound dressing applications. *Carbohydrate Polymers*, 141, 28-40.
- Dresvyanina, E. N., Grebennikov, S. F., Elokhovskii, V. Y., Dobrovolskaya, I. P., Ivan'kova, E. M., Yudin, V. E., . . . Morganti, P. (2020). Thermodynamics of interaction between water and the composite films based on chitosan and chitin nanofibrils. *Carbohydrate Polymers*, 245, 116552.
- Eberhardt, R. T., & Raffetto, J. D. (2014). Chronic Venous Insufficiency. *Circulation*, 130(4), 333-346.
- Ebube, N. K., Hikal, A. H., Wyandt, C. M., Beer, D. C., Miller, L. G., Jones, A. B. (1997). Sustained release of acetaminophen from heterogeneous matrix tablets: influence of polymer ratio, polymer loading, and co-active on drug release. *Pharmaceutical development technology*, 2(2), 161-170.
- Edwards, R., & Harding, K. G. (2004). Bacteria and wound healing. *Curr Opin Infect Dis*, 17(2), 91-96.
- El-Messery, T. M., Altuntas, U., Altin, G., & Özçelik, B. (2020). The effect of spray-drying and freeze-drying on encapsulation efficiency, in vitro bioaccessibility and oxidative stability of krill oil nanoemulsion system. *Food Hydrocolloids*, 106, 105890.

- El Fawal, G. F., Abu-Serie, M. M., Hassan, M. A., & Elnouby, M. S. (2018). Hydroxyethyl cellulose hydrogel for wound dressing: Fabrication, characterization and in vitro evaluation. *Int J Biol Macromol*, 111, 649-659.
- Ellis, S., Lin, E. J., & Tartar, D. (2018). Immunology of Wound Healing. *Curr Dermatol Rep*, 7(4), 350-358.
- Faisant, N., Siepmann, J., Richard, J., & Benoit, J. P. (2003). Mathematical modeling of drug release from bioerodible microparticles: effect of gamma-irradiation. *European Journal of Pharmaceutics and Biopharmaceutics*, 56(2), 271-279.
- Falcone, G., Mazzei, P., Piccolo, A., Esposito, T., Mencherini, T., Aquino, R. P., . . . Russo, P. (2022). Advanced printable hydrogels from pre-crosslinked alginate as a new tool in semi solid extrusion 3D printing process. *Carbohydrate Polymers*, 276, 118746.
- Fallacara, A., Baldini, E., Manfredini, S., & Vertuani, S. (2018). Hyaluronic Acid in the Third Millennium. *Polymers (Basel)*, 10(7), 701.
- Farahani, M., & Shafiee, A. (2021). Wound Healing: From Passive to Smart Dressings. *Advanced Healthcare Materials*, 10(16), 2100477.
- Fatnassi, M., Jacquart, S., Brouillet, F., Rey, C., Combes, C., & Girod Fullana, S. (2014). Optimization of spray-dried hyaluronic acid microspheres to formulate drug-loaded bone substitute materials. *Powder Technology*, 255, 44-51.
- Faure, A., York, P., & Rowe, R. C. (2001). Process control and scale-up of pharmaceutical wet granulation processes: a review. *European Journal of Pharmaceutics and Biopharmaceutics*, 52(3), 269-277.
- Frykberg, R. G., & Banks, J. (2015). Challenges in the Treatment of Chronic Wounds. *Advances in wound care*, 4(9), 560-582.
- Gajula, B., Munnamgi, S., & Basu, S. (2020). How bacterial biofilms affect chronic wound healing: a narrative review. *Internation Journal of Surgery: Global Health*. 3(2), e16.

- García, R. A., Pantazatos, D. P., Gessner, C. R., Go, K. V., Woods, V. L., Jr., & Villarreal, F. J. (2005). Molecular interactions between matrilysin and the matrix metalloproteinase inhibitor doxycycline investigated by deuterium exchange mass spectrometry. *Mol Pharmacol*, 67(4), 1128-1136.
- Gardner, S. E., Frantz, R. A., & Doebbeling, B. N. (2001). The validity of the clinical signs and symptoms used to identify localized chronic wound infection. *Wound Repair Regen*, 9(3), 178-186.
- Gentilello, L. M., Cobean, R. A., Walker, A. P., Moore, E. E., Wertz, M. J., & Dellinger, E. P. (1993). Acute ethanol intoxication increases the risk of infection following penetrating abdominal trauma. *The Journal of trauma*, 34(5), 669-674.
- Gershater, M. A., Löndahl, M., Nyberg, P., Larsson, J., Thörne, J., Eneroth, M., & Apelqvist, J. (2009). Complexity of factors related to outcome of neuropathic and neuroischaemic/ischaemic diabetic foot ulcers: a cohort study. *Diabetologia*, 52(3), 398-407.
- Ghahremankhani, A. A., Dorkoosh, F., Dinarvand, R. (2008). PLGA-PEG-PLGA tri-block copolymers as in situ gel-forming peptide delivery system: effect of formulation properties on peptide release. *Pharmaceutical development technology*, 13(1), 49-55.
- Ghatak, S., Maytin, E. V., Mack, J. A., Hascall, V. C., Atanelishvili, I., Moreno Rodriguez, R., . . . Misra, S. (2015). Roles of Proteoglycans and Glycosaminoglycans in Wound Healing and Fibrosis. *International Journal of Cell Biology*, 2015, 834893.
- Gillespie, D. L. (2010). Venous ulcer diagnosis, treatment, and prevention of recurrences. *Journal of Vascular Surgery*, 52(5, Supplement), 8S-14S.
- Gilliver, S. C., Ashworth, J. J., & Ashcroft, G. S. (2007). The hormonal regulation of cutaneous wound healing. *Clinics in dermatology*, 25(1), 56-62.

- Global burden of 369 diseases and injuries in 204 countries and territories, 1990-2019: a systematic analysis for the Global Burden of Disease Study 2019. (2020). *Lancet*, 396(10258), 1204-1222.
- Godbout, J. P., & Glaser, R. (2006). Stress-induced immune dysregulation: implications for wound healing, infectious disease and cancer. *J Neuroimmune Pharmacol*, 1(4), 421-427.
- Goldenheim, P. D. (1993). An appraisal of povidone-iodine and wound healing. *Postgraduate medical journal*, 69 Suppl 3, S97-105.
- Golub, L. M., Sorsa, T., Lee, H. M., Ciancio, S. G., Sorbi, D., Ramamurthy, N. S., . . . Konttinen, Y. T. (1995). Doxycycline inhibits neutrophil (PMN)-type matrix metalloproteinases in human adult periodontitis gingiva. *Journal of clinical periodontology*, 22 2, 100-109.
- Gómez-Ordóñez, E., & Rupérez, P. (2011). FTIR-ATR spectroscopy as a tool for polysaccharide identification in edible brown and red seaweeds. *Food Hydrocolloids*, 25(6), 1514-1520.
- Gong, C., Wu, Q., Wang, Y., Zhang, D., Luo, F., Zhao, X., . . . Qian, Z. (2013). A biodegradable hydrogel system containing curcumin encapsulated in micelles for cutaneous wound healing. *Biomaterials*, 34(27), 6377-6387.
- Gonzalez, A. C. d. O., Costa, T. F., Andrade, Z. d. A., & Medrado, A. R. A. P. (2016). Wound healing - A literature review. *Anais brasileiros de dermatologia*, 91(5), 614-620.
- Goodarzi, P., Falahzadeh, K., Nematizadeh, M., Farazandeh, P., Payab, M., Larijani, B., . . . Arjmand, B. (2018). Tissue Engineered Skin Substitutes. *Adv Exp Med Biol*, 1107, 143-188.
- Gopinath, D., Ahmed, M. R., Gomathi, K., Chitra, K., Sehgal, P. K., & Jayakumar, R. (2004). Dermal wound healing processes with curcumin incorporated collagen films. *Biomaterials*, 25(10), 1911-1917.

- Gosain, A., & DiPietro, L. A. (2004). Aging and wound healing. *World journal of surgery*, 28(3), 321-326.
- Gould, L., Abadir, P., Brem, H., Carter, M., Conner-Kerr, T., Davidson, J., . . . Schmader, K. (2015). Chronic Wound Repair and Healing in Older Adults: Current Status and Future Research. *Am Geriatr Soc*, 63(3), 427-438.
- Goy, R., Britto, D., & Assis, O. (2009). A Review of the Antimicrobial Activity of Chitosan. *Polimeros-ciencia E Tecnologia - Polimeros*, 19.
- Graves, N., Phillips, C. J., & Harding, K. (2021). A narrative review of the epidemiology and economics of chronic wounds. *Br J Dermatol*.
- Gun'ko, V. M., Savina, I. N., & Mikhalovsky, S. V. (2017). Properties of Water Bound in Hydrogels. *Gels*, 3(4), 37.
- Guo, S., & DiPietro, L. A. (2010). Factors Affecting Wound Healing. *Dent Res*, 89(3), 219-229.
- Gupta, R. C., Lall, R., Srivastava, A., & Sinha, A. (2019). Hyaluronic Acid: Molecular Mechanisms and Therapeutic Trajectory. *Front Vet Sci*, 6(192).
- Gurtner, G. C., Werner, S., Barrandon, Y., & Longaker, M. T. (2008). Wound repair and regeneration. *Nature*, 453(7193), 314-321.
- Hajhosseini, B., Longaker, M. T., & Gurtner, G. C. (2020). Pressure Injury. *Annals of Surgery*, 271(4), 671-679.
- Hamid Akash, M. S., Rehman, K., & Chen, S. (2015). Natural and Synthetic Polymers as Drug Carriers for Delivery of Therapeutic Proteins. *Polymer Reviews*, 55(3), 371-406.
- Han, G., & Ceilley, R. (2017). Chronic Wound Healing: A Review of Current Management and Treatments. *Adv Ther*, 34(3), 599-610.
- Harper, D., Young, A., & McNaught, C.-E. (2014). The physiology of wound healing. *Surgery (Oxford)*, 32(9), 445-450.

- Harris, I. R., Yee, K. C., Walters, C. E., Cunliffe, W. J., Kearney, J. N., Wood, E. J., & Ingham, E. (1995). Cytokine and protease levels in healing and non-healing chronic venous leg ulcers. *Exp Dermatol*, 4(6), 342-349.
- Hasan, N., Cao, J., Lee, J. et al (2021). Development of clindamycin-loaded alginate/pectin/hyaluronic acid composite hydrogel film for the treatment of MRSA-infected wounds. *J. Pharm Investig*, 51, 597-610.
- Hashad, R. A., Ishak, R. A. H., Fahmy, S., Mansour, S., & Geneidi, A. S. (2016). Chitosan-tripolyphosphate nanoparticles: Optimization of formulation parameters for improving process yield at a novel pH using artificial neural networks. *International Journal of Biological Macromolecules*, 86, 50-58.
- Hesketh, M., Sahin, K. B., West, Z. E., & Murray, R. Z. (2017). Macrophage Phenotypes Regulate Scar Formation and Chronic Wound Healing. *Int J Mol Sci*, 18(7).
- Hoehenwarter, W., Tang, Y., Ackermann, R., Pleissner, K.-P., Schmid, M., Stein, R., . . . Jungblut, P. R. (2008). Identification of proteins that modify cataract of mouse eye lens. *Proteomics*, 8(23-24), 5011-5024.
- Hosseini, S. M., Hosseini, H., Mohammadifar, M. A., Mortazavian, A. M., Mohammadi, A., Khosravi-Darani, K., . . . Khaksar, R. (2013). Incorporation of essential oil in alginate microparticles by multiple emulsion/ionic gelation process. *International Journal of Biological Macromolecules*, 62, 582-588.
- Huang, J. J., Xia, C. J., Wei, Y., Yao, Y., Dong, M. W., Lin, K. Z., . . . Fan, Y. Y. (2020). Annexin A1-derived peptide Ac2-26 facilitates wound healing in diabetic mice. *Wound Repair Regen*, 28(6), 772-779.
- Huang, R., Li, W., Lv, X., Lei, Z., Bian, Y., Deng, H., . . . Li, X. (2015). Biomimetic LBL structured nanofibrous matrices assembled by chitosan/collagen for promoting wound healing. *Biomaterials*, 53, 58-75.

- Huh, A. J., & Kwon, Y. J. (2011). "Nanoantibiotics": a new paradigm for treating infectious diseases using nanomaterials in the antibiotics resistant era. *J Control Release*, 156(2), 128-145.
- Huijberts, M. S., Schaper, N. C., & Schalkwijk, C. G. (2008). Advanced glycation end products and diabetic foot disease. *Diabetes Metab Res Rev*, 24 Suppl 1, S19-24.
- Iskandar, F. J. A. P. T. (2009). Nanoparticle processing for optical applications - A review. *Advanced Powder Thechnology*, 20, 283-292.
- Jacobi, J., Jang, J. J., Sundram, U., Dayoub, H., Fajardo, L. F., & Cooke, J. P. (2002). Nicotine Accelerates Angiogenesis and Wound Healing in Genetically Diabetic Mice. *Am J Pathol*, 161(1), 97-104.
- Jagetia, G. C., & Rajanikant, G. K. J. I. w. j. (2012). Acceleration of wound repair by curcumin in the excision wound of mice exposed to different doses of fractionated γ radiation. *International wound journal*, 9(1), 76-92.
- Jannesari, M., Varshosaz, J., Morshed, M., & Zamani, M. (2011). Composite poly(vinyl alcohol)/poly(vinyl acetate) electrospun nanofibrous mats as a novel wound dressing matrix for controlled release of drugs. *International journal of nanomedicine*, 6, 993-1003.
- Järbrink, K., Ni, G., Sönnergren, H., Schmidtchen, A., Pang, C., Bajpai, R., & Car, J. (2017). The humanistic and economic burden of chronic wounds: a protocol for a systematic review. *Systematic Reviews*, 6(1), 15.
- Jaya, S., Durance, T. D., & Wang, R. (2009). Effect of alginate-pectin composition on drug release characteristics of microcapsules. *Journal of Microencapsulation*, 26(2), 143-153.

- Jenning, V., Thünemann, A. F., & Gohla, S. H. (2000). Characterisation of a novel solid lipid nanoparticle carrier system based on binary mixtures of liquid and solid lipids. *International Journal of Pharmaceutics*, 199(2), 167-177.
- Jeon, O., Samorezov, J. E., & Alsberg, E. (2014). Single and dual crosslinked oxidized methacrylated alginate/PEG hydrogels for bioadhesive applications. *Acta Biomater*, 10(1), 47-55.
- Jeong, B., Bae, Y. H., & Kim, S. W. (2000). Drug release from biodegradable injectable thermosensitive hydrogel of PEG-PLGA-PEG triblock copolymers. *J Control Release*, 63(1-2), 155-163.
- Ji, S., Thulstrup, P., Mu, H., Hansen, S., van de Weert, M., Rantanen, J., & Yang, M. (2016). Effect of ethanol as a co-solvent on the aerosol performance and stability of spray-dried lysozyme. *Int J Pharm*, 513, 175-182.
- Jiang, W. G., Sanders, A. J., Ruge, F., & Harding, K. G. (2012). Influence of interleukin-8 (IL-8) and IL-8 receptors on the migration of human keratinocytes, the role of PLC- γ and potential clinical implications. *Exp Ther Med*, 3(2), 231-236.
- Jin, J., Ji, Z., Xu, M., Liu, C., Ye, X., Zhang, W., ... & Lv, Z. (2018). Microspheres of carboxymethyl chitosan, sodium alginate, and collagen as a hemostatic agent in vivo. *ACS Biomaterials Science & Engineering*, 4(7), 2541-2551
- Jung, J. A., Yoo, K. H., Han, S. K., Dhong, E. S., & Kim, W. K. (2016). Evaluation of the Efficacy of Highly Hydrophilic Polyurethane Foam Dressing in Treating a Diabetic Foot Ulcer. *Adv Skin Wound Care*, 29(12), 546-555.
- Kalwar, K. (2017). Incorporation of ciprofloxacin/laponite in polycaprolactone electrospun nanofibers: Drug release and antibacterial studies. *Materials Research Express*.

- Kamoun, E. A., Kenawy, E.-R. S., & Chen, X. (2017). A review on polymeric hydrogel membranes for wound dressing applications: PVA-based hydrogel dressings. *Journal of Advanced Research*, 8(3), 217-233.
- Kean, J. (2010). The effects of smoking on the wound healing process. *J Wound Care*, 19(1), 5-8.
- Kean, T., & Thanou, M. (2010). Biodegradation, biodistribution and toxicity of chitosan. *Advanced Drug Delivery Reviews*, 62, 3-11.
- Kerr, M., Barron, E., Chadwick, P., Evans, T., Kong, W. M., Rayman, G., . . . Jeffcoate, W. J. (2019). The cost of diabetic foot ulcers and amputations to the National Health Service in England. *Diabet Med*, 36(8), 995-1002.
- Khodaverdi, E., Tekie, F. S. M., Mohajeri, S. A., Ganji, F., Zohuri, G., & Hadizadeh, F. (2012). Preparation and Investigation of Sustained Drug Delivery Systems Using an Injectable, Thermosensitive, In Situ Forming Hydrogel Composed of PLGA–PEG–PLGA. *AAPS PharmSciTech*, 13(2), 590-600.
- Kim, J. O., Park, J. K., Kim, J. H., Jin, S. G., Yong, C. S., Li, D. X., . . . Lyoo, W. S. (2008). Development of polyvinyl alcohol–sodium alginate gel-matrix-based wound dressing system containing nitrofurazone. *International journal of pharmaceutics*, 359(1-2), 79-86.
- Koh, T. J., & DiPietro, L. A. (2011). Inflammation and wound healing: the role of the macrophage. *Expert Rev Mol Med*, 13, e23.
- Kohane, D. S. (2007). Microparticles and nanoparticles for drug delivery. *Biotechnology and bioengineering*, 96(2), 203-209.
- Kolluri, R., Lugli, M., Villalba, L., Varcoe, R., Maleti, O., Gallardo, F., . . . Beckman, J. A. An estimate of the economic burden of venous leg ulcers associated with deep venous disease. *Vasc Med*, 0(0), 1358863X211028298.

- Komaiko, J. S., & McClements, D. J. (2016). Formation of Food-Grade Nanoemulsions Using Low-Energy Preparation Methods: A Review of Available Methods. *Comprehensive Reviews in Food Science and Food Safety*, 15(2), 331-352.
- Kozen, B. G., Kircher, S. J., Henao, J., Godinez, F. S., & Johnson, A. S. (2008). An Alternative Hemostatic Dressing: Comparison of CELOX, HemCon, and QuikClot. *Acad Emerg Med*, 15(1), 74-81.
- Krajewska, B. (2004). Application of chitin-and chitosan-based materials for enzyme immobilizations: a review. *Enzyme microbial technology*, 35(2-3), 126-139.
- Krausz, A. E., Adler, B. L., Cabral, V., Navati, M., Doerner, J., Charafeddine, R. A., . . . Friedman, A. J. (2015). Curcumin-encapsulated nanoparticles as innovative antimicrobial and wound healing agent. *Nanomedicine: Nanotechnology, Biology and Medicine*, 11(1), 195-206.
- Kucińska-Lipka, J., Gubanska, I., & Janik, H. (2015). Bacterial cellulose in the field of wound healing and regenerative medicine of skin: recent trends and future perspectives. *Polymer Bulletin*, 72.
- Kucińska-Lipka, J., Gubanska, I., Lewandowska, A., Terebieniec, A., Haryńska, A., & Cieśliński, H. (2019). Antibacterial polyurethanes, modified with cinnamaldehyde, as potential materials for fabrication of wound dressings. *Polymer Bulletin*, 76, 1-18.
- Kujath, P., & Michelsen, A. (2008). Wounds - from physiology to wound dressing. *Dtsch Arztebl Int*, 105(13), 239-248.
- Kulig, D., Zimoch-Korzycka, A., Jarmoluk, A., & Marycz, K. (2016). Study on Alginate–Chitosan Complex Formed with Different Polymers Ratio. *Polymers*. 8(5), 167.
- Kung, M.-L., Lin, P.-Y., Peng, S.-W., Wu, D.-C., Wu, W.-J., Yeh, B.-W., . . . Hsieh, S. (2016). Biomimetic polymer-based Ag nanocomposites as a antimicrobial platform. *Applied Materials Today*, 4, 31-39.

- Kurahashi, T., & Fujii, J. (2015). Roles of Antioxidative Enzymes in Wound Healing. *Journal of Development Biology*, 3(2), 57-70.
- Lacerda, J. Z., Drewes, C. C., Mimura, K. K. O., Zanon, C. d. F., Ansari, T., Gil, C. D., . . . Oliani, S. M. (2018). Annexin A12–26 Treatment Improves Skin Heterologous Transplantation by Modulating Inflammation and Angiogenesis Processes. *Front Pharmacology*, 9(1015).
- Ladwig, G. P., Robson, M. C., Liu, R., Kuhn, M. A., Muir, D. F., & Schultz, G. S. (2002). Ratios of activated matrix metalloproteinase-9 to tissue inhibitor of matrix metalloproteinase-1 in wound fluids are inversely correlated with healing of pressure ulcers. *Wound Repair Regen*, 10(1), 26-37.
- Lai-Cheong, J. E., & McGrath, J. A. (2017). Structure and function of skin, hair and nails. *Medicine*, 45(6), 347-351.
- Lai, H. L., Abu'Khalil, A., & Craig, D. Q. M. (2003). The preparation and characterisation of drug-loaded alginate and chitosan sponges. *International Journal of Pharmaceutics*, 251(1), 175-181.
- Landén, N. X., Li, D., & Ståhle, M. (2016). Transition from inflammation to proliferation: a critical step during wound healing. *Cell Mol Life Sci*, 73(20), 3861-3885.
- Lawrie, G., Keen, I., Drew, B., Chandler-Temple, A., Rintoul, L., Fredericks, P., & Grøndahl, L. (2007). Interactions between Alginate and Chitosan Biopolymers Characterized Using FTIR and XPS. *Biomacromolecules*, 8(8), 2533-2541.
- Leeper, D., Assadian, O., & Edmiston, C. E. (2015). Approach to chronic wound infections. *Br J Dermatol*, 173(2), 351-358.
- Lee, B. K., Yun, Y. H., & Park, K. (2015). Smart nanoparticles for drug delivery: Boundaries and opportunities. *Chemical Engineering Science*, 125, 158-164.

- Lee, H., Park, J. W., Kim, S. P., Lo, E. H., & Lee, S. R. (2009). Doxycycline inhibits matrix metalloproteinase-9 and laminin degradation after transient global cerebral ischemia. *Neurobiol Dis*, 34(2), 189-198.
- Lee, H. M., Ciancio, S. G., Tüter, G., Ryan, M. E., Komaroff, E., & Golub, L. M. (2004). Subantimicrobial dose doxycycline efficacy as a matrix metalloproteinase inhibitor in chronic periodontitis patients is enhanced when combined with a non-steroidal anti-inflammatory drug. *J Periodontol*, 75(3), 453-463.
- Lee, K. Y., & Mooney, D. J. (2012). Alginate: properties and biomedical applications. *Prog Polym Sci*, 37(1), 106-126.
- Lee, S. H., Heng, D., Ng, W. K., Chan, H.-K., & Tan, R. B. H. (2011). Nano spray drying: A novel method for preparing protein nanoparticles for protein therapy. *International Journal of Pharmaceutics*, 403(1), 192-200.
- Lengyel, M., Kállai-Szabó, N., Antal, V., Laki, A. J., & Antal, I. (2019). Microparticles, Microspheres, and Microcapsules for Advanced Drug Delivery. *Scientia Pharmaceutica*, 87(3), 20.
- Leoni, G., & Nusrat, A. (2016). Annexin A1: shifting the balance towards resolution and repair. *Biological Chemistry*, 397(10), 971-979.
- Lepántalo, M., Apelqvist, J., Setacci, C., Ricco, J. B., de Donato, G., Becker, F., . . . Davies, A. H. (2011). Chapter V: Diabetic Foot. *European Journal of Vascular and Endovascular Surgery*, 42, S60-S74.
- Li, Boxuan and Wang, Juan and Gui, Qin and Yang, Hu, (2020). Continuous production of uniform chitosan beads as hemostatic dressings by a facile flow injection method. *J. Mater. Chem. B*, 8 (35), 7941-7946.

- Li, H., Xue, Y., Jia, B., Bai, Y., Zuo, Y., Wang, S., . . . Tang, H. (2018). The preparation of hyaluronic acid grafted pullulan polymers and their use in the formation of novel biocompatible wound healing film. *Carbohydrate Polymers*, 188, 92-100.
- Li, M., Surliel, I., Vekaria, J., Proske, J., Orbe, P., Armani, M., . . . Bilgili, E. (2018). Impact of dispersants on dissolution of itraconazole from drug-loaded, surfactant-free, spray-dried nanocomposites. *Powder Technology*, 339, 281-295.
- Li, X., Anton, N., Arpagaus, C., Belleiteix, F., & Vandamme, T. F. (2010). Nanoparticles by spray drying using innovative new technology: the Büchi nano spray dryer B-90. *J Control Release*, 147(2), 304-310.
- Li, X., Anton, N., Ta, T. M. C., Zhao, M., Messaddeq, N., & Vandamme, T. F. (2011). Microencapsulation of nanoemulsions: novel Trojan particles for bioactive lipid molecule delivery. *International journal of nanomedicine*, 6, 1313-1325.
- Li, Y., Jiang, H., Zheng, W., Gong, N., Chen, L., Jiang, X., & Yang, G. (2015). Bacterial cellulose–hyaluronan nanocomposite biomaterials as wound dressings for severe skin injury repair. *Journal of Materials Chemistry B*, 3(17), 3498-3507.
- Liem, P. H., Morimoto, N., Ito, R., Kawai, K., & Suzuki, S. (2013). Treating a collagen scaffold with a low concentration of nicotine promoted angiogenesis and wound healing. *Journal of Surgical Research*, 182(2), 353-361.
- Lin, H. Y., Chen, H. H., Chang, S. H., & Ni, T. S. (2013). Pectin-chitosan-PVA nanofibrous scaffold made by electrospinning and its potential use as a skin tissue scaffold. *J Biomater Sci Polym Ed*, 24(4), 470-484.
- Lin, Z. Q., Kondo, T., Ishida, Y., Takayasu, T., & Mukaida, N. (2003). Essential involvement of IL-6 in the skin wound-healing process as evidenced by delayed wound healing in IL-6-deficient mice. *J Leukoc Biol*, 73(6), 713-721.

- Liow, S. S., Dou, Q., Kai, D., Li, Z., Sugiarto, S., Yu, C. Y. Y., . . . Loh, X. J. (2017). Long-Term Real-Time In Vivo Drug Release Monitoring with AIE Thermogelling Polymer. *Small*, 13(7), 1603404.
- Litwiniuk, M., Krejner-Bienias, A., Speyrer, M., Gauto, A., & Grzela, T. (2016). Hyaluronic Acid in Inflammation and Tissue Regeneration. *Wounds : a compendium of clinical research and practice*, 28, 78-88.
- Liu, J.-Y., Li, Y., Hu, Y., Cheng, G., Ye, E., Shen, C., & Xu, F.-J. (2018). Hemostatic porous sponges of cross-linked hyaluronic acid/cationized dextran by one self-foaming process. *Materials Science and Engineering: C*, 83, 160-168.
- Liu, L., Tang, X., Wang, Y., & Guo, S. (2011). Smart gelation of chitosan solution in the presence of NaHCO₃ for injectable drug delivery system. *Int J Pharm*, 414(1-2), 6-15.
- Liu, W., Wang, J., McClements, D. J., & Zou, L. (2018). Encapsulation of β -carotene-loaded oil droplets in caseinate/alginate microparticles: Enhancement of carotenoid stability and bioaccessibility. *Journal of Functional Foods*, 40, 527-535.
- Liu, W., Wu, W. D., Selomulya, C., & Chen, X. D. (2011). Uniform Chitosan Microparticles Prepared by a Novel Spray-Drying Technique. *International Journal of Chemical Engineering*, 2011, 267218.
- Liu, Y., Siard, M., Adams, A., Keowen, M. L., Miller, T. K., Garza, J. F., . . . Seeram, N. P. (2018). Simultaneous quantification of free curcuminoids and their metabolites in equine plasma by LC-ESI-MS/MS. *Journal of Pharmaceutical and Biomedical Analysis*, 154, 31-39.
- Löfgren, C., Walkenström, P., & Hermansson, A.-M. (2002). Microstructure and rheological behavior of pure and mixed pectin gels. *Biomacromolecules*, 3(6), 1144-1153.

- Lollo, G., Ullio-Gamboa, G., Fuentes, E., Matha, K., Lautram, N., & Benoit, J. P. (2018). In vitro anti-cancer activity and pharmacokinetic evaluation of curcumin-loaded lipid nanocapsules. *Mater Sci Eng C Mater Biol Appl*, 91, 859-867.
- Lumbreras-Aguayo, A., Meléndez-Ortiz, H. I., Puente-Urbina, B., Alvarado-Canché, C., Ledezma, A., Romero-García, J., & Betancourt-Galindo, R. (2019). Poly(methacrylic acid)-modified medical cotton gauzes with antimicrobial and drug delivery properties for their use as wound dressings. *Carbohydrate Polymers*, 205, 203-210.
- Lupascu, F. G., Dash, M., Samal, S. K., Dubruel, P., Lupusoru, C. E., Lupusoru, R.-V., . . . Profire, L. (2015). Development, optimization and biological evaluation of chitosan scaffold formulations of new xanthine derivatives for treatment of type-2 diabetes mellitus. *European Journal of Pharmaceutical Sciences*, 77, 122-134.
- Luppi, B., Bigucci, F., Mercolini, L., Musenga, A., Sorrenti, M., Catenacci, L., & Zecchi, V. (2009). Novel mucoadhesive nasal inserts based on chitosan/hyaluronate polyelectrolyte complexes for peptide and protein delivery. *J Pharm Pharmacol*, 61(2), 151-157.
- Lv, X., Liu, Y., Song, S., Tong, C., Shi, X., Zhao, Y., ... & Hou, M. (2019). Influence of chitosan oligosaccharide on the gelling and wound healing properties of injectable hydrogels based on carboxymethyl chitosan/alginate polyelectrolyte complexes. *Carbohydrate polymers*, 205, 312-321.
- Makaremi, M., Yousefi, H., Cavallaro, G., Lazzara, G., Goh, C. B. S., Lee, S. M., . . . Pasbakhsh, P. (2019). Safely Dissolvable and Healable Active Packaging Films Based on Alginate and Pectin. *Polymers*, 11(10), 1594.
- Mangoni, M. L., McDermott, A. M., & Zasloff, M. (2016). Antimicrobial peptides and wound healing: biological and therapeutic considerations. *Exp Dermatol*, 25(3), 167-173.

- Manniello, M. D., Del Gaudio, P., Aquino, R. P., & Russo, P. (2017). Clarithromycin and N-acetylcysteine co-spray-dried powders for pulmonary drug delivery: A focus on drug solubility. *International Journal of Pharmaceutics*, 533(2), 463-469.
- Margolis, D. J., Hofstad, O., & Feldman, H. I. (2008). Association Between Renal Failure and Foot Ulcer or Lower-Extremity Amputation in Patients With Diabetes. *Diabetes Care*, 31(7), 1331-1336.
- Martin, P., & Nunan, R. (2015). Cellular and molecular mechanisms of repair in acute and chronic wound healing. *Br J Dermatol*, 173(2), 370-378.
- Masood, N., Ahmed, R., Tariq, M., Ahmed, Z., Masoud, M. S., Ali, I., . . . Hasan, A. (2019). Silver nanoparticle impregnated chitosan-PEG hydrogel enhances wound healing in diabetes induced rabbits. *International Journal of Pharmaceutics*, 559, 23-36.
- Masoud Rezvanian, Naveed Ahmad, Mohd Cairul Iqbal Mohd Amin, Shiew-Fern Ng (2017). Optimization, characterization, and in vitro assessment of alginate-pectin ionic cross-linked hydrogel film for wound dressing applications. *International Journal of Biological Macromolecules*, 97, 131-140.
- Masuda, T., Toi, Y., Bando, H., Maekawa, T., Takeda, Y., & Yamaguchi, H. (2002). Structural identification of new curcumin dimers and their contribution to the antioxidant mechanism of curcumin. *J Agric Food Chem*, 50(9), 2524-2530.
- Mathieu, D. (2006). *Handbook on hyperbaric medicine*: Springer.
- Mbhele, Z., Salemane, M., Van Sittert, C., Nedeljković, J., Djoković, V., & Luyt, A. J. C. o. M. (2003). Fabrication and characterization of silver– polyvinyl alcohol nanocomposites. *Molecules*, 15(26), 5019-5024.
- Mebert, A. M., Alvarez, G. S., Peroni, R., Illoul, C., Hélyary, C., Coradin, T., & Desimone, M. F. (2018). Collagen-silica nanocomposites as dermal dressings preventing infection in vivo. *Mater Sci Eng C Mater Biol Appl*, 93, 170-177.

- Mehvar, R. (2000). Dextrans for targeted and sustained delivery of therapeutic and imaging agents. *Journal of Controlled Release*, 69(1), 1-25.
- Mendez, M. V., Raffetto, J. D., Phillips, T., Menzoian, J. O., & Park, H.-Y. (1999). The proliferative capacity of neonatal skin fibroblasts is reduced after exposure to venous ulcer wound fluid: A potential mechanism for senescence in venous ulcers. *Journal of Vascular Surgery*, 30(4), 734-743.
- Meng, X., Lu, Y., Gao, Y., Cheng, S., Tian, F., Xiao, Y., & Li, F. (2021). Chitosan/alginate/hyaluronic acid polyelectrolyte composite sponges crosslinked with genipin for wound dressing application. *International Journal of Biological Macromolecules*, 182, 512-523.
- Merino, S., Martín, C., Kostarelos, K., Prato, M., & Vázquez, E. (2015). Nanocomposite Hydrogels: 3D Polymer-Nanoparticle Synergies for On-Demand Drug Delivery. *ACS Nano*, 9(5), 4686-4697.
- Mervis, J. S., & Phillips, T. J. (2019). Pressure ulcers: Pathophysiology, epidemiology, risk factors, and presentation. *J Am Acad Dermatol*, 81(4), 881-890.
- Michelin, R. M., Ahdoot, E., Zakhary, B. L., McDowell, M., & French, M. (2021). Choosing the Optimal Wound Dressing for Bathing After Total Knee Arthroplasty. *The Journal of Arthroplasty*, 36(3), 970-977.
- Miguel, S. P., Ribeiro, M. P., Brancal, H., Coutinho, P., & Correia, I. J. (2014). Thermoresponsive chitosan–agarose hydrogel for skin regeneration. *Carbohydrate Polymers*, 111, 366-373.
- Miller, K. J., Brown, D. A., Ibrahim, M. M., Ramchal, T. D., & Levinson, H. (2015). MicroRNAs in skin tissue engineering. *Advanced Drug Delivery Reviews*, 88, 16-36.

- Miyazaki, Y., Yakou, S., & Takayama, K. (2004). Study on jelly fig extract as a potential hydrophilic matrix for controlled drug delivery. *International journal of pharmaceutics*, 287(1-2), 39-46.
- Mladenovska, K., Cruaud, O., Richomme, P., Belamie, E., Raicki, R. S., Venier-Julienne, M. C., . . . Goracinova, K. (2007). 5-ASA loaded chitosan–Ca–alginate microparticles: Preparation and physicochemical characterization. *Int J Pharm*, 345(1), 59-69.
- Mndlovu, H., du Toit, L. C., Kumar, P., Marimuthu, T., Kondiah, P. P., Choonara, Y. E., & Pillay, V. (2019). Development of a fluid-absorptive alginate-chitosan bioplatfrom for potential application as a wound dressing. *Carbohydrate polymers*, 222, 114988.
- Moeini, A., Pedram, P., Makvandi, P., Malinconico, M., & Gomez d'Ayala, G. (2020). Wound healing and antimicrobial effect of active secondary metabolites in chitosan-based wound dressings: A review. *Carbohydrate Polymers*, 233, 115839.
- Mohanty, C., & Sahoo, S. K. (2017). Curcumin and its topical formulations for wound healing applications. *Drug Discovery Today*, 22(10), 1582-1592.
- Moore, Z., Avsar, P., Conaty, L., Moore, D. H., Patton, D., & O'Connor, T. (2019). The prevalence of pressure ulcers in Europe, what does the European data tell us: a systematic review. *J Wound Care*, 28(11), 710-719.
- Moore, Z., Cowman, S., & Conroy, R. M. (2011). A randomised controlled clinical trial of repositioning, using the 30° tilt, for the prevention of pressure ulcers. *J Clin Nurs*, 20(17-18), 2633-2644.
- Moore, Z. E., & Webster, J. (2013). Dressings and topical agents for preventing pressure ulcers. *Cochrane Database Syst Rev*(8), Cd009362.
- Morimoto, N., Takemoto, S., Kawazoe, T., & Suzuki, S. (2008). Nicotine at a low concentration promotes wound healing. *International journal of pharmaceutics*, 145(2), 199-204.

- Morton, L. M., & Phillips, T. J. (2016). Wound healing and treating wounds: Differential diagnosis and evaluation of chronic wounds. *J Am Acad Dermatol*, 74(4), 589-605; quiz 605-586.
- Moser, K., Kriwet, K., Naik, A., Kalia, Y. N., & Guy, R. H. (2001). Passive skin penetration enhancement and its quantification in vitro. *Eur J Pharm Biopharm*, 52(2), 103-112.
- Mosser, D. M. (2003). The many faces of macrophage activation. *J Leukoc Biol*, 73(2), 209-212.
- Mt, F., Mohapatra, D., Kumar, D., Chittoria, R., & Nandhagopal, V. (2015). Current concepts in the physiology of adult wound healing. *Plas Aesthet Res*, 2, 250-256.
- Mun, S.-H., Joung, D.-K., Kim, Y.-S., Kang, O.-H., Kim, S.-B., Seo, Y.-S., . . . Kweon, K.-T. (2013). Synergistic antibacterial effect of curcumin against methicillin-resistant *Staphylococcus aureus*. *Phytomedicine*, 20(8-9), 714-718.
- Munarin, F., Tanzi, M., & Petrini, P. (2013). Corrigendum to ‘Advances in biomedical applications of pectin gels’. *International Journal of Biological Macromolecules*, 51 (2012) 681–689]. (55), 307.
- Muzzarelli, R. A. A. (2009). Chitins and chitosans for the repair of wounded skin, nerve, cartilage and bone. *Carbohydrate Polymers*, 76(2), 167-182.
- Mwaura, B., Mahendran, B., Hynes, N., Defreitas, D., Avalos, G., Adegbola, T., . . . Sultan, S. (2006). The Impact of Differential Expression of Extracellular Matrix Metalloproteinase Inducer, Matrix Metalloproteinase-2, Tissue Inhibitor of Matrix Metalloproteinase-2 and PDGF-AA on the Chronicity of Venous Leg Ulcers. *European Journal of Vascular and Endovascular Surgery*, 31(3), 306-310.
- Nair, A. V., Raman, M., & Doble, M. (2016). Cyclic β -(1 \rightarrow 3) (1 \rightarrow 6) glucan/carrageenan hydrogels for wound healing applications. *RSC Advances*, 6(100), 98545-98553.

- Nandiyanto, A. B. D., & Okuyama, K. (2011). Progress in developing spray-drying methods for the production of controlled morphology particles: From the nanometer to submicrometer size ranges. *Advanced Powder Technology*, 22(1), 1-19.
- Nejati, R., Kovacic, D., & Slominski, A. (2013). Neuro-immune-endocrine functions of the skin: an overview. *Expert Rev Dermatol*, 8(6), 581-583.
- Niemiec, S. M., Louiselle, A. E., Liechty, K. W., & Zgheib, C. (2021). Role of microRNAs in pressure ulcer immune response, pathogenesis, and treatment. *International Journal of Molecular Sciences*, 22(1), 64.
- Nour, S., Baheiraei, N., Imani, R., Khodaei, M., Alizadeh, A., Rabiee, N., & Moazzeni, S. M. (2019). A review of accelerated wound healing approaches: biomaterial- assisted tissue remodeling. *Journal of Materials Science: Materials in Medicine*, 30(10), 120.
- Nussbaum, S. R., Carter, M. J., Fife, C. E., DaVanzo, J., Haught, R., Nusgart, M., & Cartwright, D. (2018). An Economic Evaluation of the Impact, Cost, and Medicare Policy Implications of Chronic Nonhealing Wounds. *Value Health*, 21(1), 27-32.
- Nyman, E., Henricson, J., Ghafouri, B., Anderson, C. D., & Kratz, G. (2019). Hyaluronic Acid Accelerates Re-epithelialization and Alters Protein Expression in a Human Wound Model. *Plast Reconstr Surg Glob Open*, 7(5), e2221.
- O'Donnell, T. F., Jr., Passman, M. A., Marston, W. A., Ennis, W. J., Dalsing, M., Kistner, R. L., . . . Gloviczki, P. (2014). Management of venous leg ulcers: clinical practice guidelines of the Society for Vascular Surgery® and the American Venous Forum. *J Vasc Surg*, 60(2 Suppl), 3s-59s.
- Oakenfull, d., & Scott, a. (1984). Hydrophobic interaction in the gelation of high methoxyl pectins. *Journal of Food Science*, 49(4), 1093-1098.
- Oakenfull, D. J. T. c., & pectin, t. o. (1991). The chemistry of high-methoxyl pectins. *The chemistry technology of pectin*, 87-108.

- Okizaki, S., Ito, Y., Hosono, K., Oba, K., Ohkubo, H., Amano, H., . . . Majima, M. (2015). Suppressed recruitment of alternatively activated macrophages reduces TGF- β 1 and impairs wound healing in streptozotocin-induced diabetic mice. *Biomed Pharmacother*, 70, 317-325.
- Olsson, M., Järbrink, K., Divakar, U., Bajpai, R., Upton, Z., Schmidtchen, A., & Car, J. (2019). The humanistic and economic burden of chronic wounds: A systematic review. *Wound Repair Regen*, 27(1), 114-125.
- Omar, A., Wright, J. B., Schultz, G., Burrell, R., & Nadworny, P. (2017). Microbial Biofilms and Chronic Wounds. *Microorganism*, 5(1), 9.
- Oropallo, A., Lantis, J., Martin, A., Rubaiay, A. A., & Wang, N. (2021). Wound care during the COVID-19 pandemic: improving outcomes through the integration of telemedicine. *J Wound Care*, 30(Sup2), S12-S17.
- Oyarzun-Ampuero, F., Vidal, A., Concha, M., Morales, J., Orellana, S., & Moreno-Villoslada, I. (2015). Nanoparticles for the Treatment of Wounds. *Current Pharmaceutical Design*, 21(29), 4329-4341.
- Pal, K., Banthia, A. K., Majumdar, D. K. (2006). Preparation of Transparent Starch Based Hydrogel Membrane with Potential Application as Wound Dressing. *Trends in biomaterials artificial organs*, 20, 59-59.
- Pallandre, S., Decker, E., & McClements, D. J. (2007). Improvement of stability of oil-in-water emulsions containing caseinate-coated droplets by addition of sodium alginate. *Journal of food science*, 72(9), E518-E524.
- Panchatcharam, M., Miriyala, S., Gayathri, V. S., & Suguna, L. (2006). Curcumin improves wound healing by modulating collagen and decreasing reactive oxygen species. *Molecular and Cellular Biochemistry*, 290(1), 87-96.

- Panyam, J., Dali, M. M., Sahoo, S. K., Ma, W., Chakravarthi, S. S., Amidon, G. L., . . . Labhasetwar, V. (2003). Polymer degradation and in vitro release of a model protein from poly (D, L-lactide-co-glycolide) nano-and microparticles. *Journal of controlled release*, 92(1-2), 173-187.
- Paomephan, P., Assavanig, A., Chaturongakul, S., Cady, N. C., Bergkvist, M., & Niamsiri, N. (2018). Insight into the antibacterial property of chitosan nanoparticles against *Escherichia coli* and *Salmonella Typhimurium* and their application as vegetable wash disinfectant. *Food Control*, 86, 294-301.
- Parani, M., Lokhande, G., Singh, A., & Gaharwar, A. K. (2016). Engineered Nanomaterials for Infection Control and Healing Acute and Chronic Wounds. *ACS Applied Materials & Interfaces*, 8(16), 10049-10069.
- Park, C. J., Gabrielson, N. P., Pack, D. W., Jamison, R. D., & Wagoner Johnson, A. J. (2009). The effect of chitosan on the migration of neutrophil-like HL60 cells, mediated by IL-8. *Biomaterials*, 30(4), 436-444.
- Pasaribu, K. M., Gea, S., Ilyas, S., Tamrin, T., & Radecka, I. (2020). Characterization of Bacterial Cellulose-Based Wound Dressing in Different Order Impregnation of Chitosan and Collagen. *Biomolecules*, 10(11), 1511.
- Patrulea, V., Ostafe, V., Borchard, G., & Jordan, O. (2015). Chitosan as a starting material for wound healing applications. *European Journal of Pharmaceutics and Biopharmaceutics*, 97, 417-426.
- Pawar, S. N., & Edgar, K. J. (2012). Alginate derivatization: a review of chemistry, properties and applications. *Biomaterials*, 33(11), 3279-3305.
- Peanparkdee, M., Iwamoto, S., & Yamauchi, R. (2016). Microencapsulation: a review of applications in the food and pharmaceutical industries. *Reviews in Agricultural Science*, 4, 56-65.

- Percival, S. L., McCarty, S., Hunt, J. A., & Woods, E. J. (2014). The effects of pH on wound healing, biofilms, and antimicrobial efficacy. *Wound Repair Regen*, 22(2), 174-186.
- Perretti, M., Chiang, N., La, M., Fierro, I. M., Marullo, S., Getting, S. J., . . . Serhan, C. N. (2002). Endogenous lipid- and peptide-derived anti-inflammatory pathways generated with glucocorticoid and aspirin treatment activate the lipoxin A4 receptor. *Nat Med*, 8(11), 1296-1302.
- Perretti, M., & D'Acquisto, F. (2009). Annexin A1 and glucocorticoids as effectors of the resolution of inflammation. *Nature Reviews Immunology*, 9(1), 62-70.
- Perretti, M., & Dalli, J. (2009). Exploiting the Annexin A1 pathway for the development of novel anti-inflammatory therapeutics. *British Journal of Pharmacology*, 158(4), 936-946.
- Pierpont, Y. N., Dinh, T. P., Salas, R. E., Johnson, E. L., Wright, T. G., Robson, M. C., & Payne, W. G. (2014). Obesity and surgical wound healing: a current review. *International Scholarly Research Notices*.
- Pilehvar-Soltanahmadi, Y., Dadashpour, M., Mohajeri, A., Fattahi, A., Sheervalilou, R., & Zarghami, N. (2018). An overview on application of natural substances incorporated with electrospun nanofibrous scaffolds to development of innovative wound dressings. *Mini reviews in medicinal chemistry*, 18(5), 414-427.
- Piñón-Balderrama, C., Leyva-Porras, C., Teran, Y., Espinosa-Solis, V., Alavrez, C., & Saavedra, Z. (2020). Encapsulation of Active Ingredients in Food Industry by Spray-Drying and Nano Spray-Drying Technologies. *Processes*, 8, 889.
- Poozesh, S., & Bilgili, E. (2019). Scale-up of pharmaceutical spray drying using scale-up rules: a review. *International Journal of Pharmaceutics*, 562, 271-292.

- Porporatto, C., Bianco, I. D., Riera, C. M., & Correa, S. G. (2003). Chitosan induces different L-arginine metabolic pathways in resting and inflammatory macrophages. *Biochem Biophys Res Commun*, 304(2), 266-272.
- Prajapati, V. D., Jani, G. K., & Kapadia, J. R. (2015). Current knowledge on biodegradable microspheres in drug delivery. *Expert opinion on drug delivery*, 12(8), 1283-1299.
- Price, R. D., Myers, S., Leigh, I. M., & Navsaria, H. A. (2005). The role of hyaluronic acid in wound healing. *American journal of clinical dermatology*, 6(6), 393-402.
- Prosdocimi, M., & Bevilacqua, C. (2012). Exogenous hyaluronic acid and wound healing: an updated vision. *Panminerva Med*, 54(2), 129-135.
- Przekora, A. (2020). A Concise Review on Tissue Engineered Artificial Skin Grafts for Chronic Wound Treatment: Can We Reconstruct Functional Skin Tissue In Vitro? , *Cells*, 9(7), 1622.
- Qin, C. X., Rosli, S., Deo, M., Cao, N., Walsh, J., Tate, M., . . . Ritchie, R. H. (2019). Cardioprotective Actions of the Annexin-A1 N-Terminal Peptide, Ac2-26, Against Myocardial Infarction. *Frontiers in Pharmacology*, 10(269).
- Raafat, D., von Bargen, K., Haas, A., & Sahl, H.-G. (2008). Insights into the mode of action of chitosan as an antibacterial compound. *Applied and environmental microbiology*, 74(12), 3764-3773.
- Rabiee, T., Yeganeh, H., & Gharibi, R. (2019). Antimicrobial wound dressings with high mechanical conformability prepared through thiol-yne click photopolymerization reaction. *Biomedical Materials (Bristol Online)*, 14(4), 21.
- Raffetto, J. D., Ligi, D., Maniscalco, R., Khalil, R. A., & Mannello, F. (2020). Why Venous Leg Ulcers Have Difficulty Healing: Overview on Pathophysiology, Clinical Consequences, and Treatment. *Journal of clinical medicine*, 10(1).

- Rai, D., Singh, J. K., Roy, N., & Panda, D. (2008). Curcumin inhibits FtsZ assembly: an attractive mechanism for its antibacterial activity. *Biochemical Journal*, 410(1), 147-155.
- Ravi Kumar, M. N. (2000). Nano and microparticles as controlled drug delivery devices. *J Pharm Pharm Sci*, 3(2), 234-258.
- Ravizza, A., De Maria, C., Di Pietro, L., Sternini, F., Audenino, A. L., & Bignardi, C. (2019). Comprehensive Review on Current and Future Regulatory Requirements on Wearable Sensors in Preclinical and Clinical Testing. *Frontiers in Bioengineering and Biotechnology*, 7(313).
- Raynal, P., & Pollard, H. B. (1994). Annexins: the problem of assessing the biological role for a gene family of multifunctional calcium- and phospholipid-binding proteins. *Biochimica et Biophysica Acta (BBA) Reviews on Biomembranes*, 1197(1), 63-93.
- Rehm, B. H. (2010). Bacterial polymers: biosynthesis, modifications and applications. *Nat Rev Microbiol*, 8(8), 578-592.
- Ribeiro, A. P. B., Masuchi, M. H., Miyasaki, E. K., Domingues, M. A. F., Stroppa, V. L. Z., de Oliveira, G. M., & Kieckbusch, T. G. (2015). Crystallization modifiers in lipid systems. *Journal of Food Science and Technology*, 52(7), 3925-3946.
- Rogers, L. C., Armstrong, D. G., Capotorto, J., Fife, C. E., Garcia, J. R., Gelly, H., . . . practice. (2020). Wound center without walls: the new model of providing care during the COVID-19 pandemic. *Wounds: a compendium of clinical research practice*, 32(7), 178.
- Rosengarh, A., & Luecke, H. (2003). A calcium-driven conformational switch of the N-terminal and core domains of annexin A1. *J Mol Biol*, 326(5), 1317-1325.
- Rosso, A., Andretto, V., Chevalier, Y., Kryza, D., Sidi-Boumedine, J., Grenha, A., . . . Lollo, G. (2021). Nanocomposite sponges for enhancing intestinal residence time following oral administration. *Journal of Controlled Release*, 333, 579-592.

- Rosso, A., Lollo, G., Chevalier, Y., Troung, N., Bordes, C., Bourgeois, S., . . . Briançon, S. (2020). Development and structural characterization of a novel nanoemulsion for oral drug delivery. *Colloids and Surfaces A: Physicochemical and Engineering Aspects*, 593, 124614.
- Rousselle, P., Braye, F., & Dayan, G. (2019). Re-epithelialization of adult skin wounds: Cellular mechanisms and therapeutic strategies. *Adv Drug Deliv Rev*, 146, 344-365.
- Ruckmani, K., Shaikh, S. Z., Khalil, P., Muneera, M. S., & Thusleem, O. A. (2013). Determination of sodium hyaluronate in pharmaceutical formulations by HPLC–UV. *Journal of Pharmaceutical Analysis*, 3(5), 324-329.
- Ryan, M. E., Usman, A., Ramamurthy, N. S., Golub, L. M., & Greenwald, R. A. (2001). Excessive matrix metalloproteinase activity in diabetes: inhibition by tetracycline analogues with zinc reactivity. *Curr Med Chem*, 8(3), 305-316.
- Sahana, T. G., & Rekha, P. D. (2018). Biopolymers: Applications in wound healing and skin tissue engineering. *Mol Biol Rep*, 45(6), 2857-2867.
- Salehi, B., Rodrigues, C. F., Peron, G., Dall'Acqua, S., Sharifi-Rad, J., Azmi, L., . . . Cruz-Martins, N. (2021). Curcumin nanoformulations for antimicrobial and wound healing purposes. *Phytoterapy Research*, 35(5), 2487-2499.
- Salvia-Trujillo, L., Martín-Belloso, O., & McClements, D. J. J. N. (2016). Excipient nanoemulsions for improving oral bioavailability of bioactives. *Nanomaterials*, 6(1), 17.
- Sansone, F., Esposito, T., Lauro, M. R., Picerno, P., Mencherini, T., Gasparri, F., . . . Aquino, R. P. (2018). Application of Spray Drying Particle Engineering to a High-Functionality/Low-Solubility Milk Thistle Extract: Powders Production and Characterization. *Molecules*, 23(7), 1716.

- Sansone, F., Mencherini, T., Picerno, P., d'Amore, M., Aquino, R. P., & Lauro, M. R. J. J. o. F. E. (2011). Maltodextrin/pectin microparticles by spray drying as carrier for nutraceutical extracts. *Journal of Food Engineering*, 105(3), 468-476.
- Sarabahi, S. T. V. K. B. S. P. Principles and practice of wound care (2012). *New Delhi: Jaypee Brothers Medical*.
- Sawicki, E., Beijnen, J. H., Schellens, J. H. M., & Nuijen, B. (2016). Pharmaceutical development of an oral tablet formulation containing a spray dried amorphous solid dispersion of docetaxel or paclitaxel. *International Journal of Pharmaceutics*, 511(2), 765-773.
- Schanté, C. E., Zuber, G., Herlin, C., & Vandamme, T. F. (2011). Chemical modifications of hyaluronic acid for the synthesis of derivatives for a broad range of biomedical applications. *Carbohydrate Polymers*, 85(3), 469-489.
- Schmid, K., Arpagaus, C., & Friess, W. (2011). Evaluation of the Nano Spray Dryer B-90 for pharmaceutical applications. *Pharmaceutical Development and Technology*, 16(4), 287-294.
- Schoener, C. A., Hutson, H. N., & Peppas, N. A. (2012). pH-responsive hydrogels with dispersed hydrophobic nanoparticles for the delivery of hydrophobic therapeutic agents. *Polym Int*, 61(6), 874-879.
- Sen, C. K., Gordillo, G. M., Roy, S., Kirsner, R., Lambert, L., Hunt, T. K., . . . Longaker, M. T. (2009). Human skin wounds: a major and snowballing threat to public health and the economy. *Wound Repair Regen*, 17(6), 763-771.
- Sen CK. (2021). Human Wound and Its Burden: Updated 2020 Compendium of Estimates. *Adv Wound Care (New Rochelle)*, 10(5):281-292.

- Serra, R., Grande, R., Butrico, L., Rossi, A., Settimio, U. F., Caroleo, B., . . . de Franciscis, S. (2015). Chronic wound infections: the role of *Pseudomonas aeruginosa* and *Staphylococcus aureus*. *Expert Rev Anti Infect Ther*, 13(5), 605-613.
- Seyfarth, F., Schliemann, S., Elsner, P., & Hipler, U. C. (2008). Antifungal effect of high- and low-molecular-weight chitosan hydrochloride, carboxymethyl chitosan, chitosan oligosaccharide and N-acetyl-D-glucosamine against *Candida albicans*, *Candida krusei* and *Candida glabrata*. *Int J Pharm*, 353(1-2), 139-148.
- Sezer, A. D., & Cevher, E. (2011). Biopolymers as wound healing materials: challenges and new strategies. *Biomaterials applications for nanomedicine*, 383-414.
- Shi, R., Geng, H., Gong, M., Ye, J., Wu, C., Hu, X., & Zhang, L. (2018). Long-acting and broad-spectrum antimicrobial electrospun poly (ϵ -caprolactone)/gelatin micro/nanofibers for wound dressing. *Journal of Colloid and Interface Science*, 509, 275-284.
- Shi, R., Sun, T. L., Luo, F., Nakajima, T., Kurokawa, T., Bin, Y. Z., . . . Gong, J. P. (2018). Elastic–Plastic Transformation of Polyelectrolyte Complex Hydrogels from Chitosan and Sodium Hyaluronate. *Macromolecules*, 51(21), 8887-8898.
- Siepmann, J., & Siepmann, F. (2012). Modeling of diffusion controlled drug delivery. *Journal of controlled release*, 161(2), 351-362.
- Silva, H. F. O., Lima, K. M. G., Cardoso, M. B., Oliveira, J. F. A., Melo, M. C. N., Sant'Anna, C., . . . Gasparotto, L. H. S. (2015). Doxycycline conjugated with polyvinylpyrrolidone-encapsulated silver nanoparticles: a polymer's malevolent touch against *Escherichia coli*. *RSC Advances*, 5(82), 66886-66893.
- Simsek-Ege, F. A., Bond, G. M., & Stringer, J. (2003). Polyelectrolyte complex formation between alginate and chitosan as a function of pH. *Journal of Applied Polymer Science*, 88(2), 346-351.

- Sinitsya, A., J. Č. k., Prutyayov, V., Skoblya, S., & V, M. (2000). Amidation of highly methoxylated citrus pectin with primary amines. *Carbohydrate Polyemers*, (4), 359-368.
- Siracusa, V., Romani, S., Gigli, M., Mannozi, C., Cecchini, J. P., Tylewicz, U., & Lotti, N. (2018). Characterization of Active Edible Films based on Citral Essential Oil, Alginate and Pectin. *Materials (Basel, Switzerland)*, 11(10), 1980.
- Smith, A. M., Moxon, S., & Morris, G. (2016). *Biopolymers as wound healing materials*. In *Wound healing biomaterials* (pp. 261-287): Elsevier
- Solans, C., & Solé, I. (2012). Nano-emulsions: Formation by low-energy methods. *Current Opinion in Colloid & Interface Science*, 17(5), 246-254.
- Sørensen, L. T. (2012). Wound healing and infection in surgery: the pathophysiological impact of smoking, smoking cessation, and nicotine replacement therapy: a systematic review. *Ann Surg*, 255(6), 1069-1079.
- Souza, J. M., Henriques, M., Teixeira, P., Fernandes, M. M., Fanguero, R., Zille, A. J. F., & Polymers. (2019). Comfort and infection control of chitosan-impregnated cotton gauze as wound dressing. *Fibers Polymers*, 20(5), 922-932.
- Sriamornsak, P., Thirawong, N., & Puttipipatkachorn, S. (2004). Morphology and buoyancy of oil-entrapped calcium pectinate gel beads. *The AAPS journal*, 6(3), e24-e24.
- Sriamornsak, P. J. S. (2003). Chemistry of pectin and its pharmaceutical uses: A review. *University International Journal*, 3(1-2), 206-228.
- Stechmiller, J., Cowan, L., & Schultz, G. (2010). The Role of Doxycycline as a Matrix Metalloproteinase Inhibitor for the Treatment of Chronic Wounds. *Biol Res Nurs*, 11(4), 336-344.
- Suh, W. H., Jang, A. R., Suh, Y.-H., & Suslick, K. S. (2006). Porous, Hollow, and Ball-in-Ball Metal Oxide Microspheres: Preparation, Endocytosis, and Cytotoxicity. *Advanced Materials*, 18(14), 1832-1837.

- Sulaeva, I., Henniges, U., Rosenau, T., & Potthast, A. (2015). Bacterial cellulose as a material for wound treatment: Properties and modifications. A review. *Biotechnol Adv*, 33(8), 1547-1571.
- Sun, G., Zhang, X., Shen, Y.-I., Sebastian, R., Dickinson, L. E., Fox-Talbot, K., . . . Gerecht, S. (2011). Dextran hydrogel scaffolds enhance angiogenic responses and promote complete skin regeneration during burn wound healing. *Proc Natl Acad Sci U S A*, 108(52), 20976-20981.
- Sun, J., & Tan, H. (2013). Alginate-Based Biomaterials for Regenerative Medicine Applications. *Materials (Basel, Switzerland)*, 6(4), 1285-1309.
- Sunarić, S. M., Denić, M. S., Bojanić, Z. Ž., & Bojanić, V. V. (2013). HPLC method development for determination of doxycycline in human seminal fluid. *Journal of Chromatography B*, 939, 17-22.
- Sundar Raj, A., Rubila, S., Jayabalan, R., Ranganathan, T. (2012). A Review on Pectin: Chemistry due to General Properties of Pectin and its Pharmaceutical Uses. *Large differences may exist between samples between molecules within a sample estimates may differ between methods of measurement*, 01 (1) 550-553.
- Sussman, G. (2014). Ulcer dressings and management. *Aust Fam Physician*, 43(9), 588-592.
- Szabo, G., Mandrekar, P. J. A. C., & Research, E. (2009). A recent perspective on alcohol, immunity, and host defense. *Alcoholism: Clinical Experimental Research*, 33(2), 220-232.
- Szekalska, M., Puciłowska, A., Szymańska, E., Ciosek, P., & Winnicka, K. (2016). Alginate: Current Use and Future Perspectives in Pharmaceutical and Biomedical Applications. *International Journal of Polymer Science*, 2016, 7697031.
- Takeo, M., Lee, W., & Ito, M. (2015). Wound healing and skin regeneration. *Cold Spring Harb Perspect Med*, 5(1), a023267.

- Tamer, T. M., Collins, M. N., Valachová, K., Hassan, M. A., Omer, A. M., Mohy-Eldin, M. S., . . . Šoltés, L. (2018). MitoQ Loaded Chitosan-Hyaluronan Composite Membranes for Wound Healing. *Materials (Basel)*, 11(4), 569.
- Tang, E. S., Chan, L., & Heng, P. W. J. A. J. o. D. D. (2005). Coating of multiparticulates for sustained release. *American Journal of Drug Delivery*, 3(1), 17-28.
- Tang, Y., Wang, X., Li, Y., Lei, M., Du, Y., Kennedy, J. F., & Knill, C. J. (2010). Production and characterisation of novel injectable chitosan/methylcellulose/salt blend hydrogels with potential application as tissue engineering scaffolds. *Carbohydrate Polymers*, 82(3), 833-841.
- Tao, Y., Qian, L.-H., & Xie, J. (2011). Effect of chitosan on membrane permeability and cell morphology of *Pseudomonas aeruginosa* and *Staphylococcus aureus*. *Carbohydrate Polymers*, 86(2), 969-974.
- Tavianatou, A. G., Caon, I., Franchi, M., Piperigkou, Z., Galesso, D., & Karamanos, N. K. (2019). Hyaluronan: molecular size-dependent signaling and biological functions in inflammation and cancer. *The FEBS Journal*, 286(15), 2883-2908.
- Teixeira, M. A., Paiva, M. C., Amorim, M. T. P., & Felgueiras, H. P. (2020). Electrospun Nanocomposites Containing Cellulose and Its Derivatives Modified with Specialized Biomolecules for an Enhanced Wound Healing. 10(3), 557.
- Teixeira, R. A. P., Mimura, K. K. O., Araujo, L. P., Greco, K. V., & Oliani, S. M. (2016). The essential role of annexin A1 mimetic peptide in the skin allograft survival. *Tissue Eng Regen Med*, 10(2), E44-E53.
- Thakur, B. R., Singh, R. K., Handa, A. K., Rao, M. (1997). Chemistry and uses of pectin-a review. *Critical Reviews in Food Science Nutrition*, 37(1), 47-73.

- Thomas, A., Harding, K. G., & Moore, K. (2000). Alginates from wound dressings activate human macrophages to secrete tumour necrosis factor-alpha. *Biomaterials*, 21(17), 1797-1802.
- Thomas, L., Zakir, F., Mirza, M. A., Anwer, M. K., Ahmad, F. J., & Iqbal, Z. (2017). Development of Curcumin loaded chitosan polymer based nanoemulsion gel: In vitro, ex vivo evaluation and in vivo wound healing studies. *Int J Biol Macromol*, 101, 569-579.
- Torres-Castro, I., Arroyo-Camarena, Ú. D., Martínez-Reyes, C. P., Gómez-Arauz, A. Y., Dueñas-Andrade, Y., Hernández-Ruiz, J., . . . Escobedo, G. (2016). Human monocytes and macrophages undergo M1-type inflammatory polarization in response to high levels of glucose. *Immunology Letters*, 176, 81-89.
- Toth, M., & Fridman, R. (2001). Assessment of gelatinases (MMP-2 and MMP-9) by gelatin zymography. *Methods Mol Med*. 57:163-74.
- Tran, N. Q., Joung, Y. K., Lih, E., & Park, K. D. (2011). In situ forming and rutin-releasing chitosan hydrogels as injectable dressings for dermal wound healing. *Biomacromolecules*, 12(8), 2872-2880.
- Trengove, N. J., Bielefeldt-Ohmann, H., & Stacey, M. C. (2000). Mitogenic activity and cytokine levels in non-healing and healing chronic leg ulcers. *Wound Repair Regen*, 8(1), 13-25.
- Tsioufis, C., Bafakis, I., Kasiakogias, A., & Stefanadis, C. (2012). The role of matrix metalloproteinases in diabetes mellitus. *Current topics in medicinal chemistry*, 12(10), 1159-1165.
- Ueno, H., Mori, T., & Fujinaga, T. (2001). Topical formulations and wound healing applications of chitosan. *Adv Drug Deliv Rev*, 52(2), 105-115.

- Uitto, V. J., Firth, J. D., Nip, L., & Golub, L. M. (1994). Doxycycline and chemically modified tetracyclines inhibit gelatinase A (MMP-2) gene expression in human skin keratinocytes. *Ann N Y Acad Sci*, 732, 140-151.
- Unnithan, A. R., Barakat, N. A. M., Tirupathi Pichiah, P. B., Gnanasekaran, G., Nirmala, R., Cha, Y.-S., . . . Kim, H. Y. (2012). Wound-dressing materials with antibacterial activity from electrospun polyurethane–dextran nanofiber mats containing ciprofloxacin HCl. *Carbohydrate Polymers*, 90(4), 1786-1793.
- Utz, E. R., Elster, E. A., Tadaki, D. K., Gage, F., Perdue, P. W., Forsberg, J. A., . . . Brown, T. S. (2010). Metalloproteinase Expression is Associated with Traumatic Wound Failure. *Journal of Surgical Research*, 159(2), 633-639.
- Uzun, M. (2018). A review of wound management materials. *Journal of Textile Engineering & Fashion Technology*, 4.
- Van Wart, H. E., & Birkedal-Hansen, H. (1990). The cysteine switch: a principle of regulation of metalloproteinase activity with potential applicability to the entire matrix metalloproteinase gene family. *Proc Natl Acad Sci U S A*, 87(14), 5578-5582.
- Vehring, R., Foss, W. R., & Lechuga-Ballesteros, D. (2007). Particle formation in spray drying. *Journal of Aerosol Science*, 38(7), 728-746.
- Venkatasubbu, G. D., & Anusuya, T. (2017). Investigation on Curcumin nanocomposite for wound dressing. *International Journal of Biological Macromolecules*, 98, 366-378.
- Venkatesan, P., & Rao, M. N. (2000). Structure-activity relationships for the inhibition of lipid peroxidation and the scavenging of free radicals by synthetic symmetrical curcumin analogues. *J Pharm Pharmacol*, 52(9), 1123-1128.
- Vowden, K., & Vowden, P. (2017). Wound dressings: principles and practice. *Surgery Oxford*, 29(10), 491-495.

- Vries, K. d. (2018). Primary care: Hydrocolloid and hydroactive wound dressings. *The Australian Journal of Pharmacy*, 99(1175), 81–83.
- Wallace, H. A., Basehore, B. M., & Zito, P. M. (2021). *Wound Healing Phases*. In *StatPearls*. Treasure Island (FL): StatPearls Publishing.
- Wan, F., Bohr, A., Maltesen, M. J., Bjerregaard, S., Foged, C., Rantanen, J., & Yang, M. (2013). Critical Solvent Properties Affecting the Particle Formation Process and Characteristics of Celecoxib-Loaded PLGA Microparticles via Spray-Drying. *Pharmaceutical Research*, 30(4), 1065-1076.
- Wang, J., de Wit, M., Boom, R. M., & Schutyser, M. A. I. (2015). Charging and separation behavior of gluten–starch mixtures assessed with a custom-built electrostatic separator. *Separation and Purification Technology*, 152, 164-171.
- Wang, Y.-C., Lee, H.-C., Chen, C.-L., Kuo, M.-C., Ramachandran, S., Chen, R.-F., & Kuo, Y.-R. (2021). The Effects of Silver-Releasing Foam Dressings on Diabetic Foot Ulcer Healing. *Journal of clinical medicine*, 10(7), 1495.
- Wang, Z., Ordoubadi, M., Wang, H., & Vehring, R. (2021). Morphology and formation of crystalline leucine microparticles from a co-solvent system using multi-orifice monodisperse spray drying. *Aerosol Science and Technology*, 1-22.
- Weller, C., & Team, V. (2019). Interactive dressings and their role in moist wound management. *In Advanced textiles for wound care* (pp. 105-134).
- Weller, C. D., Team, V., & Sussman, G. (2020). First-Line Interactive Wound Dressing Update: A Comprehensive Review of the Evidence. *Frontiers in pharmacology*, 11, 155-155.
- Werdin, F., Tennenhaus, M., Schaller, H. E., & Rennekampff, H. O. (2009). Evidence-based management strategies for treatment of chronic wounds. *Eplasty*, 9, e19.

- Westby, M. J., Dumville, J. C., Soares, M. O., Stubbs, N., & Norman, G. (2017). Dressings and topical agents for treating pressure ulcers. *Cochrane Database of Systematic Reviews* (6)6.
- Whelehan, M., & Marison, I. W. (2011). Microencapsulation using vibrating technology. *Journal of microencapsulation*, 28(8), 669-688.
- Wilkins, R. G., & Unverdorben, M. (2013). Wound cleaning and wound healing: a concise review. *Adv Skin Wound Care*, 26(4), 160-163.
- Wischke, C., & Schwendeman, S. P. (2008). Principles of encapsulating hydrophobic drugs in PLA/PLGA microparticles. *International Journal of pharmaceutics*, 364(2), 298-327.
- Wu, S., Deng, L., Hsia, H., Xu, K., He, Y., Huang, Q., . . . Peng, C. (2017). Evaluation of gelatin-hyaluronic acid composite hydrogels for accelerating wound healing. *J Biomater Appl*, 31(10), 1380-1390.
- Xia, W., Liu, P., Zhang, J., & Chen, J. (2011). Biological activities of chitosan and chitooligosaccharides. *Food Hydrocolloids*, 25(2), 170-179.
- Xiao, B., Laroui, H., Viennois, E., Ayyadurai, S., Charania, M. A., Zhang, Y., . . . Merlin, D. (2014). Nanoparticles with surface antibody against CD98 and carrying CD98 small interfering RNA reduce colitis in mice. *Gastroenterology*, 146(5), 1289-1300.e3019.
- Xie, Y., Yi, Z.-x., Wang, J.-x., Hou, T.-g., & Jiang, Q. (2018). Carboxymethyl konjac glucomannan - crosslinked chitosan sponges for wound dressing. *International Journal of Biological Macromolecules*, 112, 1225-1233.
- Xu, W.-K., Tang, J.-Y., Yuan, Z., Cai, C.-Y., Chen, X.-B., Cui, S.-Q., . . . Ding, J.-D. (2019). Accelerated Cutaneous Wound Healing Using an Injectable Teicoplanin-loaded PLGA-PEG-PLGA Thermogel Dressing. *Chinese Journal of Polymer Science*, 37(6), 548-559.
- Xu, Y. Y., Howes, T., Adhikari, B., & Bhandari, B. (2012). Investigation of Relationship between Surface Tension of Feed Solution Containing Various Proteins and Surface

- Composition and Morphology of Powder Particles. *Drying Technology*, 30(14), 1548-1562.
- Xue, J., Wang, X., Wang, E., Li, T., Chang, J., & Wu, C. (2019). Bioinspired multifunctional biomaterials with hierarchical microstructure for wound dressing. *Acta Biomaterialia*, 100, 270-279.
- Yager, D. R., Zhang, L.-Y., Liang, H.-X., Diegelmann, R. F., & Cohen, I. K. (1996). Wound Fluids from Human Pressure Ulcers Contain Elevated Matrix Metalloproteinase Levels and Activity Compared to Surgical Wound Fluids. *Journal of Investigative Dermatology*, 107(5), 743-748.
- Yamamoto, S., Saeki, T., & Inoshita, T. (2002). Drying of gelled sugar solutions—water diffusion behavior. *Chemical Engineering Journal*, 86(1), 179-184.
- Yang, X., Yang, J., Wang, L., Ran, B., Jia, Y., Zhang, L., . . . Jiang, X. (2017). Pharmaceutical Intermediate-Modified Gold Nanoparticles: Against Multidrug-Resistant Bacteria and Wound-Healing Application via an Electrospun Scaffold. *ACS Nano*, 11(6), 5737-5745.
- Yazdanpanah, L., Nasiri, M., & Adarvishi, S. (2015). Literature review on the management of diabetic foot ulcer. *World journal of diabetes*, 6(1), 37-53.
- Yip, W. L. (2015). Influence of oxygen on wound healing. *Int Wound J*, 12(6), 620-624.
- Yoon, D. S., Lee, Y., Ryu, H. A., Jang, Y., Lee, K.-M., Choi, Y., . . . Lee, J. W. (2016). Cell recruiting chemokine-loaded sprayable gelatin hydrogel dressings for diabetic wound healing. *Acta Biomaterialia*, 38, 59-68.
- Yu, Y., Shen, M., Song, Q., & Xie, J. (2018). Biological activities and pharmaceutical applications of polysaccharide from natural resources: A review. *Carbohydrate Polymers*, 183, 91-101.

- Zavan B, Vindigni V, Vezzù K, Zorzato G, Luni C, Abatange-lo G, et al. (2009). Hyaluronan based porous nano-particles enriched with growth factors for the treatment of ulcers: A placebo-controlled study. *J Mater Sci Mater Med*, 20(1):235–47
- Zhang, W., Dehghani-Sanij, A. A., & Blackburn, R. S. (2008). IR study on hydrogen bonding in epoxy resin–silica nanocomposites. *Progress in Natural Science*, 18(7), 801-805.
- Zhang, Y.-T., Li, Z., Zhang, K., Zhang, H.-Y., He, Z.-H., Xia, Q., . . . Feng, N.-P. (2017). Co-delivery of evodiamine and rutaecarpine in a microemulsion-based hyaluronic acid hydrogel for enhanced analgesic effects on mouse pain models. *International Journal of Pharmaceutics*, 528(1), 100-106.
- Zhao, R., Liang, H., Clarke, E., Jackson, C., & Xue, M. (2016). Inflammation in Chronic Wounds. *Int J Mol Sci*, 17(12), 2085.
- Zhao, Y., Huang, Z., Zhang, J., Wu, W., Wang, M., & Fan, L. (2010). Thermal degradation of sodium alginate- incorporated soy protein isolate/glycerol composite membranes. *17th IAPRI World Conference on Packaging 2010*, 402-405.
- Zheng, D., Huang, C., Huang, H., Zhao, Y., Khan, M. R. U., Zhao, H., . . . (2020). Antibacterial mechanism of curcumin: A review. *Chemistry Biodiversity*, 17(8), e2000171.
- Zielins, E. R., Atashroo, D. A., Maan, Z. N., Duscher, D., Walmsley, G. G., Hu, M., . . . Longaker, M. T. (2014). Wound healing: an update. *Regen Med*, 9(6), 817-830.
- Zorofchian Moghadamtousi, S., Abdul Kadir, H., Hassandarvish, P., Tajik, H., Abubakar, S., & Zandi, K. (2014). A Review on Antibacterial, Antiviral, and Antifungal Activity of Curcumin. *Biomed Res Int*, 2014, 186864.
- Zou, Y., Yang, X., & Scholten, E. (2018). Rheological behavior of emulsion gels stabilized by zein/tannic acid complex particles. *Food Hydrocolloids*, 77, 363-371.

Sitography

Arterial ulcers: <https://www.woundsource.com>

Chronic wounds during Covid-19: <https://www.ama-assn.org/practice-management/sustainability/physician-survey-details-depth-pandemic-s-financial-impact>

Spray drying: <https://www.europeanpharmaceuticalreview.com/article/27768/spray-drying-pharmaceutical-industry/>; <https://drug-dev.com/spray-dried-dispersions-efficient-scale-up-strategy-for-spray-dried-amorphous-dispersions/>

Wound classification: <https://www.woundcaresurgeons.org/>

Wound dressing market: <https://www.maximizemarketresearch.com/market-report/global-wound-care-market/15340/>

APPENDIX

List of publications and communications

Papers

- **Amante C**, Esposito T, Del Gaudio P, Di Sarno V, Porta A, Tosco A, Russo P, Nicolais L, Aquino RP. A Novel Three-Polysaccharide Blend In Situ Gelling Powder for Wound Healing Applications. *Pharmaceutics*. 2021 Oct 14;13(10):1680.
<https://doi.org/10.3390/pharmaceutics13101680>

- Del Gaudio, P., **Amante, C.**, Civale, R., Bizzarro, V., Petrella, A., Pepe, G., Aquino, R. P. (2020). “In situ gelling alginate-pectin blend particles loaded with Ac2-26: A new weapon to improve wound care armamentarium”. *Carbohydrate Polymers*, 227, 115305.
<https://doi.org/10.1016/j.carbpol.2019.115305>

Communications

- **Amante C.**, De Soricellis C., *Falcone G.*, Russo P., Aquino R.P., Del Gaudio P. “*In situ* gelling powders for wound healing applications: effects of polysaccharides blend and hyaluronic acid on formulation properties”. 7th International Congress of the European Polysaccharide Network of Excellence. October 11-15, 2021. Nantes, France. Oral presentation.

- **Amante C.**, De Soricellis C., Russo P., Aquino R.P., Del Gaudio P. “In-situ gelling powders based on natural polysaccharides with sodium hyaluronate as potential wound dressings”. 20th Advanced Course in Pharmaceutical Technology, September 27-29, 2021. Online. Poster presentation.

- **Chiara Amante**, Chiara De Soricellis, Giovanni Falcone, Paola Russo, Rita Patrizia Aquino, Pasquale Del Gaudio. “The influence of chitosan on in situ gelling blend powders for wound healing”. MedChem. July 26-28, 2021, Poster session on Twitter session.
- **Amante C.**, Russo P., Aquino R.P., Del Gaudio P. “ Influence of chitosan on a polysaccharide blend in situ gelling powders for wound dressing”. Nano Innovation 2020, September 15-18, 2020, Rome, Italy. Oral presentation.
- Pasquale Del Gaudio, **Chiara Amante**, Romina Sessa, Paola Russo, Rita P. Aquino. “In situ gelling polysaccharides submicrometric particles loaded with ac2-26 for wound healing”. 22nd International Symposium on Microencapsulation, 25-27 September 2019, Salvador Brazil.
- **Amante C.**, Sessa R., Chastylo V., Russo P, Aquino R.P., Del Gaudio P. “*In situ* gelling alginate-pectin blend powders loaded with Annexin A1 peptidomimetic Ac2-26 for wound healing”. 19th Advanced School in Pharmaceutical Technology “Characterization of colloidal nanocarriers”, September, 9-12, 2019, Soverato (CZ) Italy. Poster presentation.
- **Chiara Amante**, Donatella Di Pietro, Romina Sessa, Paola Russo, Rita Patrizia Aquino, Pasquale Del Gaudio. “Annexin A1 peptidomimetic Ac2-26 loaded polysaccharides particles for wound healing applications”. XIII A.It.U.N. Annual meeting. June 13-15, 2019, Relais Borgo Lanciano Castelraimondo (MC), Italy. Poster presentation.

The doctoral scholarship is co-funded by the program POR Campania FSE 2014-2020,
European Social Found “Dottorati di Ricerca con Caratterizzazione Industriale”.

